TOWARDS PHORBOXAZOLE B: THE C20-C32 FRAGMENT

Kristaps Ermanis, BSc

Doctor of Philosophy

University of York

Chemistry

September 2014

1. Abstract

Phorboxazole A and phorboxazole B are two potent cytostatic polyketides isolated from *Phorbas* marine sponge found in the Indian Ocean. Because of their excellent cytostatic activity and unprecedented structure phorboxazoles have been a very attractive target for synthetic chemists and eleven total syntheses have been reported.

(+)-Phorboxazole A: R^1 = H, R^2 = OH
(+)-Phorboxazole B: R^1 = OH, R^2 = H

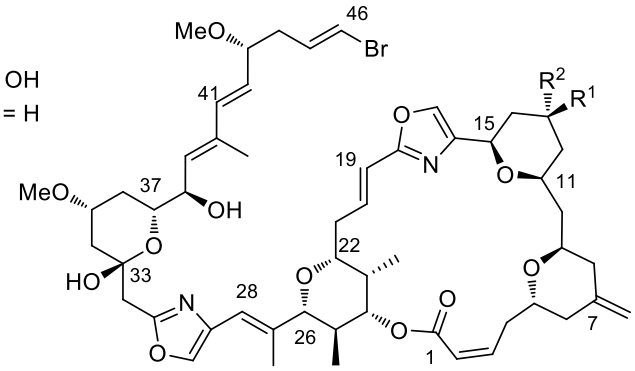

A novel and efficient synthesis of the C20-C32 core fragment of phorboxazoles has been developed. Key steps were: an enantioselective aldol reaction, a diastereoselective crotylation and, a diastereoselective oxy-Michael reaction. The synthesis was 7 steps long with an overall yield of 31%. A stereodivergent oxy-Michael reaction was further investigated in a computational study and analogue study.

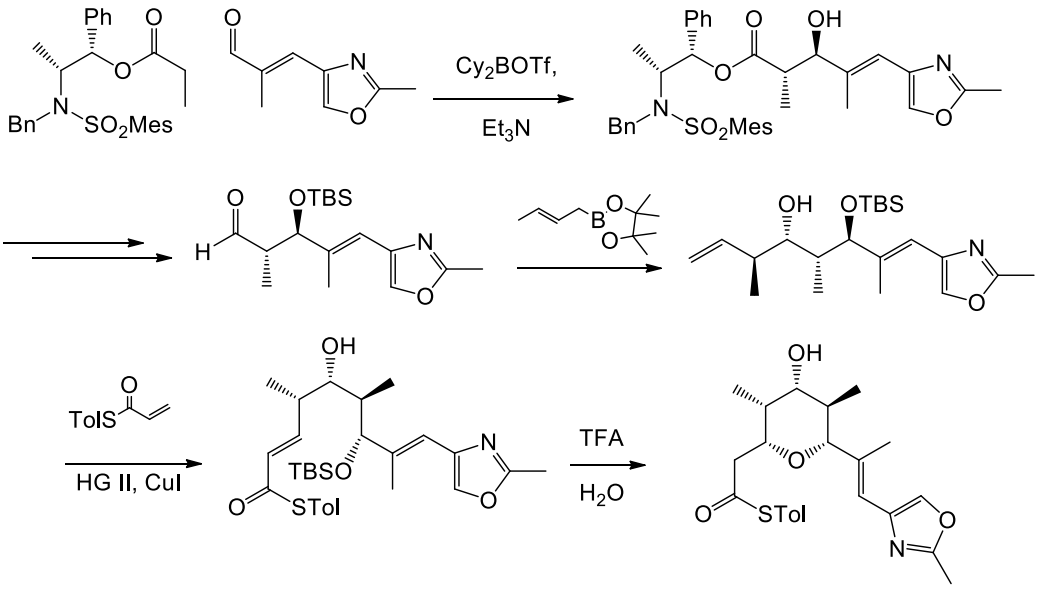

2. Contents

3. List of Tables

4. List of Figures

5. Acknowledgements

I would first of all like to thank my supervisor Dr. Paul Clarke for giving me the opportunity to work on such an exciting and challenging project. His advice, motivation and belief in me have been invaluable throughout the last four years. I am grateful to the University of York and Wild Fund for funding. I would like to thank the analytical services at the University of York, in particular Heather Fish and Karl Hale for their assistance in acquiring data.

I would also like to thank the wonderful people I have had the pleasure of working in the group with – Laurence, Joby, Phil, Bun, Helen, Nimesh, Ugur, Josh and Andy. In particular I wish to thank Paul and Nimesh for proof reading this manuscript. Any mistakes that remain are mine alone.

Finally, I wish to thank the people in my life I love so dearly. A special thank you to my Mum and my wonderful wife Liga – without their support this thesis would not be complete.

6. Declaration

I hereby declare that the substance of this thesis has not been submitted, nor is currently being submitted, in candidature for any other degree.

I also declare that the work embodied in this thesis is the result of my own investigations and in the event the work of others has been used this has been fully acknowledged in the text.

7. Introduction

7.1 Natural product synthesis today

Total synthesis of natural products has been one of the principal driving forces in the organic chemistry since the early days of the field. In the 170 years the field has seen incredible advancements that have successively demonstrated proof-of-concept (urea), biomimicry (tropinone), feasible complexity (strychnine, vitamin B-12, erythronolide), programmability (prostaglandins, ginkolide) and finally pushing the limits of chemical synthesis (palyotoxin, erythropoietin).[1]

Total synthesis has made many important contributions to the wider field of chemistry. One of them is the structure confirmation and revision of natural products. Despite the power of modern crystalographic and spectroscopic methods, between 1990 and 2004 the structures of more than 300 natural products have been reassigned. More importantly, total synthesis accounts for the vast majority of these structure revisions.[2] One well known case of structure reassignment is diazonamide A. Lindquist published its structure in 1991 based on X-ray studies which are considered the gold standard in the structure elucidation (Figure 1).[3] However, 10 years later Harran revised the structure by total synthesis.[4]

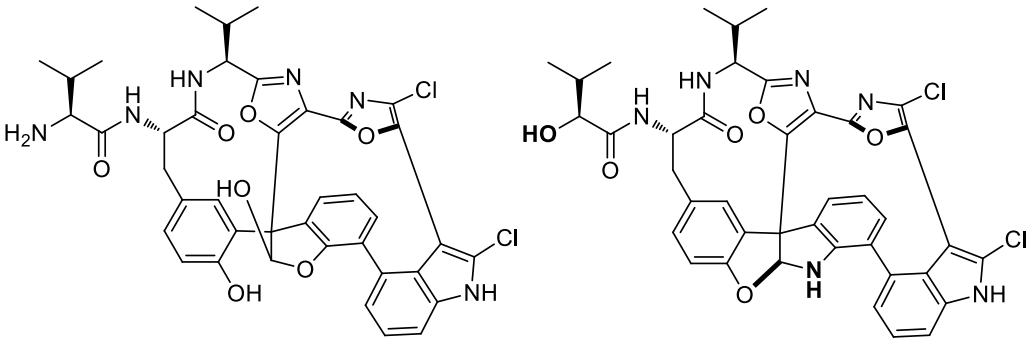

Figure 1: Proposed and revised structures of diazonamide A[4]

Other significant contributions of total synthesis are new chemical insights, for example, Barton's seminal work on conformational analysis was inspired by the synthetic efforts towards the steroids in the mid-20th century.[5] Similarly, in many cases new synthetic methodology has been developed to allow the synthesis of new classes of molecules. One well-known example is Evans' development of asymmetric alkylation and aldol methodology which gave access to the complex antibiotic cytovaricin.[6] The role of total synthesis in the development of new natural product based drugs is of particular importance.

Since prehistoric times people have used plants and other natural substances in traditional medicine to treat a wide spectrum of diseases. Nowadays natural products continue to be an important source of the new drugs.[7] Among all new chemical entities approved between 1981 and 2010, 6% were natural products, 28% were natural product derived, 25% mimicked the action of a natural product and 5% contained the pharmacophore of a natural product. The number of approved compounds has been steadily declining from a peak of 70 in 1987 to only 20 in 2010. In contrast, the proportion of natural products and their derivatives have been slowly increasing, reaching an impressive 50 percent in 2010. The pharmaceutical industry seems to have recognized this trend and is shifting away from large libraries of simple compounds and towards smaller, more focused libraries of more complex, natural product-like collections.[7]

Synthesis plays an important part in the natural product drug development. It is usually used to prepare semi-synthetic analogues with improved pharmacological properties, important examples being antimalarial artemisinin analogues and the Taxol derived anticancer drug DHA-paclitaxel.[8,9] In other cases it is possible to prepare simplified fully synthetic analogues, as for example the majority of compounds in the blockbuster cholesterol-lowering statin class.

In many cases, the development of natural products into drugs is hindered by significant supply issues. This is because the source organism is not always known and when it is known, the active compound often is found in only miniscule quantities. The answer to these supply issues would seem to be total chemical synthesis.

Nowadays it is generally accepted that synthesis of compounds of any complexity can be achieved, given enough time and resources. However, the vast majority of the reported total syntheses provide only milligram quantities of the target compound. These amounts are insufficient for significant biological studies and therefore have little impact in drug development, especially when the compound cannot be simplified without the loss of activity. Fortunately, in the last decade several groups have successfully addressed this issue with an increased focus on scalability of the total syntheses. They have succeeded in the production of several highly complex natural products in multigram quantities for biological studies. For example, the Smith III group synthesized 1.0 g of spongistatin and Novartis achieved the synthesis of more than 60 grams of discodermolide.[10,11] The development of the complex natural product halichondrin **3** into the drug eribulin **8** is particularly remarkable, as it is undoubtedly the most complex fully-synthetic drug molecule ever approved by FDA. The effort included the synthesis of more that 200 structural analogues of this complex molecule and culminated in 33 step industrial process that provided eribulin in 300 g batches (Scheme 1).[12]

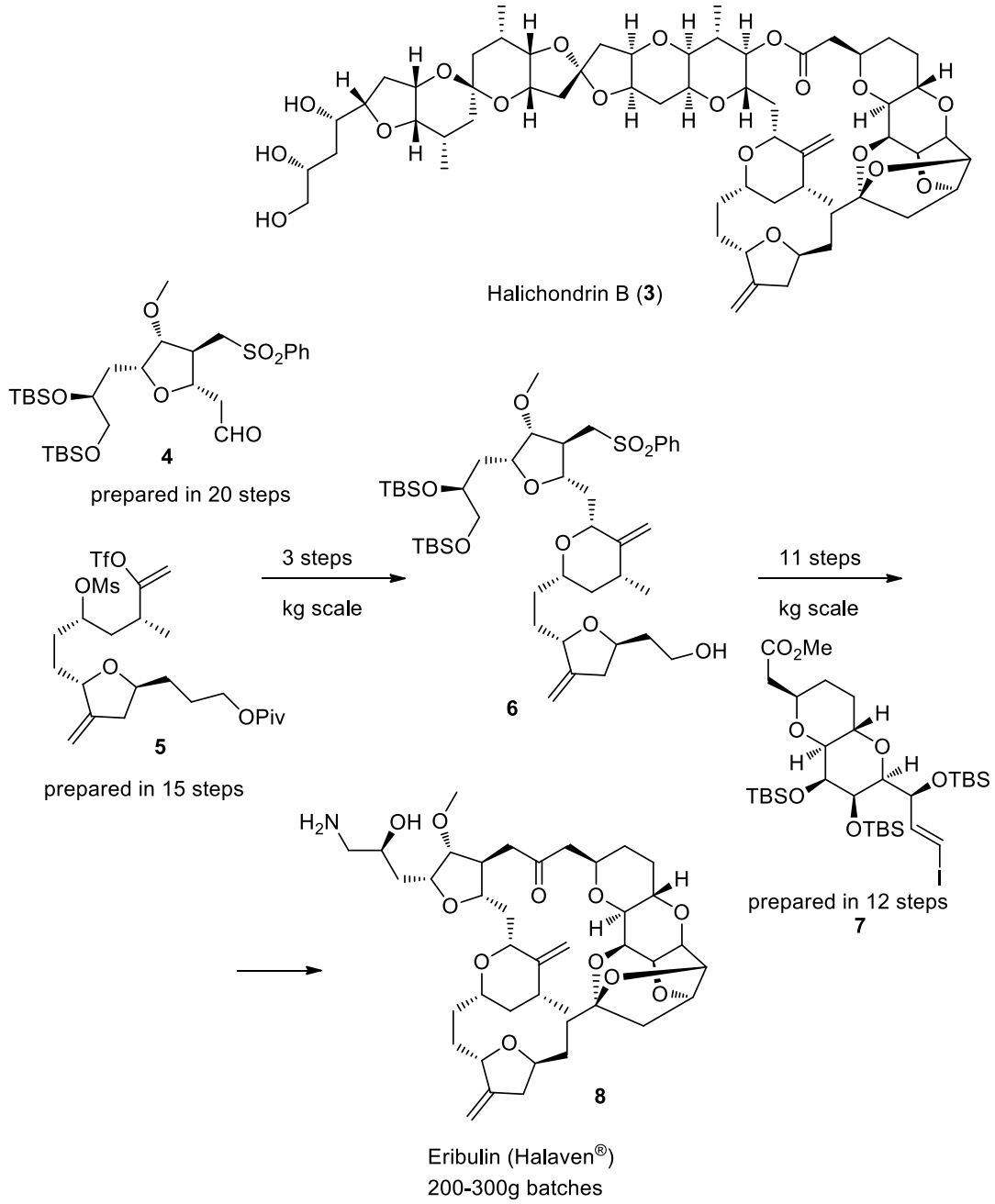

Scheme 1: Development and production of Eribulin

With the excellent potential of natural products as biologically active molecules and the increased focus on the scalability of the syntheses, one can only expect the role of total synthesis in chemistry, biology and medicine to increase in the coming years.

7.2 Phorboxazoles

Phorobxazoles A (**9**) and B (**10**) (Figure 2) are complex natural products isolated from *Phorbas* sponge. Their structure, relative and absolute stereochemistry was elucidated in 1996 by Searle and Molinski.[13-15] The structures of these natural products include four substituted tetrahydropyran (THP) rings, two 2,4-substituted oxazole rings, 15 stereogenic centres and seven double bonds. These structural features are organised into a C1-C26 macrolide ring and a C27-C46 tail. Three of the THP rings have *cis* geometry and the remaining one has *trans* geometry.

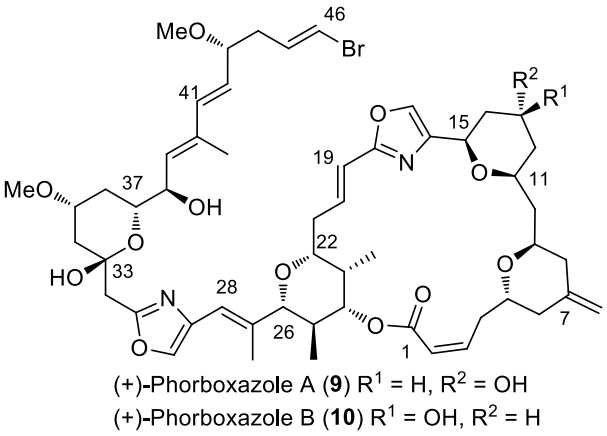

Figure 2: The structures of phorboxazoles

The importance of the phorboxazoles arises not only from the complex and unique structure of these molecules but also from their biological activity. They exhibit impressive cytostatic activity against the National Cancer Institute's (NCI) panel of 60 human tumour cell lines with mean GI values of 1.6×10^{-9} M. Most of the cells were completely inhibited even at the lowest test concentration. This makes the phorboxazoles among the most potent cytostatic agents known.

Compound	NALM-6 Leukemia IC_{50} (nM)	BT-20 Breast cancer IC_{50} (nM)	U373 Brain tumour IC_{50} (nM)
9	1.7	3.4	6.7
11	4.8	12.6	27.4
12	5.2	11.3	29.2
13	>2000	>2000	>2000
14	>2000	>2000	>2000
15	>2000	>2000	>2000
16	>2000	>2000	>2000
17	>2000	>2000	>2000

Table 1: Effect of (+)-phorboxazole A and various structural analogues on proliferation of human cancer cells[17]

After the first total synthesis of (+)-phorboxazole A (**9**) was published by Craig Forsyth,[16] the biological activity of a number of synthetic analogues was evaluated to find out which parts of the molecule were essential for its cytostatic activity.[17]

The analogues were tested against the human B-lineage acute lymphoblastic leukaemia cell line NALM-6, human breast cancer cell line BT-20, and human brain tumor (glioblastoma) cell line U373 (Table 1, Figure 3). The results showed that minor structural modifications do not have significant impact on the anticancer activity. For example, both **11** and **12** retain most of their biological activity, despite having modifications at C46 and C33, respectively. However, it was clear that portions of the macrolide, the central oxazole and the polyene sidechain were necessary for retention of high levels of activity, as shown by the inactive compounds **13-17**.

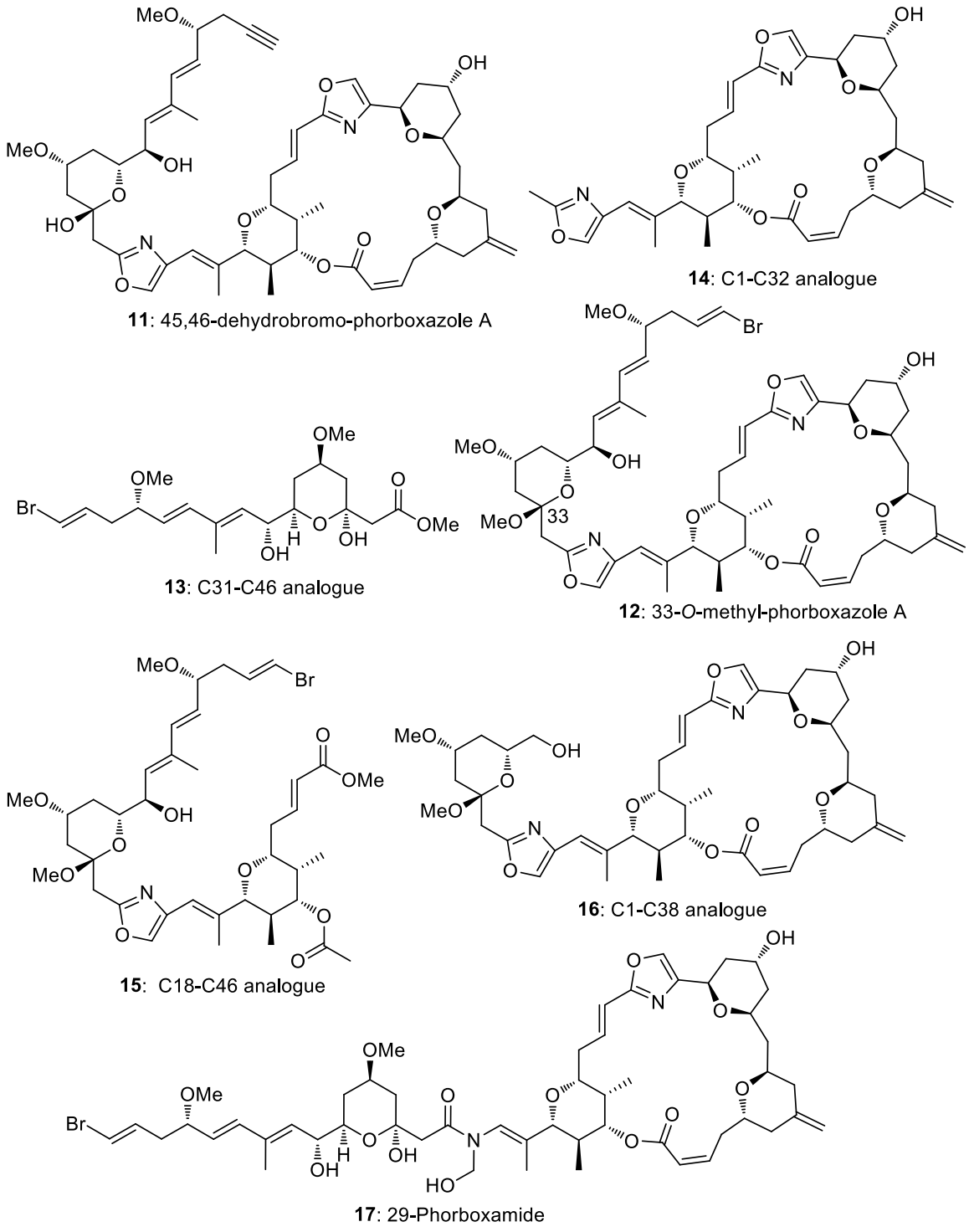

Figure 3: Forsyth's synthetic analogues of (+)-phoroboxazole A[17]

Several other phorboxazole analogues have since been prepared by Smith III's group (Figure 4).[18] It was found that the 46-chlorophorboxazole **18** possessed improved cytotoxicity in the picomolar range. To simplify the synthesis of these compounds, the C11-C15 tetrahydropyran ring was replaced with an acetal to give analogue **19**, which

retained most of the biological activity. Combination of these two modifications gave compound **20** with a similar activity to phorboxazoles. Interestingly, the methylation at C33 caused a drastic decrease in the biological activity. It appears that with the removal of the alcohol in the C11-C15 ring, at least one of the remaining two hydrogen bond donors has become much more important. In the same study the results from compounds with a truncated tail indicates that the *Z* geometry of the C2-C3 double bond is also crucial for cytotoxicity.

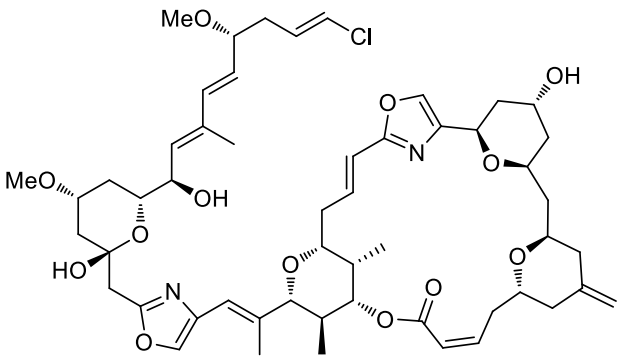

18
GI_{50} 0.38 nM (KM20L2, colon)

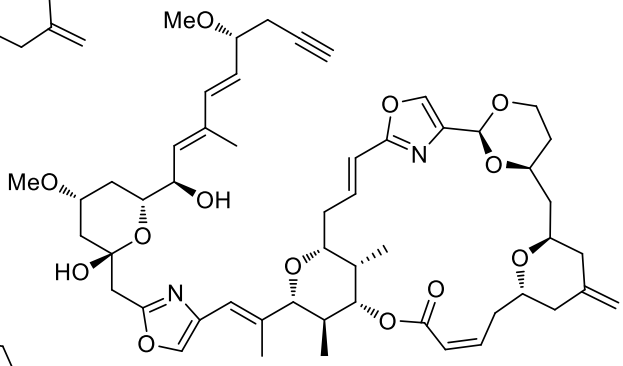

19
GI_{50} 11.8 nM (KM20L2, colon)

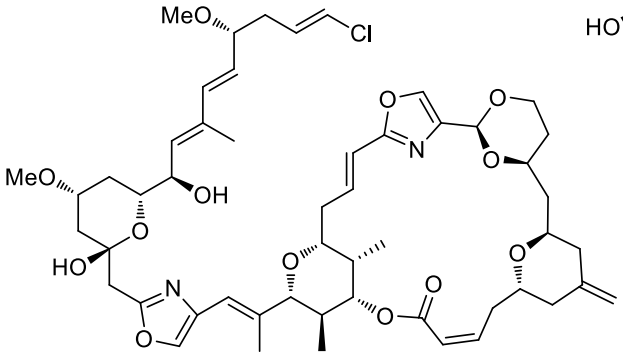

20
GI_{50} 2.33 nM (HCT-116, colon)

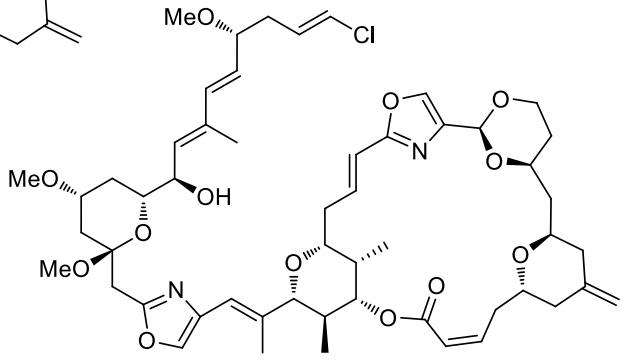

21
GI_{50} 94.5 nM (HCT-116, colon)

Figure 4: Smith's synthetic analogues of phorboxazole A[18]

The mechanism of the biological activity of this class of natural products has not been studied extensively because of the low quantities available of this natural product. However, it has been found that phorboxazoles arrest the cell cycle at the S-phase and do not affect tubulin. The studies by Forsyth have also shown that fluorescently labelled phorboxazole analogues promote the association of cyclin-dependent kinase 4 (cdk4) with intermediate filaments of the cytoskeleton.[19] This kinase is a crucial part of the signalling pathway that lets the cell proceed through G1/S phase. It is often altered in melanomas, glioblastomas, breast and cervical cancers and has been extensively studied as an anticancer drug target.[20] Phorboxazole induced sequesteration of this kinase upon cytoskeleton probably disrupts its function and inhibits the cell growth. This represents a unique mode of activity and more studies in this area are needed and investigation of *in vivo* activity and protein cocrystallisation studies would be particularly welcome. Unfortunately this requires orders of magnitude larger amounts of this compound than is available from natural sources and therefore presents a challenge to synthetic chemists.

7.3 Previous syntheses of the C20-C32 fragment

The unique structural features and the astonishing biological activity combined with the limited amounts available from nature have all made the phorboxazoles very attractive targets for total synthesis. It is therefore not surprising that to date eight total syntheses of phorboxazole A[16,21-27] and three of phorboxazole B have been published. [28-30] In addition to full synthesis, several synthetic studies of the various fragments have also been published.[30-33]

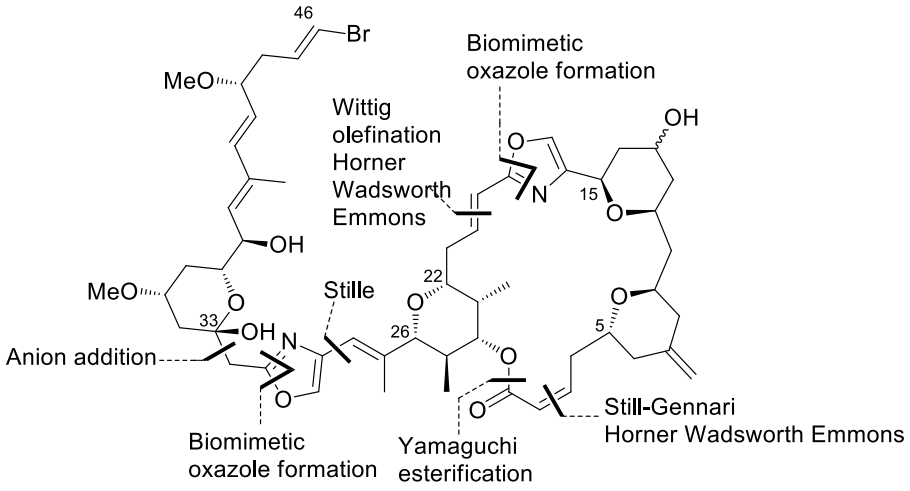

Figure 5: Examples of disconnections used to split the molecule into more simple components.

Most of the molecules stereocentres are in the THP rings. The common strategy in the synthesis of phorboxazoles has been to disconnect the molecule in three fragments of comparable complexity - the C1-C19 *bis*-pyran unit, C20-C32 core fragment and the C33-C46 tail fragment (Figure 5). This allows chemists to synthesize the THP rings separately and then join the fragments together using known coupling procedures. The tail fragment has been attached *via* anion addition to a lactone, a Stille coupling or a biomimetic oxazole formation. The core fragment and the *bis*-pyran unit is joined step-wise, with the northern connection made by either Wittig olefination, Horner-Wadsworth-Emmons olefination or biomimetic oxazole formation. The southern connection is generally made by either Yamaguchi macrolactonization or by Still-Genari or Horner-Wadsworth-Emmons olefination.

A diverse range of chemistry has been used to synthesize the C20-C32 core fragment, which contains five of the molecule's fifteen stereogenic centres. The key step in all of the syntheses is the formation of the tetrahydropyran ring.

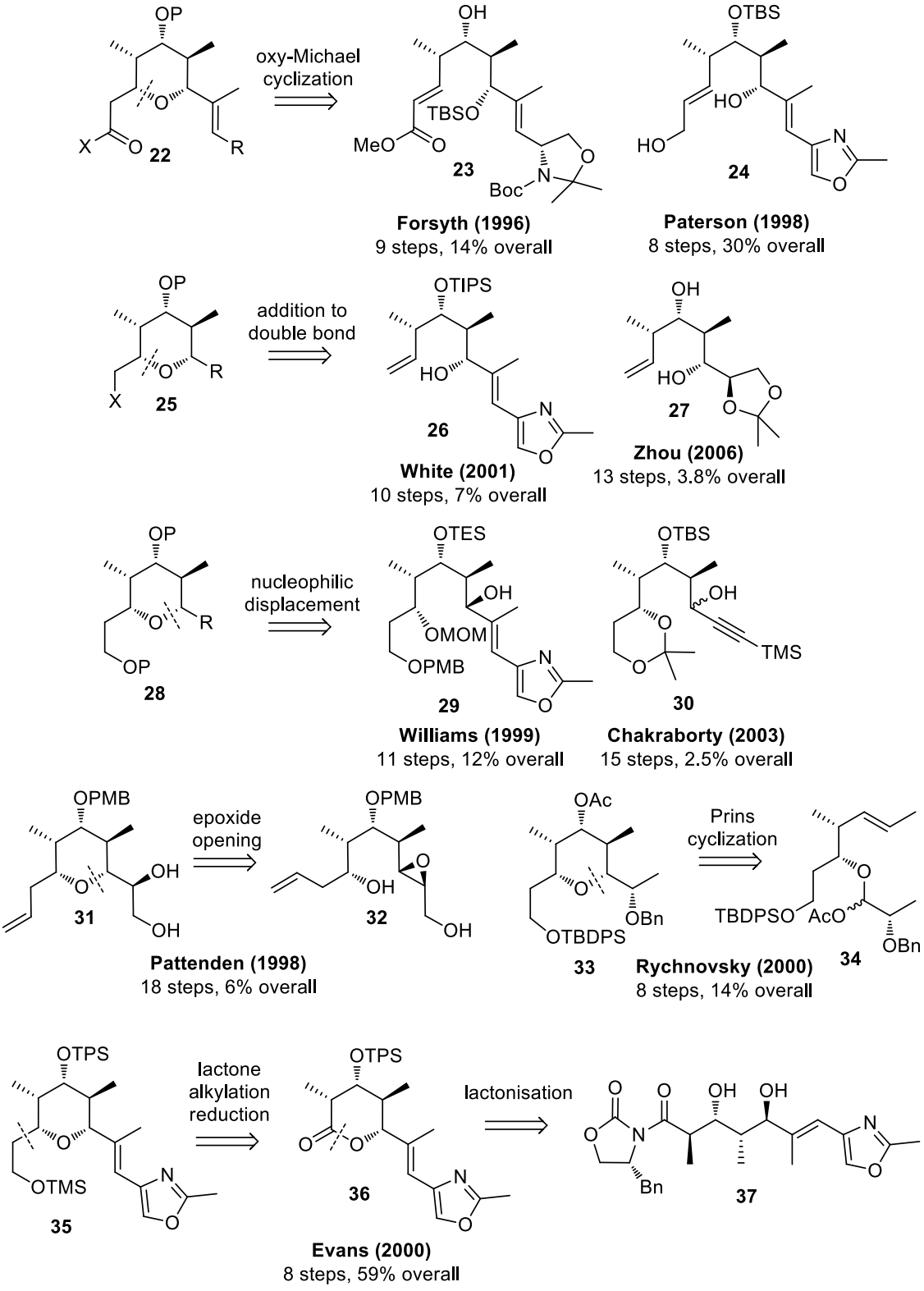

Figure 6: Linear approaches to the C20-C32 fragment

The most popular strategy for installation of the stereocentres has been the synthesis of enantiomerically enriched linear precursors prior to cyclisation (Figure 6). Forsyth and Paterson both chose to use variations of oxy-Michael reaction to close the

ring, while White and Zhou chose additions to a terminal alkene as the ring closing step. Nucleophilic intramolecular displacement of an alcohol was used by both Williams and Chakraborty. Pattenden opted for an epoxide opening, while Rychnovsky made use of an intramolecular Prins cyclisation. Finally, Evans used a stepwise strategy of first forming a lactone and then elaborated the molecule by an alkylation and reduction.

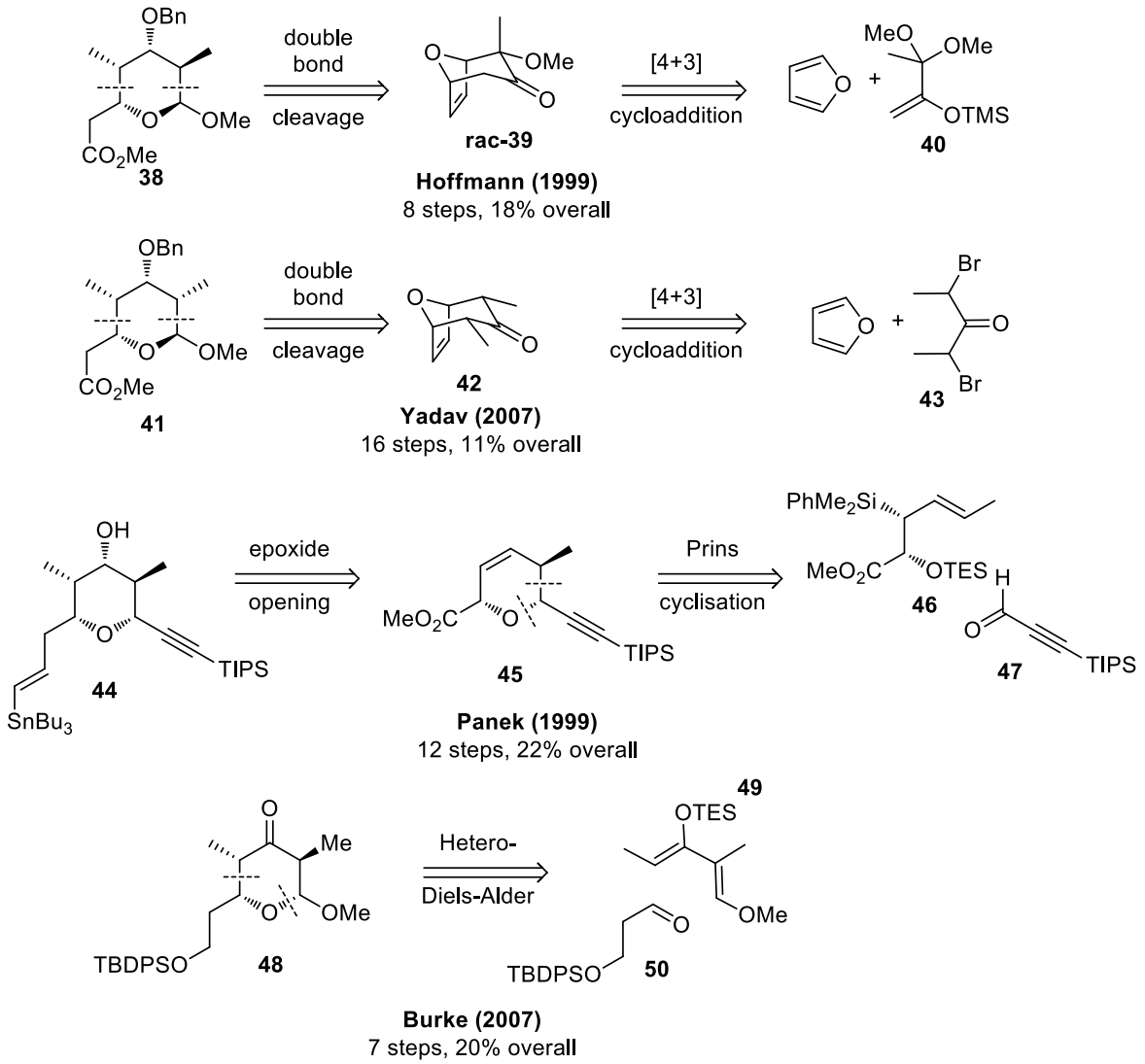

Figure 7: Cycloaddition approaches to the C20-C32 fragment

The rest of the syntheses can be broadly called as cycloaddition approaches (Figure 7). Hoffman and Yadav chose fairly similar strategies of achieving the tetrahydropyran ring *via* a cleavage of a bicyclic intermediates **rac-39** and **42** which in turn were formed in a [4+3] cycloadditions. Panek used an intermolecular Prins cyclization to

form the dihydropyran **45** which was further elaborated to the final product. Finally, Burke rapidly formed the core fragment *via* an enantioselective hetero-Diels-Alder reaction.

In total, thirteen research groups have achieved the synthesis of this fragment. The syntheses range from seven to eighteen steps in length and from 2.5 to 59 percent in overall yield. These studies will now be discussed in more detail.

The first synthesis of the core fragment was published by Forsyth and co-workers.[31] The precursor **54** was synthesized from the previously synthesized compound **51** (Scheme 2). This was achieved by diastereoselective (*E*)-enol borinate aldol reaction with the unsaturated aldehyde **52**, which gave compound **53** with three of the five stereocentres installed. The final stereogenic centre in the precursor was installed using Evans-Saksena β-hydroxy directed ketone reduction methodology.

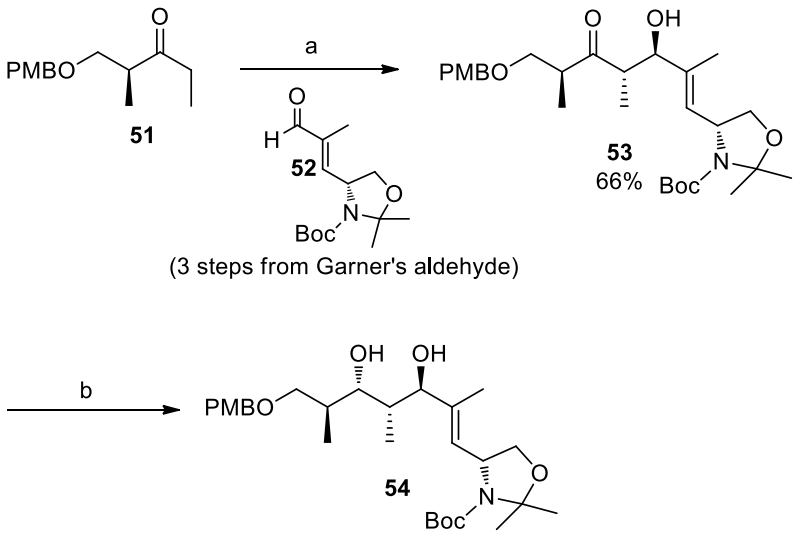

Reagents and conditions: a) i) Cy_2BCl, Et_3N ii) **52** b) $Me_4NBH(OAc)_3$, 89%

Scheme 2: Forsyth's assembly of enantiomerically enriched acyclic precursor **54**

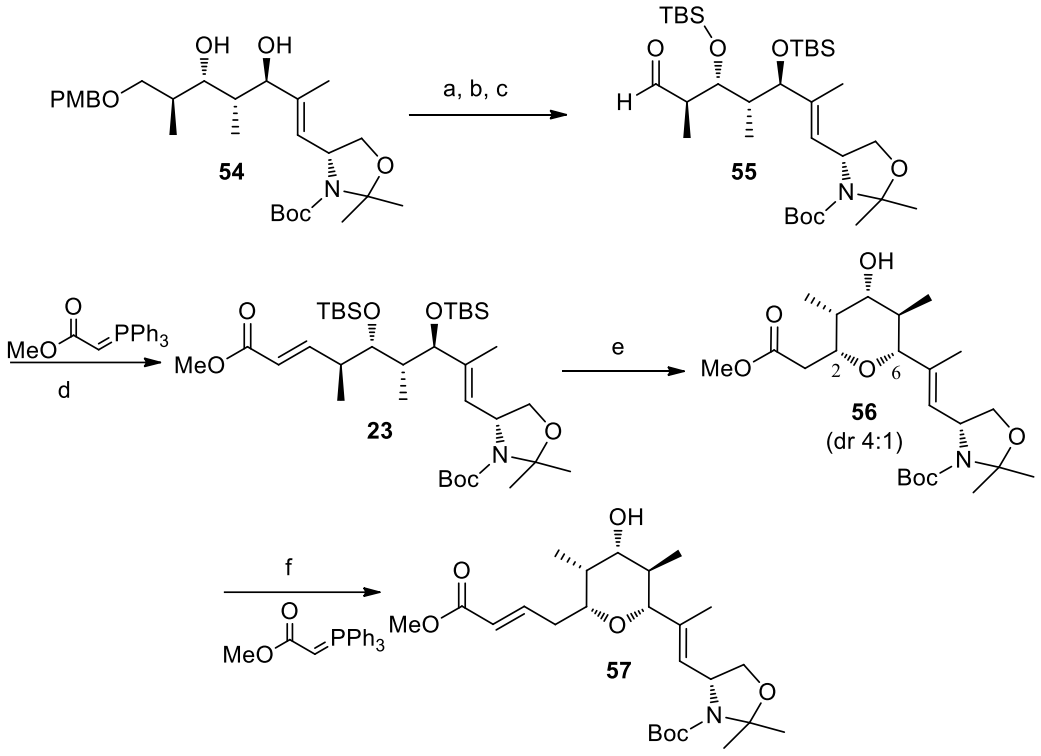

Reagents and conditions: a) TBSOTf, Et_3N b) DDQ c) DMP, 77% over 3 steps d) Methyl (triphenylphosphoranylidene)acetate, 96% e) TBAF, THF, 46% 72h f) i) DIBAL ii) Methyl (triphenylphosphoranylidene)acetate, 70%

Scheme 3: Intramolecular hetero-Michael cyclisation to form 2,6-*cis* THP **57**

Protection of the diol **54**, followed by PMB removal, oxidation and Wittig reaction gave the ester **23** (Scheme 3). Deprotection with TBAF effected the oxy-Michael reaction and formed the tetrahydropyran ring in only 46% yield as 4:1 mixture of diastereomers. Finally, reduction of the ester and another Wittig reaction gave the final core fragment **57** in nine steps from a previously known compound and 14% overall yield.

A similar approach to the core fragment was reported in a synthetic study published by Pattenden and co-workers in 1998.[32] Commercially available starting material **58** was converted into aldehyde **59** through protection of the alcohol, reduction of the ester and reoxidation to the aldehyde (Scheme 4). Diastereoselective addition of crotylborane **60** gave compound **61** in good yield and formed two stereogenic centres in one step. This was subjected to a further five steps to afford the aldehyde **62**.

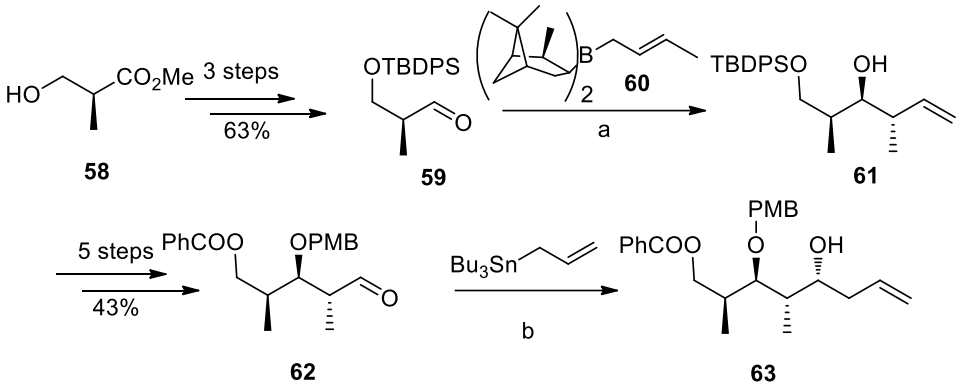

Reagents and conditions: a) **60**, Et_3N, H_2O_2, 76% b) allyltributyltin, $BF{\cdot}OEt_2$, 94%, dr: 98:2

Scheme 4: Pattenden's synthesis of the enantiomerically enriched acyclic precursor **63**

Felkin-Anh controlled addition of allyltributyltin resulted in formation of **63** with excellent yield and diastereoselectivity. A further five steps transformed the alkene **63** in **64** (Scheme 5). Sharpless asymmetric epoxidation formed **65** and furnished the final stereocentre in excellent yield and diastereoselectivity prior to cyclisation. Fluoride promoted the removal of the TES protecting group from the hydroxyl and titanium isopropoxide effected the intramolecular epoxide opening to give THP **31**. This is the longest published synthesis of the core fragment and took 18 steps and gave **31** in 6% overall yield.

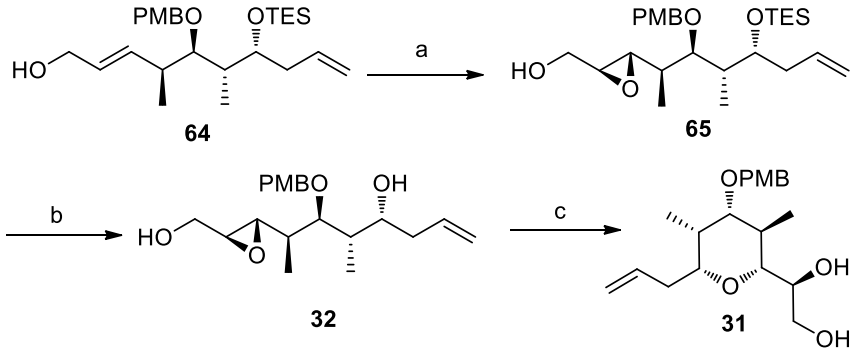

Reagents and conditions: a) (+)-DET, Ti(O*i*-Pr)$_4$, TBHP, 95% b) TBAF, 94% c) Ti(O*i*-Pr)$_4$, 76%

Scheme 5: Intramolecular epoxide opening

Although Paterson and co-workers have not published a synthesis of phorboxazoles, a synthetic study of the C20-C32 core fragment was reported in 1998.[33]

This synthesis is another example of the use of an asymmetric aldol reaction to install the stereochemistry of the core fragment (Scheme 6).

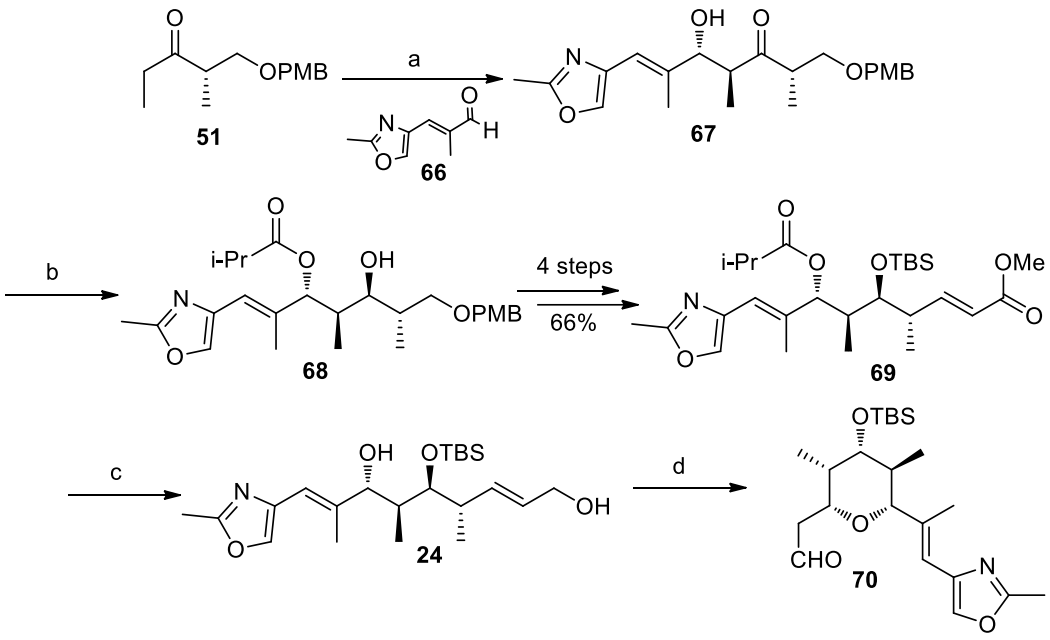

Reagents and conditions: a) i) Cy_2BOTf, $EtNMe_2$ ii) **66**, 94% b) *i*-PrCHO, SmI_2, 86% c) DIBAL, 86% d) $SO_3 \cdot py$, DMSO, Et_3N, 81%, dr 4:1

Scheme 6: Paterson's use of an intramolecular hetero-Michael addition

The synthesis starts with a chiral ketone **51** which is converted into β-hydroxyketone **67** in excellent yield and diastereoselectivity through an *anti*-selective boron-enolate aldol reaction with a known aldehyde **66**. Next, a modified Evans-Tischenko reduction of the ketone revealed the 1,3-*anti* reduction product **68**. A further four steps were necessary to synthesize the α,β-unsaturated ester **69**, which upon reduction gave the alcohol **24**. Subsequent Parikh-Doering oxidation revealed the aldehyde which immediately underwent cyclisation to form the core fragment **70** in good yield and moderate diastereoselectivity. The synthesis is only eight steps long with 30% overall yield from **51**.

Another synthetic study was reported by Williams and co-workers in 1999.[34] In this study Evans' oxazolidinone auxiliaries **71** and *ent*-**71** were used in successive

asymmetric aldol reactions to set up the four stereocentres and give the precursor **75** in only five steps. Thus, the *Z*-enolate of **71** reacted with aldehyde **72** to give the *syn* product **73** in 96% yield (Scheme 7). Protection of the alcohol, cleavage of the auxiliary and oxidation yielded the aldehyde **74**. Another *syn* selective aldol reaction using *ent*-**71** formed **75** in 83% yield over 2 steps.

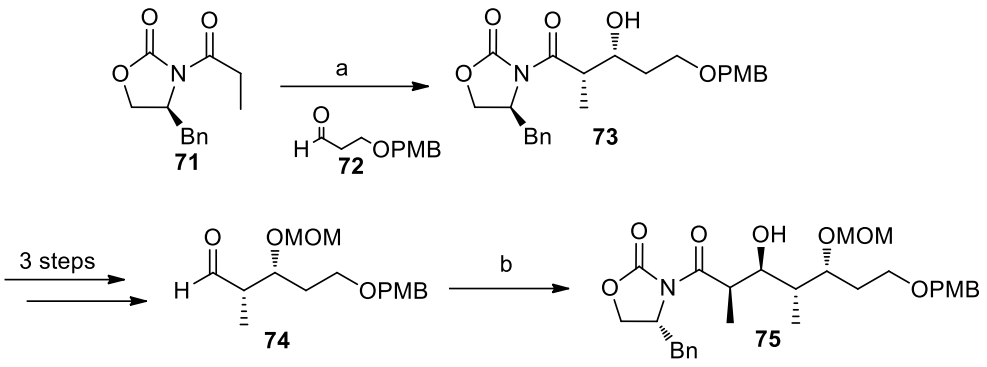

Reagents and conditions: a) i) Bu_2BOTf, Et_3N ii) **72**, 96% b) *ent*-**71**, Et_3N, Bu_2BOTf, 83%

Scheme 7: Williams' use of consecutive asymmetric aldols

Protection of the alcohol **75** and the cleavage of the auxiliary with BnOLi formed the benzyl ester. Claisen condensation of the ester with ethyl diethylphosphonate gave **76** in good yield (Scheme 8). Horner-Emmons condensation with aldehyde **77** and subsequential Luche reduction gave the cyclisation precursor **29**. In the presence of triflic anhydride and pyridine this formed a single tetrahydropyran product **79** *via* the proposed transition state **78**, however in only 40% yield. Overall, Williams' route to this fragment was eleven steps long with most steps proceeding in good yield with the exception of the cyclisation resulting in 12% overall yield.

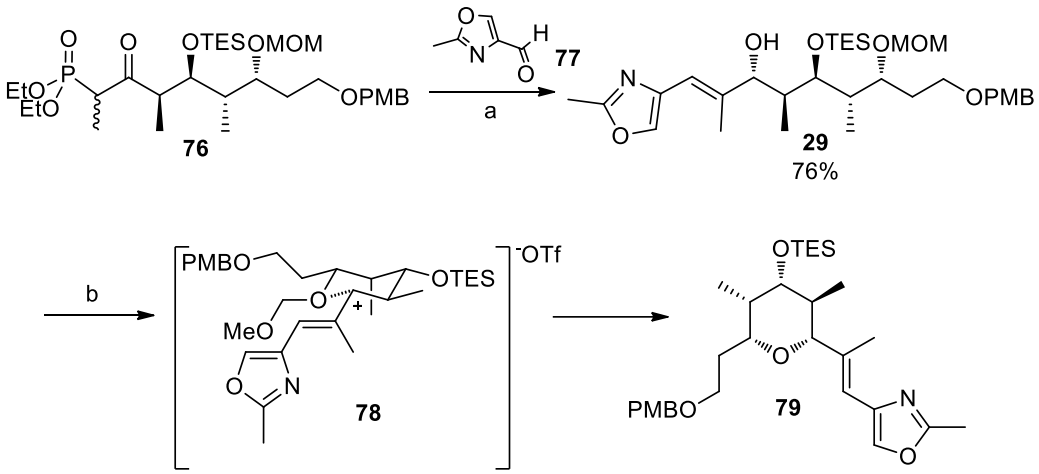

Reagents and conditions: a) i) NaH, **77** ii) $NaBH_4$, $CeCl_3 \cdot 7H_2O$, 76% b) Tf_2O, pyridine, 40%

Scheme 8: Cyclisation via allyl cation formation

Evans and co-workers reported a total synthesis of (+)-phorboxazole B (**10**) in 2000.[28] The approach to the core fragment started with an *anti*-selective aldol reaction between (*E*)-boron enolate of **80** and aldehyde **66** which yielded **81** in 97% yield and excellent diastereoselectivity (Scheme 9). This was diastereoselectively reduced using hydroxyl directed borohydride reduction which gave 1,3-*anti* diol **37** as a single diastereomer and in 87% yield. From this a lactone was formed in a base catalyzed cyclisation which also served to remove the auxiliary. Subsequential TPS protection gave the lactone **36**.

Hemiketal **82** was formed in a reaction between the lactone **36** and the anion of *t*-butyl acetate (Scheme 10). When treated with triethylsilane and Lewis acid, the hemiketal **82** was reduced to the tetrahydropyran **84**. In this transformation the Lewis acid allows the formation of the oxocarbenium anion **83** which was then diastereoselectively reduced by a pseudoaxial delivery of the hydride anion. This reaction proceeded in high yield and with excellent diastereoselectivity.

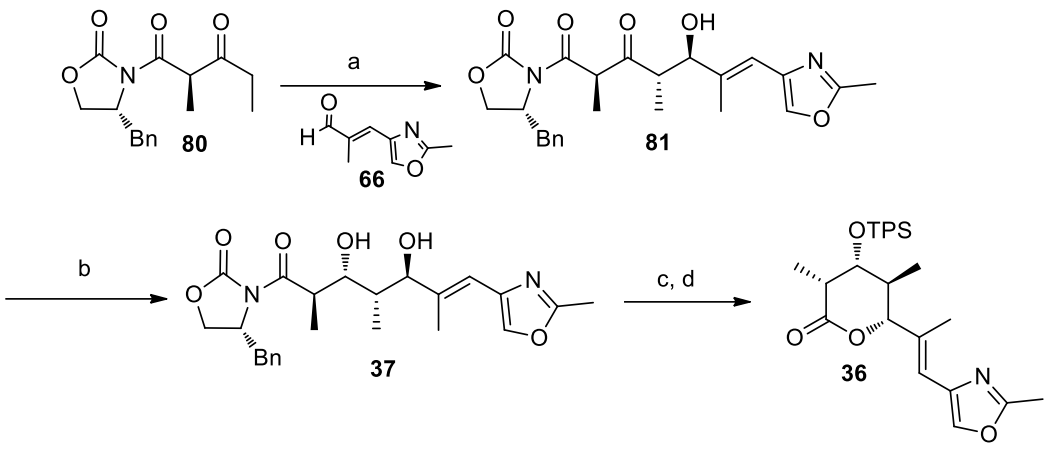

Reagents and conditions: a) i) Cy_2BOTf, $EtNMe_2$ ii) **66**, 97%, dr 94:6 b) $Me_4NBH(OAc)_3$, 87% c) DBU d) TPSCl, imidazole, 81% over 2 steps

Scheme 9: Evans' route to the penta-substituted THP core *via* lactone **36**

The final core fragment was furnished in a reduction of the *t*-butyl ester to the alcohol and protection of the resulting alcohol. Overall, Evans' synthesis of the C20-C32 fragment is a remarkable example of stereoselective synthesis as it produced the core fragment in only eight steps in an impressive overall yield of 59%.

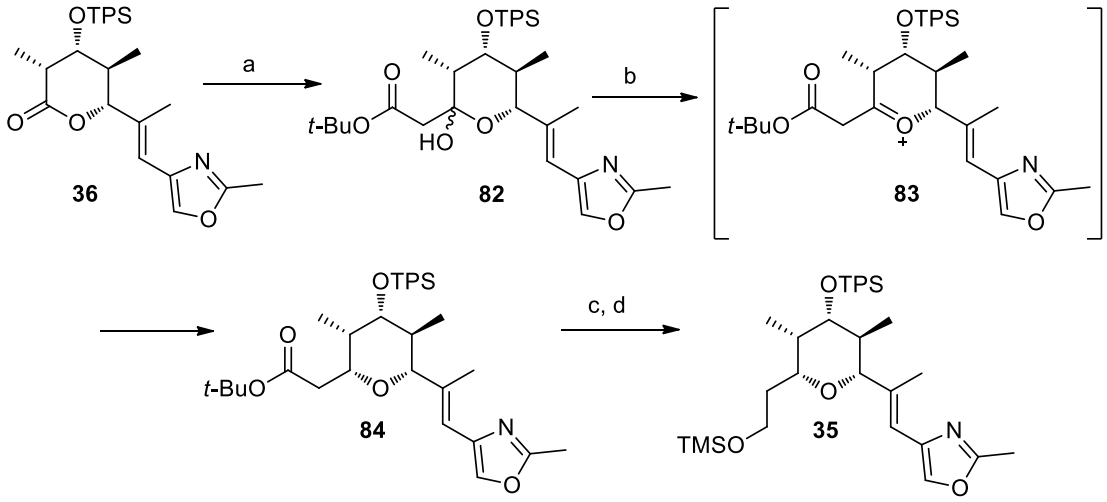

Reagents and conditions: a) *t*-butyl acetate, LDA b) Et_3SiH, $BF_3{\cdot}OEt_2$, 91% over 2 steps, dr >20:1 c) $LiAlH_4$ d) TMSCl, DMAP, imidazole, 95% over 2 steps

Scheme 10: Diastereoselective reduction of of hemiketal **82**

In a synthetic study published in 2001, White employs successive asymmetric crotylations to install the required stereochemistry of the C20-C32 fragment.[35] The synthesis starts with a crotylation of known aldehyde **66**, which yields **85** in 67% yield and

with excellent diastereoselectivity (Scheme 11). Hydroxyl protection, dihydroxylation of the alkene and diol cleavage gave the aldehyde **87**. Then in another crotylation reaction two more stereogenic centres were successfully installed, yielding **88** in only 53% yield as a 6:1 mixture of diastereomers.

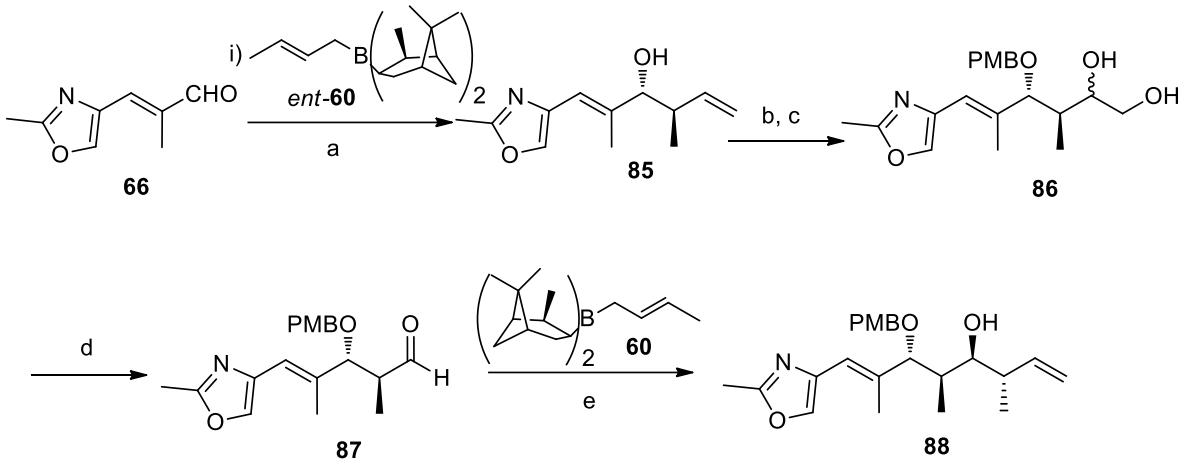

Reagents and conditions: a) i) *ent*-**60** ii) $NaHCO_3$, H_2O_2, 67%, dr >96:4, er >96:4 b) NaH, PMBCl, *n*-Bu_4NI c) OsO_4, NMO, THF, H_2O, 75% over 2 steps d) $NaIO_4$, 98%
e) **60**, ethanolamine, MeOH, 53%, dr 6:1

Scheme 11: White's use of iterative asymmetric crotyl additions

Protection of the alcohol followed by mild PMB removal gave the cyclisation precursor **26** (Scheme 12). The tetrahydropyran ring was then formed as a single diastereomer by a palladium catalyzed intramolecular alkoxycarbonylation reaction in presence of methanol under carbon monoxide atmosphere. This methodology had previously been developed in White's group and usually requires an equivalent of the palladium catalyst. On this occasion, however, acetonitrile cosolvent was found to be necessary and this caused the deactivation of the palladium catalyst. As a result, three equivalents of the catalyst were required for the reaction to go to completion. Nevertheless, the reaction gave 86% yield, which is the highest yield in a cyclization reaction reported in any of the syntheses of the core fragment to date. In a more recent study the amount of palladium catalyst has been reduced to 10 mol% while retaining the yield of the reaction *ca* 60%. This was accomplished by switching from palladium(II) acetate to palladium(II)

chloride and addition of *p*-benzoquinone oxidant.[27] Reduction of the ester and Dess-Martin oxidation of the resulting alcohol furnished the core fragment as aldehyde **90**. This route was ten steps long with the overall yield of 7%.

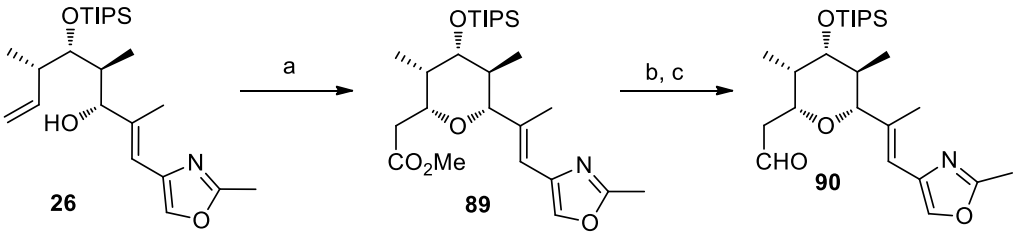

Reagents and conditions: a) $Pd(OAc)_2$, CO, MeOH, MeCN, 86% b) $LiAlH_4$
c) DMP, 67% over 2 steps

Scheme 12: Pd(II)-mediated cyclisation to the C20 – C32 THP

Zhou and co-workers reported a similar approach to White's in a synthetic study published in 2006.[29] Like White, they chose to use successive crotylations to set up the stereocentres in the cyclisation precursor and then form the tetrahydropyran ring *via* hydroxyl attack on an activated alkene (Scheme 13).

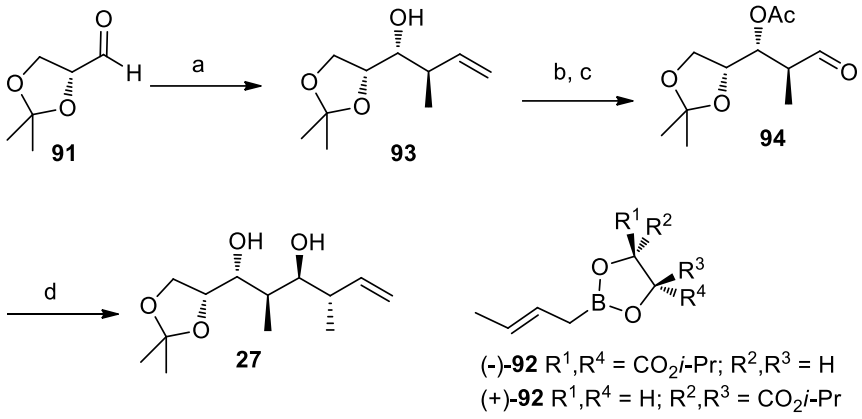

Reagents and conditions: a) (+)-**92**, 65% b) Ac_2O, Et_3N, DMAP c) O_3, 81% over 2 steps
d) (-)-**92**, 70%

Scheme 13: Zhou's use of iterative asymmetric crotyl additions

Thus, starting with chiral aldehyde **91**, they first formed two stereocentres in a crotylation reaction, using chiral boronate (+)-**92**. This gave **93** in 65% yield. The hydroxyl was then acetylated and the double bond transformed into the aldehyde **94** *via* ozonolysis.

The second crotylation was then performed, using the chiral boronate (-)-**92**, which gave the diol **27** in good yield. When treated with mercury(II) acetate and iodine, the diol **27** cyclized to form the tetrahydropyran **95** in 86% yield (Scheme 14). The free hydroxyl was protected with PMB group, S_N2 displacement of the iodine with cyanide formed a nitrile, which was then reduced to an alcohol. Protection of the alcohol formed compound **96**. Periodate cleavage of the protected diol revealed the aldehyde and subsequent methyllithium addition and Dess-Martin oxidation yielded ketone **97**. Finally, an (*E*)-selective Horner-Wadsworth-Emmons olefination was performed to give the C20-C32 core fragment **99**. Overall the route took 13 steps to form the fragment in 3.8% yield.

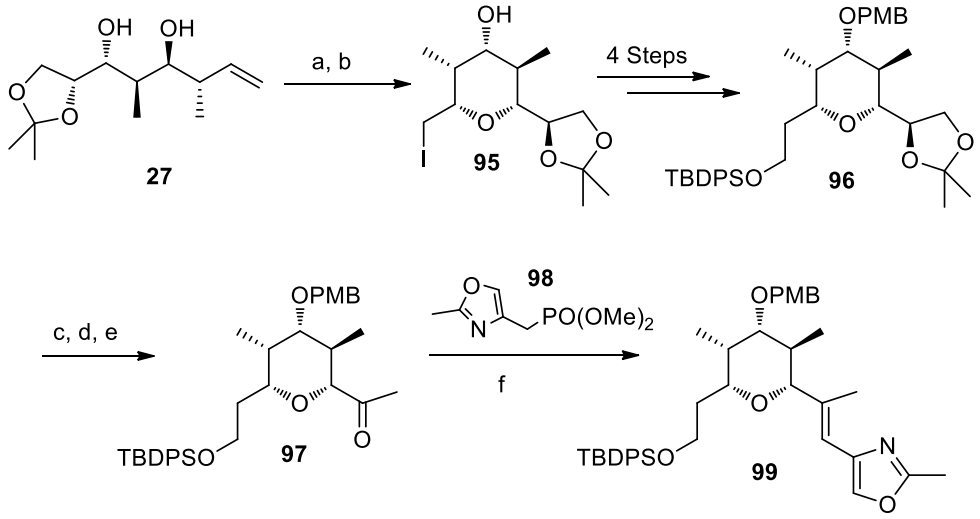

Reagents and conditions: a) $Hg(OAc)_2$ b) I_2, 86% over 2 steps c) HIO_4 d) MeLi e) DMP, 58% over 3 steps f) LDA, **98**, 78%

Scheme 14: Hg(II) promoted cyclisation to the C20 – C32 THP core.

An innovative synthesis of the C20-C32 fragment of the phorboxazoles was reported by Smith and co-workers in 1999.[36] In this synthesis the tetrahydropyran ring along with one of the stereogenic centres is formed in a Petasis-Ferrier rearrangement of a dioxanone. The synthesis makes use of an aldol reaction between Evans' oxazolidinone auxiliary derived boron enolate of **71** and aldehyde **100** to install the first two stereogenic centres (Scheme 15). The auxiliary is then cleaved using lithium hydrogen peroxide to

yield the acid **101**. *Bis*-silylation and subsequential TMSOTf-promoted condensation with aldehyde **102** yielded dioxanone **103**. This was transformed into the sulfone **104** in four steps.

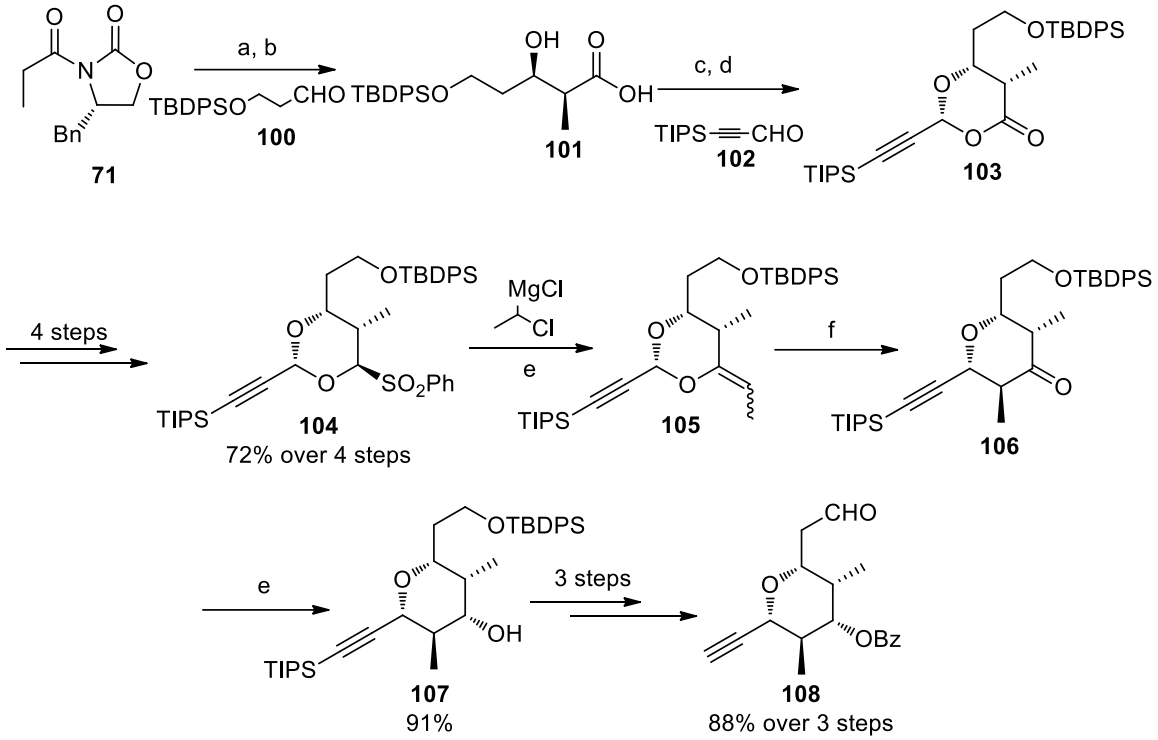

Reagents and conditions: a) Et_3N, *n*-Bu_2BOTf, **100** b) LiOOH, 84% over 2 steps c) HMDS d) TMSOTf, **102**, 66% e) *n*-BuLi, chloroethylmagnesium chloride, 95%, *E*:*Z* 1:1 f) Me_2AlCl, 90% e) $NaBH_4$, 91%

Scheme 15: Smith's synthetic study towards the core THP unit

Julia olefination was then used to install a double bond and form **105** as 1:1 mixture of stereoisomers. Fortunately, it was found that when subjected to Petasis-Ferrier rearrangement conditions, only the desired diastereomer **106** was formed in 90% yield. Diastereoselective reduction of the ketone formed the last stereocentre and gave **107** in 91% yield. Protection of the alcohol, TBDPS removal and oxidation furnished the final C20-C32 fragment **108** in thirteen steps and 20% overall yield. This synthesis was later shortened to only ten steps and it provided multigram quantities of this fragment.[22]

Although Rychnovsky and co-workers have not published a full synthesis of phorboxazole, a synthetic study was reported by their group in 2000.[37] It exploits the Prins

cyclisation methodology developed in the group. The synthesis starts with a coupling reaction between the aldehyde **100** and chiral boronate **109**, which gives alcohol **110** (Scheme 16). From this and chiral acid **111** the ester **112** was formed. The ester was then reduced to hemiacetal with DIBAL and acylated to give **34**. When this was exposed to boron trifluoride diethyletherate and acetic acid, Prins cyclisation was effected and the tetrahydropyran **33** was formed as a single diastereomer.

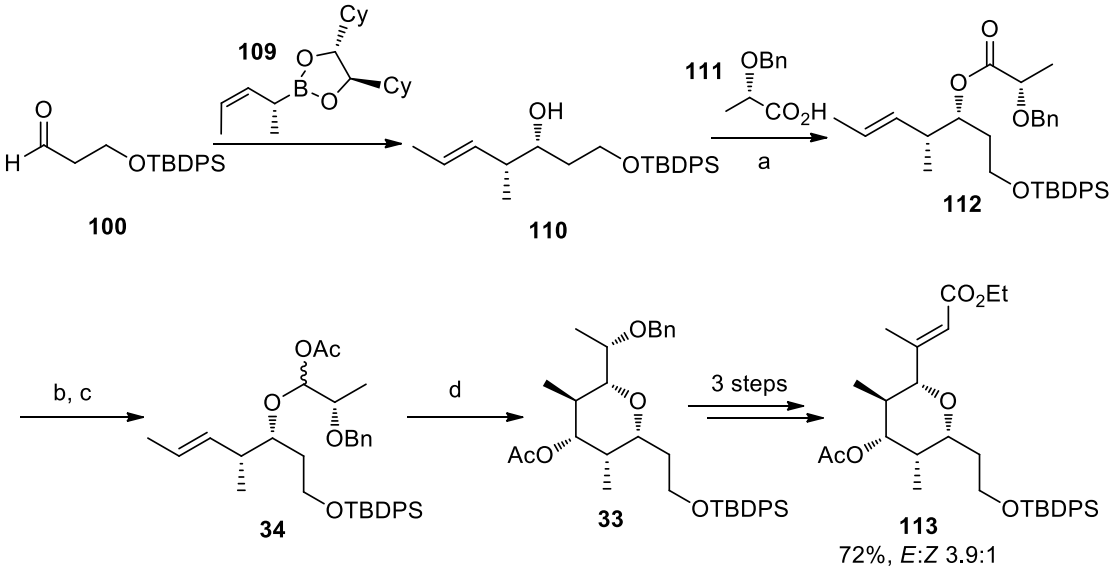

Reagents and conditions: a) **111**, DCC, 53% over 2 steps b) DIBAL c) Ac_2O, pyridine, DMAP, 91% over 2 steps d) $BF_3{\cdot}OEt_2$, AcOH, 52%

Sheme 16: Rychnovsky's use of a Prins cyclisation

Benzyl group removal, oxidation and olefination furnished the C20-C32 fragment **113** in 14% overall yield and only eight steps. However, it is worth noting that this fragment still lacks the oxazole functionality and therefore the length of this synthesis cannot be directly compared to that of others.

An unusual and rapid synthesis of the core fragment was reported by Burke in 2007.[38] It starts with an enantioselective hetero-Diels-Alder reaction between Danishefsky's diene **49** and aldehyde **50** in Jacobsen's conditions to give **48** (Scheme 17).

This reaction formed the tetrahydropyran ring and three of the five stereocentres in the correct configuration in one pot through the silyl enol ether **115**.

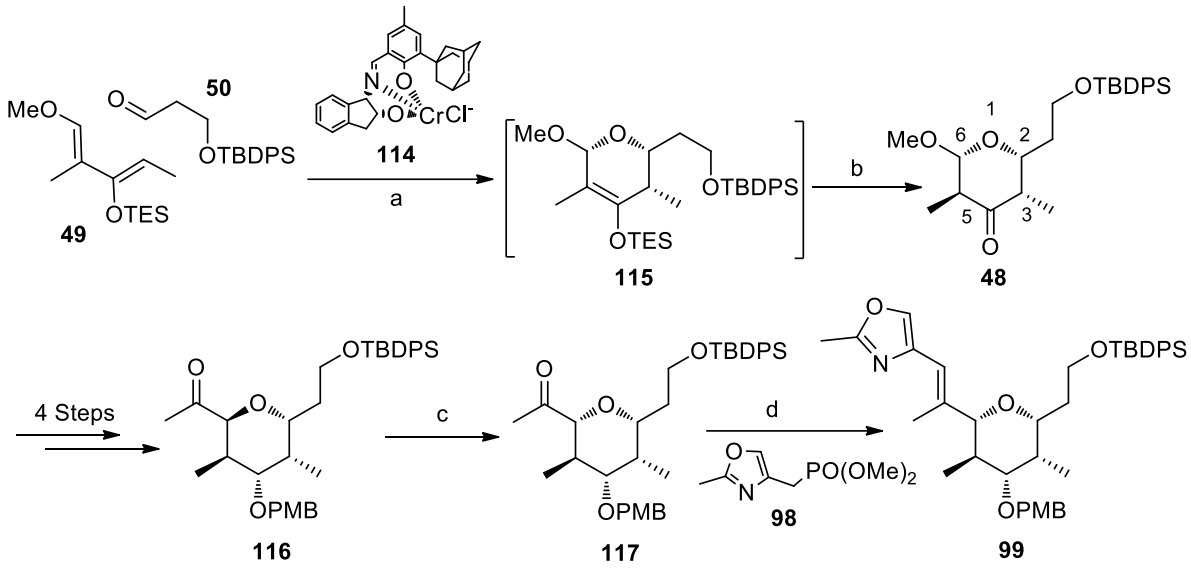

Reagents and conditions: a) 2 mol% **114** b) HF, pyridine, 77%, 91% ee c) KHMDS, LiCl, 91% d) LDA, **98**, 68%

Scheme 17: Burke's rapid construction of the C22-C26 THP

Diastereoselective reduction of the ketone formed alcohol which was then PMB protected. An axial nitrile group was subsequently introduced at C6 which was then converted to the ketone **116** by treatment with trimethylaluminium in the presence of catalytic $Ni(acac)_2$. As the stereocentre at C6 was at the wrong configuration, epimerization was achieved by exposing the ketone to KHMDS to give **117**. Finally olefination with phosphonate ester **98** gave the desired C20-C32 fragment of phorboxazoles. This route is remarkable by its brevity, being only seven steps in length with an overall yield of 20%.

Hoffman and co-workers reported application of their THP forming methodology to the core fragment of phorboxazoles in 1999.[39] They achieved the synthesis of **33** in eight steps from known starting materials (Scheme 18). The route starts with a Lewis acid promoted [4+3] cycloaddition between furan and silyl enol ether **40** to give **rac-39** in 77%

yield and good stereoselectivity (dr 6:1 / MeO_{eq} : MeO_{ax}). Diastereoselective methylation and SmI_2 reduction yielded the *bis*-methylated tetrahydropyran ring with an 3,5-*anti* relationship.

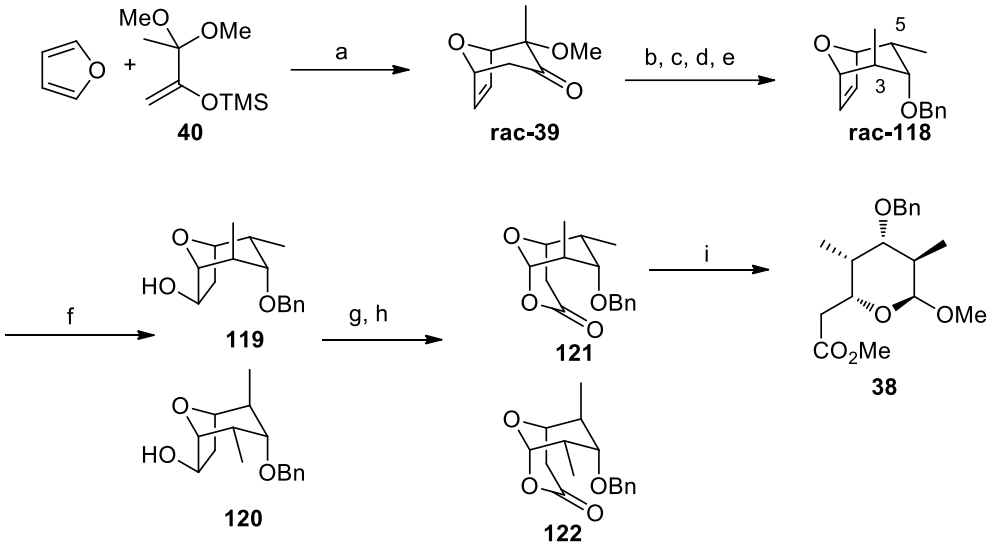

Reagents and conditions: a) TMSOTf b) LDA, TMEDA, MeI, 86% c) SmI_2, Zn, 97% d) DIBAL e) NaH, BnBr, 85% over 2 steps f) $(-)\text{-}(Ipc)_2BH$, NaOH, H_2O_2, 93% g) PCC/SiO_2, DCM h) *m*-CPBA, $NaHCO_3$ 82% over 2 steps i) H_2SO_4, MeOH, 84%

Scheme 18: Hoffmann's [4+3] cycloaddition

Ketone was then reduced and protected to give **rac-118**. Subsequent asymmetric hydroboration yielded alchol as mixture of diastereomers **119** and **120** in 93% yield. Oxidation with PCC and Baeyer-Villiger reaction produced separable mixture of lactones **121** and **122**. Finally, methanolysis of **121** gave **38** in 84%. This route was eight steps long with an overall yield of 18%. However, the final product **38** lacks the oxazole functionality and has the incorrect stereochemistry at C26. Therefore the final fragment requires significant further functionalisation before the length of this route can be directly compared with that of the other routes.

A similar strategy for the synthesis of the core fragment was used by Yadav (Scheme 19).[40] The approach starts with the compound **42** that was synthesized in a [4+3] cycloaddition from furan and 2,4-dibromopentanone **43**.

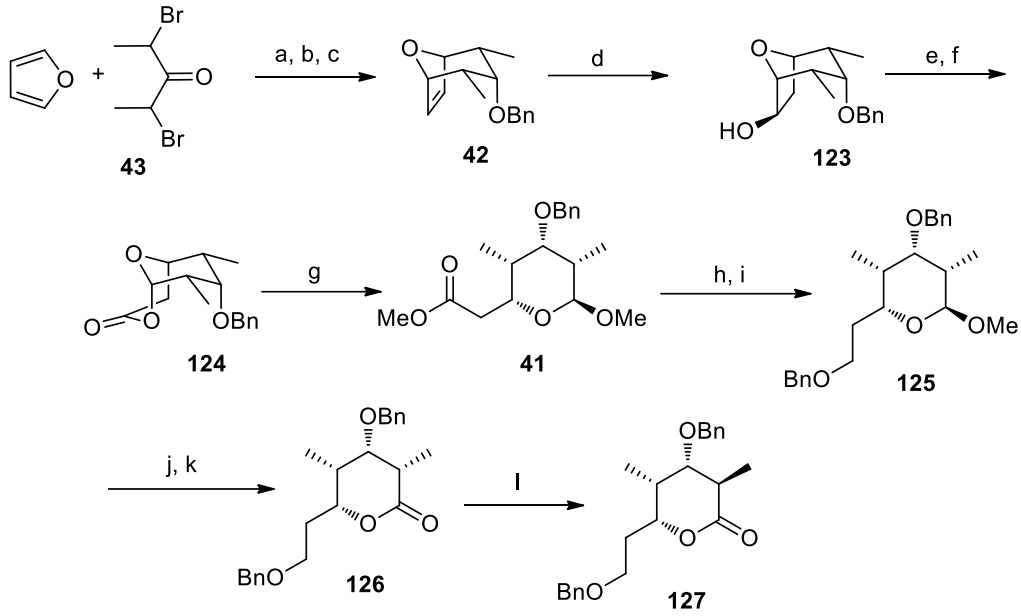

Reagents and conditions: a) Zn, Cu, DME b) DIBAL, THF c) NaH, BnBr, THF, 57% over 3 steps d) (-)-Ipc_2BH, H_2O_2, NaOH, 96% e) PCC, DCM f) *m*-CPBA, $NaHCO_3$, DCM g) H_2SO_4, MeOH 85% over 3 steps h) $LiAlH_4$, THF i) NaH, BnBr, THF, quant. over 2 steps j) AcOH, H_2O k) PCC, NaOAc, 55% over 2 steps l) DBU, THF, 95%

Scheme 19: Yadav's [4+3] cycloaddition

Asymmetric hydroboration, PCC oxidation and Baeyer-Villiger oxidation yielded the bicyclic lactone **124**. This was then hydrolyzed in acidic conditions to give the acetal **41**. Reduction of the ester and protection of the resulting primary alcohol gave compound **125** in quantitative yield. The acetal was then hydrolyzed and oxidized to a lactone **126** in 55% yield over two steps. The α-methyl group was then epimerized by application of base to yield compound **127**. The functionalized tetrahydropyran ring was achieved *via* acetylide addition and hemiketal reduction to give **129** as a single diastereomer (Scheme 20). Finally, *oxy*-mercuration and modified Julia olefination furnished the C20-C32 fragment **132** as 9:1 mixture of *E* and *Z* isomers. This is one of the longest published synthesis of this fragment being 17 steps long with 11% overall yield.

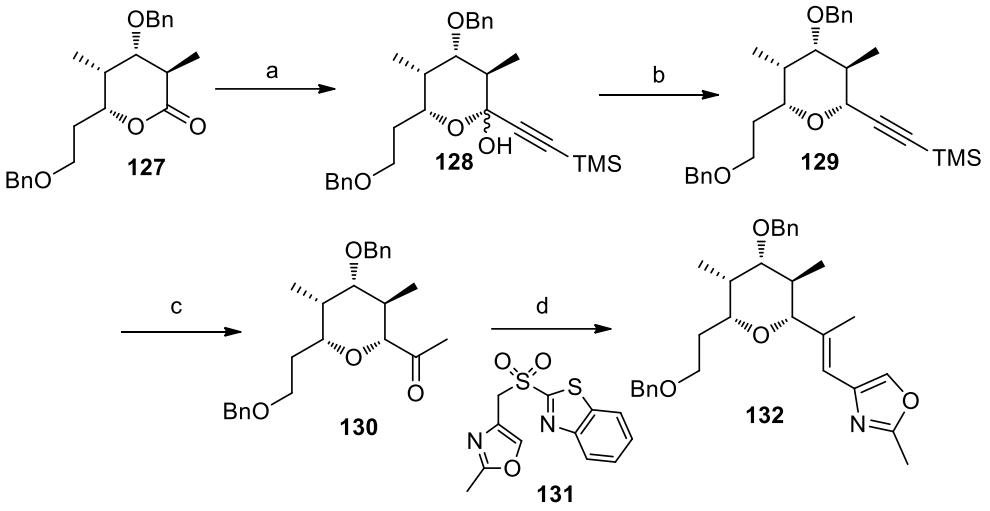

Reagents and conditions: a) *n*-BuLi, TMSCCH, THF, 90% b) Et_3SiH, $BF_3{\cdot}OEt_2$, MeCN, DCM c) HgO, H_2SO_4, acetone, 85% over 2 steps d) NaHMDS, **131**, THF, 70% brsm, 9:1 *E*/*Z*

Scheme 20: Completion of C20-C32 fragment by Yadav

Chakraborty group's approach to the core fragment starts with an aldol reaction between chiral oxazolidinethione derived ester **133** and aldehyde **134** that gives non-Evans *syn* product **135** in 78% yield and as a single diastereomer (Scheme 21).[41] The auxiliary was then removed by $NaBH_4$ reduction and the resulting alcohol was protected as a TBDPS ether **136**. This was followed by an enantioselective epoxidation to produce **137**. The epoxide was then diastereoselectively reduced using titanocene chloride and zinc. Unexpectedly, the major product in this reaction was the β-elimination product **138**. This byproduct was converted in the desired product **139** *via* a regioselective hydrogenation.

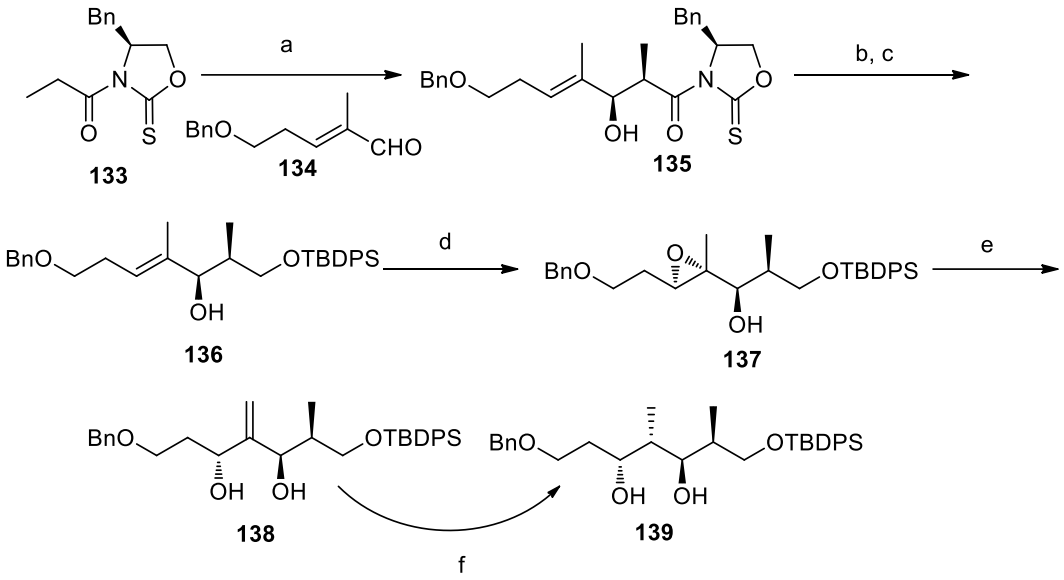

Reagents and conditions: a) **134**, $TiCl_4$, DIPEA, DCM, 78% b) $NaBH_4$, EtOH c) TBDPSCl, Et_3N, DMAP, DCM, 68% over 2 steps d) $Ti(OiPr)_4$, (-)-DIPT, TBHP, DCM, 4Å MS, 81% e) Cp_2TiCl_2, Zn, $ZnCl_2$, THF f) H_2, Pd/C, NH_4OAc, MeOH, 65% over 2 steps

Scheme 21: Chakraborty's synthesis of the stereotetrad

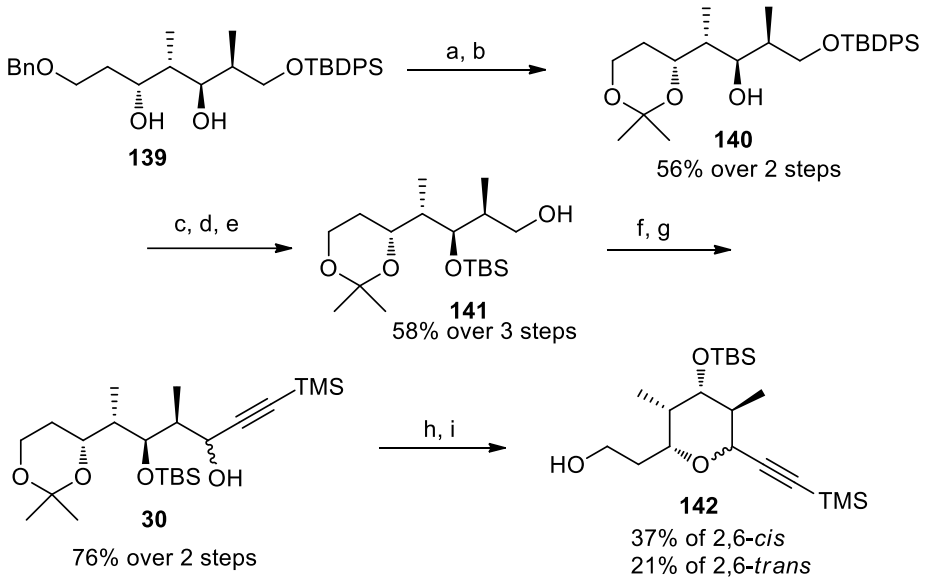

Reagents and conditions: a) H_2, Pd/C, MeOH b) 2,2-dimethoxypropane, CSA, DCM, 56% over 2 steps c) TBAF, THF d) TBSOTf, 2,6-lutidine, DCM e) HF·py, THF, 58% over 3 steps f) SO_3·py, Et_3N, DMSO, DCM g) TMSCCH, *n*-BuLi, 76% over 2 steps h) MsCl, DMAP, py i) CSA, DCM

Scheme 22: Completion of the C20-C32 core fragment by Chakraborty

Five more steps of protecting group manipulation gave the primary alcohol **141** (Scheme 22). It was oxidized to an aldehyde and treated with lithium trimethylsilylacetylide to give alkynol **30** as a mixture of diastereomers. Mesylation and

acid-mediated acetonide removal resulted in a spontaneous ring closure to give C20-C28 core fragment **142** in 37% yield and its 2,6-*trans* diastereomer in 21% yield. Overall, this route was 15 steps long with an overall yield of only 2.5%.

A different strategy was published by Panek and coworkers in 2001 (Scheme 23).[42] It starts with a Lewis acid catalyzed formal [4+2] Prins-type annulation between aldehyde **47** and protected hydroxyalkene **46** and gives the dihydropyran **45** in good yield. This was then then transformed into the epoxide **143**, again in a good yield and diastereoselectivity.

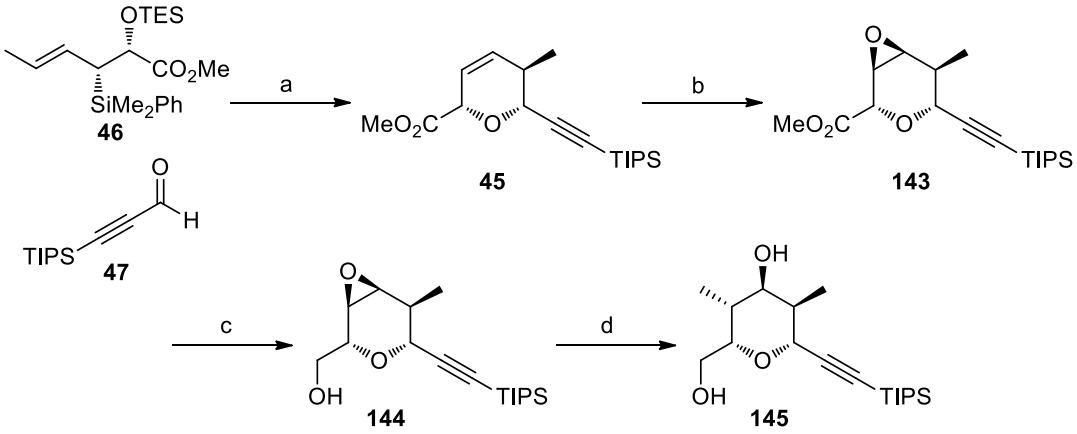

Reagents and conditions: a) TMSOTf, DCM, 65% b) *m*-CPBA, CCl_4, 85%, dr 13:1 c) $LiAlH_4$, THF, 92% d) CH_3MgBr, CuI, THF, 90%

Scheme 23: Panek's synthesis of the tetrahydropyran ring

The ester was reduced to the alcohol and the epoxide was opened with methylmagnesium bromide to give the pentasubstituted core **145**. The primary alcohol was then transformed into an alkyne **146** *via* a triflation and S_N2 displacement (Scheme 24). The configuration of the alcohol on the THP ring was inverted by first oxidising it to a ketone and then reducing with $LiAlH_4$. Finally, bromination of the alkyne and palladium catalyzed hydrostannation furnished the C19-C28 fragment **44** in 12 steps and 12% overall yield.

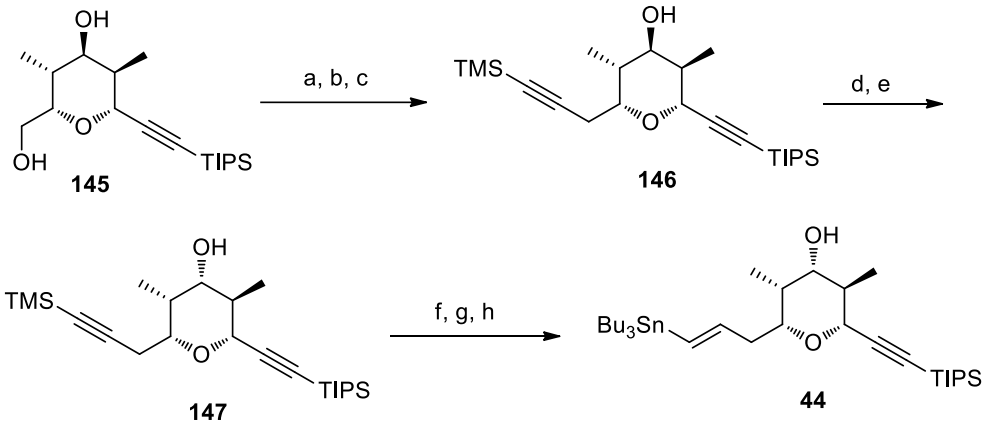

Reagents and conditions: a) Tf_2O, py, DCM b) TMSOTf, 2,6-lutidine c) LDA, THF, TMSCCH, HMPA, 80% over 3 steps d) DMP, DCM e) $LiAlH_4$, THF, 86% over 2 steps, dr 8:1 f) TMSOTf, 2,6-lutidine g) NBS, $AgNO_3$ h) Bu_3SnH, $PdCl_2(PPh_3)_2$, 70% over 3 steps

Scheme 24: Panek's conclusion of the C20-C32 core fragment synthesis

As can be seen from the syntheses reviewed here, the core fragment of phorboxazoles has been a very attractive target for synthetic chemists, both as a part of total syntheses and also to showcase methodologies for THP formation. The approaches are quite diverse and can be broadly grouped in cycloaddition and linear precursor cyclization strategies. The synthesis by Evans (Scheme 9 and 10) is a particularly nice example of synthetic methodology, having a 60% overall yield for this complex fragment. The Diels-Alder approach employed by Burke (Scheme 17) is also impressive because of its concise nature.

7.4 Previous efforts towards C20-C32 fragment in Clarke group

The Maitland-Japp reaction developed in the group has proven to be a versatile methodology in the diastereoselective synthesis of tetrahydropyran rings and has been applied to the synthesis of several natural products.[43-45] As part of the groups' efforts towards the synthesis of phorboxazole B (**10**), applications of this reaction to the synthesis of the core fragment were also explored.[46]

The synthetic study started with Masamune-Abiko auxiliary derived ester **148**, which is known to give good results in the asymmetric synthesis of *anti* aldol products (Scheme 25). Thus, in a Cy_2BOTf and Et_3N promoted aldol reaction the *anti* aldol product **149** was synthesized in 91% yield and in high diastereoselectivity (dr 14:1 *anti*:*syn*). The auxiliary was first cleaved with sodium methoxide to give the methyl ester in 83% and a subsequent Claisen condensation with *t*-butyl acetate provided the β-ketoester **150** in 75% yield.

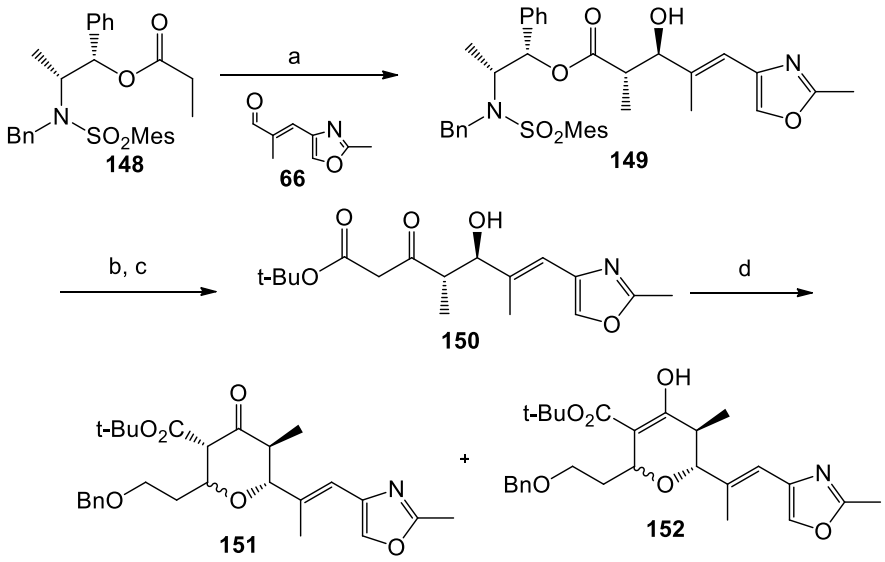

68%, ratio of diastereomers: 1:1 (*trans*) : 1.1 (*cis*)

Reagents and conditions: a) Cy_2BOTf, Et_3N, **66**, DCM, 91%, dr 14:1 b) NaOMe, MeOH c) LDA, *t*-BuOAc, THF, 62% over 2 steps d) $BnO(CH_2)_2CHO$, $Sc(OTf)_3$, DCM

Scheme 25: THP forming Maitland-Japp reaction

Lewis acid-catalysed Maitland-Japp cyclisation with an aldehyde was then attempted to give the pentasubstituted tetrahydropyran ring. Numerous reaction conditions were tested, but unfortunately, all of them gave complex mixture of 2,6-*cis*/*trans* diastereomers **151** and interconverting keto/enol tautomers **152**. Even worse, in all cases the desired 2,6-*cis* tetrahydropyran was the minor product in the mixture and, because of the difficult separation of this mixture, insufficient amounts of material were available to continue the synthesis.

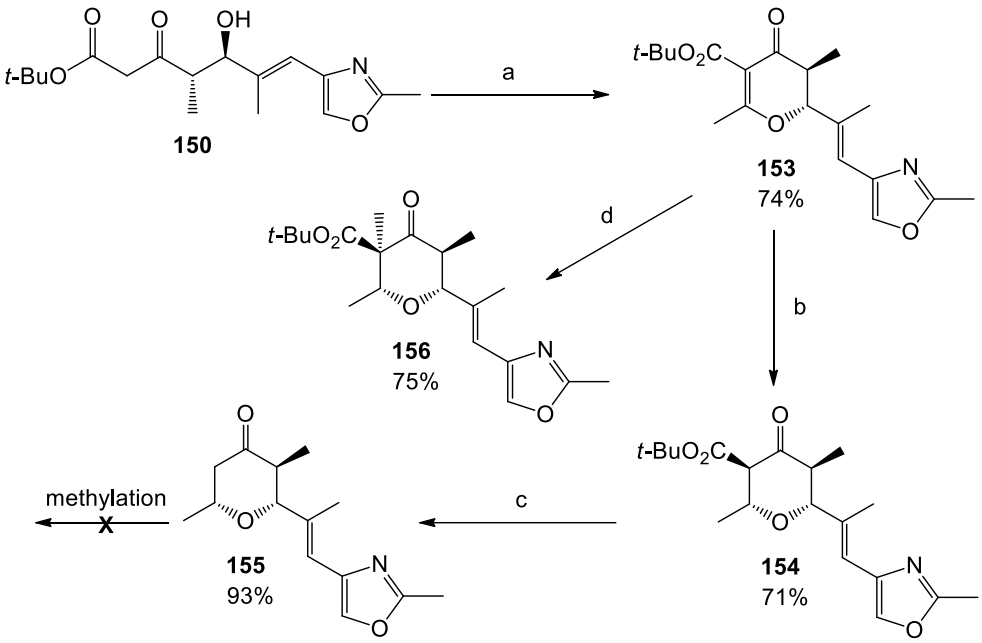

Reagents and conditions: a) $MeC(OMe)_2NMe_2$, toluene, 74% b) L-Selectride, THF, 71% c) microwave, DMF, H_2O, 93% d) L-Selectride, THF, MeI, 75%

Scheme 26: DHP forming Maitland-Japp reaction

For this reason it was decided to switch to the dihydropyran-forming version of Maitland-Japp reaction, also developed previously in our group. Reaction between β-ketoester **150** and the dimethyl acetal of dimethylacetamide provided the dihydropyran **153** in 74% yield (Scheme 26). This was then reduced diastereoselectively with L-Selectride to tetrahydropyran **154** in 71% yield. Alternatively, when the enolate resulting from the L-Selectride reduction was trapped with MeI, the tetrahydropyran **156** was obtained in 75%

yield as a single diastereomer a with correctly installed axial methyl group present at the C23 position of the phorboxazoles.

To continue the synthesis of the core fragment, the tetrahydropyran **154** was heated in a microwave oven, which effected the removal of the *t*-butyl ester and decarboxylation. It was hoped that the remaining methyl group could then be installed with kinetic deprotonation of **155** and a kinetic quench with MeI. However, in all cases the starting material was isolated unchanged.

It was then rationalised that the fragment **156** could be used to complete the synthesis of the core fragment, if the ester group could be removed stereospecifically. To this effect, the ketone was diastereoselectively reduced and the resulting alcohol was protected as the PMB ether to give compound **157** in 69% yield over two steps (Scheme 27). Next, the ester was reduced to give the aldehyde **158** in 72% yield. Unfortunately, when decarbonylation was attempted in the presence of stoichiometric amount of Wilkinson's catalyst, no reaction was observed.

Since the stereospecific removal of the ester had failed, it was decided to decarboxylate anyway. To achieve this, the ester **156** was first treated with TFA and then heated in toluene at reflux. Following this, the ketone functionality was reduced with sodium borohydride, which proceeded in 60% yield and gave the alcohol **159** as a 2:3 mixture of diastereomers. This completed the synthesis of the C21-C32 tetrahydropyran core of the phorboxazoles, being epimeric at C23.

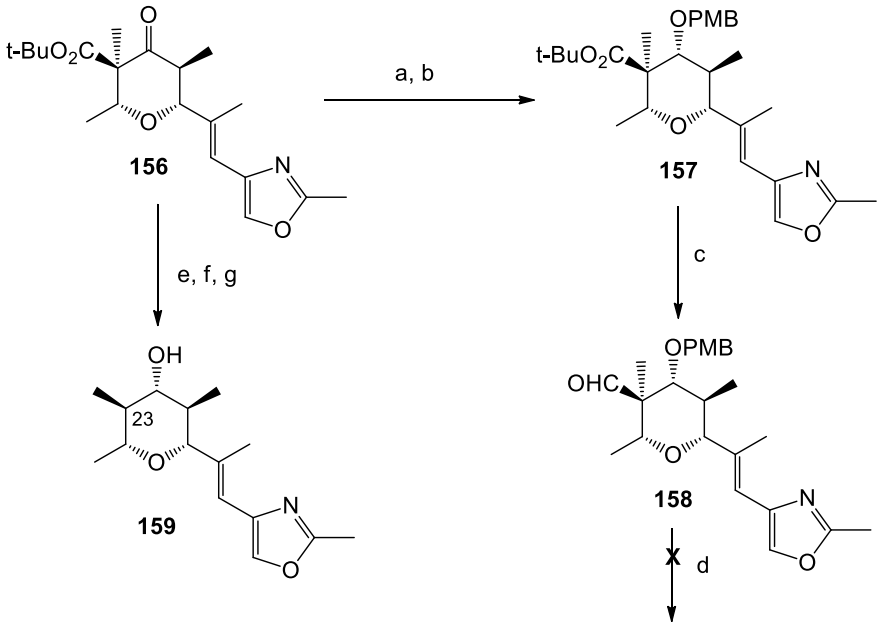

Reagents and conditions: a) DIBAL, DCM b) KH, THF, PMBCl, 69% over 2 steps c) DIBAL, toluene, 72% d) $RhCl(PPh_3)_3$, toluene e) TFA, DCM f) toluene, reflux g) $NaBH_4$, MeOH, 56% over 3 steps, dr 2:3 at C24

Scheme 27: Synthesis of the epi-23 C20-C23 phorboxazole core fragment

8. Results and Discussion

8.1 Retrosynthetic analysis

The Maitland-Japp reaction developed in the group has proven to be a versatile methodology for the diastereoselective synthesis of tetrahydropyran rings and has been applied to the synthesis of several natural products.[43, 44] However, previous attempts in the group at synthesis of the core fragment of the phorboxazole B (**10**) using the Maitland-Japp reaction had proved unsuccessful,[46] and therefore we set out to develop an alternative route.

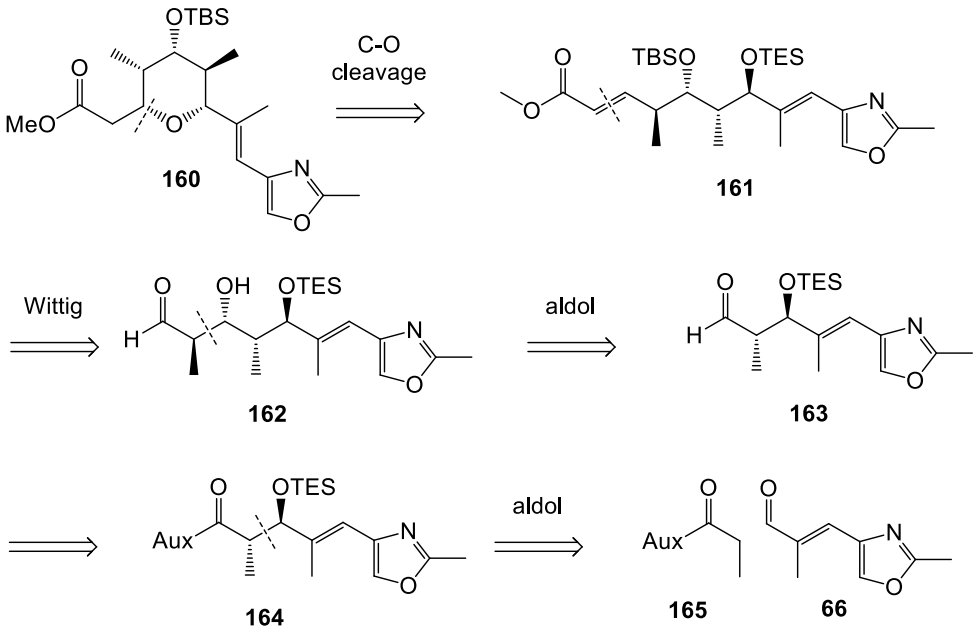

Scheme 28: Our retrosynthetic analysis of the C20-C32 fragment of phorboxazoles

As part of our efforts in synthesizing phorboxazole B (**10**) we performed a retrosynthetic analysis of the C20-C32 core fragment of this natural product (Scheme 28). We reasoned that the core fragment **160** could be simplified to a linear precursor **161** *via* a C-O bond cleavage. A Wittig disconnection would lead from the unsaturated ester to a simpler aldehyde **162**. Finally, two consecutive aldol disconnections give a known

aldehyde **66** and a chiral auxiliary derived compound **165** and thus a blue-print for the synthetic strategy of the C20-C32 core fragment.

8.2 Synthesis of the stereotetrad

In the forward sense, a crucial part of the synthesis is the installation of the four stereocentres of the cyclization precursor (Scheme 29). For the installation of the first two stereocentres the use of an asymmetric auxiliary-controlled, *anti* selective aldol reaction was envisaged. After the cleavage of the auxiliary and protection of the alcohol, the second two stereocentres could be installed *via* either a Felkin-Anh controlled aldol reaction or a crotylation reaction.

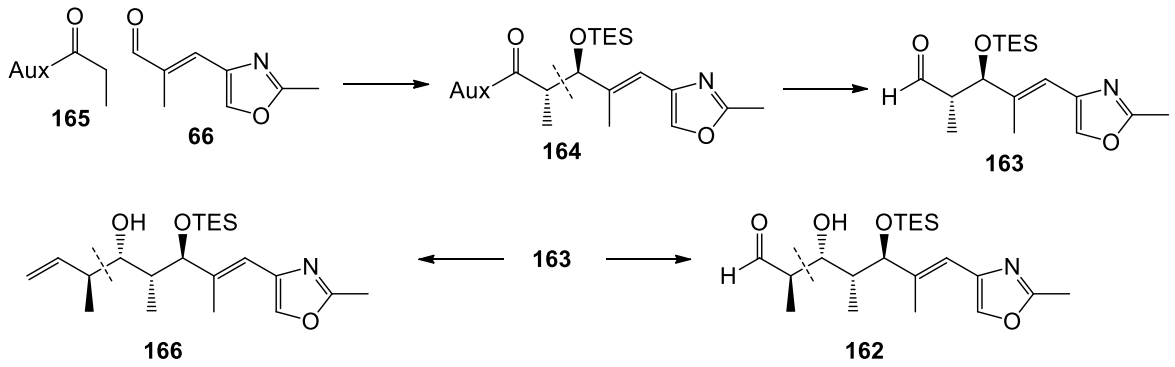

Scheme 29: Forward synthetic plan for the stereotetrad of the core fragment

The aldol reaction is a very popular way of forming carbon-carbon bonds, especially when relative and absolute stereocontrol is important. The asymmetric aldol reaction was pioneered by Evans in 1981 using the now well-known chiral oxazolidinone auxiliary approach (Scheme 30).[47] The Evans aldol reaction has become the gold standard of aldol processes. The proposed explanation to the observed enantioselectivity is shown in Scheme 31.

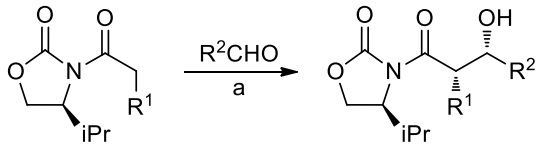

Reagents and conditions: a) *n*-Bu_2BOTf, DIPEA, then aldehyde

Scheme 30: Evans' auxiliary approach to aldol products

Evans auxiliary derived ester boron enolates exist as the *Z* isomer **169** (Scheme 31). These can then react with the aldehyde *via* two alternative Zimmerman-Traxler transition states **170** and **171**. While in most similar transition states the most favoured one is determined by steric repulsion forces, in this case dipole minimization is more important. In both transition states the steric interactions are minimized and in **170** the overall dipole is minimized because the oxazolidinone carbonyl group is pointing away from the aldehyde and enolate oxygen atoms. Conversely, in **171** the dipole is maximized as all the polar carbon-oxygen bonds are pointing the same way.

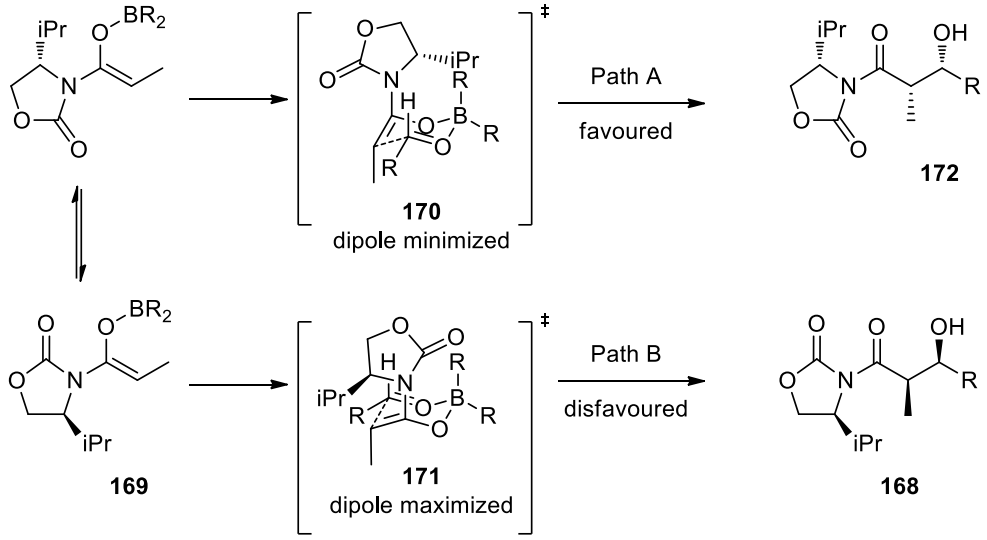

Scheme 31: Enantiomeric pathways when using Evans auxiliary

One important limitation of Evans' methodology is the inability to produce the *anti* aldol products. This problem has been solved by several modifications to Evans protocol. The earliest was reported by Heathcock in 1991 in which the precoordination of

the aldehyde with Et_2AlCl enabled the production of the *anti* product (Scheme 32).[48] This precoordination disrupts the cyclic transition state and the reaction takes place *via* the open transition state **173** instead. The bulky Lewis acid ensured that the attacking aldehyde is oriented so as to minimize all steric interactions and give the *anti* product.

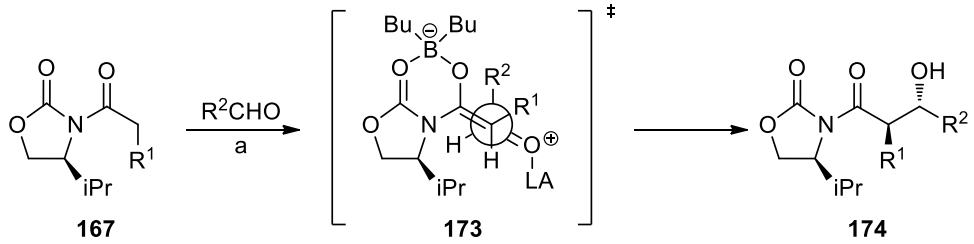

167 **173** **174**

Reagents and conditions: a) *n*-Bu_2BOTf, DIPEA, then R^2CHO precomplexed with Et_2AlCl;

Scheme 32: Heathcock's modification to Evans' aldol reaction

Another modification was reported more recently by Evans that makes use of catalytic amounts of magnesium salts to access the *anti* aldol products (Scheme 33). The reaction involves the silylation of the formed *Z*-enolate which reacts with an aldehyde presumably through an open transition state **176** similar to that proposed by Heathcock. The observed yields were in excess of 88% and the diastereomeric ratios in most cases were better than 20:1.[49]

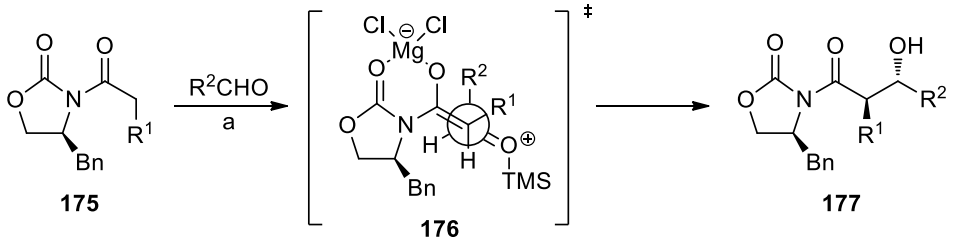

175 **176** **177**

Reagents and conditions: a) 0.1 eq $MgCl_2$, R^2CHO, Et_3N, TMSCl, EtOAc;

Scheme 33: Modification to Evans' aldol reaction

An alternative auxiliary has been developed by Masamune and Abiko (Scheme 34).[50] This is a particularly attractive approach as the auxiliary is accessible in 3 steps from norephedrine and both enantiomers of norephedrine are commercially available. The authors found that both *syn* and *anti* diastereomers are accessible using this methodology.

The choice of reagents used for the enolization was critical for both good yields and selectivities. Thus, the combination of dibutylboron triflate and DIPEA formed the *Z*-enolate and gave mostly the *syn* aldol product. Alternatively, the use of dicyclohexylboron triflate and triethylamine allowed the synthesis of the *anti* product *via* an *E*-enolate in an impressive 98% yield and greater than 98:2 diastereoselectivity. The accessibility of the auxiliary precursors and the robustness of this procedure has made this a popular way of forming *anti* aldol products and has been applied to several total syntheses, including those of apmhidinolide A, rhizopodin and leiodermatolide.[51-53]

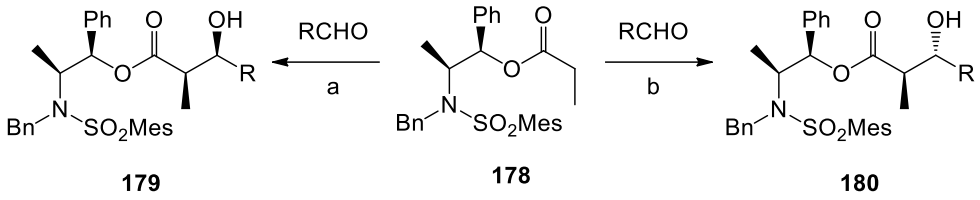

179 **178** **180**

Reagents and conditions: a) Bu_2BOTf, DIPEA, RCHO b) Cy_2BOTf, TEA, RCHO;
Scheme 34: Masamune-Abiko aldol reaction

While the chiral auxiliary approach remains the most popular and best developed, several important catalytic enantioselective aldol methodologies have also been developed in the last 20 years. The generation of *anti* geometries has been a challenging problem in the catalytic processes as well.

Kobayashi reported a catalytic route towards *anti* aldol products in 2002 (Scheme 35).[54] This methodology makes use of zirconium Lewis acid with a BINOL-derived ligand **183** as the catalyst. It provides good yields and enantioeselectivities along with good to excellent *anti* selectivities. Interestingly, this reaction provides the *anti* product regardless of the double bond geometry of the silyl enol ether. This indicates that the transition state of the reaction is likely acyclic.

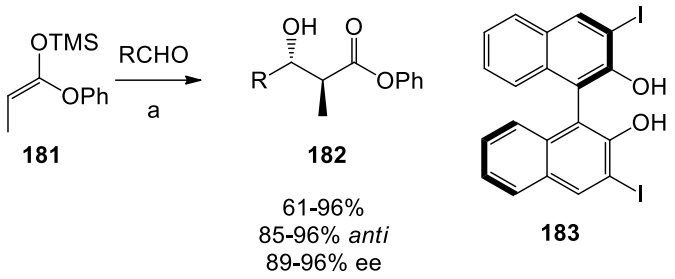

Reagents and conditions: a) RCHO, 10 mol% $Zr(OtBu)_4$, 12 mol% **183**, 80 mol% PrOH, 20 mol% H_2O, toluene, 0 ˚C, 18 h

Scheme 35: Kobayashi Zr-catalyzed *anti*-selective aldol reaction

An impressive methodology using chiral Lewis base catalyst has been developed by Denmark (Scheme 36).[55] It uses the BINOL-derived phosphamide catalyst **186** and similarly to Kobayashi's study, the reaction gives the *anti* product regardless of the geometry of the double bond in the silyl enol ether.

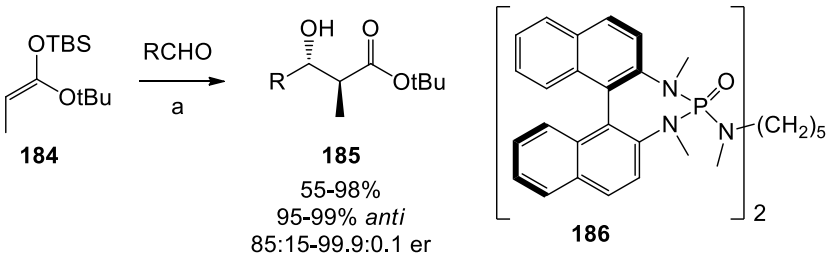

Reagents and conditions: a) 1.1 eq $SiCl_4$, 1 mol% **186**, DCM, -78 ˚C

Scheme 36: Denmark's organic Lewis base catalyzed *anti*-selective aldol reaction

Because of the high yields and diastereoselectivites reported and the easy access to the auxiliary, we chose the Masamune-Abiko boron enloate approach to begin the implementation of our synthetic strategy. Massamune-Abiko auxiliary derived ester **148** had been already prepared in large quantities for previous synthetic studies in the group. The original route had been followed using (+)-norephedrine as the starting point (Scheme 37).

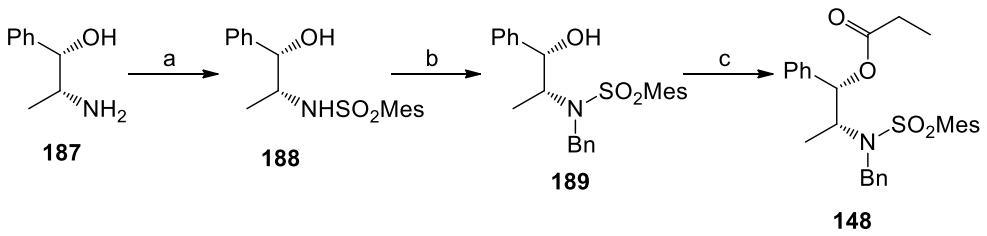

Reagents and conditions: (i) Et_3N, $MesSO_2Cl$, CH_2Cl_2, 12 h, 98%; (ii) Cs_2CO_3, BnBr, MeCN, reflux, 90 min, 93%; (iii) py, propionyl chloride, CH_2Cl_2, 0 ˚C, 4 h, 96%.

Scheme 37: Preparation Massamune-Abiko auxiliary

In addition to the ester **148**, both the dicyclohexylboron triflate **192** and the aldehyde **66** had to be prepared before the aldol reaction could be attempted. Dicyclohexylboron triflate was prepared in two steps from cyclohexene **190**, borane dimethylsulfide complex and triflic acid (Scheme 38).[56] Cyclohexene was first hydroborated by adding borane dimethylsulfide complex and stirring for 3 hours at 0 ˚C. Solvent was then removed, the dicyclohexylborane **191** suspended in hexane and triflic acid added at room temperature. This gave the dicyclohexylboron triflate in 70% yield and its solution in hexane was then stored in the fridge and used in subsequent aldol reactions. Great care had to be taken in the preparation and handling of this reagent as it is water and air sensitive and decomposes at temperatures above 0 ˚C.

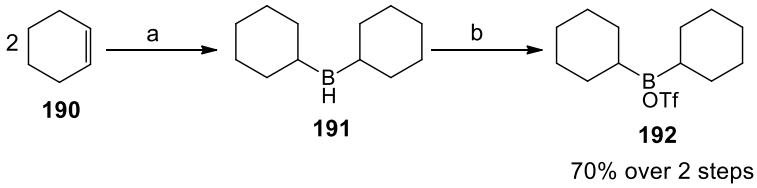

Reagents and conditions: a) $BH_3{\cdot}Me_2S$, Et_2O, 0 ˚C, 3 hours b) TfOH, hexane, rt, 70% over 2 steps

Scheme 38: Preparation of the dicyclohexylboron triflate

A modified industrial route first developed by GlaxoSmithKline was used to prepare the aldehyde **66.**[57] A condensation between DL-serine methyl ester **193** and ethyl acetimidate hydrochloride gave the oxazoline **194** (Scheme 39). This was then oxidised to the oxazole carboxylic ester by mixture of bromotrichloromethane and base. In this

reaction the ester is first brominated in the α position followed by elimination to reveal the oxazole.

While several routes to the oxazolaldehyde **198** have been explored in previous studies, it was found that the $LiAlH_4$ reduction of a Weinreb amide was the most reliable and scalable route. Thus, the carboxylic ester was first hydrolyzed to the acid **196** and then transformed into the Weinreb amide **197**. This was then reduced to the oxazole aldehyde **198**. Finally, the aldehyde was submitted to a Wittig reaction with a commercially available stabilized Wittig reagent **199**, which gave the desired unsaturated aldehyde **66** with an excellent *E* selectivity.

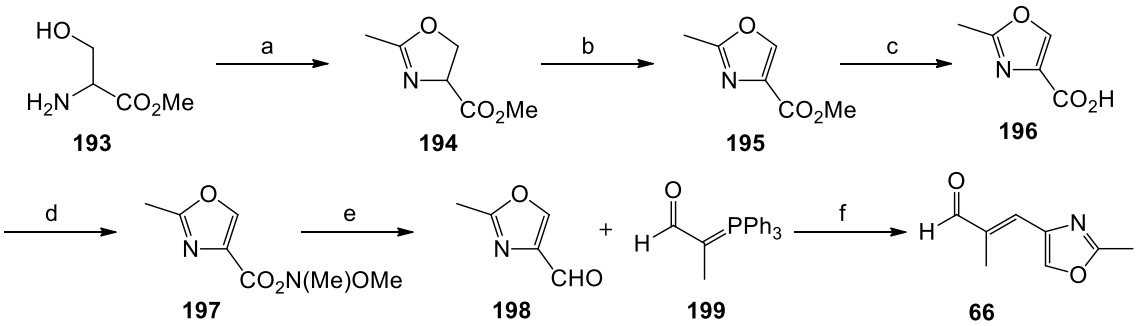

Reagents and conditions: a) Ethyl acetimidate·HCl, NEt_3, CH_2Cl_2, rt, 16 h, 72%; b) $BrCCl_3$, DBU, CH_2Cl_2, 0 °C, 16 h, 62% c) i) 32% NaOH, H_2O rt, 1 h; ii) 37% HCl, 0 °C, 1 h, 57%; d) NH(Me)OMe·HCl, EDC, NEt_3, CH_2Cl_2, H_2O, rt, 2 h, 61%; e) $LiAlH_4$, THF, -35 °C, 1 h, 79% f) benzene, reflux, 20 h, 96%

Scheme 39: Preparation of the aldehyde **66**

The aldol reaction was then attempted (Scheme 40). As the enolate geometry determines the relative stereochemistry and we required the *anti* relationship between the two stereocentres created in the reaction, it was important to prepare the (*E*)-boron enolate. This was accomplished by adding the sterically undemanding base triethylamine and the bulky Lewis acid dicyclohexylboron triflate to the ester **148** at -78 °C, followed by the addition of the aldehyde **66**. To our delight, the reaction gave 91% yield as 14:1 mixture of

diastereomers. It was also found that the reaction could be scaled up to several grams without any appreciable loss in selectivities or yield.

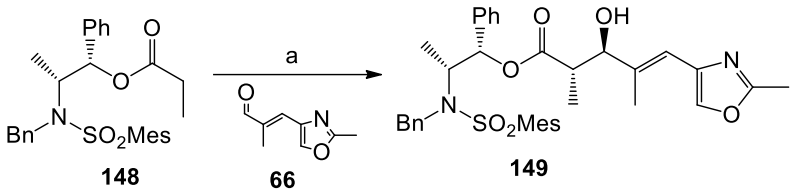

Reagents and conditions: a) i) Cy_2BOTf, Et_3N, DCM, -78 ˚C ii) **66**, 91%, dr 14:1

Scheme 40: Aldol reaction

The absolute stereochemistry of the product of this aldol reaction is determined by the bulky auxiliary group. It has been proposed that the reaction between the (*E*)-dicylohexylboron enolate of the ester **148** can proceed *via* transition states **200** and **201** (Figure 8). It could be that **200** will be the disfavoured one as there is significant steric clash between the phenyl group of the auxiliary and the methyl group of the (*E*)-boron enolate.[58]

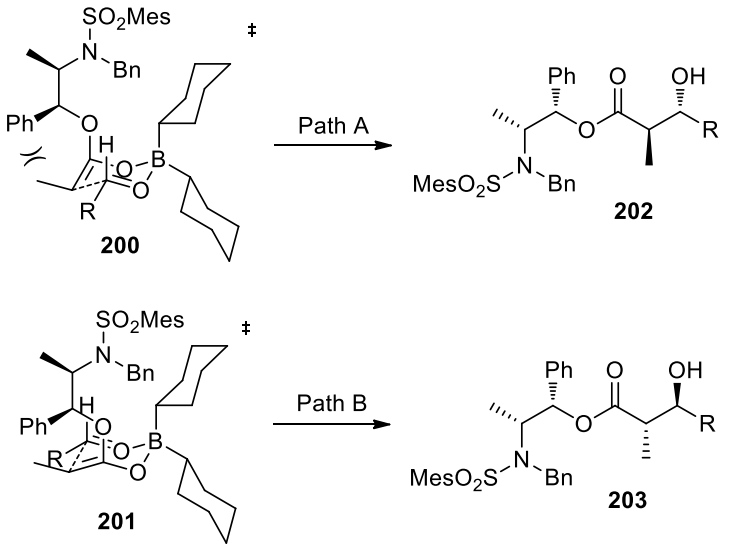

Figure 8: Enantiomeric pathways when using Masamune-Abiko auxiliary

Based on a molecular mechanics study using MMFF94 force field, we propose an alternative explanation (Figure 9).

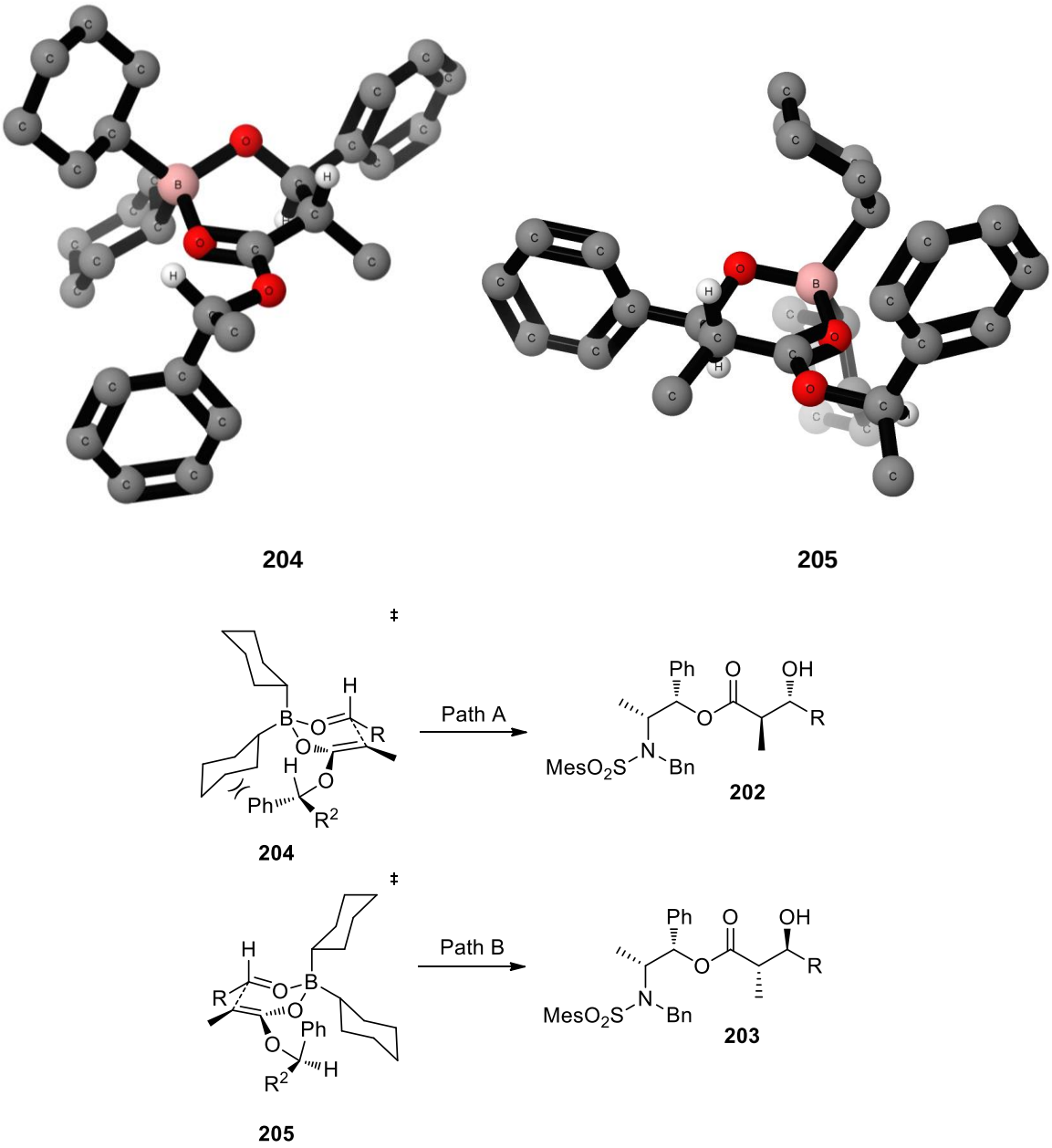

Figure 9: Alternative molecular mechanics based enantiomeric pathways when using the Masamune-Abiko auxiliary

The norephedrine derived ester is by far the sterically largest substituent and therefore it is quite unlikely that it would favour axial position in the transition state. The rotation to a pseudo-equatorial postition means that the transition states are actually in a half-chair configuration. Half-chair transition states are not quite as common as chair-like transition states, however they have been encountered in, for example, theoretical studies of enamine aldol reactions.[59] It is also worth noting that half-chair transition states are only

plausible in *E*-boron enolate aldol reactions, because the *Z* enolate geometry in a half-chair transition state would mean that the α-substituent is pointing towards the aldehyde, thus blocking the approach.

The key difference between the two diastereomeric transition states **204** and **205** appears to be the interaction between the cyclohexyl substituents on the boron reagent and the phenyl substituent on the auxiliary. The sulfonamide substituent is the largest portion of the auxiliary and would always be positioned away from the large cyclohexane rings of the boron reagent. In the higher energy transition state **204** this means that the hydrogen atom is pointing at the gap between the two cyclohexyl ring, while the phenyl substituent is clashing with one of the cyclohexyl substituents. In the lower energy diastereomeric transition state **205** the phenyl ring is pointing towards the gap between the two cyclohexyl rings, thus avoiding the highly undesirable phenyl-cyclohexyl interaction.

The overall difference in energy of these transition states is approximately 10 kJ/mol which is consistent with the observed diastereoselectivity. It must be noted, however, that molecular mechanics is not the best tool for transition state studies. While **204** and **205** provide a plausible rationale for the overall stereoinduction, it is unlikely that these are the actual transition state structures as the molecular orbital overlap for the formation of the bond would be quite limited. Therefore the actual explanation is probably more complex and requires higher level computational analysis. The probable complexity of the explanation might be the reason why one has not been suggested in a published paper in the almost 20 years since the first report of the Masamune-Abiko aldol reaction.

To continue our synthesis of the core fragment, we attempted to protect the aldol product **149** with a TES group. However, both TES triflate in pyridine and TES chloride and imidazole in DMF failed to give the desired product. Therefore we switched to TBS protection using TBS triflate and employing 2,6-lutidine as base. This gave us the

protected aldol product **206** in high yield (Scheme 41). With the hydroxyl group successfully protected, the Massamune-Abiko auxiliary was cleaved using DIBAL. Unfortunately this reaction resulted in overreduction and gave the alcohol **207**. This issue has been reported in other studies using Masamune-Abiko auxiliary.[60] The reason for the difficult cleavage is probably the significant steric bulk of the auxiliary. The cleaved auxiliary is left as an alcohol **189** and could be isolated and reused.

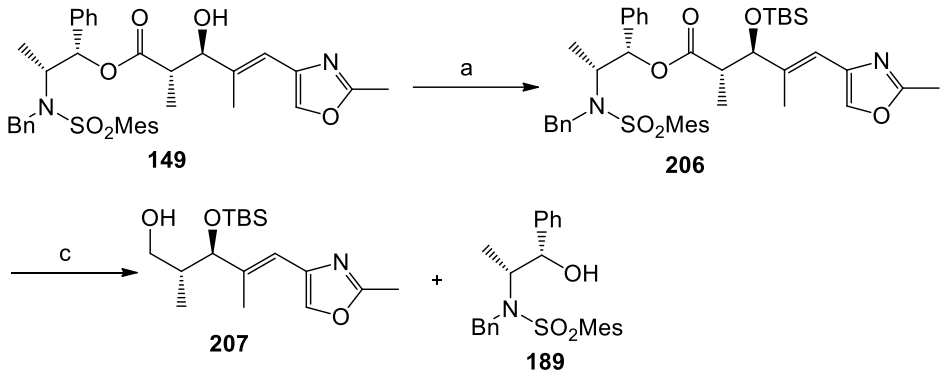

Reagents and conditions: a) TBSOTf, 2,6-lutidine, DCM, 93% c) DIBAL, DCM, 0 ˚C, 82%

Scheme 41: DIBAL cleavage of the auxiliary

Because of the difficulties in protecting the aldol product we also explored a sodium methoxide cleavage of the auxiliary (Scheme 42). This reaction gave the ester **208** in moderate yield which was subsequently protected with a TBS group to give **209**. However, we chose not to use this route because of the moderate yields of both steps and also because of the extended reaction times required for methoxide cleavage. The reaction takes 3 days and compares quite unfavourably with DIBAL cleavage, which only takes 10 minutes.

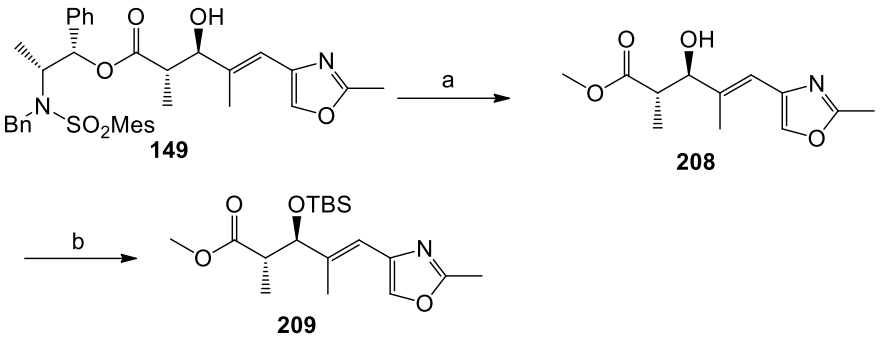

Reagents and conditions: a) NaOMe, MeOH, 0 ˚C - rt, 68% b) 2,6-lutidine, TBSOTf, DCM, 0 ˚C, 56%

Scheme 42: Methoxide cleavage of the auxiliary

Since the auxiliary cleavage using DIBAL gave the overreduction product **207**, it was necessary to reoxidize it to aldehyde before we could continue the synthesis. To this end, Parikh-Doering oxidation was attempted. However, it only gave traces of the required aldehyde **210**. As an alternative reagent for the oxidation we chose Dess-Martin periodinane. While DMP is commercially available, it is quite expensive, so we opted to prepare it ourselves following a literature procedure.[61] Notably, this procedure uses Oxone® instead of the potassium bromate as the oxidant in the first step, which makes the procedure significantly safer and more convenient. With DMP in hand, alcohol **207** was reoxidized and gave the desired aldehyde **210** in 94% yield and in high purity so it did not require purification by column chromatography before submission to the next step (Scheme 43).

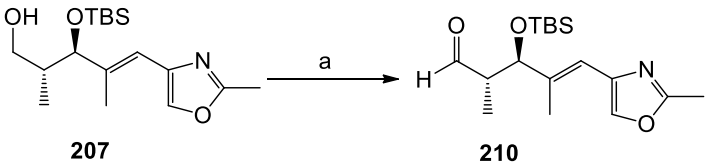

Reagents and conditions: a) DMP, DCM, 0 ˚C - rt, 94%

Scheme 43: Dess-Martin oxidation

To install the the next two stereocentres, we first experimented with boron enolate Felkin-Anh controlled aldol reaction. However, this reaction did not give the

required product and only starting material could be identified in the crude reaction mixture (Scheme 44). Therefore we explored boron mediated crotylation as an alternative means of setting up the two stereocentres.

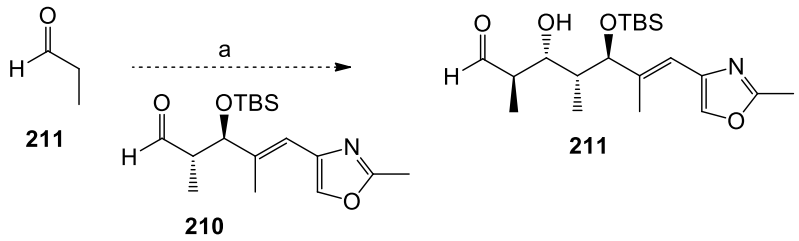

Reagents and conditions: a) Cy_2BOTf, Et_3N, **134**, DCM, -78 ˚C

Scheme 44: Attempted diastereoselective aldol reaction

In the last 30 years the allylboration of carbonyl compounds has become a popular tool in the chemist's toolbox for carbon-carbon bond formation with a high level of stereocontrol (Scheme 45).[62]

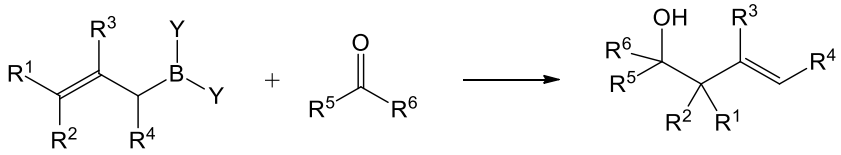

Scheme 45: Allylboration of carbonyl compounds

In reactions of this type allylboron reagents react with several classes of carbonyl compounds, including aldehydes, ketones and imines. In the most common case, however, the substrate is an aldehyde and the product of this reaction is a homoallylic secondary alcohol. One of the key early developments was the realisation by Hoffmann and Zeiss that the addition of allylboron reagents to alcohols were highly stereoselective and predictable (Scheme 46).[63] They found that the double bond geometry of the crotylboronate reagent determines the relative stereochemistry of the product. Thus, *E*-crotylboronates generally give the 1,2-*anti* products and *Z*-crotylboranes give the 1,2-*syn* products with excellent diastereoselectivity in most cases.

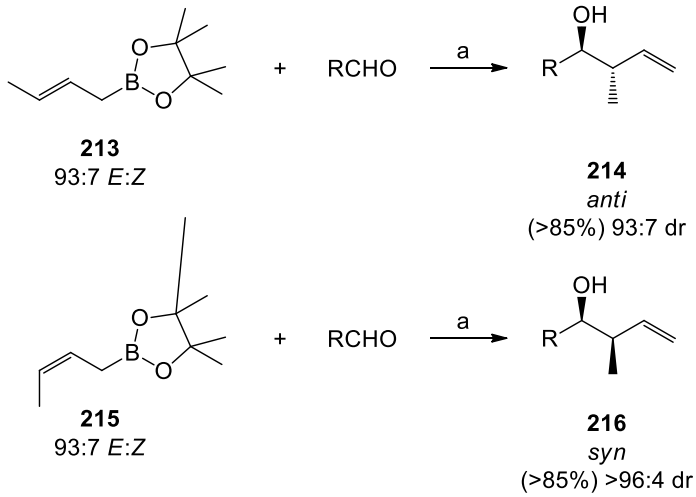

Reagents and conditions: a) Et_2O, -78 °C to rt

Scheme 46: Stereocontrol in allylboration reaction

What makes this observation particularly useful is the comparatively easy preparation of the *E* and *Z* crotylboron reagents in a highly stereoselective way from the corresponding alkenes (Scheme 47). Other notable ways of preparation of more complex allylboron reagents include hydroboration, olefin metathesis and transition metal catalyzed allylic substitution reactions.[64-66]

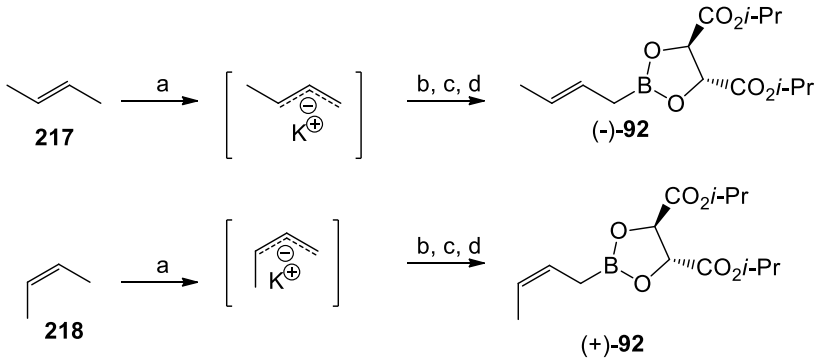

Reagents and conditions: a) *t*-BuOK, *n*-BuLi, THF, -78 ˚C to -50 ˚C b) (*i*-PrO)$_3$B, -78 ˚C c) 1 N HCl, Et_2O d) (+)-DIPT, $MgSO_4$, >75% over 4 steps

Scheme 47: Stereoselective boronate synthesis

Absolute stereocontrol in allylboration reactions has also been well developed and can be achieved both by using substrate control and reagent control. For example,

when α-chiral aldehydes are used as substrates in allylation reactions with achiral reagents, generally good levels of stereoinduction can be achieved.

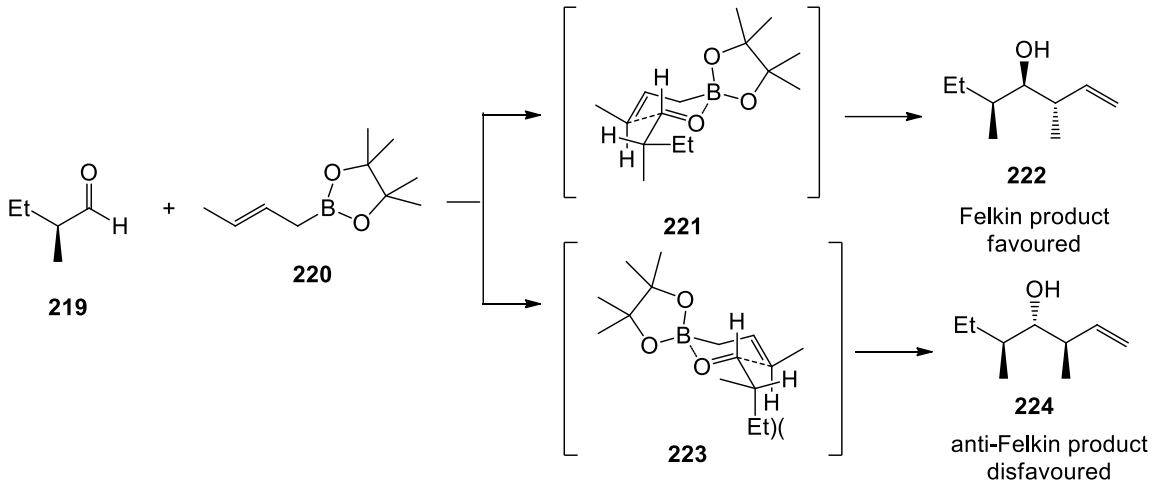

Scheme 48: Stereoinduction model for additions of *E*-boronate to α-chiral aldehyde

From the attack of *E*-crotylboronates on aldehydes the Felkin-Anh products are generally obtained (Scheme 48). However, the Felkin-Anh model cannot explain all the observed diastereoselectivites and a different explanation has been proposed by Roush.[67] He argued that the major factor was instead the minimization of *syn*-pentane interactions between the γ-substituents of the allyl unit and the α-carbon of the aldehyde. Thus, in the reaction between aldehyde **219** and the crotylboronate **220**, the lowest energy transition state would be **221**, in which the largest group of the aldehyde is pointing away from the reactive centres. This transition state best minimizes so-called gauche-gauche interactions. In the alternative transition state **223** slightly more important steric interactions between the ethyl group and the γ-hydrogen atom of the boronate cannot be avoided and thus this transition is less favoured and leads to an 83:17 diastereomeric ratio in favour of the Felkin product.

Further support for Roush's model is given by the similar reaction between the same aldehyde and the *Z*-crotylboronate **225** in which the major product is the anti-Felkin

product **229** (Scheme 49). Roush's model, however, successfully explains this selectivity based on the same principles as above.

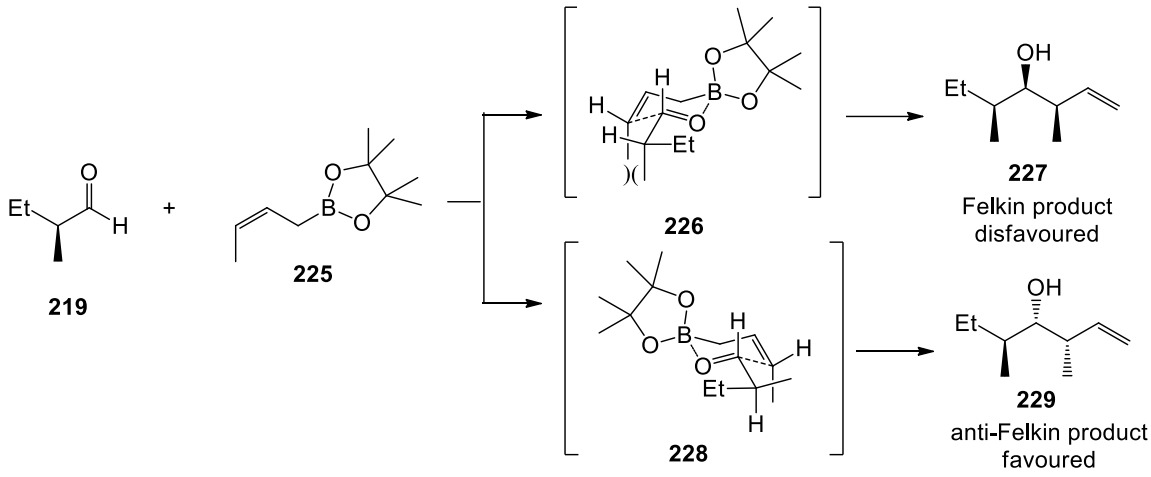

Scheme 49: Stereoinduction model for additions of *Z*-boronate to α-chiral aldehyde

Various levels of absolute stereocontrol can also be achieved by reagent control. A great variety of chiral boron reagents have been developed, with the chirality being installed both as an auxiliary on the boron and also in the allylic part of the reagent (Figure 10).

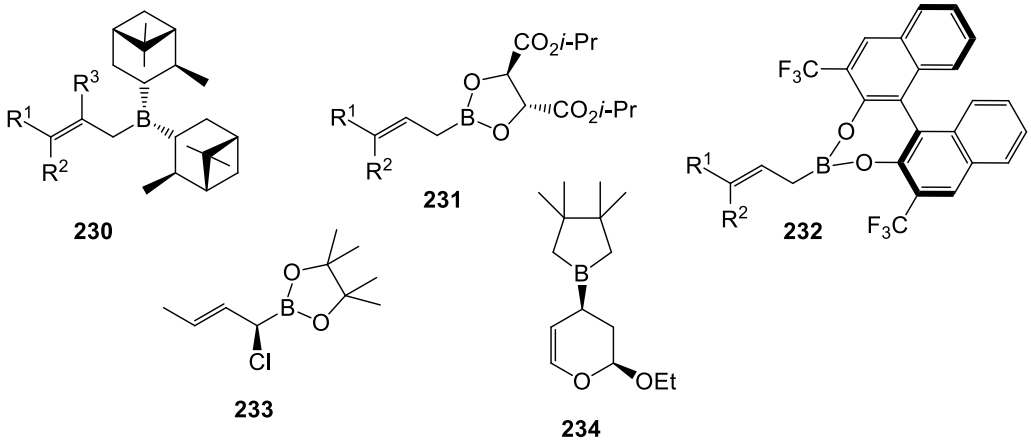

Figure 10: Some examples of chiral allylation agents

The bis(isopinocampheyl)borane derivatives **230** and diisopropyl tartrate boronate derivatives **231** both generally achieve high levels of stereocontrol and are by far the most often used in synthesis. Both Pattenden and White made use of

bis(isopinocampheyl)borane reagents in the synthesis of the C20-C32 core fragment of phorboxazoles with great results (Schemes 4 and 11). Similarily, Zhou used the boronate ester **231** in his approach to the core fragment (Scheme 13). Catalytic enantioselective crotylations have also been an active area of research recently and various different approaches have been developed.[68]

Allylborations have been applied to countless total syntheses. A nice example showing both the strengths and the challenges of the reaction is the total synthesis of calyculin C by Armstrong (Scheme 50).[69] The chiral *E*-crotylborane **60** was added to the complex aldehyde **235** to install two new stereocentres in excellent diastereoselectivity and good yield. The resulting terminal alkene was cleaved to the corresponding aldehyde **236** *via* ozonolysis. Another crotylation using the same reagent **60** was attempted. However this time the reagent was mismatched with the substrate and failed to achieve good stereocontrol. The reaction gave essentially equal amounts of both *anti* products **237** and **238**. Fortunately, the terminal alkenes could be separated and the desired isomer **238** was carried forward to complete the total synthesis of calyculin C.

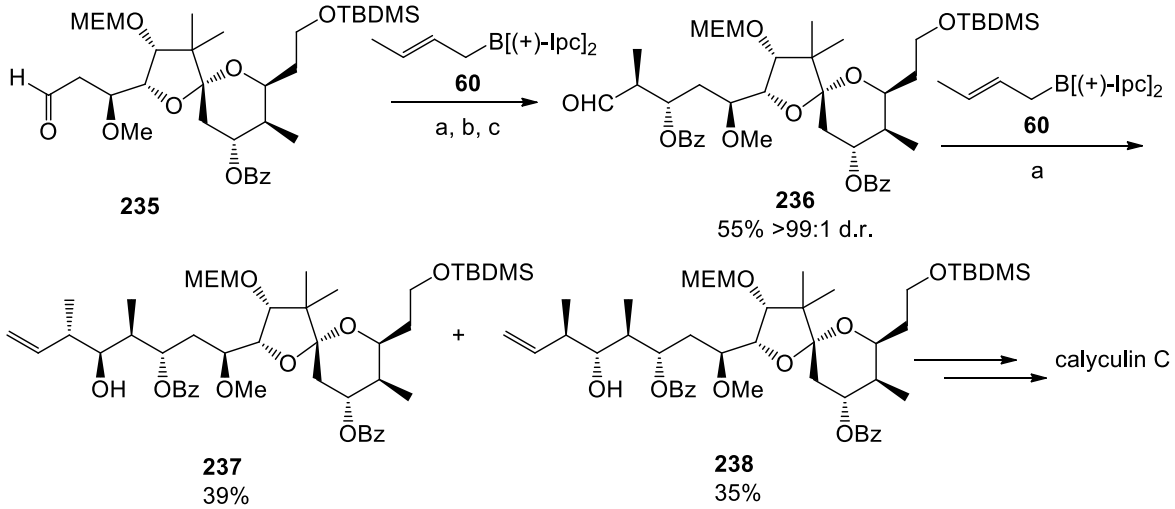

Reagents and conditions: a) **89**, THF, -78 ˚C b) BzCl, pyridine, 89%

c) O_3, Me_2S, PBu_3, DCM, -78 ˚C

Scheme 50: Application of asymmetric crotylation reactions to the total synthesis of calyculin C

To avoid similar problems with the potential mismatch between the stereochemistry of the aldehyde and the crotylation reagent, it was decided for the synthesis of the core fragment to use an achiral crotylating reagent (Scheme 51). Pinacol ester **220** developed by Hoffmann had been shown to give good stereoinduction and diastereoselectivity.[63] It is commercially available and was therefore chosen for further study.

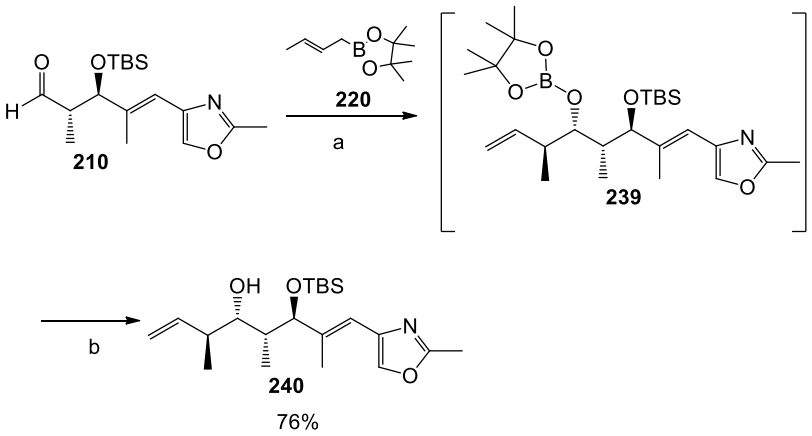

: *Reagents and conditions*: a) **220**, hexane, rt, 18 h b) ethanolamine, DCM, 4 h, 86%

Scheme 51: Diastereoselective crotylation

The reaction is very convenient from the practical point of view, as the substrate and the reagent are simply stirred together in hexane at room temperature overnight. At the end of the reaction the resulting secondary alcohol is left as the boronic ester **239**. This is generally removed during the workup procedure by stirring vigorously with either tris-ethanol amine or ethanolamine. Fortunately, the reaction proceeded to give the product **240** in 86% yield and the NMR spectrum of the reaction mixture showed a single diastereomer. The stereochemistry of the product at this point was assumed based on literature precedent. It was hoped that after successful synthesis of the THP ring the relative stereochemistry would be confirmed by NOE studies. After the synthetic studies described in the next chapters it was shown that the assumed stereochemistry of the terminal alkene **240** was indeed the correct one.

The high diastereoselectivity of this reaction can be explained by comparing two possible transition states of this reaction – **241** and **243** (Figure 11). Transition state **241** leads to the product **242**, while **243** leads to product **244**. In both transition states the large oxazole containing substituent would adopt position furthest away from the cyclic transition structure. In **243** this forces the α-methyl group close to the cyclic transition state, which is unfavourable because of the interaction with the terminal methyl group of the crotylboronic acid pinacol ester. As there is no such interaction in the transition state **241**, this reaction path should be the dominant and product **242** the major product, which is also what we observed.

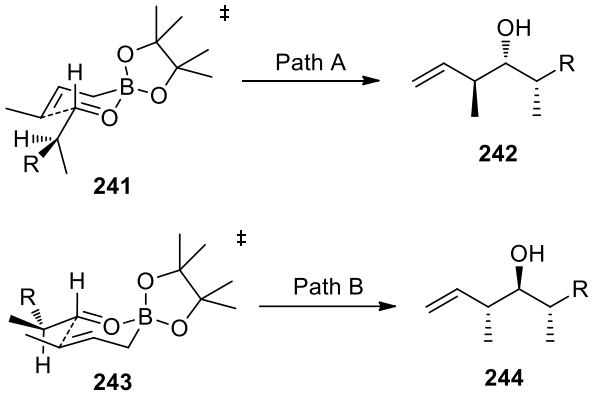

Figure 11: Diastereomeric pathways of crotylation

8.3 Oxy-Michael cyclization

It was envisaged to use olefin cross-metathesis to convert the terminal alkene into the oxy-Michael substrate.

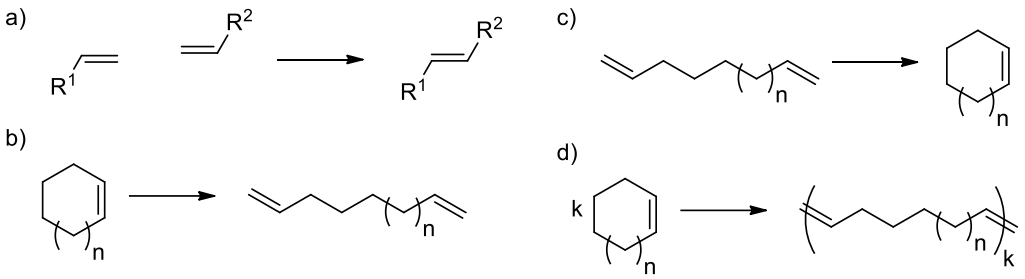

Scheme 52: The main classes of olefin metathesis reactions

The main classes of olefin metathesis reactions are shown in Scheme 52. Probably the most useful of these is cross-metathesis (a), which couples two different alkenes. Ring-opening and ring-closing metathesis are also widely used (b, c), especially to access structures that would be difficult to achieve otherwise. Ring-closing metathesis is especially useful for preparation of macrocycles. Finally, ring-opening metathesis polymerisation is a quite important process industrially for the preparation of polymers (d).[70]

Of all these processes cross metathesis presents a unique challenge of selectivity and reactivity. If both alkenes are of similar reactivity and used in similar amounts, in a purely statistic reaction only 50% yield can be expected of the cross-metathesis product. This can be alleviated by the use of multiple equivalents of the more accessible olefin. Thus, the use of 4 equivalents of one of the coupling partners increases the maximum theoretical yield to 80%. Additionally, since intermolecular processes are involved, the reactions are inherently slower than their intramolecular counterparts. This is also made worse by the fact that the effective catalyst loadings are often lower because of the need to use one of the coupling partners in excess.[71]

Olefin metathesis reaction was first discovered in 1960, when it was observed that the mixture of lithium aluminium tetraheptyl and titanium(IV) chloride caused the polymerisation of norbornene.[72] During the next decades various other metal compounds were successfully applied to reactions of this type. Mechanistic details were also gradually

worked out with key intermediates isolated. However, the olefin metathesis did not see wide application in organic synthesis. This was largely due to the poor substrate scope and also the air and moisture sensitivity of the catalysts, which required the use of Schlenk lines and glove boxes.

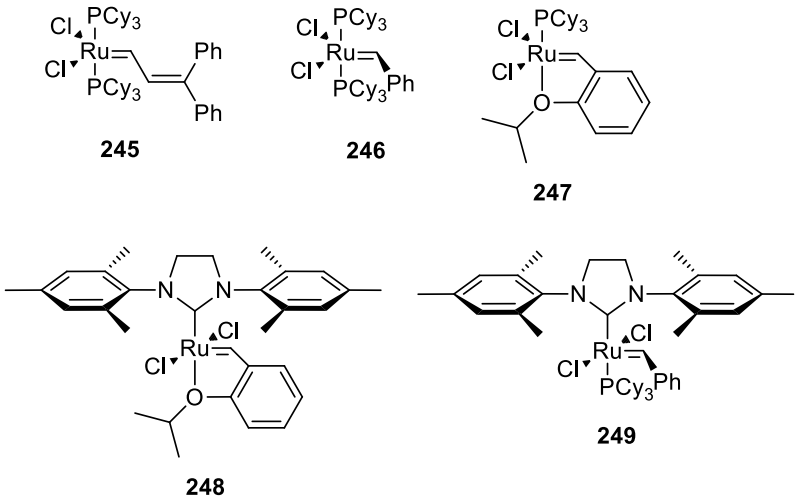

Figure 12: Ruthenium olefin metathesis catalysts

Breakthrough in the area came in 1992 with the development of well-defined ruthenium catalysts for this reaction by Grubbs.[73] More than 400 ruthenium based catalysts have since been prepared, but the most well known are the first and second generation Grubbs catalysts **246** and **249**, and the first and second generation Hoveyda-Grubbs catalysts **247** and **248** (Figure 12).[74]

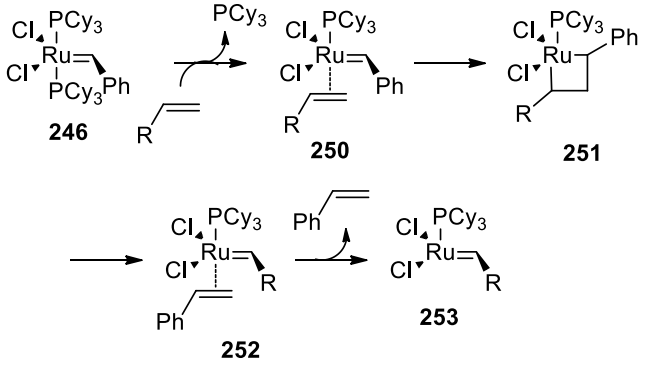

Scheme 53: Mechanism of olefin metathesis initiation

All of the catalysts in general use are actually precatalysts. They are $16e^-$ species, while the active species in the reaction are $14e^-$. For the reaction to be initiated, these $14e^-$ must be generated and the rate of the initiaton is an important property of the catalysts. In many cases there is a trade-off between the stability of a catalyst and its rate of initiation. The mechanism of the initiation is now generally accepted to be a dissociative one (Scheme 53).[75] One of the ligands first dissociates from the metal centre and leaves it in a $14e^-$ configuration. Alkene then coordinates and forms a metalocyclobutane **251** in a cycloaddition reaction. After this the metalocyclobutane cycloreverts to release the initial carbene ligand and to form the active form of the catalyst **253**.

This catalyst then goes on to catalyze the olefin metathesis *via* the catalytic cycle first proposed by Chauvin (Scheme 54).[76] In a productive cross-metathesis a different alkene then adds and forms the metallocyclobutane ring **255**, which then cycloreverts to form the product **257**. This last step leaves the catalyst as the methylidene complex **258**. This is generally thought as the most fragile species in the catalytic cycle and most of the decomposition pathways involve this complex. Finally, another molecule of the first olefin coupling partner adds to the catalyst and the active species is regenerated *via* retro-cycloaddition and release of ethene.

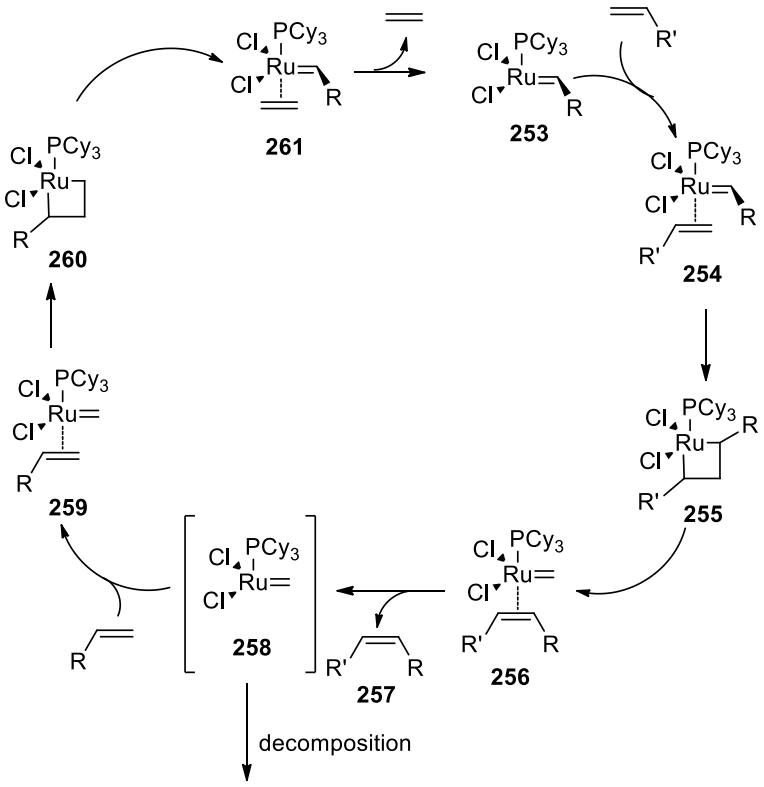

Scheme 54: The catalytic cycle of olefin metathesis

In the last 5 years ring-closing metathesis has become a quite popular way of synthesizing tetrahydropyran rings in the total synthesis of natural products. Thus, Fuwa used ring-closing metathesis in the synthesis of neopeltolide to form dihydropyran **263** from the diene precursor **262.**[77] The dihydropyran ring was then hydrogenated to achieve the tetrahydropyran ring of the neopeltolide (Scheme 55).

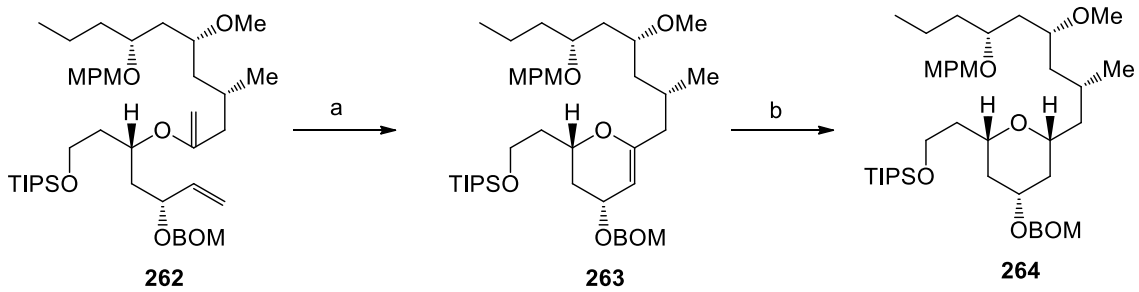

Reagents and conditions: a) Grubbs 2nd gen **247**, toluene, 70 ˚C, 67% b) H_2 (0.8 MPa), 10% Pd/C, 1:1 EtOAc/MeOH, rt, 6.5 h, 81%

Scheme 55: Application of ring-closing metathesis to the synthesis of the THP ring of neopeltolide

Olefin metathesis is generally under thermodynamic control, and the formation of *E* double bonds are usually favoured. Therefore one of the more recent exciting developments in this area have been the Z selective catalysts. For example, Shrock, Hoveyda and Dixon applied a *Z* selective tungsten catalyst **267** to the synthesis of epothilone C and achieved 95% Z selectivity in the ring-closing metathesis step (Scheme 56).[78] Grubbs first generation catalysts only gave 50 to 60 percent *Z* selectivity in the same reaction.

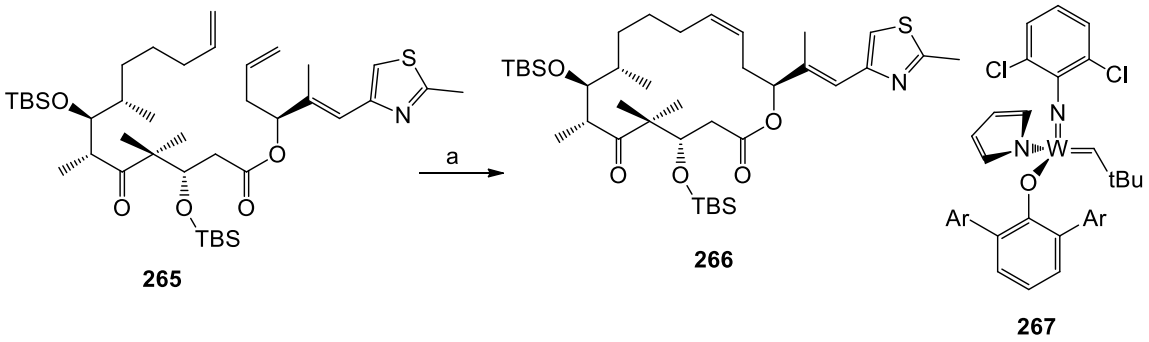

265 **266** **267**

Reagents and conditions: a) 6.5 mol% **267**, mesitylene, 0.6 Torr, 22 ˚C, 4.0 h, 83%, 95:5 *Z*:*E*

Scheme 56: Application of *Z*-selective metathesis.to the synthesis of epothilone

Enantioselective catalysts for olefin metathesis have also been developed and applied to the synthesis of natural products (Scheme 57). On their approach towards africanol, Hoveyda and Shrock used enantioselective ring-opening metathesis to achieve a fused bicyclic scaffold **269** with good enantioselectivity.[79] This scaffold would be quite difficult to achieve asymmetrically by other means.

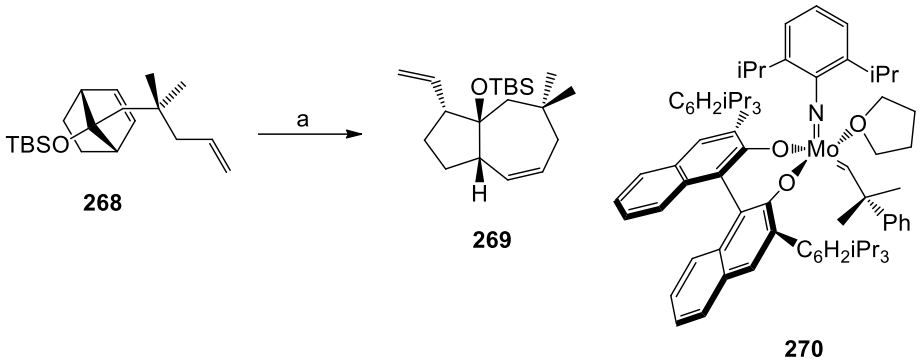

268 **269** **270**

Reagents and conditions: a) 3.0 mol% **270**, pentane, 22^{0}C, 6.0 h, 97%, 87% ee

Scheme 57: Application of asymmetric ring-opening ring-closing metathesis to the synthesis of africanol

Around the time when our studies in the cross-metathesis reaction could be started, we became aware of a recent publication by Fuwa in which they use an oxy-Michael reaction on thioesters to prepare tetrahydropyran rings with good 2,6-*cis* diastereoselectivities (Scheme 58).[80,81] As this methodology promised much higher diastereoselectivities than have been achieved in a classical oxy-Michael reaction, we decided to explore this methodology first.

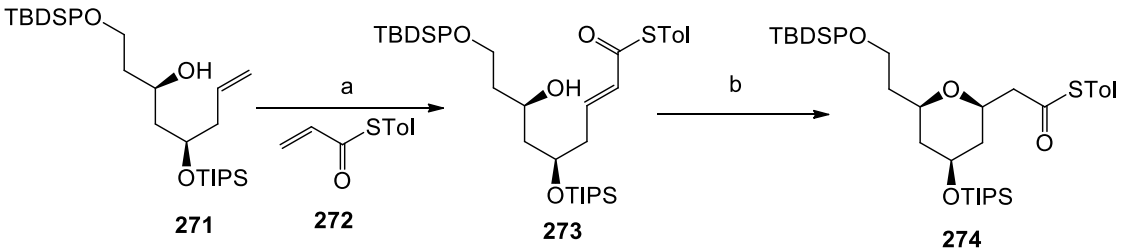

271 **272** **273** **274**

Reagents and conditions: a) 10 mol% HG II **248**, DCM, reflux, **272** b) 20 mol% CSA, DCE, 70 ˚C, 8 h, 90%, dr >20:1

Scheme 58: THP synthesis methodology published by Fuwa.

To this end *p*-tolylacryloylthioester **272** had to be prepared. As Fuwa and coworkers did not provide the experimental procedure for the synthesis of **272**, we attempted to work out the reaction conditions ourselves. However, this seemingly simple reaction proved to be quite a challenge. Pyridine, triethylamine, sodium hydride were all tested as bases in this reaction, but no satisfying conditions were found. In all cases the

major product was *bis*-addition product **277** along with large amounts of polymerization products. The best yield achieved was 24%, however, this still contained small amounts of **277**, which could have impacted the metathesis reaction.

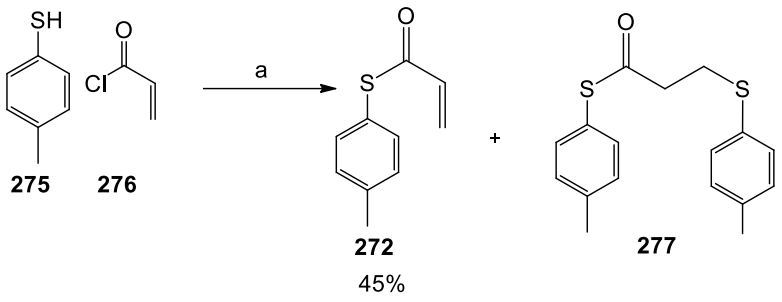

Reagents and conditions: a) i) $NaBH_4$, 15% NaOH ii) BHT, cyclohexane

Scheme 59: Synthesis of the thioester **272**

Unfortunately, our first attempts at the metathesis reaction failed and confirmed that the coupling partner **272** was of insufficient purity. Therefore we consulted the authors of the original publication[80] and followed the procedure they used for the preparation of coupling partner (Scheme 59). In this procedure the nucleophile is sodium thiolate, which makes it a harder nucleophile and less prone to react at the soft β position of the acrolyl chloride. Also, several additives are used to improve the yield and reduce the side reactions. Sodium borohydride is added to the preparation of sodium thiolate to avoid the formation of disulfides. To avoid the polymerization of both arcrolyl chloride and the product, BHT is added to reaction. In addition, the procedure provided by Fuwa contained some useful pointers about the purification of the product. Pleasingly, the reaction proceeded in higher yield (45%) and provided us with thioester **272** of much higher purity.

To achieve good cross-metathesis yield, usually the more accessible of the coupling partners is used in an excess. However, electron poor alkenes homodimerize relatively slowly and therefore Fuwa was able to use only relatively modest excess of 3 equivalents of the thioester and achieve good cross-coupling yields. Following their procedure, a cross metathesis between **272** and **240** was attempted using 10 mol% loading

of Hoveyda-Grubbs 2nd generation catalyst. When this failed, it was determined that for the reaction to take place, one equivalent of the Grubbs catalyst was needed. The likely reason for this was the sulfide byproduct **277** contamination in the initial batches of thioester starting material which could have reduced the activity of the catalyst.

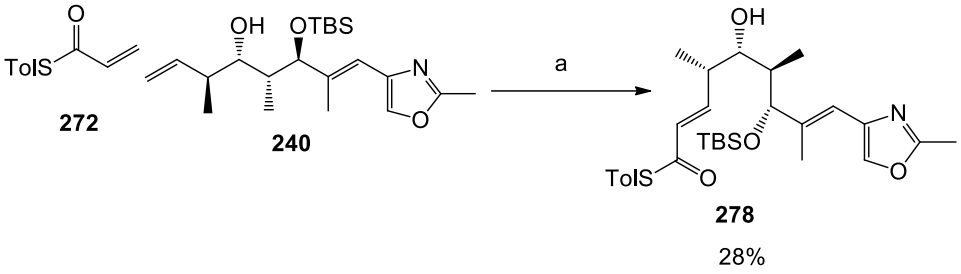

Reagents and conditions: a) 20 mol% HG II, toluene, 55 ˚C, 20 h

Scheme 60: Metathesis reaction

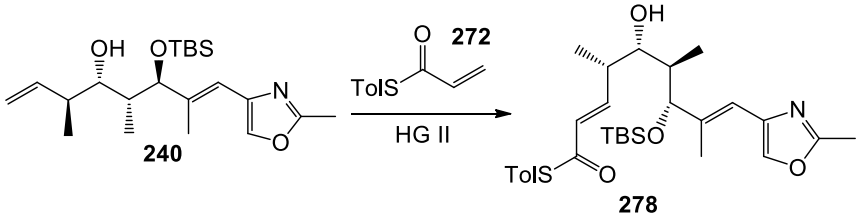

Scheme 61: Optimisation of metathesis reaction

entry	catalyst loading	solvent	temp.	best yield (average)
a	10 mol%	DCM	35 ˚C	0%
b	100 mol%	DCM	35 ˚C	71%
c	20 mol%	DCM	35 ˚C	38%
d	20 mol%	toluene	55 ˚C	62% (28%)
e	20 mol%	toluene	70 ˚C	20%
f	20 mol%	toluene	90 ˚C	0%
g	20 mol%	toluene	reflux	0%
h	50 mol%	DCM	35 ˚C	71% (50%)
i[a]	20 mol%	toluene	55 ˚C	Traces
j[b]	20 mol%	toluene	55 ˚C	25%

[a] 30 mol% $Ti(iOPr)_4$ was added. [b] 2 eq $Ti(iOPr)_4$ was added.

Table 2: Optimization of the metathesis reaction

When pure acryloylthioester **272** was obtained, the cross metathesis reaction was carried out in various conditions, varying catalyst loading and temperature (Scheme 61, Table 2). The pure starting material allowed the catalyst loading to be reduced to a more reasonable 20 mol%, however at 35 °C the reaction still gave only moderate yields (entry **c**). To see if higher temperatures could improve the yield, toluene was used as solvent and the reaction was probed at several temperatures up to reflux. While increasing temperature to 55 °C gave a comparatively good yield of 62%, further increases in temperature resulted in poor yields because of the apparent decomposition of the starting materials (entry **d-g)**. Although we had found conditions which gave reasonable yield, repeating this reaction gave widely varying yields, the average yield being only 28%. To provide material for probing the final step of the synthesis, it was decided to increase the catalyst loading to 50 mol% (entry **h**). Fortunately, the increased catalyst loading improved the yield of the reaction to 71% and allowed us to probe the cyclization step on a small scale.

In the meantime the efforts in optimisation of the metathesis reaction were continued. Both starting materials were repurified by flash chromatography to exclude any contaminant influence on the reaction. However, this did not improve the yields and indicated that any problem with the reaction must be inherent to the substrate.

Fürstner has reported that stable chelating complexes can form between the catalyst and the substrate and can significantly reduce yields in metathesis reactions (Scheme 62).[82] His solution to this problem was the use of mild Lewis acids as an additives to olefin metathesis reactions.

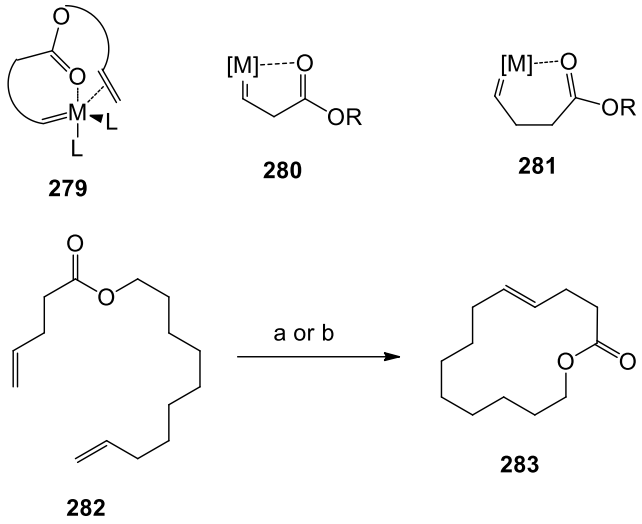

Reagents and conditions: a) 5 mol% Grubbs 0th gen **245**, DCM, 25 ˚C, 3 d, 22% b) 5 mol% **245**, 5 mol% Ti(O*i*-Pr)$_4$, DCM, 40 ˚C, 3 d, 55%

Scheme 62: Effect of Lewis acid on ring-closing metathesis and stable intermediates proposed by Fürstner

In the synthesis of a simple macrocycle **283**, it was found that the addition of 5 mol% of titanium(IV) isopropoxide boosted the yield from 22% to 55%. By analogy, it was hypothesized that in our case the complex **284** could form in the reaction conditions and be the cause of the reduction of catalyst activity (Figure 13). Unfortunately, when titanium(IV) isopropoxide was added to the reaction, no improvement in yields was observed (Table 2, entries **i** and **j**).

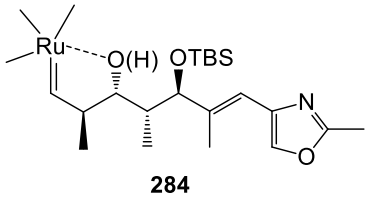

Figure 13: Proposed catalyst-substrate complex

Strategies for the protection of the free alcohol were also explored to test if this can reduce any unwanted interactions between the substrate and the catalyst (Scheme 63).

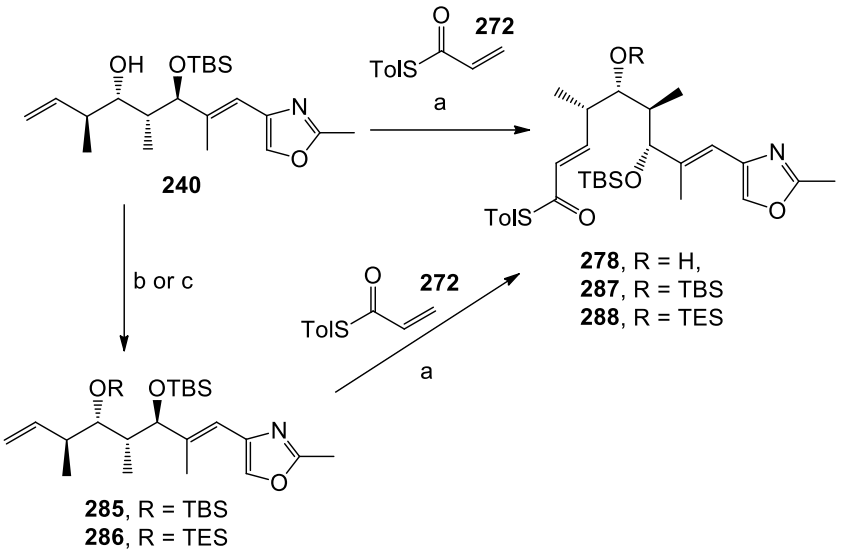

Reagents and conditions: a) 20 mol% HG II, **272**, toluene, 55 ˚C, 20 h b) TBSOTf, DCM, 2,6-lutidine c) TESOTf, DCM, 2,6-lutidine

Scheme 63: Alcohol protecting strategies for the metathesis reaction

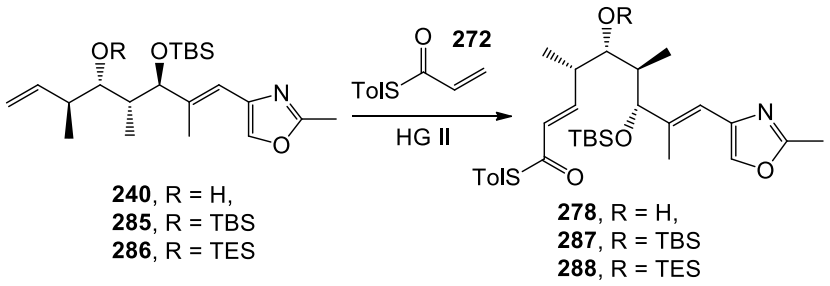

Scheme 64: Further optimisation of the metathesis reaction

entry	R	catalyst loading	solvent	temp.	co-catalyst	best yield (average)
a	TBS	30 mol%	toluene	45 °C		50%
b	TBS	20 mol%	toluene	45 °C		31%
c	TES	20 mol%	toluene	45 °C		62% (38%)
d	TES	20 mol%	ether	reflux	CuI 20 mol%	41%
e	TES	30 mol%	ether	reflux	CuI 20 mol%	38%
f	TES	30 mol%	ether	reflux	NaI 20 mol%	41%
g	**H**	**30 mol%**	**ether**	**reflux**	**CuI 20 mol%**	**79% (67%)**

Table 3: Further optimization of the metathesis reaction

Both TES and TBS protected alcohols (**285** and **286**) were prepared in moderate to good yields. Using these compounds in the metathesis reaction improved the yields to about 45% on average (Table 3, entries **a-c**). While this was an improvement, together with the modest yields of the protection step, the strategy did not provide overall benefit.

Several other strategies have been employed to boost the yields in challenging metathesis reactions. For example, Kadyrov and Grela have used fluorinated solvents in the notoriously difficult formation of tetrasubstituted alkenes *via* a ring-closing metathesis reaction (Scheme 65).[83] When used in combination with ruthenium indenylidene catalyst **291**, trifluoromethylbenzene allowed essentially a tripling of the yield from 28% to 94%. This marked increase in activity has been suggested to be caused by the formation π-π complexes between the solvent and the indenylidene ligand.

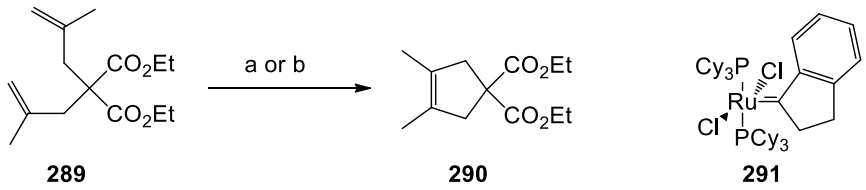

289 **290** **291**

Reagents and conditions: a) 2 mol% **291**, DCE, 70 ˚C, 3 h, 28% b) 2 mol% **291**, $CF_3C_6H_5$, 70 ˚C, 3 h, 94%

Scheme 65: The use of fluorinated solvents for promotion of RCM

Lipshutz *et al* has reported the use of CuI and NaI co-catalysts as a way to improve yields in challenging metathesis reactions (Scheme 66).[84] The authors proposed that iodide ion stabilizes the catalyst, thus increasing its overall activity. They also proposed that copper acts as the phosphine scavenger, however this mode of action would not apply to our reaction conditions as Hoveyda-Grubbs 2nd generation catalyst does not have a phosphine ligand.

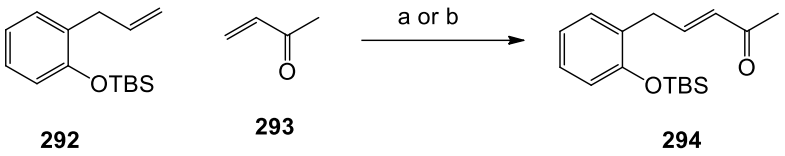

292 **293** **294**

Reagents and conditions: a) 3 eq **293**, 2 mol% **247**, Et_2O, 22 ˚C, 15 h, 43% b) 3 eq **293**, 2 mol% **247**, 3 mol% CuI, Et_2O, 22 ˚C, 15 h, 85%

Scheme 66: The use of CuI additive for the enhancement of cross-metathesis reaction yields

Intrigued by this approach we decided to test if the addition of CuI co-catalyst could solve our problems. Initial reactions using the TES protected substrate **286** did not give promising results (entries **d-f**). However, when the reaction was applied to the unprotected substrate **240** the use of CuI improved the yield to 79% (Scheme 67). We were very glad when this result was confirmed in repeated experiments and that it was also robust to moderate scale up.

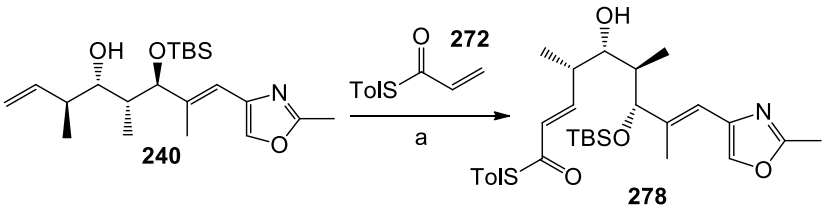

Reagents and conditions: a) 20 mol% HG II, CuI 20 mol%, **141**, Et_2O, reflux, 3 h, 79%

Scheme 67: Optimised metathesis reaction

This result is particularly impressive because the reaction times could be significantly reduced from 20 hours to 3 hours and the reaction temperatures were also reduced from 55 ˚C to 35 ˚C - the boiling point of diethyl ether. Thus the simple addition of copper(I) iodide co-catalyst gave at least an order of magnitude improvement in the activity of the ruthenium catalyst.

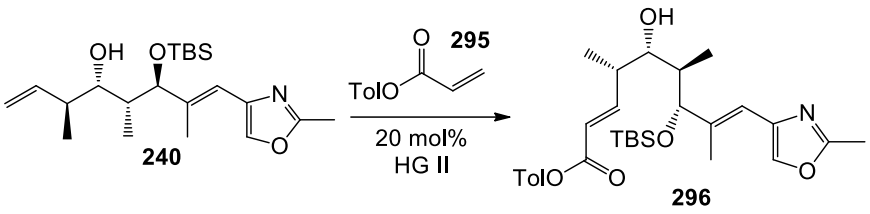

Scheme 68: Synthesis of the oxo-esters

entry	solvent	temp.	best yield (average)
a	DCM	35 °C	36%
b	toluene	55 °C	60% (48%)

Table 4: Synthesis of the oxo-esters

We also prepared the ester analogue **295** of the thioester **272** and used it in metathesis reaction (Table 4, entries **a** and **b**). This was done mainly to later compare the reactivities and selectivities of both cyclization precursors in the oxy-Michael reaction. Metathesis reaction in DCM in 35 °C gave poor yield, however switching to toluene and raising the temperature to 55 °C improved the yield to 60%. Similarly to the case of thioester, the yields were highly variable and generally quite poor. When direct comparison experiments with repurified starting materials were conducted, the yields from both the oxo-ester and thioester reactions were essentially the same. This indicates that it is unlikely that either the thioester or any contaminants in any of the starting materials were the source of our problems in the cross-metathesis reaction. It is instead probable that the oxazole moiety in the substrate was complexing with the catalyst and inhibiting the reaction. It has been shown previously that oxazole containing fragments can be poor substrates for cross-metathesis.[85] Very similar cross-metathesis reactions were later conducted in our group on substrates without the oxazole moiety. It was found that the catalyst loadings in these reactions could be significantly lowered and the reactions were also significantly faster, thus indirectly suggesting that the vinyloxazole moiety was indeed the cause of our

troubles. Our studies on analogues with other substituents will be discussed in more detail in section 9.5.

With the metathesis reaction successfully optimized, we were now in position to close the tetrahydropyran ring using oxy-Michael reaction. Historically the oxy-Michael reaction has been much less developed when compared to the classical Michael reaction and this is due to several factors. One of them is the poor nucleophilicity of the alcohols arising from their high pK_a values and the inherent reversibility of the reaction (Scheme 69).[86] This has generally been solved by the use of more nucleophilic surrogates, for example, peroxide instead of a hydroxyl. One can also achieve better results by the use of more acidic alcohols, like phenols, however this limits the substrate scope.

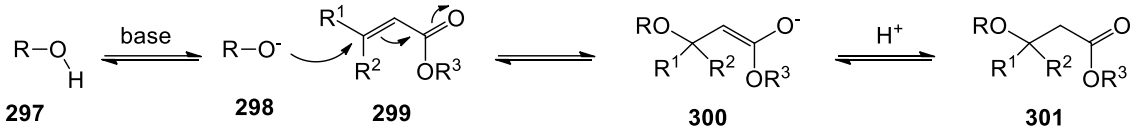

Scheme 69: General mechanism of the oxy-Michael reaction

This approach was used in an organocatalytic oxy-Michael/Michael domino reaction to synthesize 4H-chromenes (Scheme 70).[87] In this reaction the chiral proline-derived catalyst **304** forms an iminium ion with the alkynal **303**. This then reacts in an oxy-Michael reaction to give the allenamine intermediate **305**. Finally, the allenamine reacts in a Michael reaction to give the products in excellent yields up to 98% and with excellent enantioselectivites.

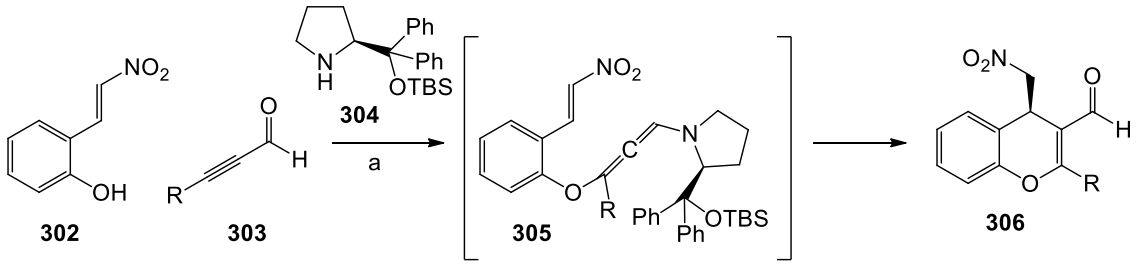

Reagents and conditions: a) 15 mol% **304**, toluene, 0 ˚C, 92-97%, 98-99% ee

Scheme 70: Oxy-Michael/Michael cascade in the synthesis of chromenes

Another elegant solution to achieving catalytic enantioselective oxy-Michael reaction has been reported by You (Scheme 71).[88] By using the chiral BINOL derived phosphoric acid **309** and molecular sieves they achieved a catalytic intramolecular desymmetrizing oxy-Michael reaction and formed the products **308** in good yields and enantioselectivities. This methodology was then applied to the synthesis of three small biologically active natural products cleroindicins D (**310**), C (**311**) and F (**312**).

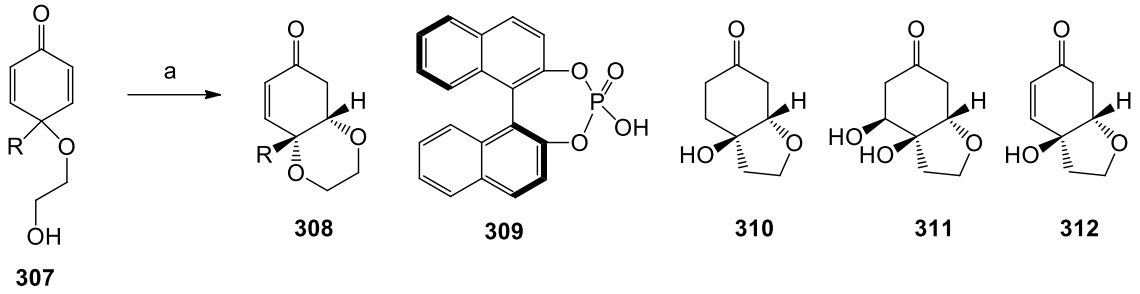

Reagents and conditions: a) 10 mol% **309**, DCM, rt, 0.5-3 h

Scheme 71: You's desymmetrization of cyclohexadienones *via* oxy-Michael reaction

In the last two decades intramolecular oxy-Michael reaction has gradually been developed into an attractive approach to the synthesis of tetrahydropyran rings. Both Forsyth and Paterson used the oxy-Michael reaction as the key step in their syntheses of the core fragment of phorboxazoles (Scheme 3 and 6). Lee's synthesis of leucascandrolide A illustrates nicely both the challenges of stereocontrol in this type of reaction and also how these challenges can be overcome (Scheme 72).[89]

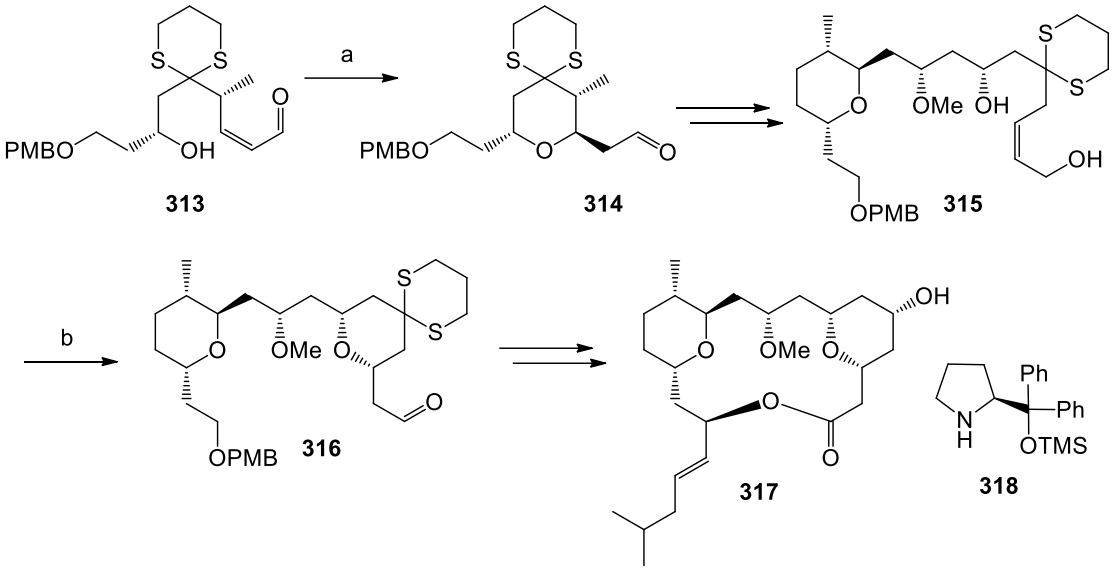

Reagents and conditions: a) 20 mol% **318**, 20 mol% BzOH, DCM, -40 ˚C 98%, dr >20:1 b) MnO_2, DCM, 25 ˚C, 12 h, 86%, dr >20:1

Scheme 72: Lee's use of oxy-Michael reactions in the synthesis of leucascandrolide A

Thus, the α,β-unsaturated aldehyde **313** was prepared *in situ* from the corresponding allylic alcohol. However, under reaction conditions the yield of the cyclized product **314** was only 12% and gave the tetrahydropyran ring as 1:1 mixture of 2,6-*cis* and 2,6-*trans* diastereomers. To speed up the reaction, pyrrolidine base was used and this increased the yield to 98%, but gave only the undesired 2,6-*cis* isomer. Lowering the temperature switched the diastereoselectivity to 7:1 in favour of 2,6-*trans* product. While the authors do not provide explanation for this shift to the other product, it is likely that the imine catalyzed reaction switches from the thermodynamic control to kinetic control at lower temperatures. Finally, they found that use of chiral proline-derived amine **318** improved the diastereoselectivity to greater than 20:1 and gave the desired product in 98% yield. After a few more steps they synthesized another cyclization precursor **315**. As this time the desired product was the 2,6-*cis* product, the initial conditions worked fine and gave the product in good yield and excellent diastereoselectivity.

After the successful optimisation of the metathesis reaction we were in position to try to achieve the oxy-Michael cyclization. We reasoned that it would be possible to do the

deprotection and cyclization in one step, and to that end we tested both camphorsulfonic acid (CSA) and tetrabutylammonium fluoride as the TBS removal agents (Scheme 73, Table 5).

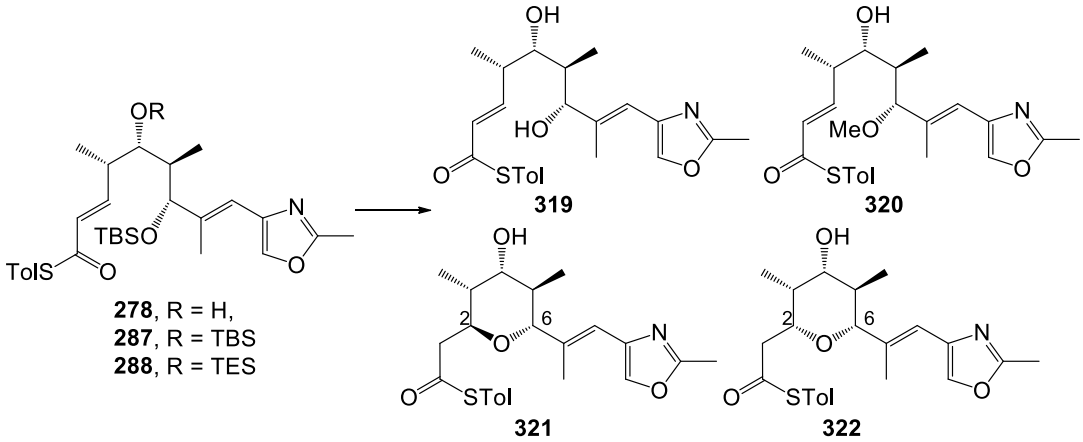

Scheme 73: Investigation of the Oxy-Michael reaction on thioesters

Entry	R	Conditions	Yield
a	H	0.2 eq CSA, DCE/MeOH 3:1, 30 °C	**319** (56%), **322** (trace)
b	H	0.5 eq CSA, DCE/MeOH 3:1, 55 °C	**322** (20%), dr 10:1
c	TBS	0.5 eq CSA, DCE/MeOH 3:1, 45 °C	no reaction
d	TES	0.5 eq CSA, DCE/MeOH 3:1, 45 °C	**322** (26%), **320** (32%)
e	TES	0.5 eq CSA, DCE/iPrOH 3:1, 45 °C	**322** (trace)
f	TES	0.1 eq TsOH, THF/H_2O 20:1, rt	no reaction
g	TES	TFA/H2O/DCM 4:1:5, rt	**322** (35%)
h	**H**	**TFA/H2O/DCM 4:1:5, 0 °C - rt**	**322 (71%), dr 13:1**
i	**H**	**1 eq TBAF, 0.2 eq AcOH, THF, rt**	**321 (35%), dr >20:1**
j	H	1 eq TBAF, THF, rt	decomposition

Table 5: Investigation of the Oxy-Michael reaction on thioesters

In both cases the cyclization precursor underwent cyclization immediately after deprotection. We were surprised to find, however, that each method of deprotection and cyclization gave a different diastereomer in high diastereoselectivity. Camphorsulfonic acid catalyzed deprotection and cyclization yielded the required 2,6-*cis* THP ring **322** with good diastereoselectivity (dr 10:1, entry **b**) while buffered fluoride TBS removal provided

the 2,6-*trans* tetrahydropyran **321** with excellent diastereoselectivity (dr >20:1, entry **i**). Unbuffered TBAF gave only the decomposition of the starting material, likely due to the highly basic nature of the TBAF (entry **j**).

While the observed stereodivergence was very intriguing (Scheme 74), the yields of these reactions were far from satisfying. The acid catalyzed cyclization in particular needed optimization as the 2,6-*cis* product had the required geometry for the C20-C32 core fragment of phorboxazoles. Since this coincided with experiments in metathesis reaction using the protected substrates and the first silyl ether deprotection did not seem to be slow or difficult, these doubly protected cyclization precursors **287** and **288** were used for further experiments.

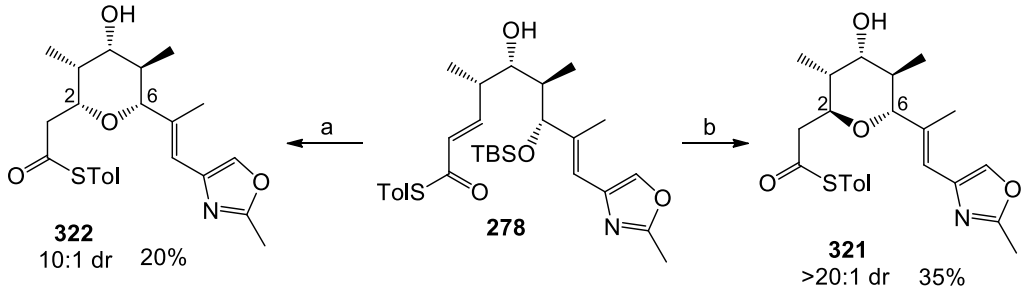

Reagents and conditions: a) 20 mol% CSA, DCM, MeOH, 55 ˚C b) 1.5 eq TBAF, 20 mol% AcOH, THF, rt

Scheme 74: Stereodivergent oxy-Michael reaction

With TBS as the other protecting group, deprotection proved to be impossible under the conditions investigated (entry **c**), therefore it was not used for any further experiments. Triethylsilyl protected compound gave slightly improved yield of the 2,6-*cis* product (26%), however, the formation of significant amounts of the methylated product was also observed (entry **d**). To avoid the methylation, we tried using isopropanol instead of methanol, however, this gave only trace amounts of the products (entry **e**). It was then decided to look at other Brønsted acids as catalysts for the deprotection and cyclization. In the presence of tosylic acid in THF/water mixture no reaction was observed and the

starting material was reisolated (entry **f**). A mixture of TFA, DCM and water gave the desired 2,6-*cis* product in higher yield and of higher purity (entry **g**). Encouraged by this result we repeated the reaction using the original cyclization precursor without the TES protecting group and lowered the initial temperature to 0 °C. These changes significantly improved the yield of the reaction to 71%, and provided the desired tetrahydropyran (entry **h**).

The structures of tetrahydropyrans **322** and **321** were determined using ^{1}H NMR and NOE techniques. The 400 MHz ^{1}H NMR spectrum of both fragments exhibited peaks in three main regions: 6-8 ppm for aromatic and alkene protons, 2.5-4.5 ppm for protons on a carbon bound to oxygen and α to the thioester and 1-3 ppm for the remaining protons.

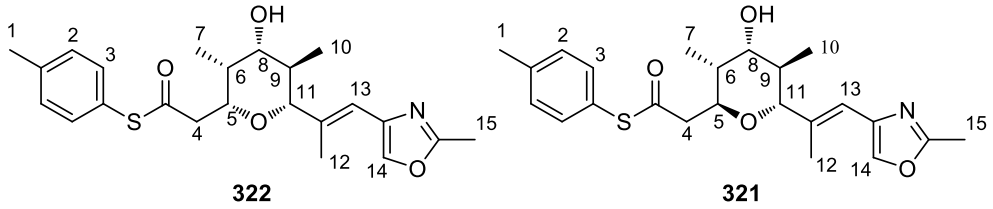

Figure 14: Numbering for NMR analysis of 2,6-*cis* THP **156** and 2,6-*trans* THP **157**

For the 2,6-*cis* THP **322** singlet peak at 7.49 ppm was assigned as the oxazole proton H-14. Two doublets at 7.26 and 7.20 ppm with matching coupling constants of 8.1 Hz were assigned as H-2 and H-3, respectively. A singlet 6.18 ppm was assigned as the alkene proton H-13. A ddd at 4.02 ppm with coupling constants of 6.8, 6.8 and 1.9 Hz was assigned as the H-5, because it matched the coupling constants exhibited by the diastereotopic H-4 protons at 2.97 and 2.76 ppm. Also, its third coupling constant of 1.9 Hz is consistent with axial-equatorial coupling to H-6. A dd at 3.52 ppm was assigned as H-8, as it has a diaxial 10.3 Hz coupling to H-9 and an axial-equatorial 4.6 Hz coupling with H-6 – both consistent with the proposed stereochemistry of the THP ring. A doublet at 3.49 ppm was assigned as H-11 – its single coupling constant of 10.1 Hz is consistent with a transdiaxial coupling to H-9. Both of doublets of doublets at 2.97 and 2.76 showed a

large 15.2 Hz coupling to each other in addition to H-5 and were therefore both assigned as H-4. The two singlets at 2.45 and 2.36 were assigned as the H-15 and H-1 methyl groups, respectively. A qdd at 1.99 ppm with *J* values of 6.9, 4.6 and 1.9 Hz was assigned as H-6 and confirmed by NOE experiments, which will be discussed shortly. A singlet at 1.93 ppm was assigned as the H-12 methyl group. A ddq at 1.71 with *J* values of 10.3, 10.1 and 6.5 Hz was assigned as H-9, and two doublets at 1.02 and 0.85 ppm as the H-7 and H-10 methyl group – all assignments greatly aided by NOE experiments (Figure 15).

NOE experiments on the 2,6-*cis* THP **322** were conducted in benzene-d_6 to increase distance between two key protons – H-8 and H-11, which would otherwise give ambiguous results. Irradiation of H-5 returned a large correlation with H-11 (7.5%), confirming the 2,6-*cis* geometry of this compound. It also showed a correlation with H-4 and H-6, thus allowing unambiguous assignment of the latter. Another key interaction is between the H-9 proton and the H-7 methyl group, again showing that the two substituents are on the same side of the ring and the assumed stereochemistry is correct.

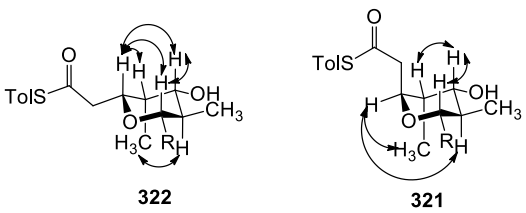

Figure 15: NOE correlations of 2,6-*cis* THP **322** and 2,6-*trans* THP **321**

For the 2,6-*trans* THP **321** singlet peak at 7.49 ppm was assigned as the oxazole proton H-14. Two doublets at 7.27 and 7.19 ppm with matching coupling constants of 8.0 Hz were assigned as H-2 and H-3, respectively. A singlet 6.26 ppm was assigned as the alkene proton H-13. A ddd at 4.35 ppm with coupling constants of 7.3, 7.3 and 2.0 Hz was assigned as the H-5, because it matched the coupling constants exhibited by the diastereotopic H-4 protons at 3.16 and 2.92 ppm. Also, its third coupling constant of 2.0

Hz is consistent with equatorial-equatorial coupling to H-6. A doublet at 3.78 ppm was assigned as H-11 – its single coupling constant of 10.0 Hz is consistent with a transdiaxial coupling to H-9. A dd at 3.72 ppm was assigned as H-8, as it has a diaxial 9.2 Hz coupling to H-9 and an axial-equatorial 4.2 Hz coupling with H-6 – both consistent with the proposed stereochemistry of the THP ring. Both of doublets of doublets at 3.16 and 2.92 showed a large 14.4 Hz coupling to each other in addition to H-5 and were therefore both assigned as H-4. The two singlets at 2.45 and 2.36 were assigned as the H-15 and H-1 methyl groups, respectively. A qdd at 1.99 ppm with *J* values of 6.9, 4.2 and 2.0 Hz was assigned as H-6 and confirmed by NOE experiments. A singlet at 1.94 ppm was assigned as the H-12 methyl group. A ddq at 1.89 with *J* values of 10.0, 9.2 and 6.5 Hz was assigned as H-9, and two doublets at 1.16 and 0.90 ppm as the H-7 and H-10 methyl group – all assignments aided by NOE experiments (Figure 15).

NOE experiments on the 2,6-*trans* THP **321** were conducted in $CDCl_3$. Irradiation of H-5 showed no correlation with H-11, confirming the 2,6-*trans* geometry of this compound. It also showed a correlation with H-7 methyl group (2.4%) and H-9 proton (1.7%), further confirming that all three substituents are on the same side of the ring and helping the assignment of the signals. Another key interaction is between the H-8 proton and the H-11 proton, again showing that the two atoms are on the same side of the ring and that the assumed stereochemistry is correct.

We were happy to confirm the structure of the 2,6-*cis* THP **322** and to conclude our synthesis of the C20-C32 core fragment of phorboxazoles in such an efficient manner. Overall our synthesis was 7 steps long with a 31% overall yield and compares very favourably in both regards with syntheses reported so far.

To explore further the factors influencing the diastereoselectivity of this reaction, the oxo-ester analogue **296** of the cyclization precursor **278** was prepared. Cyclization was

then attempted using both of the previously described methods. While the TFA catalyzed the deprotection of the **296**, it failed to effect cyclization (Table 6, entry **a**). The buffered fluoride procedure, however, yielded the 2,6-*trans* cyclised product in 71% yield and excellent diastereoselectivity (entry **b**). Unbuffered fluoride TBS removal was also attempted, but just like in the case of thioesters, it caused the decomposition of the starting material.

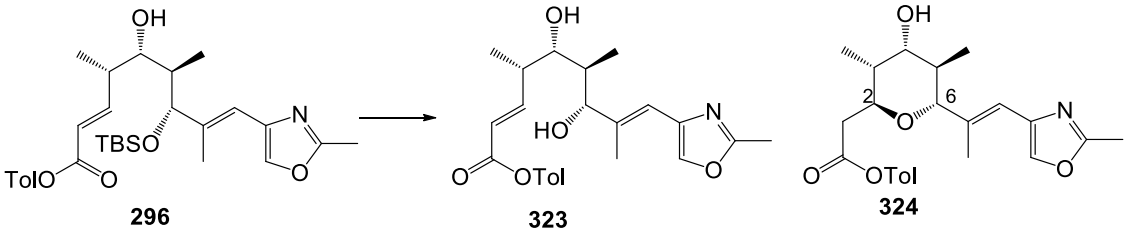

Scheme 75: Investigation of the Oxy-Michael reaction on oxo-esters

entry	conditions	yield
a	TFA/H_2O/DCM 4:1:5, 0 °C - rt	**323** (68%)
b	**1 eq TBAF, 0.2 eq AcOH, THF, rt**	**324 (71%), dr >20:1**
c	1 eq TBAF, THF, rt	decomposition

Table 6: Investigation of the Oxy-Michael reaction on oxo-esters

To test if the TBAF and acidic conditions are under kinetic or thermodynamic control, crossover experiments were also conducted (Scheme 76). When 2,6-*trans* THP **321** was submitted to the acidic cyclization conditions, no interconversion was detected. The 2,6-*cis* THP **322** was also submitted to TBAF conditions and no interconversion was observed, only gradual degradation of the starting material. This strongly suggests that in both cases the reactions are under kinetic control.

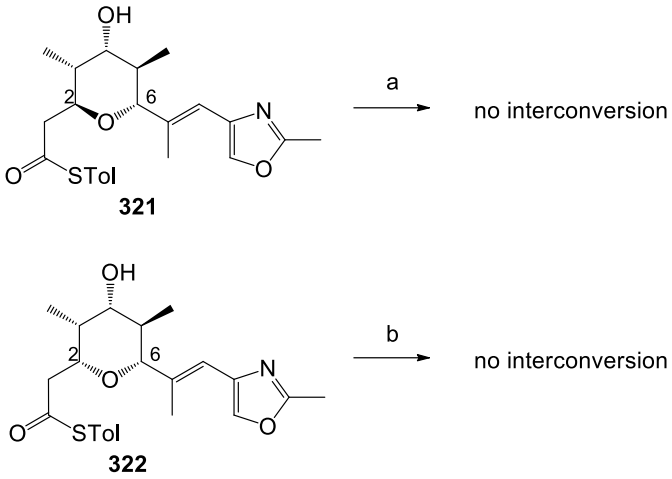

Reagents and conditions: a) TFA, DCM, H_2O, rt b) 1.5 eq TBAF, 20 mol% AcOH, THF, rt

Scheme 76: Crossover experiments

While the remarkably effective stereodivergence is intriguing, its mechanistic causes are not entirely clear. Fuwa in their study of thioester cyclization observed a similar stereodivergence – camphorsulfonic acid catalyzed reaction gave the 2,6-*cis* tetrahydropyran while potassium *t*-butoxide gave the 2,6-*trans* product (Scheme 77).[81] Based on the studies of Houk and Strozier[90] Fuwa proposed that the acid-catalyzed reaction has an allylic cationic transition state and proceeds *via* an S_N1-type mechanism (Scheme 78). The transition state **329** is the chair-like transition state and would give the 2,6-*cis* product. It would be favoured because all of the steric interactions are minimised. In contrast, the chair-like transition state **330** leading to the 2,6-*trans* product would be disfavoured because of a steric interaction between the thioester α carbon and the 4-axial hydrogen atom.

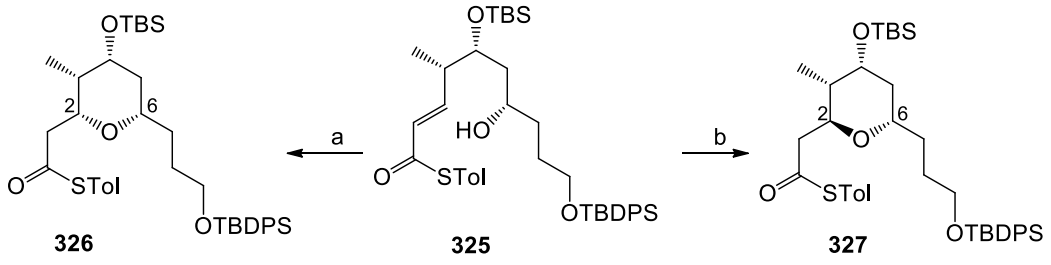

Reagents and conditions: a) CSA, DCE, 70 ˚C, 92%, dr 14:1 b) KO*t*-Bu, THF, -78 ˚C, 85%, dr 4:1

Scheme 77: Stereodivergent Oxy-Michael reaction encountered by Fuwa

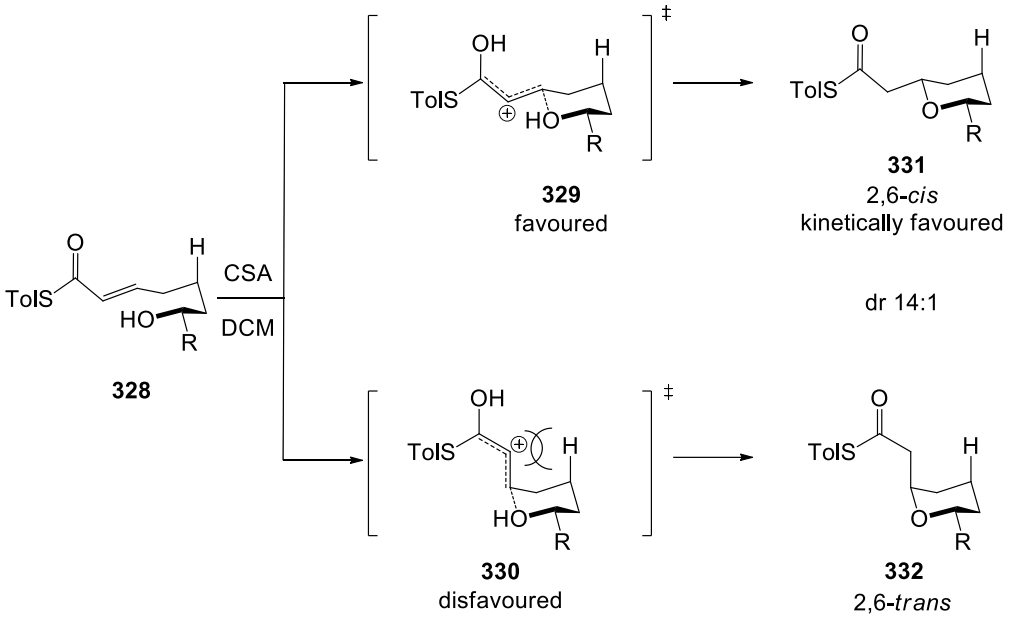

Scheme 78:The transition states for acid catalyzed cyclization proposed by Fuwa

For the potassium butoxide mediated cyclization Fuwa *et al.* propose two very similar transition states (Scheme 79). The main difference in this case is a proposed chelating interaction between the potassium ion and the substrate in the transition state **334** that leads to the 2,6-*trans* product. Fuwa proposes that the coordination of the thioester oxygen and the alkoxide to the potassium ion stabilises this transition state in spite of the same unfavourable steric interactions as in the acidic case. In the alternative transition state **333** the thioester oxygen atom would be too far away for chelation and thus the 2,6-*cis* product would be kinetically disfavoured in these conditions. While this is certainly a plausible explanation for the 2,6-*trans* selectivity encountered by Fuwa, the chelation cannot explain our observations as in our conditions there are no coordinating cations in the reaction mixture.

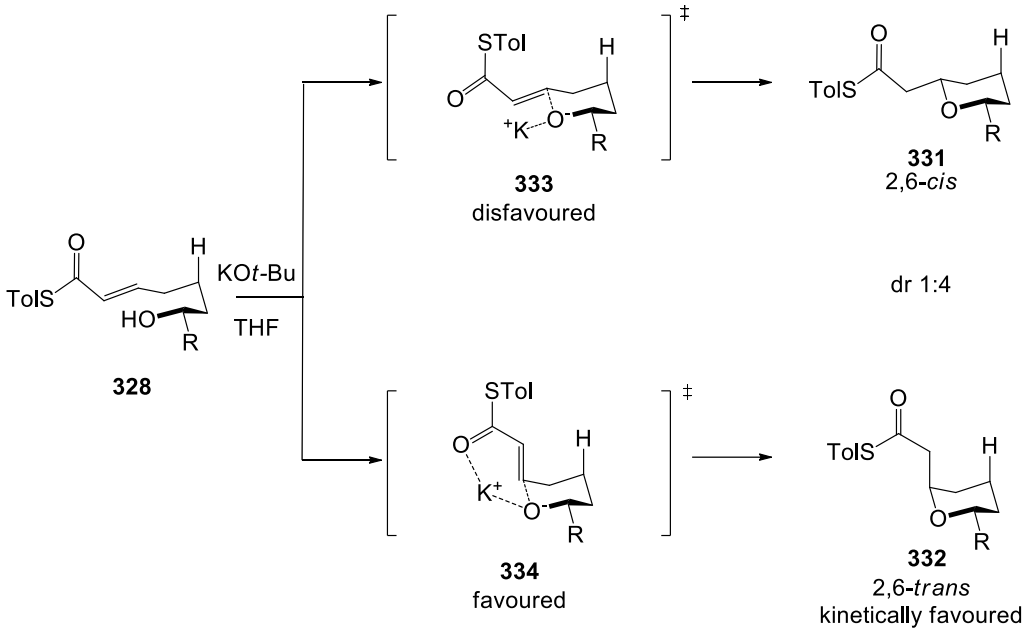

Scheme 79: The transition states for base catalyzed cyclization proposed by Fuwa

Soon after the initial report by Fuwa, Urpi and Romea published their work on total synthesis of (+)-herboxidiene.[91] In their studies towards this natural product they envisioned forming the tetrahydropyran ring *via* a base catalyzed oxy-Michael reaction (Scheme 80). They reasoned that the reaction would give 2,6-*cis* product as the thermodynamic product. Unfortunately, the oxy-Michael reaction gave a disappointing 1.8:1 *cis*:*trans* mixture of diastereomers. They proposed that the 2,6-*trans* product arises from the transition state **338** where the 4-hydroxyl group forms an intramolecular hydrogen bond and stabilizes the boat-like transition state. Support to this explanation is given by the fact that only after the removal of the 4-hydroxyl group the undesired 2,6-*trans* product could be equilibrated cleanly to the 2,6-*cis* product.

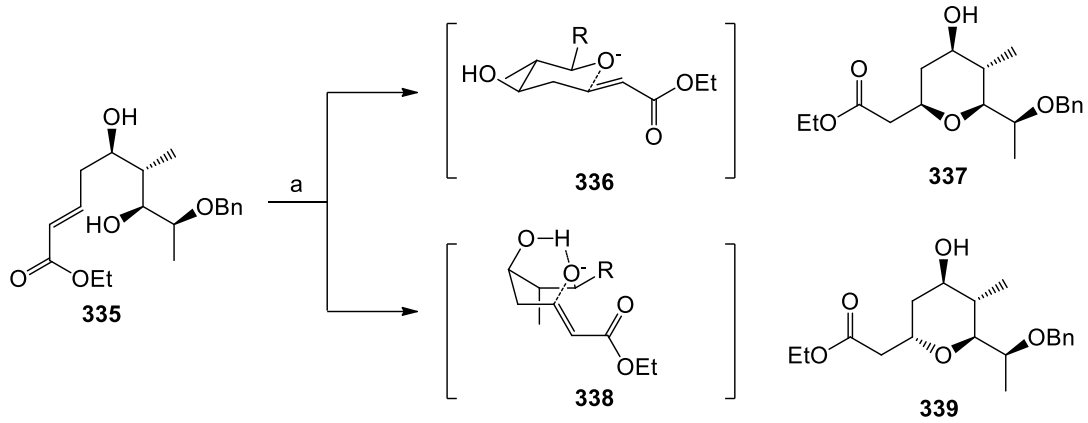

Reagents and conditions: a) DBU, toluene, 100 ˚C, 5h

Scheme 80: Urpi's rationale for the lack of stereochemistry in base mediated oxy-Michael reaction

Soon after we reported our synthesis of the C20-C32 core fragment,[92] Paterson's group reported their use of oxy-Michael reactions in the synthesis of the western fragment of madeirolide (Scheme 81).[93] They had initially envisaged the use of the oxy-Michael reaction on oxo-esters to form the tetrahdyropyran ring, just like they had done with good effect in the synthesis of the core fragment of phorboxazoles (Scheme 6). However, when they attempted this cyclization in basic conditions, they achieved the synthesis of the undesired 2,6-*trans* tetrahydropyran with excellent diastereoselectivity. They offer a similar explanation to that of Urpi and Romea - that the 2,6-*trans* selectivity arises from a boat like transition state featuring an intramolecular hydrogen bond between the 4-hydroxyl group and the alkoxide nucleophile. It is worth noting that as potassium butoxide was used as the base, in principle the chelating interaction with the potassium ion could also be used to explain the 2,6-*trans* selectivity.

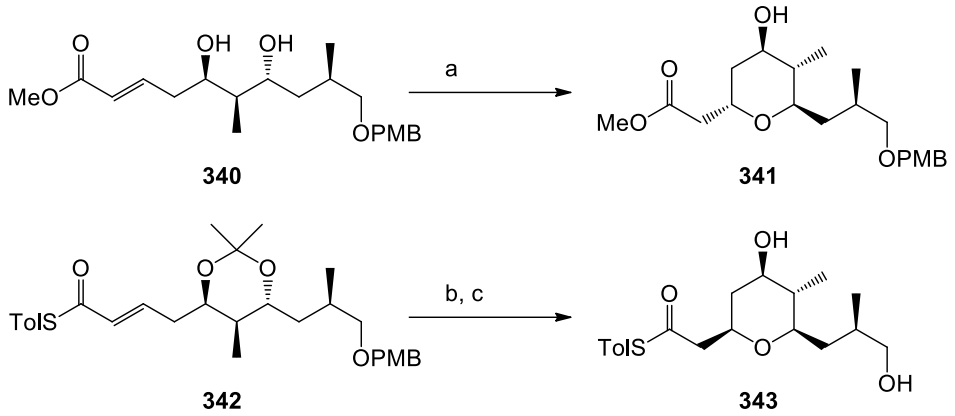

Reagents and conditions: a) *t*-BuOK, THF, -78 ˚C – rt, 3 h, 78%, dr >20:1 b) TsOH, DCM, 4.5 h c) DDQ, DCM, pH 7 buffer, 0 ˚C, 1 h, 61% over 2 steps, dr >20:1

Scheme 81: Stereodivergence in Paterson's synthesis of the C1-C11 fragment of madeirolide

Paterson *et al.* then decided to work around this unexpected result by using Fuwa's methodology. They prepared the corresponding thioester **342** and submitted it to Fuwa's cyclization conditions to give the desired 2,6-*cis* tetrahydropyran with excellent diastereoselectivity and yield.

Overall it can be seen that with the rise of popularity of oxy-Michael reaction as a way of forming the THP rings, several interesting observations have been made in the last few years regarding the stereocontrol of this reaction. Previously, when the 2,6-*cis* tetrahydropyrans were desired, the thermodynamic control was usually relied upon for stereocontrol. However, as we have seen in this chapter, the production of the 2,6-*cis* product is by no means guaranteed even under thermodynamic conditions. Therefore Fuwa's development of kinetic conditions for highly selective formation of the 2,6-*cis* THP rings is very welcome.

The Clarke group along with several other groups have observed a stereodivergence to a larger or lesser degree. More interestingly, the mechanistic causes of this stereodivergence are not entirely clear and would therefore be an interesting field of further study. Tetrahydropyran rings in both the 2,6-*cis* and 2,6-*trans* configurations are quite often encountered in natural products of biological interest. Therefore a well

understood and general way of providing both diastereomers would be an exciting advance in this area. For this reason we decided to investigate the stereodivergence in more detail in a computational study, which will be discussed in the next chapter.

8.4 Computational investigations

8.4.1 Background. Along with the rise of the power of computers, computational methods are increasingly becoming an extremely useful tool for a synthetic chemist. The four major classes of computational methods are molecular mechanics, semi-empirical methods, *ab initio* methods and density functional theory.[94]

Molecular mechanics are the simplest set of methods in common use today. The main characteristic of this class is that all covalent bonds are modelled as a classical spring. Thus for every bond several parameters are assigned, including spring constant and equilibrium length. The downside is that these methods are fully empirical and can only be reliably used for compounds that have similar bonds to those that were used in the parametrization of the force field. Another drawback is that molecular mechanics cannot be used to model reactions as the bond formation and breaking cannot be modelled. On the other hand, these techniques are exceedingly fast and for this reason were the first to become useful to the organic chemist. Because of the speed of this approach, nowadays it is particularly useful for the modelling of biological molecules, like proteins, carbohydrates, DNA and RNA. In several impressive studies the whole ribosome and the entirety of human immunodeficiency virus were modelled at all-atom detail. [95,96]

The semi-empirical methods were developed mainly to overcome the inability of molecular mechanics to model bond forming and breaking. It was developed from the basic Hückel method to cover all electrons in a molecule, not just those in π systems.

Again, these systems need parametrization based on experimental data or higher level calculations and therefore can only be applied to similar problems. While this approach is slower than molecular mechanics, it is still very fast. It was quite popular about 20 years ago, but nowadays because of the lack of accuracy and rise of computing power, more sophisticated methods have largely replaced semi-empirical calculations. They are still used as the first step of larger computational studies involving higher-level methods. Another modern application of semi-empirical methods is, for example, modelling of proteins at quantum-mechanical level.[97] In these cases, the speed is the most important factor in the choice of the method because of the sheer scale of the problem.

A much higher precision is generally offered by the the *ab initio* class of computational methods. The Hartree-Fock self-consistent field method was the first one developed, but since then a range of post-Hartree-Fock approaches have been developed, such as Møller-Plesett perturbation theory and coupled-cluster methods. These were developed since the earliest days of the field, but because of the computational complexity for a long time they were impractical for all but the simplest systems and were of little use to organic chemists. Breakthrough was achieved by Pople who realised that the Slater-type orbitals can be approximated by several Gaussian orbitals. Even though the description of a single orbital required several Gaussian functions, the computational simplification was still remarkable and along with the improvements in computer hardware have made these methods much more accessible. Based on this principle he and others developed the well-known program GAUSSIAN. For these and other contributions he was awarded the 1998 Nobel Prize in Chemistry along with Kohn, who developed the density functional theory.

The final class of the computational chemistry techniques is the density functional theory. The basic principle of this class is that the ground-state properties of a system are defined simply by the electron density distribution instead of the positions and

mutual interactions of every individual electron. This reduces the problem of N electrons with 3N degrees of freedom to the problem of electron density with just 3 spatial degrees of freedom. This simplifies the problem significantly and gives access to larger systems while retaining most of the precision of pure *ab initio* methods. Initially, this approach was only used in solid state physics, but with the developments in accuracy, in the last 20 years it has become the method of choice for the modelling of organic reactions. The most popular functional by far is still the B3LYP,[98] but several others have been developed with improved treatment of non-bonding interactions, including M06 and ωB97 families. [99,100]

The encountered ability to switch the diastereoselectivites of the oxy-Michael reaction intrigued us. Also, it was not entirely clear to us why oxo-esters were completely unreactive in the conditions that were so efficient for thioesters. Therefore we decided to investigate the factors governing the diastereoselectivites and reactivities of these cyclization reactions by conducting a computational study.

Thus, the questions that would ideally be answered by this study were:

1. Why are the TBAF mediated cyclizations 2,6-*trans* selective?
2. Why are the acid mediated cyclizations 2,6-*cis* selective?
3. Why are only thioesters reactive in the acidic conditions?

8.4.2. Fluoride mediated cyclization. We started by investigating the TBAF effected deprotection and cyclization. We assumed that the deprotection is fast and has no influence on the diastereoselectivity of the reaction. The TBAF conditions of the reaction mean that the active molecule is the alkoxide **344** (Scheme 82), which then attacks the conjugate double bond to form either the 2,6-*trans* enolate **345** or the 2,6-*cis* enolate **346**. Both enolates are then quenched to the corresponding products **321** and **322** upon workup. Our previous crossover experiments also suggested that the reaction is under kinetic control and therefore the modelling of transition states would be necessary.

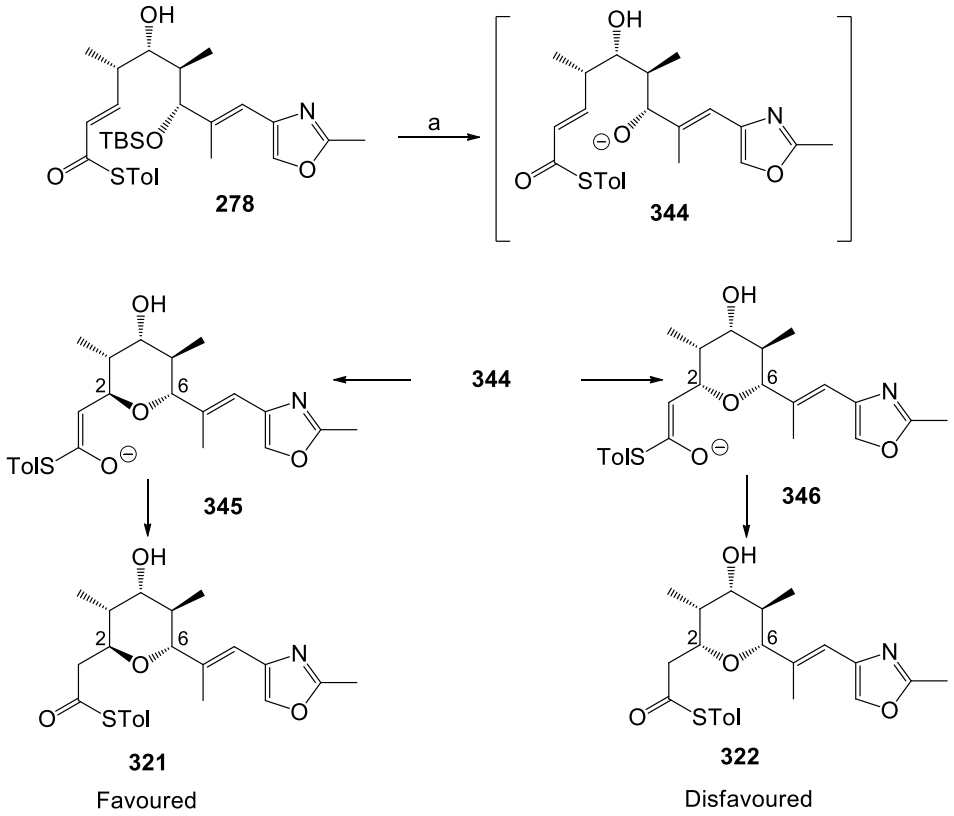

Reagents and conditions: a) 1.5 eq TBAF, 0.2 eq AcOH, THF, rt

Scheme 82: Computational mechanistic investigations of TBAF cyclization

Initially a comprehensive conformational search was conducted at the molecular mechanics level of theory using MMFF94 force field. Energetically most favourable conformations as well as conformations that seemed to be "close" to the expected transition states were then submitted for a further geometry optimisation step at DFT level of theory using B3LYP functional and 6-31G* basis set. The two obtained geometries are shown in Figure 16. It is worth noting that in both conformations the negative charge on oxygen is stabilised by a intramolecular hydrogen bond formed with the hydroxyl group as well as by an anion-induced dipole interaction with the tolyl ring. Both conformations are also already in a hairpin shape with the only difference being the orientation of the double bond. Conformation **347** has the β-hydrogen of the thioester pointing upwards and would give the 2,6-*cis* THP upon cyclization, while in **348** the β-hydrogen is pointing downwards and would give the 2,6-*trans* product. The **348** is lower in energy than **347** by 11.4 kJ/mol

and this could contribute to the *trans* diastereoselectivity of the reaction, if the activation energy turned out to be small. The energy of **348** was chosen as reference point for all other energies in the investigations of this system.

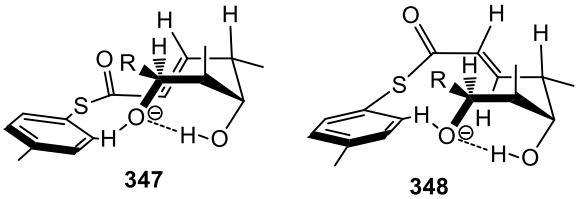

347

Rel. enthalpy 11.4 kJ/mol

C-O	3.32 Å
O…HO	1.51 Å
O…HAr	2.15 Å

348

Rel. enthalpy 0.0 kJ/mol

C-O	2.88 Å
O…HO	1.54 Å
O…HAr	2.08 Å

Figure 16: Low energy conformations of thioester alkoxide

A search for the transition states leading to the two diastereomers was conducted. At first a coordinate scan was executed at the DFT level by fixing the alkoxide – β carbon distance at 0.2 Å intervals. When the approximate transition state geometry was found, it was further refined using direct search of the precise transition state geometry. Two alternative transition states were found - **349** and **350**, corresponding to the *cis* and the *trans* products (Figure 17). Overall the reaction energy barrier is 24.5 kJ/mol for the 2,6-*cis* and 10.0 kJ/mol for the 2,6-*trans* product, both of which are quite low and is consistent with the observed speed of the reaction (complete in less than 10 minutes at room temperature). The *trans* transition state is 14.5 kJ/mol lower in energy than the *cis* transition state, which is consistent with the observed diastereoselectivity of the reaction (>20:1 in favour of 2,6-*trans* product). One possible reason for this energy difference is the eclipsing interaction of the β and γ hydrogen atoms of the thioester, which is present in the 2,6-*cis* transition state **349**, but not the 2,6-*trans* transition state **350**. However, this could only constitute approximately one third of the energy difference. One other reason could be the increased bond strain of thioester in the *cis* conformation **349** as the double bond orientation is less favourable for the rotation of the tolyl substituent to reach the

alkoxide. Also, there could be some contribution from the pseudo-1,3-diaxial interaction between the hydrogen atoms that would be in the 2- and 6- positions in the finished product. It might be more pronounced than usual because the protons are pointing slightly towards each other to allow the alkoxide attack from a trajectory close to the Bürgi-Dunitz angle.

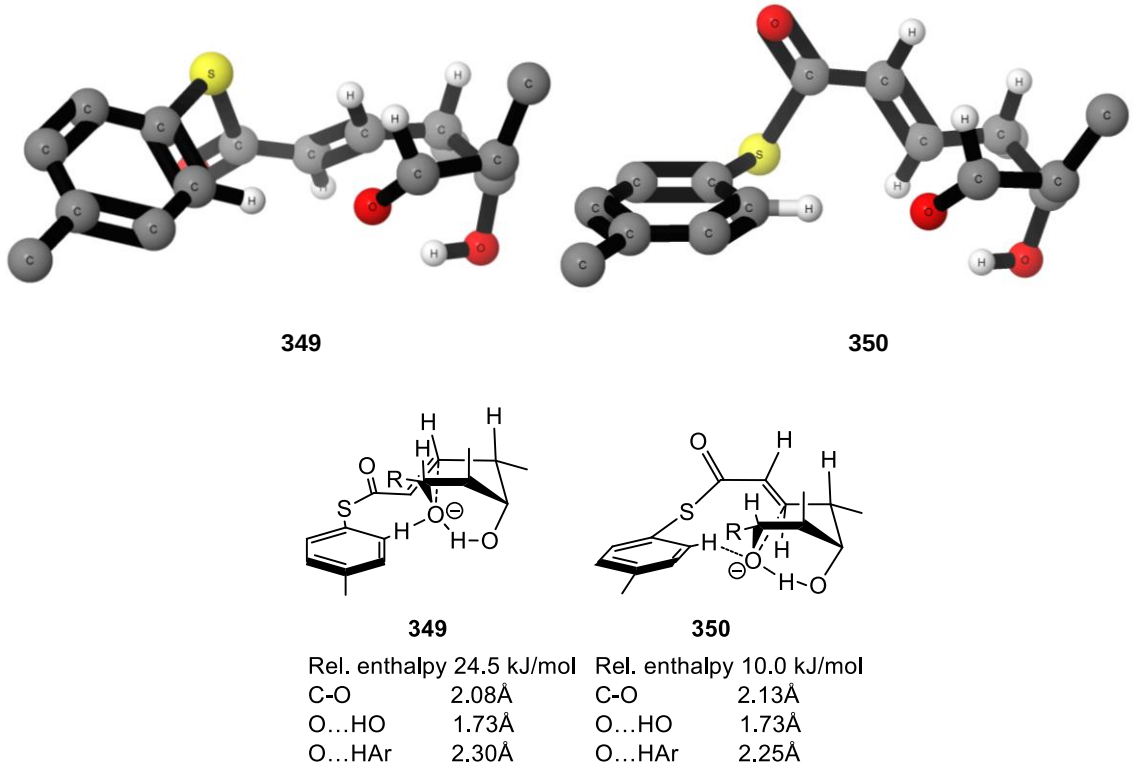

Figure 17: Transition states of thioester anion cyclization in basic conditions

For the next step, the conformation search was repeated for the cyclized thioester enolate products of the reaction. This process was complicated somewhat by the fact that the reaction can potentially give 2,6-*trans* and 2,6-*cis* diastereomers as well as *E* and *Z* enolate geometries for each: 4 potential intermediates in total. It was also discovered that the molecular mechanics conformation search algorithm was quite conservative when applied to the constrained geometries of our tetrahydropyran products. Thus, to check if a boat conformation might be energetically more favourable we had to modify the structure manually and repeat the conformation search.

Unsurprisingly, all the *Z*-enolates turned out to be significantly higher in energy than the *E*-enolates. The reason for this is that *Z* enolates have the bulky tolyl substituent clashing with the tetrahydropyran ring. The lowest energy conformation for the *trans*-product **167** was the simple chair conformation with the tolyl thioester enolate substituent in an axial position; this had the relative energy of -34.8 kJ/mol (Figure 18).

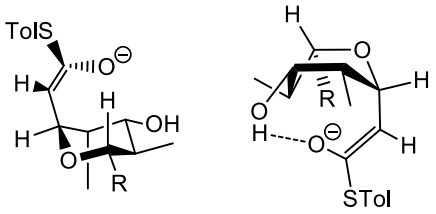

351 Rel. enthalpy -34.8 kJ/mol

352 Rel. enthalpy -43.9 kJ/mol

Figure 18: Low energy conformations of the basic thioester cyclization products

As expected, the lowest energy conformation of the *cis* product **352** is 9.1 kJ/mol lower at -43.9 kJ/mol. However, the geometry of the conformation was somewhat surprising. Instead of the chair conformation with both of the large substituents in 2 and 6 positions in equatorial positions, the enolate takes a boat conformation so as to allow the formation of a hydrogen bond between the enolate oxygen and the hydroxyl group. The energetical gain from the stabilization of the enolate appears to outweigh any reduction of steric interactions a chair conformation would give.

An energy diagram was then constructed for this reaction (Figure 19). From this the reaction appears to be under kinetic control, because the energy barrier for the reverse reaction is significantly higher than the forward reaction. Also, the observed major product of this reaction is the *trans*-product, even though the thermodynamically more stable is the *cis*-product, which further suggests kinetic control. It is also worth noting that these results and the boat-like transition state in particular match the transition states proposed by Urpi and Romea and also Paterson (Scheme 80).

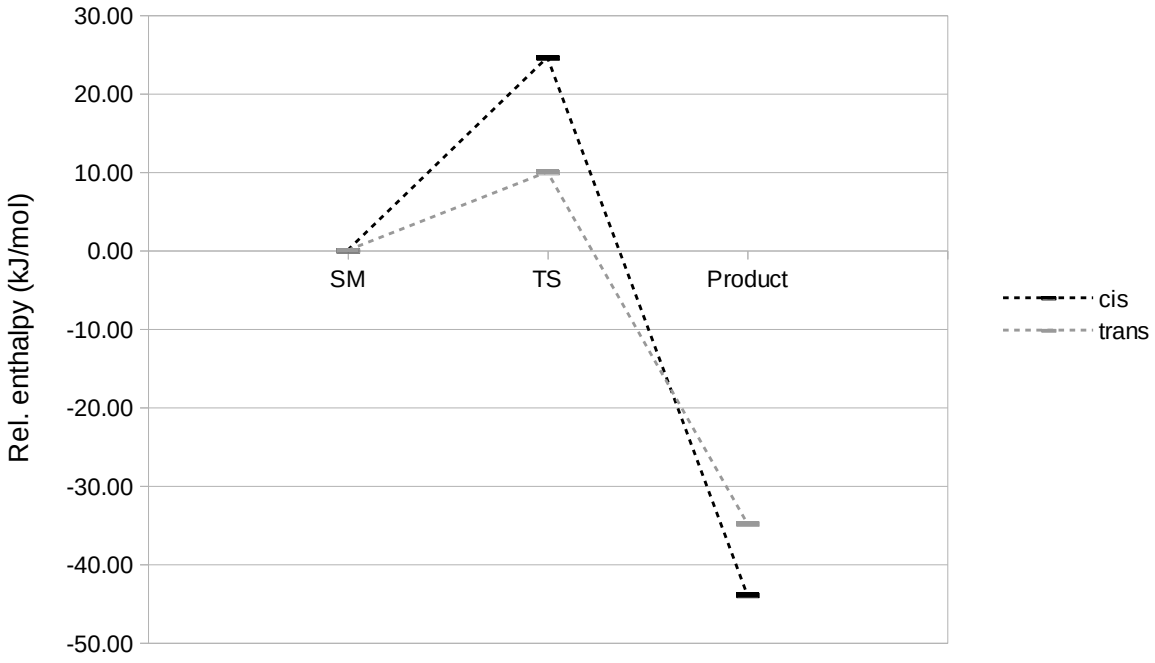

Figure 19: Energy diagram of the TBAF mediated thioester cyclization

With the thioester cyclization study complete, the process was repeated with the oxoester analogue. The uncyclized alkoxide conformation search gave three low energy conformations **353**, **354** and **355** (Figure 20). Again, the lowest energy conformation is the pseudo-*trans* hairpin conformation **353** with a hydrogen bond between alkoxide and hydroxyl group and an induced dipole-anion interaction between alkoxide and the *ortho* hydrogen of the tolyl ring. The energy of this conformation was set to 0.0 kJ/mol in this study. The pseudo-*cis* conformation **355** was also found to be having relatively low energy of 22.4 kJ/mol. The final conformation **354** has a comparatively straight chain geometry with the intramolecular hydrogen bond between alcohol and alkoxide as the only notable interaction. The relative energy of this conformation is 21.5 kJ/mol which puts it just below the pseudo-*cis* conformation **354**.

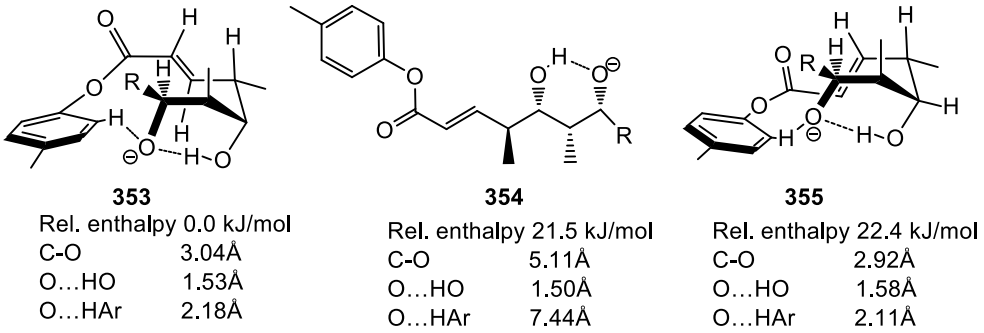

Figure 20: Low energy conformations of the oxoester alkoxide

In a similar process to that described previously, the two diastereomeric transition states **356** and **357** were found (Figure 21). The 2,6-*trans* transition state **356** again is very similar to the conformation **353** and it's energy is 22.9 kJ/mol, which is higher than in the thioester analog but still quite low. The 2,6-*cis* transition state **357** is slightly unusual as its tolyl ring is pointing away from the forming ring and has no interaction with the alkoxide. This is probably the result of the shorter bond lengths of the oxoester which causes the bond strain to be too large for the induced dipole - anion interaction to give a net reduction of the energy. The 2,6-*cis* transition state is 11.5 kJ/mol higher in energy than the 2,6-*trans* transition state. Assuming kinetic control, the results again are consistent with the observed diastereoselectivity of this reaction (>20:1 *trans*:*cis*).

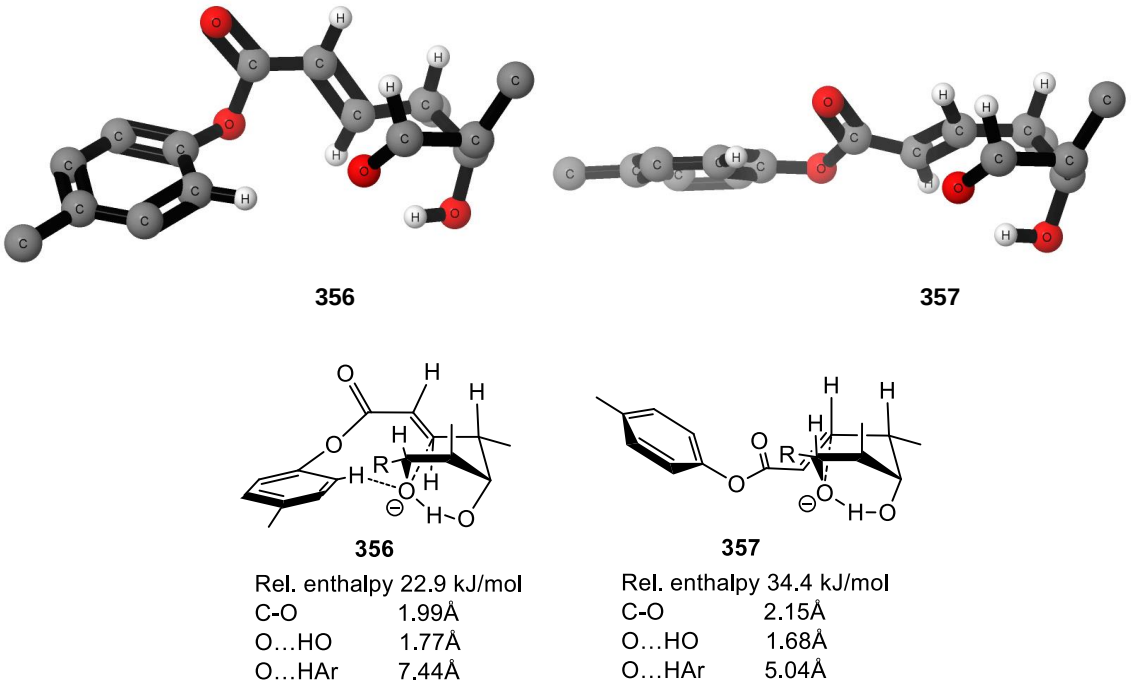

Figure 21: Transition states of oxoester anion cyclization

The conformation search for the products of the reaction gave no surprises and the lowest energy conformations of the *cis* and *trans* products turned out to have almost identical geometries to their thio- analogues (Figure 22). The *trans* product takes a chair conformation **358** with the ester enolate in axial position and it's relative energy is -2.8 kJ/mol. The *cis* enolate takes a boat conformation **359** and has a relative energy of -7.0 kJ/mol.

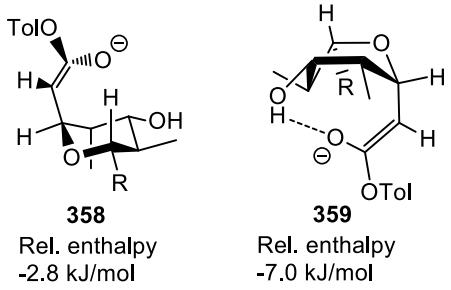

Figure 22: Low energy conformations of the basic thioester cyclization products

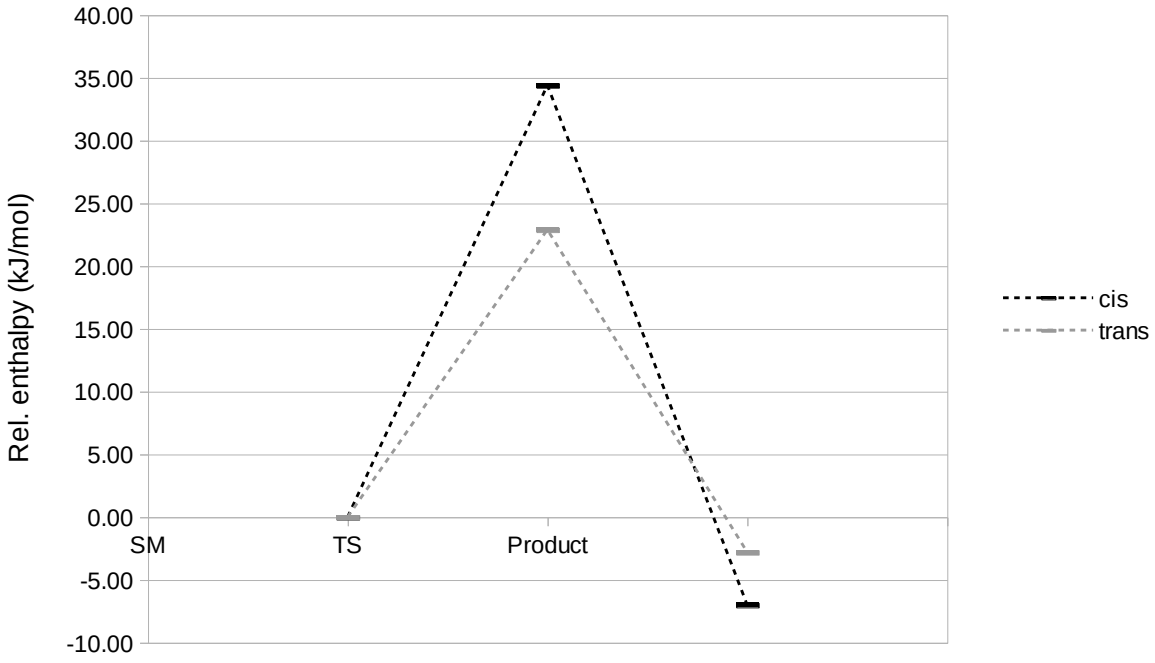

Figure 23: Energy diagram of the TBAF mediated oxoester cyclization

With this information in hand an energy diagram of the reaction was constructed and it became apparent that it is quite different when compared to that of the thioester reaction (Figure 23). The 2,6-*trans* transition state is still significantly lower in energy and the 2,6-*cis* product is still the energetically more favoured product. However, in this case it is not clear from the calculations if the reaction is under kinetic or thermodynamic control as the energy barriers for the forward and reverse reactions appear to be quite similar in magnitude. This makes the computational results hard to reconcile with experimental results. If the reaction is under kinetic control then the computations are correct about the relative energies of the transition states and incorrect about the relative energies of the products. And if the reaction is under thermodynamic control, it is *vice versa*.

The most straightforward cause of these inconsistencies could be the chosen computational method, and the basis set in particular. While the 6-31G* basis set generally gives good results, the addition of diffuse functions to the basis set is often found to

improve the results for anions and weak interactions like hydrogen bonds. As our system has both, we will repeat the calculations for the ester cyclization using the 6-31+G* basis set, which includes diffuse functions.

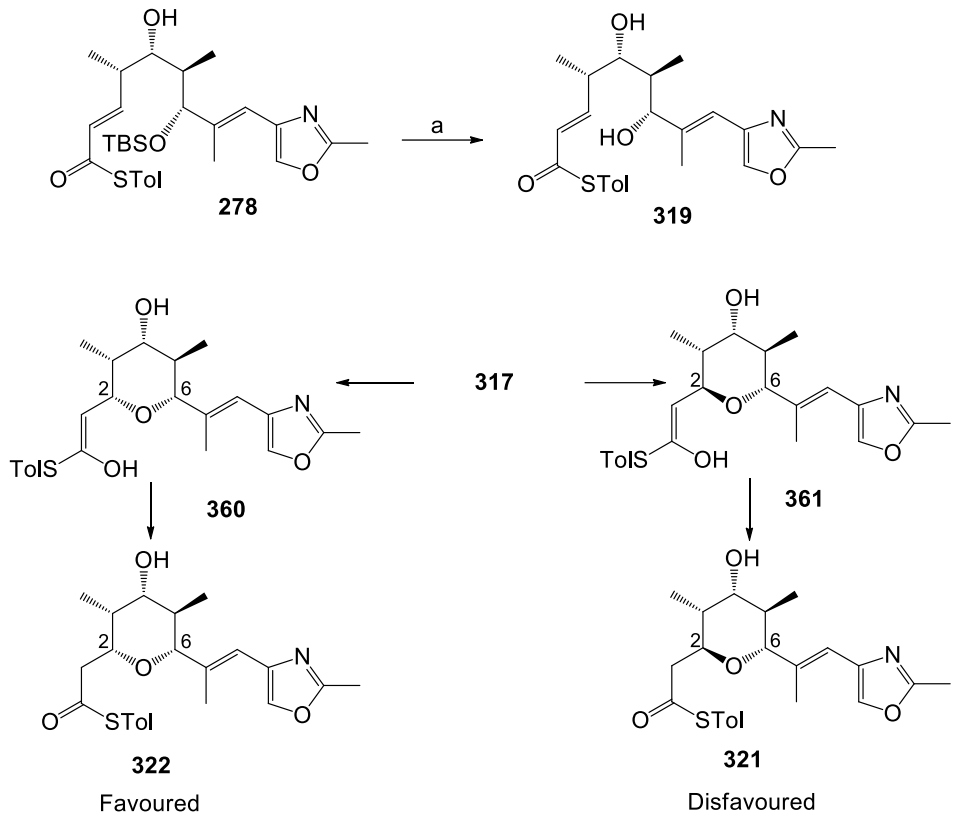

Reagents and conditions: a) TFA/DCM/H_2O, rt

Scheme 83: Computational mechanistic investigations of acid-mediated cyclization

8.4.3. Acid mediated cyclization. With the successful completion of the modelling of TBAF mediated cyclization, we turned our attention to the acid mediated cyclization (Scheme 83). This reaction posed quite a few interesting questions. It gives the opposite diastereomer to the TBAF mediated process and as shown by Fuwa and us, it is likely under kinetic control. This means that a simple thermodynamic preference for the 2,6-*cis* diastereomer is not an adequate explanation for the observed stereocontrol. One might suggest that the 2,6-*cis* product is produced simply because the chair-like instead of boat-like conformation is now the lowest energy transition state in acidic conditions. But what causes this change of conformational preference? It could be the reduced basicity of

the alcohol when compared to the alkoxide. Alternatively, it could also be the increased solvation and formation of hydrogen bonds between the 4-hydroxyl group and the highly protic environment thus making it a much worse hydrogen bond donor.

The lack of a generally accepted mechanism for the cyclization was another complication. Fuwa proposed an allylic cation type mechanism, however, they have not reported any further experimental support for it. Furthermore, our optimised reaction conditions differ quite significantly from those used by Fuwa. They use catalytic amounts of acid, aprotic solvent, elevated temperatures and extended reaction times. In contrast, our conditions feature a large excess of the acid, which also serves as part of the solvent mixture, thus making this a highly protic environment. These conditions enable the reaction to run at room temperature and to be complete in only 6 hours, hence the differences in conditions could imply significant differences in the mechanism.

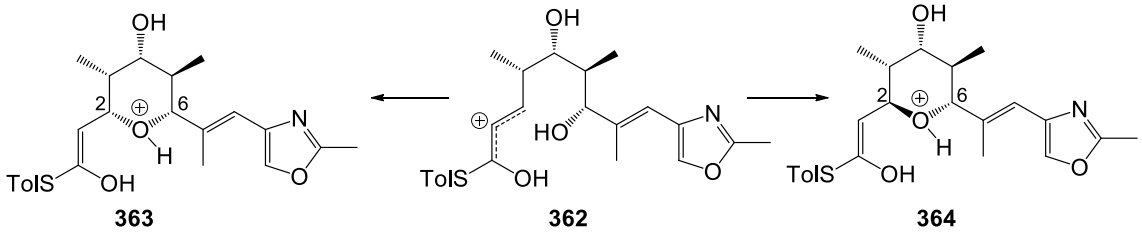

Scheme 84: Allylic cation mechanism

Firstly, it was decided to test if the allylic carbocation mechanism could indeed be the mechanism for this reaction (Scheme 84). To this end, the conformational search was conducted at molecular mechanics level for the protonated cyclization precursor **362** as well as for the two possible cyclization products **363** and **364**. The lowest energy conformations of **362** were then submitted to the DFT calculations. As can be seen in Figure 24, the lowest energy conformation for the protonated cyclization precursor features a hydrogen bond network linking the protonated thioester and the two hydroxyl groups. When the lowest energy conformations of the products were submitted to geometry optimisation at the DFT level, the tetrahydropyran ring opened back up during the process.

This implies that there is no energy barrier for the opening of the ring and that the protonated cyclized products are unstable. This makes it highly unlikely that they would be the intermediates in the actual mechanism.

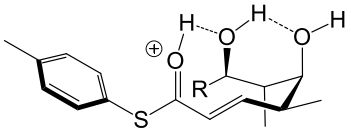

365

Figure 24: Lowest energy conformation of the protonated cyclization precursor

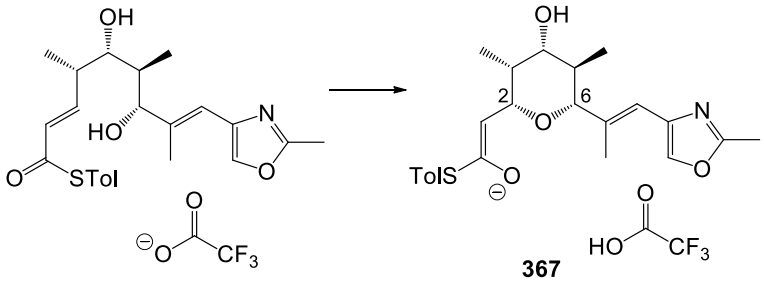

366 **367**

Scheme 85: Trifluoroacetate ion mediated cyclization

After a period of probing calculations, it was found that the intermediates can be stable, if the proton is removed from the tetrahydropyran oxygen. This would require a Brønsted base, and in the reaction conditions there are only a few possible candidates. Hydroxyl anion would be present in only extremely small quantities. Trifluoroacetic acid, however, would be almost completely dissociated in these concentrations and the trifluoroacetate anion could therefore act as a Brønsted base in the reaction. With that in mind we then conducted a study on simplified reaction conditions with only the trifluoroacetate ion present along the cyclization precursor (Scheme 85). This was not meant as an accurate representation of the reaction conditions, but more as an opportunity to learn more about the possible mechanisms for the reaction. Also, if viable transition states were found, then it would be far easier to later include protonation or solvent molecules in a stepwise fashion to make the model more realistic.

Thus to this end a conformational search and the DFT calculations for the starting material and the 2,6-*cis* enolate intermediate were performed once again. It was found that this time the intermediate was stable. Encouraged by these results we then took the transition state-like conformations of the stable intermediates and gradually increased the C-O distance and optimised the geometries at the Hartree-Fock level and using 3-21G basis set. It was found that the proton transfer takes place when the C-O distance is around 1.72 Å. This optimised structure was used a starting point for the transition state search. We were happy to find that this approach allowed us to find the transition state for the trifluoroacetate mediated 2,6-*cis* cyclization (Figure 25).

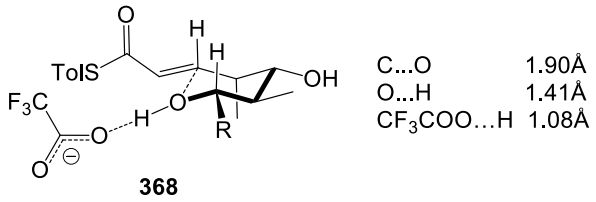

368

Figure 25: Transition state for trifluoroacetate mediated oxy-Michael cyclization

With the minimal transition state as a guide, it was now possible to explore more realistic models of the reaction. Since the trifluoroacetic acid would be almost completely dissociated in the reaction conditions, it seemed reasonable that the hydroxonium ion would be the counterion in the transition state. Also, if the proton would be transferred to the thioester oxygen atom, this might still increase the electrophilicity of the conjugated double bond and thus promote the reaction (Scheme 86).

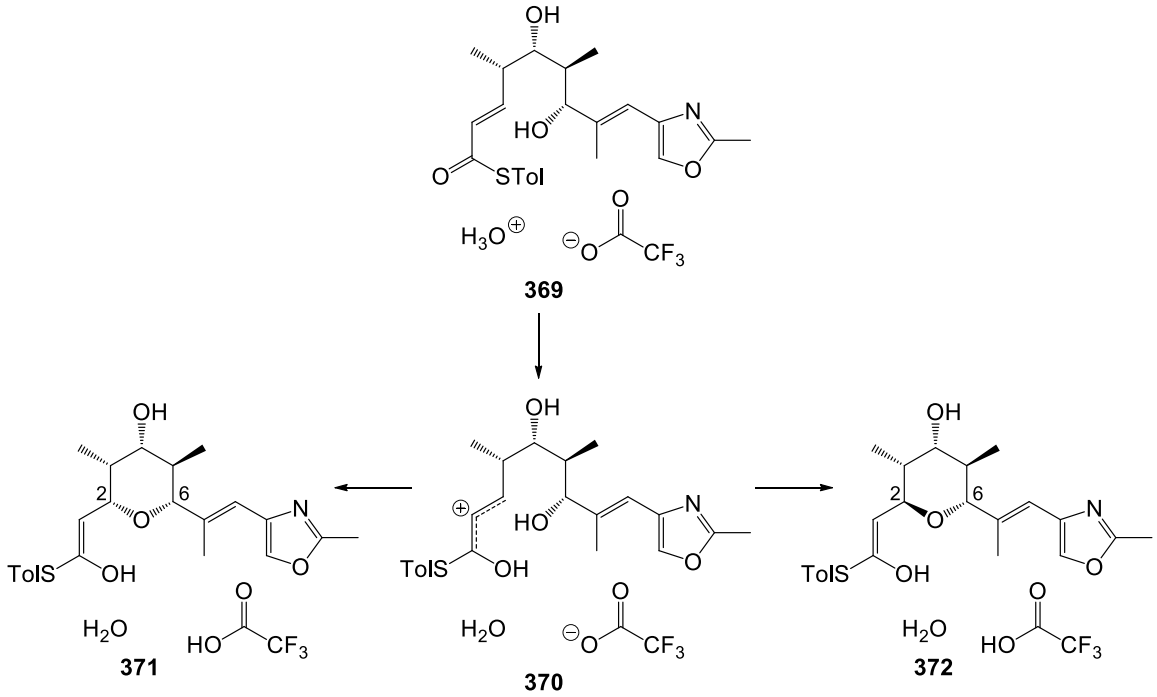

Scheme 86: Computational mechanistic investigations

With that in mind, a hydroxonium ion was added to the system and the conformational search for the starting materials and products was performed as previously. The search for the transition states was subsequently started. First, a preoptimization at the DFT level was done, by fixing the C-O distance at 1.90 Å and the alcohol O-H distance at 1.41 Å, using the simplified transition state **368** as a guide. After this a transition state search was conducted and the lowest energy transition states are shown in Figure 26.

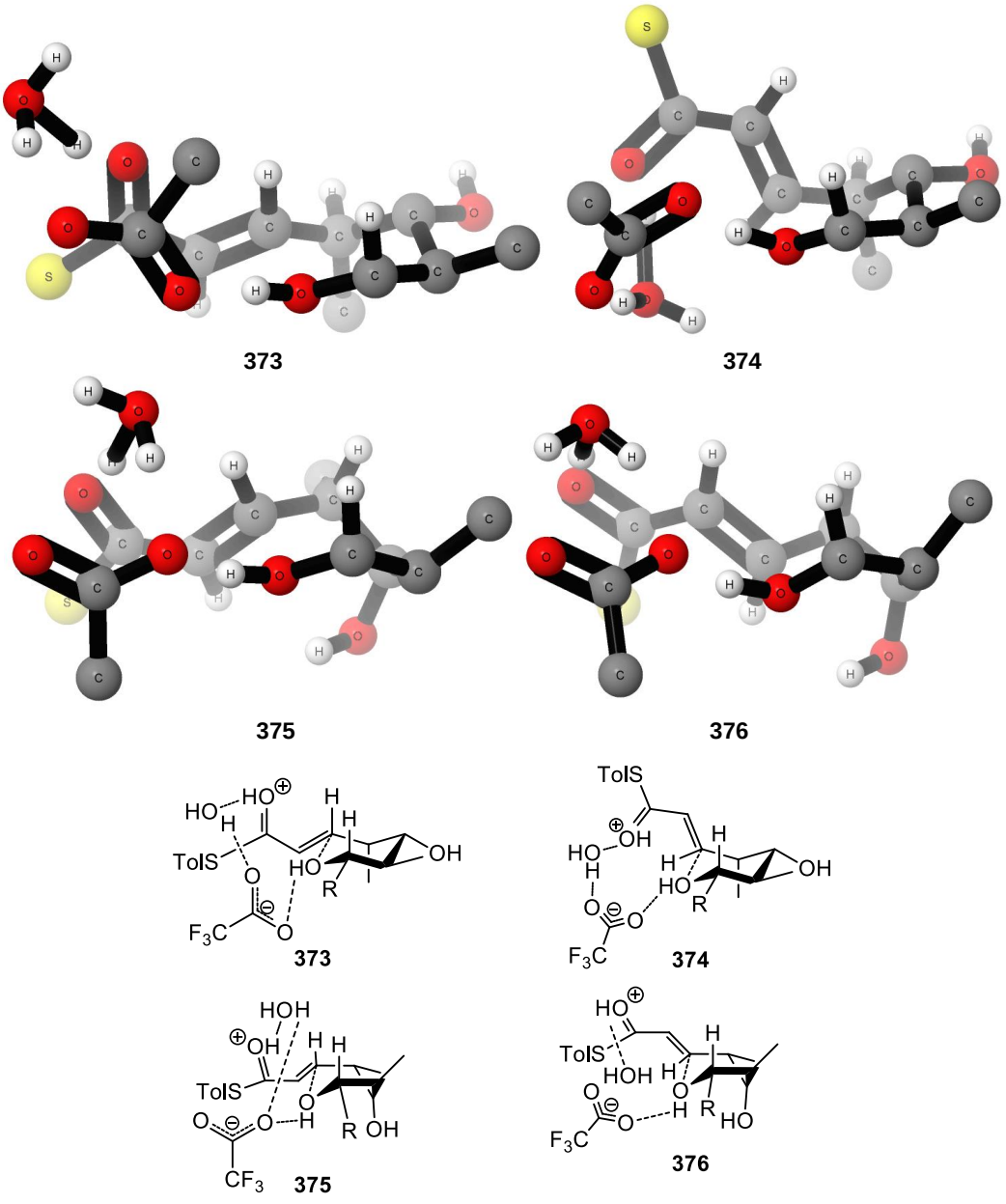

Figure 26: Transition states for trifluoroacetate-hydroxonium mediated oxy-Michael cyclization

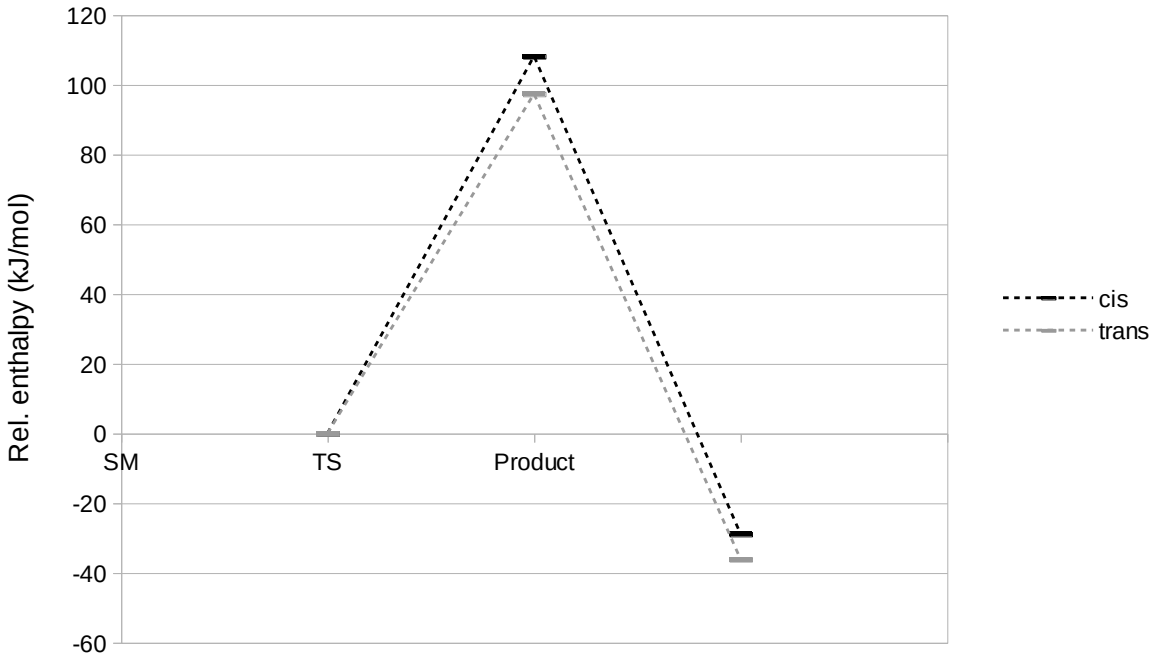

Figure 27: Energy diagram for the trifluoroacetate-hydroxonium mediated oxoester cyclization

The full energy diagram could then be constructed (Figure 27). It was encouraging to see that the energy barrier for this reaction was within the range of room temperature reactions.[94] We were, however, disappointed to find out that the relative energies of the transition states predicted that the reaction would be 2,6-*trans* selective which contradicted experimental observations. Interestingly, the boat and chair transition states are very similar in energy, as the intramolecular hydrogen bond between the alcohols is much weaker now and does not stabilise the boat-like structure to such a great extent. Another notable feature of the transition states is the hydrogen bond network that can be seen in all of the structures. It is easy to imagine that this network would act as a path through which the proton from the alcohol could be efficiently delivered to the thioester oxygen.

While these candidate structures certainly gave valuable insights, it was clear from the predicted selectivity and the high activation energy that the search for the true transition states was not at the end. After giving the problem some thought, we wondered if

the hydroxonium ion would really be present in the transition state. It could just as likely act as a proton source that delivers the proton to the thioester oxygen and plays no role in the mechanism after that.

We repeated the conformation search process with the protonated thioester-trifluoroacetate ion complex. Using the same preoptimization and transition state search sequence as previously, new transition states were found relatively quickly (Figure 28).

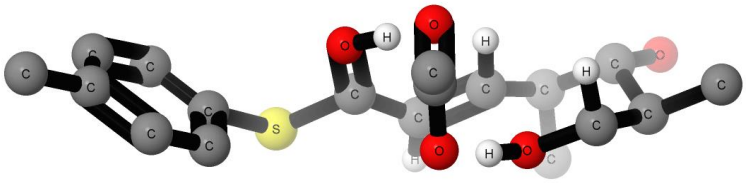

377

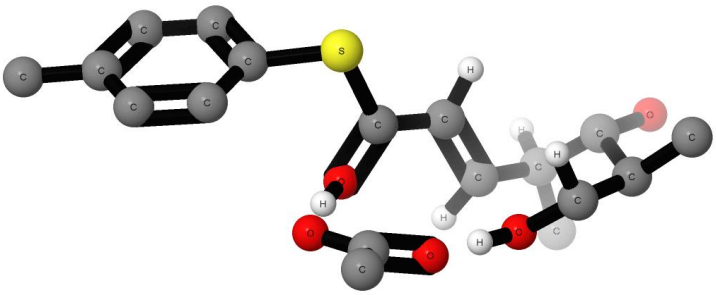

378

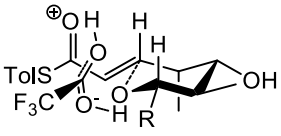

377

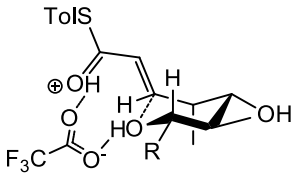

378

Figure 28: Transition states for trifluoroacetate-hydroxonium mediated oxy-Michael cyclization

This time the boat-like transition state was significantly higher in energy in both the 2,6-*trans* and the 2,6-*cis* cases. In both transition states there are two hydrogen bonds connecting the trifluoroacetate ion to the alcohol and to the protonated thioester. More importantly, the relative energies of the transition states now match the observations with the 2,6-*cis* being the favoured product. Also the predicted activation enthalpy for the

reaction is significantly lower than in the hydroxonium ion case. Thus this appears to be the more plausible reaction mechanism not simply because it happens to give the right selectivity, but also because this pathway would be several orders of magnitude faster than the alternative one.

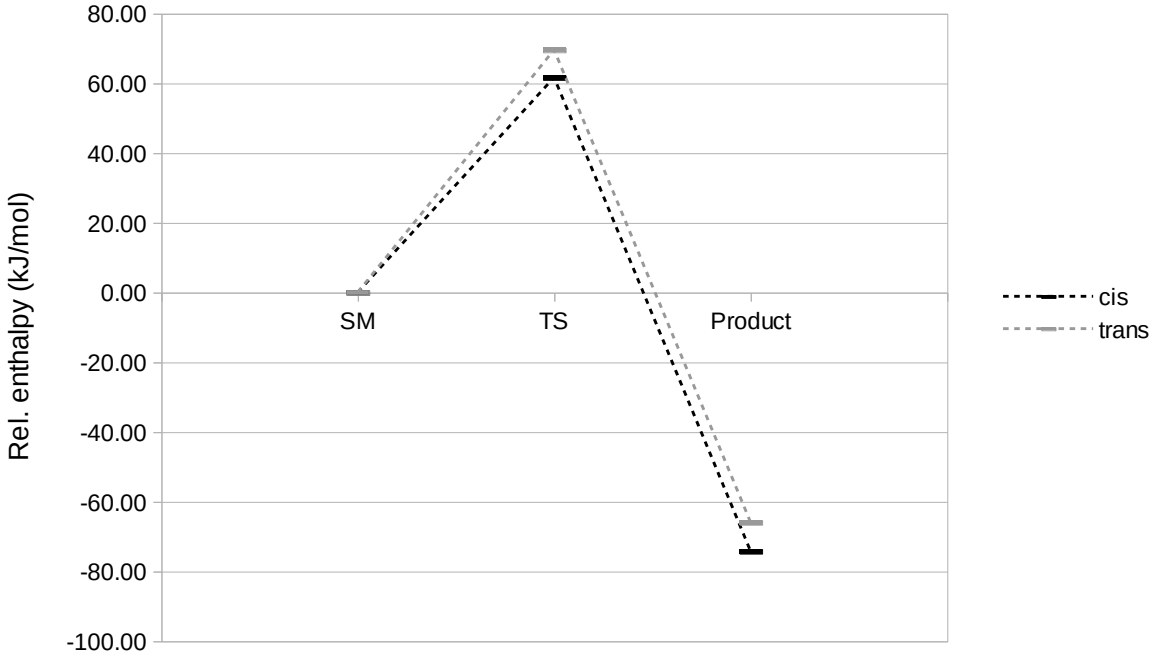

Figure 29: Energy diagram for the trifluoroacetic acid mediated oxoester cyclization

The last remaining question for the computational study was the dramatic difference in the reactivity of thioesters and oxoesters in this oxy-Michael cyclization. To gain better understanding of the causes of the difference in the reactivity, we modelled the same reaction as previously, but with the oxo-ester as the substrate. Only the 2,6-*cis* pathway was modeled as we were primarily interested only in the reactivity of the substrate. We found a similar transition state as in the thioester case, however, the energy profile of the reaction showed a much higher transition state energy. This difference of more that 20 kJ/mol would make the oxo-ester reaction roughly 100 times slower. While this matched the experimental observations, it did not explain them. The transition state geometries are quite similar and therefore it is very unlikely that the steric effects are the

cause for the dramatic difference. An alternative cause would be the electronic reasons; that for some reason the oxo-ester is a less efficient electrophile than a thioester. Conveniently, all DFT calculations output the coefficients for the atomic orbitals that combine to make each molecular orbital, as well as the energy of each molecular orbital. This information could be used to determine both the overall reactivity of the molecule from the energies of HOMO and LUMO, as well as the relative reactivity of different sites in the molecule from the orbital coefficients.

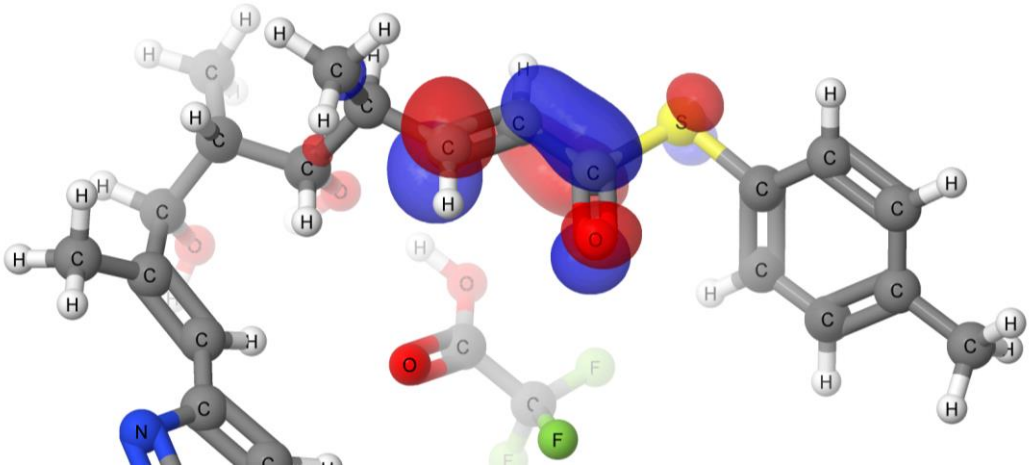

Figure 30: LUMO of the thioester-TFA complex

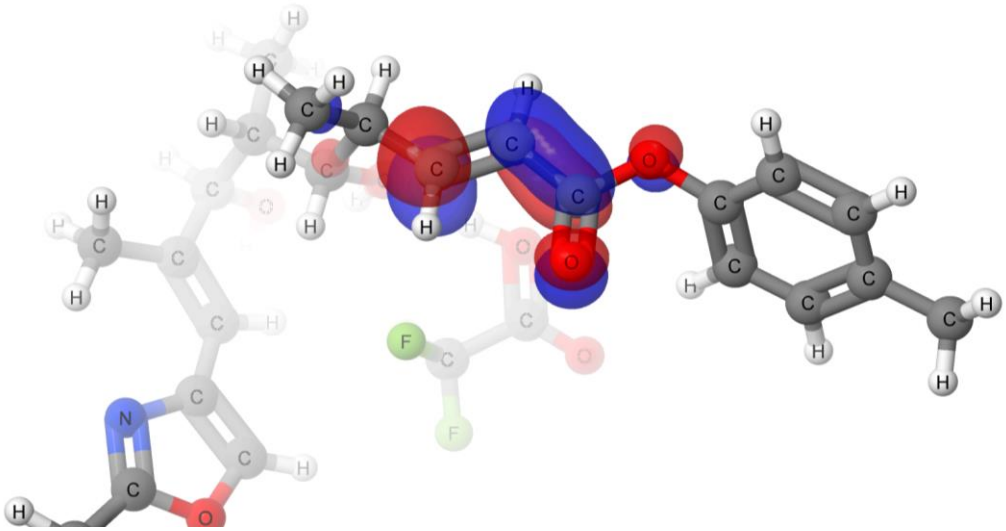

Figure 31: LUMO of the oxoester-TFA complex

The nucleophile is the same in both reactions, the only difference is in the electrophile. Therefore any differences in the electronic structure regarding the reactivity of the molecule should present themselves in the LUMO of the substrate. Two very similar and low lying conformations of the thioester-TFA and the oxoester-TFA complex were compared and the LUMO of both are shown in Figure 30 and 31. The energies for the LUMO is -1.43 eV for the thioester and -1.06 eV for the oxoester. While this difference is relatively small, it is significant and shows that the sulfur atom makes the LUMO more accessible for nucleophiles. As can be seen from Figures 30 and 31, the LUMO electron density distribution is very similar for both substrates, so any difference in the reactivity should be the result of the overall energy difference and not the distribution of the electron density.

Possible explanation for the difference in the LUMO energies between thioesters and oxoesters might be that sulfur lone pair has a weaker overlap with the C=O π^* orbital because of the size difference. This would make the system more ketone like and more electrophilic in comparison with the esters.[101]

We also looked at the HOMOs of the cyclization precursors (Scheme 32 and 33). The HOMO of the thioester is largely localized in the vinyloxazole substituent with a small amount of density on the alcohol nucleophile. This illustrates the poor nucleophilicity of the alcohol and is in sharp contrast with the corresponding alkoxide where the majority of the electron density resides on the oxygen atom. Surprisingly, the HOMO of the normal ester is localized in the tolylester end of the molecule with no electron density on the alcohol. It is only the next orbital down (e.g. HOMO(-1)) that is analogous to the thioester HOMO (Figure 51). Overall this means that for the thioester cyclization to take place, a HOMO-LUMO gap of -4.45 eV must be overcome, while for the ester it is -5.04 eV – a significant difference.

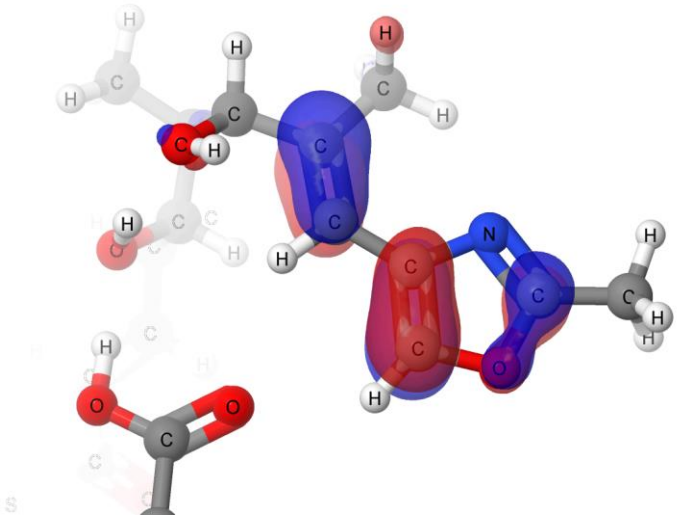

Figure 32: HOMO of the thioester-TFA complex

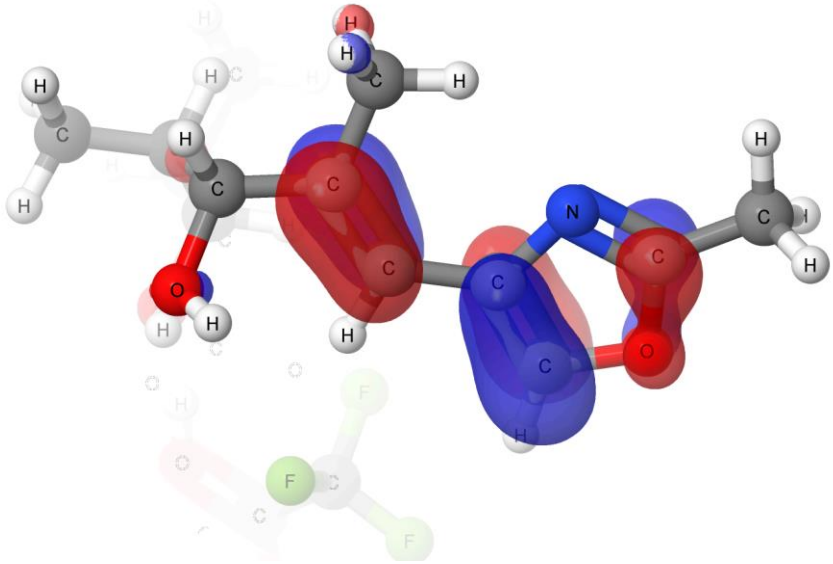

Figure 33: HOMO(-1) of the oxoester-TFA complex

In conclusion, during the computational studies the mechanistic cause for the switch of the diastereoselectivity in the oxy-Michael cyclizations has been successfully determined. The most important factor appears to be the conformation of the transition state. Fluoride mediated cyclizations go through a boat-like transition state which causes the reactions to be highly 2,6-*trans* selective. In contrast, the acid mediated cyclizations have a more conventional chair-like transition state and are highly 2,6-*cis* selective. We

have also explained the difference in the reactivity of the thioesters and oxoesters in the acid mediated cyclizations. The major difference appears to be of electronic nature, where the LUMO of thioesters is significantly lower than in the case of normal esters.

8.5 Synthetic studies on stereodivergence

After the successful computational explanation of the observed experimental facts, we were eager to put these insights to a test. This coincided with an arrival of an ERASMUS exchange student Ugur Kaya. Together we designed a route to a range of simplified cyclization precursors. These precursors would have no subsituents in the 3, 4 and 5 positions and would test the computational predictions that the 4-hydroxyl substituent is crucial for the 2,6-*trans* selectivity in the TBAF conditions and the stereodivergence phenomenon.

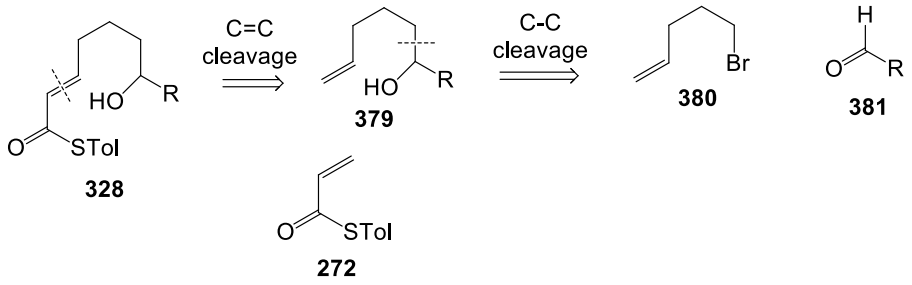

Scheme 87: Retrosynthesis of simplified cyclization precursors

Retrosynthetically, the cyclization precursors **328** could be simplified *via* a C=C cleavage to the alkenols **379** and the already known acryloylthioester **272** (Scheme 87). The alkenols can then be simplified to commercially available bromopentene **380** and a range of aldehydes **381**.

In the forward sense the route would start with a Grignard reaction between the aldehydes and 5-bromopentene. The thioester moiety would then be attached in a

metathesis reaction as in the original route to the C20-C32 core fragment. Finally, cyclizations in the two conditions would be conducted.

Ugur set out to implement the plan. The Grignard reactions worked well with benzaldehyde, nonanal and isobutyraldehyde with yields 72%, 53% and 26% respectively (Scheme 88, Table 7). The low yield from the pivalaldehyde reaction is likely because of the volatility of the product.

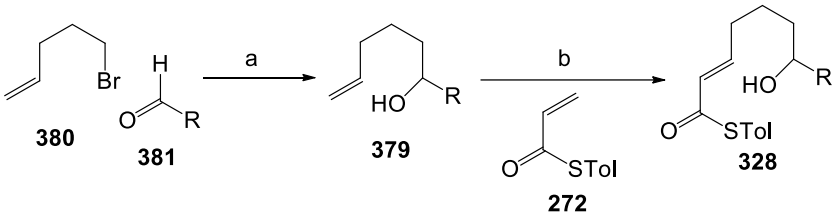

Reagents and conditions: a) Mg, THF b) **170**, 10 mol% HG II, 15 mol% CuI, Et_2O

Scheme 88: Preparation of simplified cyclization precursors

entry	R	yield for a	yield for b
a	Ph	72%	67%
b	*i*-Pr	26%	88%
c	C_7H_{15}	53%	71%

Table 7: Preparation of simplified cyclization precursors

These compounds were then converted in the cyclization precursors using the copper(I) iodide assisted olefin metathesis reaction. All of the reactions proceeded smoothly giving good yields In fact, it was observed that the catalyst was still present at the end of the reaction and therefore reduction of the catalyst loading from 20% to 10% was trialled. The reactions still proceeded to completion and hinted that the ultimate cause of our previous problems with the metathesis reaction might lie in the vinyloxazole substituent.

With the cyclization precursors in hand, cyclizations could be attempted (Scheme 89, Table 8). The standard acidic conditions were applied as in the original study. Just like

in the original study by Fuwa and ourselves, the acidic conditions reliably produced the 2,6-*cis* products in moderate to good yields and variable, but generally good diastereoselectivities. A key indication of successful cyclization in the NMR spectra was the appearance of a new peak for all substrates in the 3.7-4.1 ppm region, which was assigned as the H-2. Also, an already familiar pair of doublet of doublets could be observed in 2.6-3.0 ppm region and were assigned as the α-protons of the thioester. The relative stereochemistry of the products were ascertained by NOE studies, by looking for any interaction between the 2- and 6- protons in particular (Figure 34). Irradiation of H-2 always showed a correlation with H-6 and *vice versa*. The magnitudes of the interaction were 2.1-3.2%, depending on the substituent.

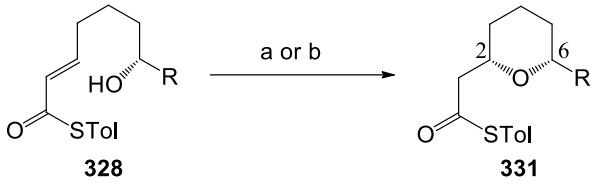

328 **331**

Reagents and conditions: a) TFA/DCM/H_2O, rt b) 30 mol% TBAF, 6 mol% AcOH, THF, rt

Scheme 89: Cyclization of simplified cyclization precursors

entry	R	yield for a	dr for a	yield for b	dr for b
a	Ph	56%	8:1	53%	>20:1
b	*i*-Pr	47%	4:1	27%	>20:1
c	C_7H_{15}	36%	5:1	25%	>20:1

Table 8: Cyclization of simplified cyclization precursors

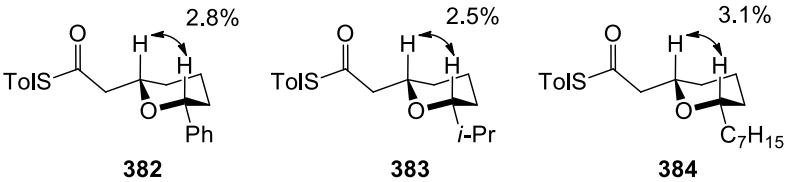

382 **383** **384**

Figure 34: NOE correlations of 2,6-*cis* simplified tetrahydropyrans

The TBAF conditions were slightly modified by using substoichiometric amount of TBAF equivalents (0.3 eq) and a proportional amount of the acetic acid buffer. As these cyclization precursors do not contain the silyl protecting group, it was hypothesized that a catalytic amount of the TBAF should suffice. When tested on the simplified substrates, these conditions successfully promoted the cyclization. Interestingly, the major products had the same 2,6-*cis* relative stereochemistry as from the acidic conditions. It appears that some of the functionality in the original cyclization precursor was crucial for the stereodivergence and hints that our computational model for the 2,6-*trans* selectivity might be correct.

Encouraged by the results, we decided to reintroduce just the hydroxyl at the 4-position. Retrosynthetically, we expected to end syntheses just like previously by using olefin metathesis to introduce the thioester (Scheme 90). Then it was reasoned, that the best way to install the hydroxyl in the desired position would be *via* a Mukaiyama aldol reaction between a methylketone and 4-butenal.

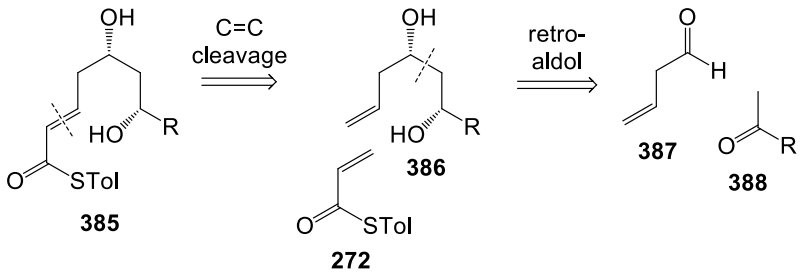

Scheme 90: Retrosynthetic plan for the reintroduction of 4-hydroxyl group

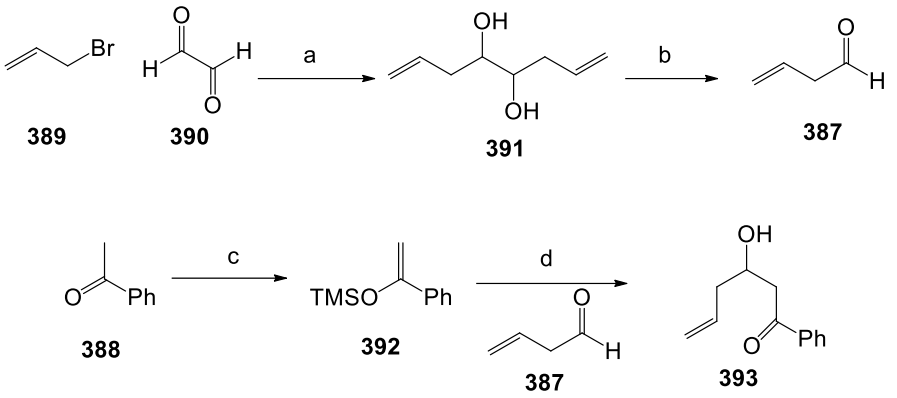

Reagents and conditions: a) Sn, H_2O, THF, μW, 73% b) $NaIO_4$, H_2O, DCM, rt, 68% c) Et_3N, TMSCl, MeCN, 40 ˚C, 99% d) **181,** $TiCl_4$, DCM, 27%

Scheme 91: Initial synthetic studies for hydroxy reintroduction

With the plan in hand, we set out to prepare the hydroxylated cyclization precursors (Scheme 91). The first desired silyl enol ether **388** could be prepared from acetophenone, trimethylsilyl chloride and triethylamine as the base. The 4-butenal also needed to be prepared as it is not commercially available. The commonly used preparation is somewhat counterintuitive: the aldehyde is produced from **391** *via* a diol cleavage reaction. Many alternative methods (e.g. alcohol oxidation) would cause this aldehyde to isomerize to the conjugated aldehyde. The 4-butenal is very volatile and therefore is not usually isolated but used as a solution. With both starting materials in hand the aldol reaction was carried out and it gave the desired β-hydroxyketone **393** in moderate yield.

Reduction of the β-hydroxyketone **393** to the alcohol could potentially produce a mixture of 1,3-*syn* and 1,3-*anti* diastereomers. If this mixture was carried forward, the cyclization could potentially give up to 4 different diastereomers, which would make the analysis of the results extremely difficult. It was therefore decided to conduct the cyclizations on diastereomerically pure starting materials. Fortunately, the diastereoselective reductions of β-hydroxyketones is a fairly well developed area and the general approach to 1,3-*syn* diols is the Narasaka reduction (Scheme 92).[102]

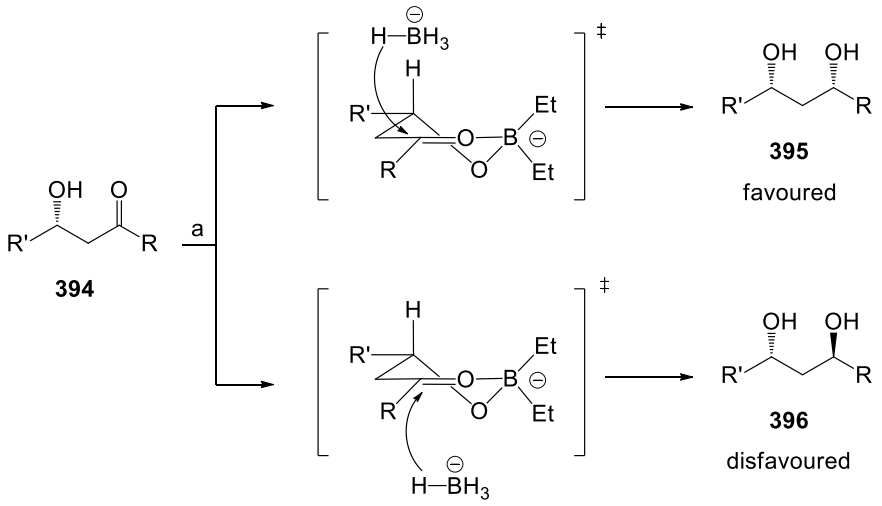

Reagents and conditions: a) Et_3B, $NaBH_4$, MeOH, THF, -78 ˚C

Scheme 92: Diastereoselectivity in Narasaka reduction

Diethylmethoxyborane is generated *in situ* and used as a chelating Lewis acid to form a cyclic intermediate. An external hydride source is then used to reduce the ketone. The hydride can attack axially either from the top or the bottom of the intermediate. Since only an attack from the top would produce an initial chair conformation, the corresponding transition state is lower in energy and therefore the production of the 1,3-*syn* diol **395** is favoured.

The complementary approach to the 1,3-*anti* diols β-hydroxyketones is the Evans-Saksena reduction (Scheme 93).[103,104] In this case, the alcohol is used as a directing group to which the borohydride reducing agent complexes. Hydride is then delivered intramolecularly to the ketone *via* two possible chair-like transition states **397** and **398**. The hydride delivery from the side of the alcohol is preferred as this minimizes any steric interactions in the cyclic transition state. Thus the transition state **397** is favoured and 1,3-*anti* diol is the major product in the reaction.

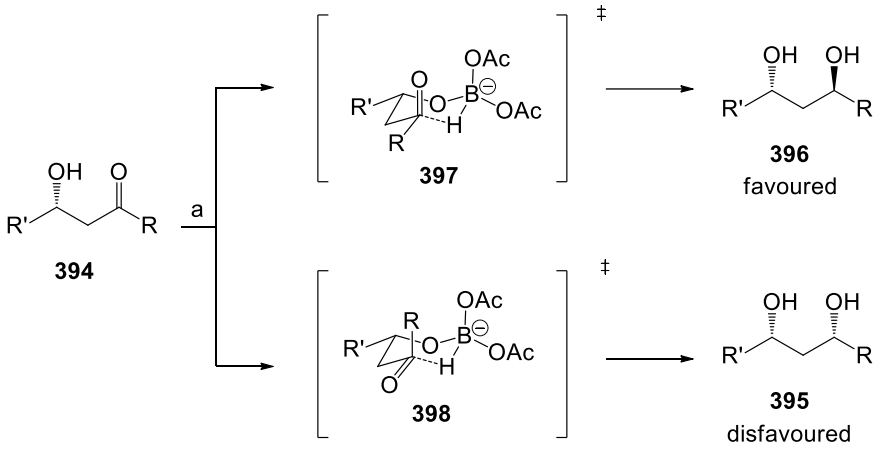

Reagents and conditions: a) $Me_4N(AcO)_3BH$, MeCN/AcOH, -40 ˚C

Scheme 93: Diastereoselectivity in Evans-Saksena reduction

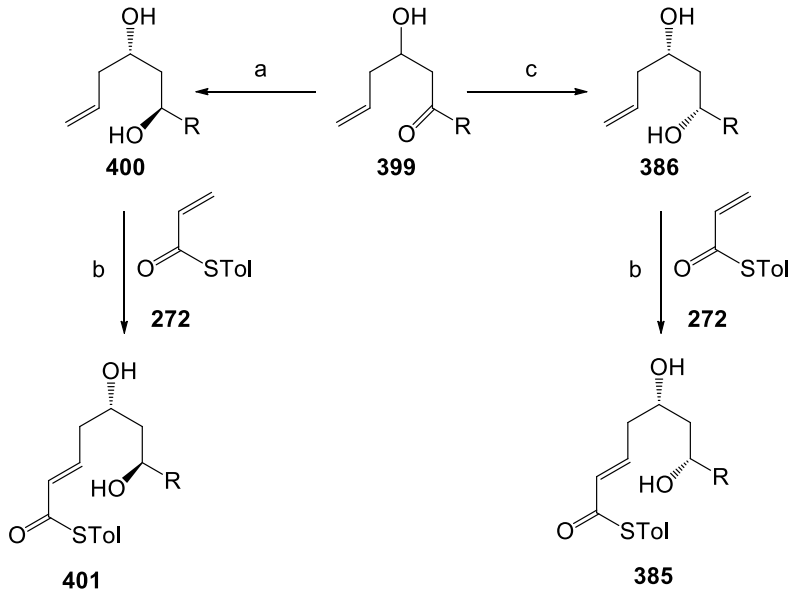

Reagents and conditions: a) Et_3B, $NaBH_4$, MeOH, THF, -78 ˚C b) 10 mol% HG II, 15 mol% CuI, Et_2O, c) $Me_4N(AcO)_3BH$, MeCN/AcOH, -40 ˚C

Scheme 94: Preparation of hydroxy subtituted cyclization precursors

entry	R	yield for a	yield for b	yield for c	yield for d
a	Ph	58%	94%	61%	62%
b	*i*-Pr	43%	75%	83%	54%
c	$-C_7H_{15}$	78%	86%	86%	53%

Table 9: Preparation of hydroxy substituted cyclization precursors

Both of these reduction strategies were used on the β-hydroxyketones prepared by Ugur and me (Scheme 94, Table 9). The Narasaka reduction gave 1,3-*syn* alkenediols in

moderate to good yields. Evans-Saksena gave 1,3-*anti* alkenediols in good to excellent yields. The diastereoselectivties in both reactions were always good (dr >5:1) and the minor diastereomer could be seperated by careful column chromatography. All alkenediols were then transformed into the α,β-unsaturated thioesters using the usual copper(I) iodide assisted olefin metathesis conditions in good to excellent yields. As previously, the reactions proceeded to completion with only 10 mol% of the catalyst.

With the cyclization precursors in hand, it was possible to test if the alcohol in the 4 position has reintroduced the stereodivergence (Scheme 95 and 96, Table 10 and 11). The cyclizations could be effected using either the fluoride or the acid mediated conditions and gave the cyclized products in moderate to good yields. The key difference from the unsubstituted series is that in all cases the fluoride conditions now produced the 2,6-*trans*-tetrahydropyrans in good to excellent diastereoselectivites. The only exception was the *n*-heptyl-**402**, which was produced only in 3:2 selectivity.

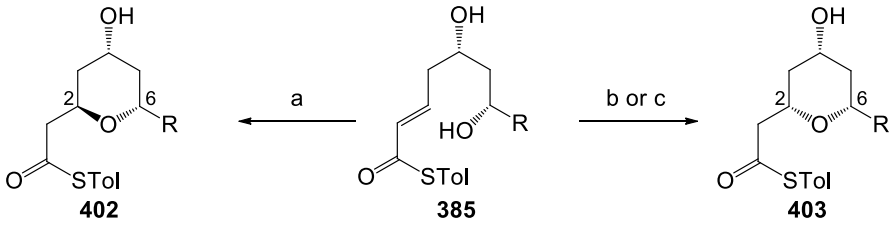

Reagents and conditions: a) 30 mol% TBAF, 6 mol% AcOH, THF, rt b) CSA, DCE, 80 ˚C c) TFA/DCM/H_2O, rt

Scheme 95: Oxy-Michael cyclizations on 1,3-*anti* diol substrates

entry	**R**	**yield for a**	**dr for a**	**yield for b/c**	**dr for b/c**
a	Ph	40%	6:1	58%	10:1
b	*i*-Pr	69%	7:1	66%	>20:1
c	$-C_7H_{15}$	41%	3:2	47%	>20:1

Table 10: Oxy-Michael cyclizations on 1,3-*anti* diol substrates

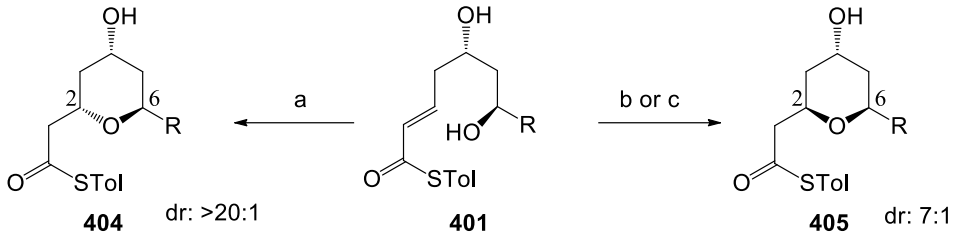

Reagents and conditions: a) 30 mol% TBAF, 6 mol% AcOH, THF, rt b) CSA, DCE, 80 ˚C c) TFA/DCM/H_2O, rt

Scheme 96: Oxy-Michael cyclizations on 1,3-*syn* diol substrates

entry	R	yield for a	dr for a	yield for b	dr for b
a	Ph	40%	>20:1	74%	7:1
b	*i*-Pr	69%	8:1	66%	15:1
c	-C_7H_{15}	48%	>20:1	65%	>20:1

Table 11: Oxy-Michael cyclizations on 1,3-*syn* diol substrates

In contrast, the acidic conditions produced the 2,6-*cis*-tetrahydropyrans in good to excellent diastereoselectivities in all cases. The trifluoroacetic acid conditions worked well with isopropyl and *n*-heptyl substituted cyclization precursors and gave the cyclized products in good yields. The same conditions failed on the phenyl substituted substrates and only the decomposition of the starting material was observed. An MSc project student Alan Jeuken during his time in our lab successfully optimized this reaction and found that Fuwa's original conditions worked much better for this particular substrate. When the precursors phenyl-**403** and phenyl-**405** were exposed to a solution of CSA in dichloroethane and stirred at 80 ˚C overnight, the 2,6-*cis*-tetrahydropyrans were produced in good yields and good diastereoselectivites.

A key indication of successful cyclization in the NMR spectra was the appearance of a new peak for all substrates in the 3.7-4.5 ppm region, which was assigned as the H-2. Also, the familiar pair of doublet of doublets could be observed in 2.4-3.0 ppm region and were assigned as the α-protons of the thioester. The relative stereochemistry of

the products was ascertained by NOE studies, by looking for any interaction between the 2- and 6- protons in particular (Figure 35).

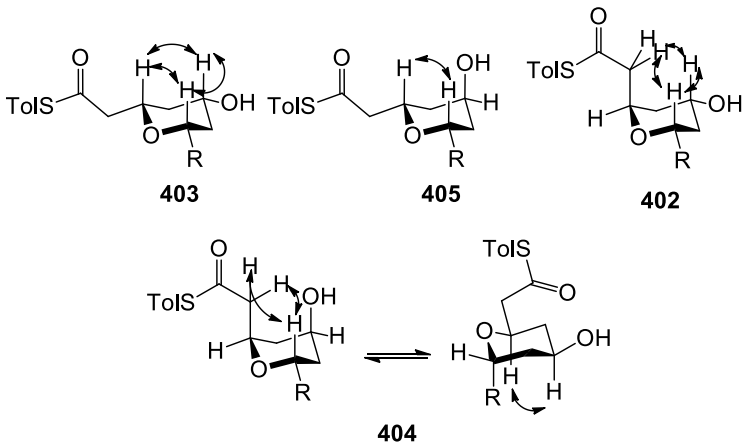

Figure 35: NOE correlations of 4-OH tetrahydropyrans

The NOE studies of the 2,6-*cis* compounds in both series (**403** and **405**) were the most straightforward. The most prominent through-space interaction was between the H-2 and H-6 protons and had a magnitude between 4.5% and 6.2%. In the **403** series weaker interactions between H-2 and H-4 and H-6 and H-4 could also be detected (1.5-2.0%).

In the 2,6-*trans* series no through-space interaction could be detected between the H-2 and H-6. For the diastereomeric series **402**, a comparatively weak (1.7-2.1%) interaction between H-4 and H-6 was shown. Also, correlations between the thioester α-protons and the H-6 were present in this series. The diastereomeric series **404** featured two significant NOE interactions. The first was between the thioester α-protons and the H-6 (1.0-2.5%) and the second was between H-2 and H-4. This suggests that these compounds likely exist in an equilibrium between two chair conformations. In one of the conformations the thioester is in an axial position and therefore close to the H-6, while in the other the H-2 and H-4 are both axial and therefore exhibit a mutual NOE correlation.

The reappearance of the stereodivergence along with the reintroduction of the extra alcohol group provides strong support for our computational explanation of this phenomenon. One final test for our proposed mechanism for the 2,6-*trans* selectivity

would be the protection of the newly introduced hydroxyl prior to the cyclization. If the computational hypothesis is correct, this should switch off the stereodivergence once again and provide the 2,6-*cis* tetrahydropyran from both conditions.

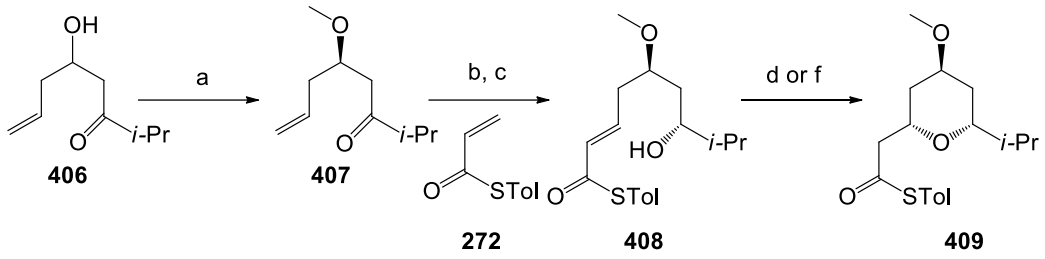

Reagents and conditions: a) Ag_2O, MeI, MeCN, reflux, 64% c) $NaBH_4$, MeOH, rt c) 10 mol% HG II, 15 mol% CuI, Et_2O, 34% over 2 steps d) 30 mol% TBAF, 6 mol% AcOH, THF, rt, traces f) TFA/DCM/H_2O, rt, 48%

Scheme 97: Synthesis and cyclization of methoxy substituted cyclization precursor

To this end the β-hydroxyketone **406** was methylated using methyl iodide and silver(I) oxide. The resulting β-methoxyketone **407** was treated with sodium borohydride to give the β-methoxyalcohol as a 60:40 mixture of diastereomers. They were inseparable at this stage, therefore the mixture was carried forward through the olefin metathesis step to give the thioester in good yield. The diastereomers could be separated at this stage by repeated preparative TLC. The major diastereomer was submitted to both acidic and TBAF-mediated cyclization conditions. As it was expected, both conditions produced the 2,6-*cis* product. The acidic conditions gave product cleanly and in good yield. The cyclization in the TBAF conditions, however, proceeded extremely slowly. When more TBAF was added to the reaction, more of the cyclized product was formed, but at the cost of much more pronounced thioester hydrolysis. The ^{1}H NMR spectrum of the crude reaction mixture showed very small amounts of the cyclized product, but it was clear that the THP produced was the 2,6-*cis* diastereomer. Thus, it has been shown that the hydrogen bond donor is required for the 2,6-*trans* selectivity in TBAF mediated tetrahydropyran formation.

Having studied the exquisite and complementary stereocontrol of the oxy-Michael cyclizations on a range of substrates, we wondered if it could be useful in natural product synthesis. The reaction had already been applied to the C20-C32 core fragment of phorboxazoles, however, it would be more elegant, if both 2,6-*cis* and 2,6-*trans* isomers were natural products. It turned out that diospongins A (**412**) and B (**414**) offer such an opportunity to demonstrate the stereodivergence methodology (Scheme 98). Evenmore, both natural products should be accessible in one step from cyclization products **411** and **413** already synthesized during this study.

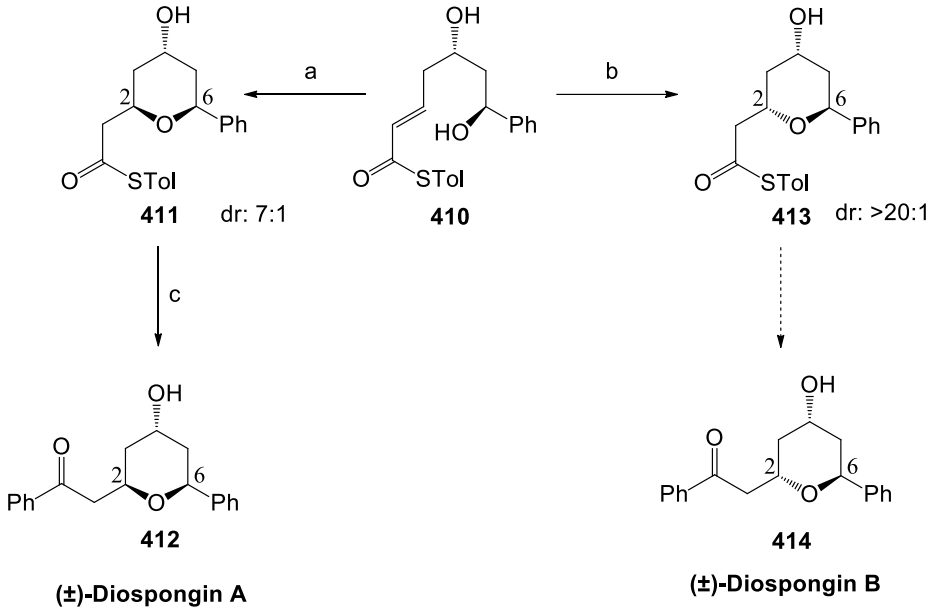

Reagents and conditions: a) CSA, DCE, 80 ˚C b) 30 mol% TBAF, 6 mol% AcOH, THF, rt c) 5 mol% $Pd_2(dba)_3$, $PhB(OH)_2$, CuTC, 4 mol% $(EtO)_3P$, THF, rt, 75%

Scheme 98: Stereodivergent route to (±)-Diospongin A and (±)-Diospongin B

Thus Alan was given the task to convert the thioesters into the phenylketones. Following the example of Fuwa, Liebeskind–Srogl coupling was successfully used on the 2,6-*cis* tetrahydropyran and the (±)-diospongin A was furnished in 75% yield. The same reaction was attempted on the 2,6-*trans* diastereomer, but unfortunately the initial attempts of this reaction failed. Alan's time in the lab had ran out at this point, however, it is expected that this reaction will be optimised in near future. A paper detailing the

computational and analogue studies as well as the application to natural product synthesis is currently being prepared and will be submitted in the near future.

8.6 Conclusion and future work

We have successfully developed a novel synthesis of the core fragment of the phorboxazole B in 7 steps and 31% overall yield. The key steps are an *anti*-selective Masamune-Abiko boron enolate aldol reaction, diastereoselective Hoffmann crotylation and a diastereoselective oxy-Michael cyclization. Only one enantioselective reaction was used, which installed two stereocentres. The other three were installed *via* diastereoselective means. The results have been reported in a paper in *Organic Letters*.[92]

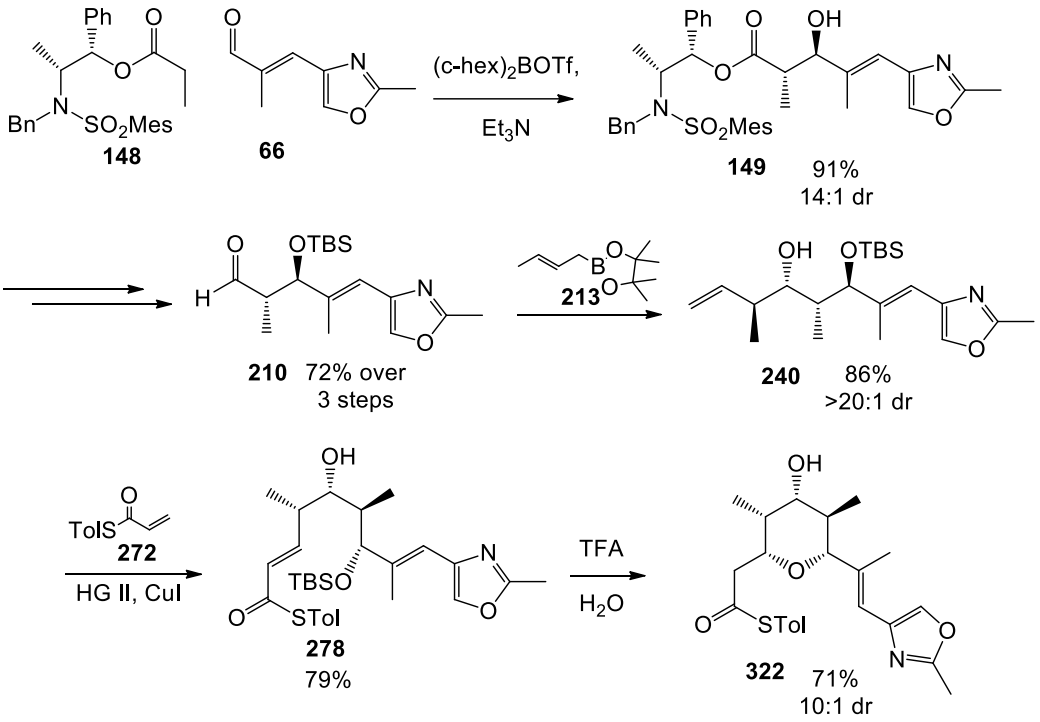

Scheme 99: The synthesis of the C20-C32 fragment

An intriguing stereodivergence was observed in the oxy-Michael cyclization and was studied further using computational techniques. The mechanistic causes were explained. The 2,6-*cis* producing acid mediated cyclization takes place *via* a chair-like transition state. The 2,6-*trans* producing TBAF mediated cyclization occurs through a boat-like transition state and the *pseudo*-4-hydroxyl appeared to be crucial for the diastereoselectivity.

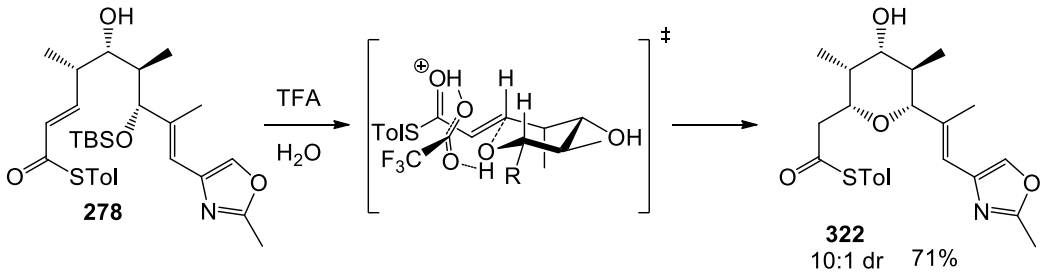

Scheme 100: Computational rationale for 2,6-*cis* selectivity of acid mediated cyclization

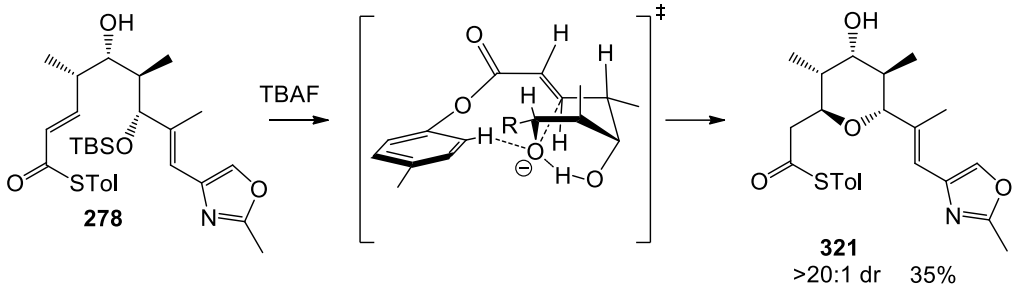

Scheme 101: Computational rationale for 2,6-*trans* selectivity of TBAF mediated cyclization

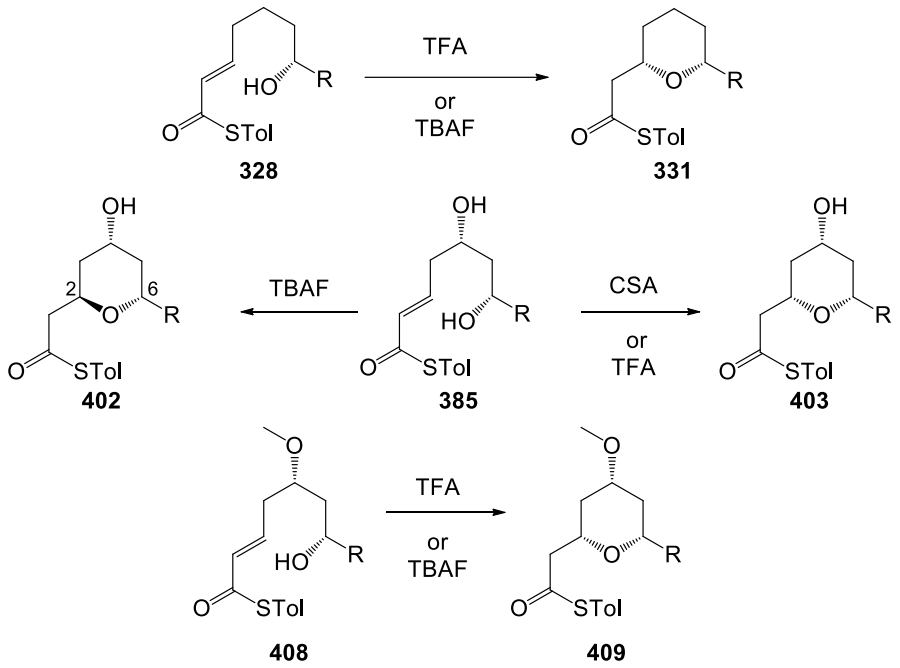

Scheme 102: Synthetic studies on stereodivergence

Synthetic verification for the computational insights was conducted. Removal of the extra hydroxyl from the substrates caused the disappearance of stereodivergence, as predicted by calculations. Reintroduction of alcohol allowed the observation of the

stereodivergence once again. Finally, protection of the alcohol switched it off again, showing that a hydrogen bond donor is crucial for the stereodivergence.

Future work will involve the incorporation of the core fragment in the macrocycle of the phorboxazole B. A route to C1-C19 fragment has been developed previously in the group. The successful synthesis of C20-C32 fragment will now allow the synthesis of the C1-C32 macrocycle by coupling the two fragments. This will be achieved *via* a Wittig olefination and Yamaguchi macrolactonization and will conclude the formal synthesis of phorboxazole B.

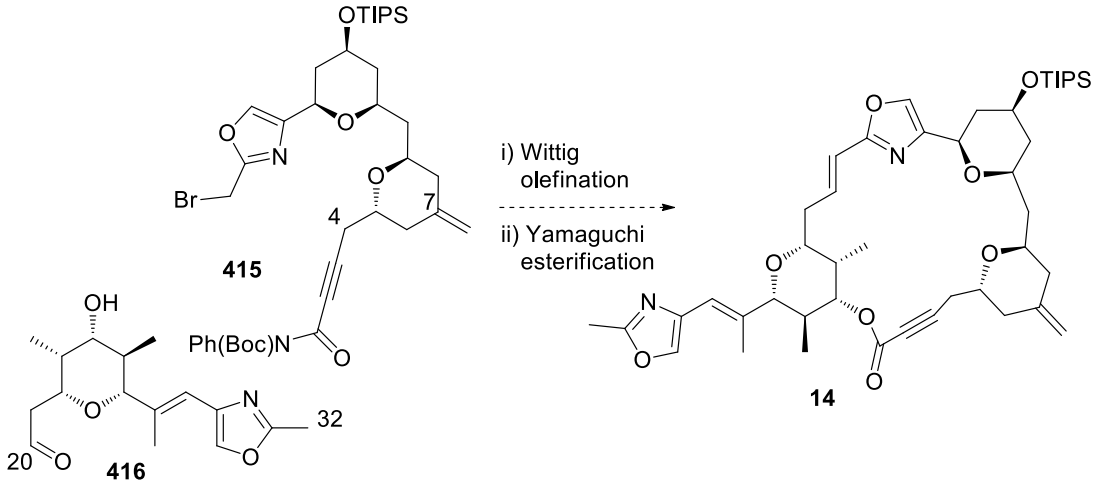

Scheme 103: Synthesis of C1-C32 macrolactone

A 2nd generation synthesis of the C1-C19 fragment using the newly developed stereodivergent oxy-Michael reaction will also be investigated.

9. Experimental

9.1 General experimental

Melting points were determined using a Stuart SMP3 apparatus. Optical rotations were carried out using a JASCO-DIP370 polarimeter and $[\alpha]_D$ values are given in 10^{-1}deg.cm^2.g^{-1}. Infra-red spectra were acquired on a ThermoNicolet Avatar 370 FT-IR spectrometer. Nuclear magnetic resonance spectra were recorded on a Jeol ECX-400, a Jeol ECS-400, Bruker DRX 500 or a Bruker AV700 spectrometer at ambient temperature; chemical shifts are quoted in parts per million (ppm) and were referenced as follows: chloroform-*d*, 7.26 ppm; DMSO-d_6, 2.54 ppm for ^{1}H NMR; chloroform-*d*, 77.0 ppm; DMSO, 128.0 ppm for ^{13}C NMR. Coupling constants (*J*) are quoted in Hertz. Mass spectrometry was performed by the University of York mass spectrometry service using electron spray ionisation (ESI) technique. Thin layer chromatography was performed on glass-backed plates coated with Merck Silica gel 60 F_{254}. The plates were developed using ultraviolet light, acidic aqueous ceric ammonium molybdate, basic aqueous potassium permanganate or ethanolic anisaldehyde. Liquid chromatography was performed using forced flow (flash column) with the solvent systems indicated. The stationary phase was silica gel 60 (220–240 mesh) supplied by Fluorochem or silica gel Merck TLC grade 11695 supplied by Sigma-Aldrich. Hexane, DCM, toluene, THF were all purified using Innovative Technology Solvent Purification System; triethylamine were distilled from calcium hydride. All other solvents and reagents were used as received from commercial suppliers. All numbering on the structures below is for the benefit of characterisation and does not necessarily conform to IUPAC rules.

9.2 Experimental procedures

2-Methyl-4-carbomethoxy ester oxazoline (194)

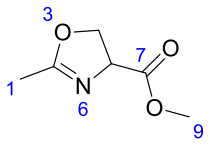

To a solution of *DL*-serine methyl ester hydrochloride (20 g, 0.13 mol) and ethyl acetimidate hydrochloride (17.5 g, 0.14 mol) in DCM (250 mL) was added triethylamine (25 g, 0.25 mol) over a 20 minute period. The mixture was stirred at room temperature under a N_2 atmosphere for 16 hours. The salts formed were filtered through a pad of celite and washed with diethyl ether (500 mL). The filtrate was concentrated and the solid formed was washed with diethyl ether (500 mL). The ether extracts were combined and concentrated to give a pale yellow oil. The crude material was purified by Kugelrhor distillation to give a colourless oil (13.2 g, 72 %). The ^{1}H NMR data were found to be in agreement with the literature.[105]

^{1}H NMR (400 MHz, $CDCl_3$): δ 4.72 (1H, ddq, *J* = 10.5, 8.0, 1.0 Hz, H-5), 4.48 (1H, dd, *J* = 8.5, 8.0 Hz, H-4), 4.40 (1H, dd, *J* = 10.5, 8.5 Hz, H-4), 3.78 (3H, s, H-9), 2.03 (3H, d, *J* = 1.0 Hz, H-1) ppm.

2-Methyl-4-carbomethoxy ester oxazole (195)

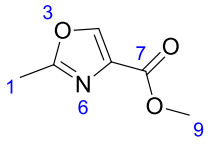

A solution of methyl oxazole **194** (13.0 g, 0.091 mol) in DCM (100 mL) stirring at 0 °C under N_2 was treated with DBU (27.7 g, 0.182 mol). The mixture was stirred for 15

minutes and was then treated with $BrCCl_3$ (19.8 g, 0.100 mol) and left to stir for 16 hours at 0 °C gradually warming to room temperature. The mixture was partitioned between ethyl acetate (250 mL) and a 2 M aqueous solution of HCl (200 mL). The layers were separated and the aqueous layer washed with ethyl acetate (250 mL). The combined organic layers were washed with a saturated solution of $NaHCO_3$ (2 × 400 mL), brine (2 × 400 mL), dried ($MgSO_4$), filtered and concentrated to give an off-white solid. The crude material was purified by flash chromatography on a silica gel column using a 5% ethyl acetate in petroleum ether to give a white solid (8.0 g, 62%). The ^{1}H NMR data were found to be in agreement with the literature.[106]

^{1}H NMR (400 MHz, $CDCl_3$): δ 8.14 (1H, s, H-4), 3.91 (3H, s, H-9), 2.50 (3H, s, H-1) ppm.

2-Methyloxazole-4-carboxylic acid (196)

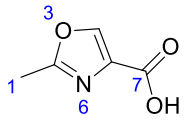

To a solution of 2-methyl-4-carbomethoxy ester oxazole **195** (8.0 g, 0.057 mol) in H_2O (20 mL) stirring at room temperature, was added a 32% aqueous solution of NaOH (10.0 g, 0.081 mol). The reaction was stirred for 1 hour and was then treated with a 37% aqueous solution of HCl (5.9 g, 0.060 mol). The reaction was cooled to 0 °C and left to stand for 1 hour. The solids were filtered and washed with cold H_2O (30 mL) to give a white solid (4.1 g, 57%). The ^{1}H NMR data were found to be in agreement with the literature.[57]

^{1}H NMR (400 MHz, DMSO): δ 8.49 (1H, s, H-4), 2.42 (3H, s, H-1) ppm.

_N_-Methoxy-_N_,2-dimethyloxazole-4-carboxamide (197)

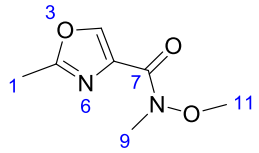

2-Methyoxazole-4-carboxylic acid **196** (4.1 g, 0.032 mol) and _N_,_O_-dimethylhydroxylamine hydrochloride (3.01 g, 0.032 mol) were suspended in DCM (15 mL) and H_2O (1.5 mL). The reaction was treated with triethylamine (4.5 g, 0.044 mol) and was then stirred at room temperature for 1 hour to give a clear solution which was cooled to 0 °C. 1-(3-Dimethylaminopropyl)-3-ethylcarbodiimide hydrochloride (7.3 g, 0.038 mol) was suspended in DCM (30 mL) and then cooled to 0 °C. The solution of carboxylic acid was added to the slurry of diimide maintaining the temperature < 10 °C. Once the addition was complete the solution was allowed to warm to room temperature and then stirred for 1 hour. A solution of citric acid (2.5 g) in H_2O (10.4 mL) was added and the layers were separated. The aqueous solution was washed with DCM (2 × 20 mL). The organic extracts were combined and then washed with H_2O (30 mL) and concentrated to give an orange solid (3.3 g, 61%). The ^{1}H NMR data were found to be in agreement with the literature.[57]

^{1}H NMR (400 MHz, $CDCl_3$): δ 8.03 (1H, s, H-4), 3.71 (3H, s, H-11), 3.34 (3H, s, H-9), 2.47 (3H, s, H-1) ppm.

2-Methyloxazole-4-carboxaldehyde (198)

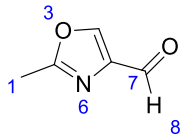

A solution of *N*-methoxy-*N*,2-dimethyloxazole-4-carboxamide **196** (3.3 g, 19 mmol) in THF (200 mL) stirring at -35 °C under a N_2 atmosphere was treated with a 1.0 M solution of $LiAlH_4$ in THF (19 mL, 19 mmol). The reaction was stirred for 1 hour and was treated with a 20% aqueous solution of Rochelle's salt (60 mL). The mixture was warmed to room temperature and stirred for 2 hours. The mixture was then partitioned between diethyl ether (200 mL) and H_2O (200 mL). The organic layer was separated and the aqueous layer washed with diethyl ether (200 mL). The combined organic layers were washed with brine (300 mL), dried ($MgSO_4$) and concentrated *in vacuo* to give a brown solid (1.7 g, 79%). The ^{1}H NMR data was found to be in agreement with the literature.[105]

^{1}H NMR (400 MHz, $CDCl_3$): δ 9.89 (1H, s, H-8), 8.15 (1H, s, H-4), 2.52 (3H, s, H-1) ppm.

(*E*)-2-methyl-3-(2'-methyl-oxazol-4'-yl)-propenal (66)

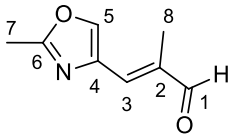

2-(Triphenylphosphoranylidene)-propionaldehyde (2.8 g, 8.8 mmol) was added to a solution of (2'-methyl-oxazol-4'-yl)-formaldehyde (**198**) (780 mg, 7.0 mmol) in benzene (60 mL) at room temperature under an atmosphere of N_2. The reaction was heated under reflux for 20 hours, filtered and washed with pentane, resulting in precipitate formation in the filtrate. This precipitate was removed by filtration and washed with pentane. The

filtrate was dried ($MgSO_4$), filtered, and concentrated *in vacuo* to yield an off-white solid. The solid was successively extracted with pentane, and the combined organic extracts were dried ($MgSO_4$), filtered, and concentrated *in vacuo* to yield a pale yellow solid. Flash column chromatography (50% ethyl acetate in petroleum ether) gave **66** as a pale yellow solid (1.01 g, 96%). The ^{1}H NMR data were found to be in agreement with the literature.[105]

^{1}H NMR ($CDCl_3$, 400 MHz): δ 9.55 (1H, s, H-1), 7.83 (1H, q, *J* = 1.2 Hz, H-5), 7.07 (1H, s, H-3), 2.51 (3H, s, H-8), 2.08 (3H, d, *J* = 1.2 Hz, H-7) ppm;

2-(*N*-Benzyl-*N*-mesitylenesulfonyl)amino-1-phenyl-1-propyl 3'-hydroxy-2',4'-dimethyl-5'-(2-methyloxazol-4-yl)pent-4'-enoate (**149**)

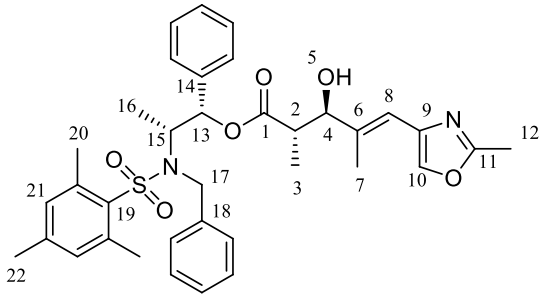

Triethylamine was added to a solution of 2-(*N*-benzyl-*N*-mesitylenesulfonyl)amino-1-phenyl-1-propyl propionate **148** (1.60 g, 3.33 mmol) in DCM (31 mL) at room temperature, under an atmosphere of N_2. The reaction mixture was cooled to -78 ^{o}C, and a pre-cooled 1.0 M solution of dicyclohexylboron triflate in hexanes (10.0 mL, 10.0 mmol) in DCM (10 mL) was added to the reaction mixture *via* cannula. After stirring for 3 hours at -78 ^{o}C, (*E*)-2-methyl-3-(2-methyloxazol-5-yl)acrylaldehyde **29** (604 mg, 3.76 mmol) was added as a solution in DCM (10 mL). After stirring for 3 hours at -78 ^{o}C, the reaction was warmed to room temperature and quenched with an aqueous solution of pH 7 phosphate buffer (20 mL), followed by methanol (40 mL) and hydrogen peroxide (30% w/w in H_2O) (10 mL). The phases were separated and the aqueous was further

extracted with DCM (3 × 50 mL). The combined organics were washed with brine (50 mL), dried (Na_2SO_4), and concentrated *in vacuo* to a yellow oil, which was purified by flash silica gel column chromatography (35% diethyl ether in hexanes) to yield **149** as an off-white solid (1.91 g, 91%).

$[\alpha]^{24}_D$ -40.3 (c = 0.785, $CHCl_3$); **Melting point** 70-72 ^oC; **IR** (film, NaCl): υ_{max} 2979, 2939, 1738, 1604, 1585, 1496, 1150 cm^{-1}; **^{1}H NMR** (400 MHz, $CDCl_3$): δ 7.49 (1H, s, H-10), 7.14-7.37 (8H, m, Ar), 6.89 (2H, s, H-21), 6.80-6.87 (2H, m, Ar), 6.23 (1H, bs , H-8), 5.82 (1H, d, *J* = 3.9 Hz, H-13), 4.81 (1H, d, *J* = 16.6 Hz, H-17), 4.60 (1H, d, *J* = 16.6 Hz, H-17), 4.23 (1H, dd, *J* = 9.3, 3.5 Hz, H-4), 4.07 (1H, dq, *J* = 7.0, 3.9 Hz, H-15), 2.62-2.72 (2H, m, H-2 + H-5), 2.50 (6H, s, H-20), 2.44 (3H, s, H-12), 2.29 (3H, s, H-22), 1.95 (3H, d, *J* = 0.8 Hz, H-7), 1.15 (3H, d, *J* = 7.0 Hz, H-16), 0.98 (3H, d, *J* = 7.2 Hz, H-3) ppm; **^{13}C NMR** (100 MHz, $CDCl_3$): δ 174.5, 160.9, 142.5, 138.8, 138.2, 138.1, 137.4, 135.8, 133.4, 132.1, 128.4, 128.3, 127.8, 127.6, 127.0, 125.7, 118.5, 79.9, 78.3, 56.8, 48.2, 43.5, 22.9, 20.8, 14.2, 13.7, 13.3, 13.3 ppm; **MS** (ESI): m/z 631 (M^+); HRMS: found: (M^+) 631.2851. $C_{36}H_{43}N_2O_6S$ requires (M^+) 631.2836.

2-(*N*-Benzyl-*N*-mesitylenesulfonyl)amino-1-phenyl-1-propyl 2',4'-dimethyl-3'-(dimethyl (1,1-dimethylethyl)silyloxy)-5'-(2-methyloxazol-4-yl)pent-4'-enoate (**206**)

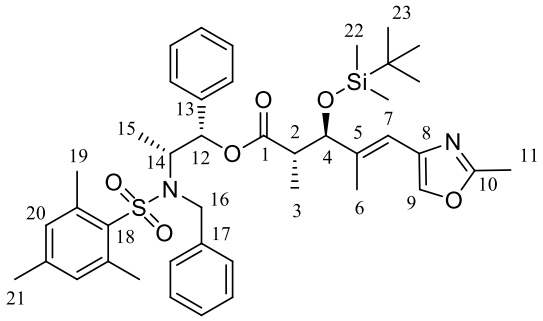

A solution of 2-(*N*-benzyl-*N*-mesitylenesulfonyl)amino-1-phenyl-1-propyl 3'-hydroxy-2',4'-dimethyl-5'-(2-methyloxazol-4-yl)pent-4'-enoate **148 (**0.800 g, 1.27 mmol) in DCM (5 mL) was cooled to 0 ^{o}C under an atmosphere of N_2. To this solution 2,6-lutidine (0.442 mL, 3.8 mmol) and t-butyldimethylsilyl triflate (0.585 mL, 2.54 mmol) were added. After stirring for 1 hour at 0 ^{o}C, the reaction was quenched with a 1 M aqueous solution of HCl (8 mL). The phases were separated and the aqueous was further extracted with DCM (3 × 20 mL). The combined organics were dried (Na_2SO_4), filtered and concentrated *in vacuo* to a yellow oil, which was further purified by flash silica gel column chromatography (25% ethyl acetate in hexanes) to yield **206** as a yellow oil (0.880 g, 93%)

$[\alpha]^{24}_{D}$ -37.8 (c = 1.105, $CHCl_3$); **IR** (film, NaCl): υ_{max} 2933, 2856, 1744, 1604, 1456, 1323, 1254, 1154 cm^{-1}; **^{1}H NMR** (400 MHz, $CDCl_3$) δ 7.47 (1H, s, H-9), 7.13-7.33 (8H, m, Ar), 7.02-7.10 (2H, m, Ar), 6.88 (2H, s, H-20), 6.14 (1H, d, *J* = 1.1 Hz, H-7), 5.67 (1H, d, *J* = 6.1 Hz, H-12), 4.91 (1H, d, *J* = 16.1 Hz, H-16), 4.39 (1H, d, *J* = 16.1 Hz, H-16), 4.26 (1H, d, *J* = 9.5 Hz, H-4), 4.01 (1H, m, H-14), 2.63-2.73 (1H, m, H-2), 2.44 (3H, s, H-11), 2.40 (6H, s, H-19), 2.32 (3H, s, H-21), 1.85 (3H, d, *J* = 1.1 Hz, H-6), 1.56 (9H, s, H-23), 1.16 (3H, d, *J* = 6.7 Hz, H-15), 0.77 (3H, d, *J* = 7.3 Hz, H-3), -0.01 (3H, s, H-22), -0.05 (3H, s, H-22) ppm; **^{13}C NMR** (100 MHz, $CDCl_3$): δ 173.4, 160.8, 142.3, 140.3, 138.5,

138.0, 137.4, 135.5, 132.8, 132.1, 128.4, 128.3, 128.1, 127.8, 127.3, 126.3, 118.5), 80.5, 77.5, 56.6, 48.1, 44.9, 25.8, 25.6, 22.8, 20.8, 18.0, 14.8, 14.1, 13.7, 13.3, -4.9, -5.1 ppm; **MS** (ESI): m/z 745 ($M+H^+$), 767 ($M+Na^+$); HRMS: found: ($M+H^+$) 745.3721, ($M+Na^+$) 767.3540,. $C_{42}H_{57}N_2O_6SSi$ requires ($M+H^+$) 745.3701, $C_{42}H_{56}N_2NaO_6SSi$ requires ($M+Na^+$) 767.3521.

(*E*,2*R*,3*R*)-2,4-dimethyl-3-(dimethyl(1,1-dimethylethyl)silyloxy)-5-(2-methyloxazol-4-yl) pent-4-enol (207)

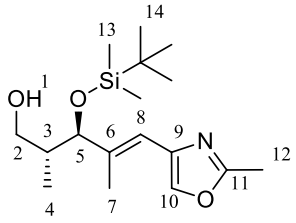

A solution of 2-(*N*-benzyl-*N*-mesitylenesulfonyl)amino-1-phenyl-1-propyl 2',4'-dimethyl-3'-(dimethyl (1,1-dimethylethyl)silyloxy)-5'-(2-methyloxazol-4-yl)pent-4'-enoate **206** (1.12 g, 1.50 mmol) in DCM (3 mL) was cooled to 0 ^oC under an atmosphere of N_2. To this 1 M solution of diisobutylaluminium hydride (4.50 mL, 4.50 mmol) was added dropwise over a 3 minute period. After stirring for 15 minutes at 0 ^oC, the reaction was quenched with 0.5 M aqueous solution of Rochelle's salt (40 mL). The mixture was diluted with diethyl ether (50 mL) and stirred vigorously for 2 hours. The phases were separated and the aqueous was further extracted with diethyl ether (2 x 30 mL). Brine was added to the aqueous phase and it was further extracted with diethyl ether (2 x 30 ml). The combined organics were dried (Na_2SO_4), filtered and concentrated *in vacuo* to give a yellow oil, which was further purified by flash silica gel column chromatography (30% ethyl acetate in hexanes) to yield **207** as a clear oil (400 mg, 82%).

[α]^{24}D +40.0 (c = 0.500, $CHCl_3$); **IR** (film, NaCl): υ_{max} 3413, 2957, 2857, 1643, 1061 cm^{-1}; **^{1}H NMR** (400 MHz, $CDCl_3$): δ 7.49 (1H, s, H-10), 6.18 (1H, s, H-8), 3.99 (1H, d, *J* = 7.9 Hz, H-5), 3.67-3.60 (2H, m, H-2), 2.83 (1H, br m, H-1), 2.45 (3H, s, H-12), 1.88-1.93 (4H, m, H-3 + H-7), 0.90 (9H, s, H-14), 0.81 (3H, d, *J* = 7.0 Hz, H-4), 0.11 (3H, s, H-14) , -0.01 (3H, s, H-14) ppm; ^{13}C NMR (100 MHz, $CDCl_3$): δ 160.9, 140.3, 137.9, 135.6, 117.5, 84.7, 67.0, 38.9, 26.0, 18.2, 14.5, 14.0, -4.3, -5.1 ppm; **MS** (ESI): m/z 326 ($M+H^+$), 348 ($M+Na^+$); HRMS: found: ($M+H^+$) 326.2139, ($M+Na^+$) 348.1968 $C_{17}H_{32}NO_3Si$ requires ($M+H^+$) 326.2146, $C_{17}H_{31}NNaO_3Si$ requires ($M+Na^+$) 348.1965.

(*E*,2*S*,3*R*)-2,4-Dimethyl-3-(dimethyl(1,1-dimethylethyl)silyloxy)-5-(2-methyloxazol-4-yl) pent-4-enal (210)

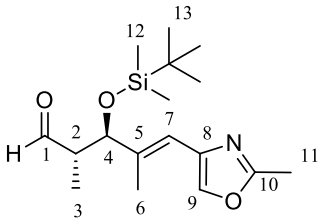

A solution of 2,4-dimethyl-3-(dimethyl(1,1-dimethylethyl)silyloxy)-5-(2-methyloxazol-4-yl) pent-4-enol **207 (**0.280 g, 0.86 mmol) in DCM (8 mL) was cooled to 0 ^oC under an atmosphere of N_2. To this, Dess-Martin periodinane (730 mg, 1.72 mmol) was then added in one portion. The reaction mixture was then allowed to warm to room temperature. After stirring for 1 hour at room temperature, the reaction was quenched with 2 M aqueous NaOH solution (15 mL). The mixture was then extracted with diethyl ether (3 x 50 mL). The combined organics were washed with aqueous saturated $NaHCO_3$ solution, dried (Na_2SO_4), filtered and concentrated *in vacuo* to give a clear oil (262 mg, 94%), which was used in the next step without further purification.

[α]^{24}D +7.0 (c = 0.570, $CHCl_3$); **IR** (film, NaCl): υ_{max} 2956, 2931, 2857, 1728, 1254, 1108 cm^{-1}; **^{1}H NMR** (400 MHz, $CDCl_3$): δ 9.77 (1H, d, *J* = 2.8 Hz, H-1), 7.50 (1H, s, H-9), 6.23 (1H, br s, H-7), 4.24 (1H, d, *J* = 8.2 Hz, H-4), 2.22 (1H, dqd, *J* = 8.2, 7.0 and 2.8 Hz, H-2), 2.46 (3H, s, H-11), 1.89 (3H, d, *J* = 0.9 Hz, H-6), 0.91 (3H, d, *J* = 7.0 Hz, H-3), 0.86 (9H, s, H-13) , 0.05 (3H, s, H-12) , -0.03 (3H, s, H-12) ppm; **^{13}C NMR** (100 MHz, $CDCl_3$): δ 204.7, 160.9, 138.7, 137.5, 135.7, 118.0, 80.3, 60.4, 50.5, 29.7, 25.7, 18.1, 13.8, 11.1, -4.5, -5.3 ppm; **MS** (ESI): m/z 324 ($M+H^+$); HRMS: found: ($M+H^+$) 324.1994. $C_{17}H_{30}NO_3Si$ requires ($M+H^+$) 324.1989.

(3*S*,4*S*,5*R*,6*R*,*E*)-6-(dimethyl(1,1-dimethylethyl)silyloxy)-3,5,7-trimethyl-8-(2-methyloxazol-4-yl)octa-1,7-dien-4-ol (240)

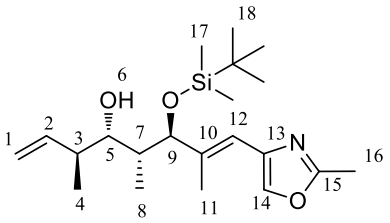

E-crotyl boronic acid pinacol ester (914 μL, 4.50 mmol) was cooled to 0 ^oC under an atmosphere of N_2. To this, a solution of 2,4-dimethyl-3-(dimethyl(1,1-dimethylethyl)silyloxy)-5-(2-methyloxazol-4-yl) pent-4-enal **210 (**1.15 g, 3.60 mmol) in dry hexane (5 mL) was then added. The reaction mixture was then allowed to warm to room temperature. After stirring for 17 hours at room temperture, a solution of ethanolamine (900 μL) in DCM (900 μL) was added. The mixture was then stirred for further 4 hours. The mixture was then concentrated *in vacuo* and purified by flash silica gel column chromatography (10% ethyl acetate in hexanes) to yield **240** as a clear oil (1.16 g, 86%).

[α]^{24}D +29.8 (c = 1.435, $CHCl_3$); **IR** (film, NaCl): υ_{max} 3498, 2955, 2930, 2857, 1586, 1463, 1383, 1253, 1106 cm^{-1}; **^{1}H NMR** (400 MHz, $CDCl_3$): δ 7.46 (1H, s, H-14), 6.27 (1H, bs, H-12), 5.76 (1H, ddd, J = 17.1, 10.2 and 8.4 Hz, H-2), 5.10 (1H, dd, J = 17.1 and 1.8 Hz, H-1), 5.05 (1H, dd, J = 10.2 and 1.8 Hz, H-1), 4.17 (1H, d, *J* = 5.5 Hz, H-9), 3.63 (1H, m, H-5), 2.70 (1H, bs, H-6), 2.45 (3H, s, H-16), 2.18-2.28 (1H, m, H-3), 1.89 (3H, d, *J* = 0.9 Hz, H-11), 1.78-1.87 (1H, m, H-7), 0.84-0.94 (15H, m, H-4 + H-8 + H-18), 0.08 (3H, s, H-17) , -0.01 (3H, s, H-17) ppm; **^{13}C NMR** (100 MHz, $CDCl_3$): δ 160.7, 142.5, 139.9, 138.1, 135.4, 116.1, 115.1, 81.8, 73.0, 60.4, 41.9, 37.1, 25.9, 18.1, 16.5, 15.1, 13.9, 10.1, -4.7, -5.3 ppm; **MS** (ESI): m/z 402 ($M+Na^+$); HRMS: found: ($M+Na^+$) 402.2419. $C_{21}H_{37}NNaO_3Si$ requires ($M+Na^+$) 402.2435.

_S_-_p_-Tolyl prop-2-enethioate (272)

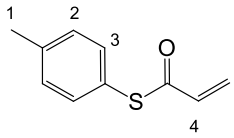

Butylated hydroxytoluene (35.7 mg, 0.162 mmol, 0.01 eq.) and acryloyl chloride (1.34 mL, 16.5 mmol, 1.5 eq.) were dissolved in cyclohexane (7 mL). In a separate flask $NaBH_4$ (13.4 mg, 0.35 mmol, 0.03 eq.) and 4-methylbenzenethiol (1.38 g, 11.0 mmol) were added in order to 15% aq. NaOH (5 mL). This mixture was stirred for 1 hour at room temperature. Under ice-cooling, this mixture was added over a period of 10 minutes to the acryloyl chloride solution. After the reaction mixture was stirred for 30 minutes at 55-60 ºC, it was allowed to cool to room temperature and then extracted with diethyl ether (3 x 4 mL). The combined organic layers were washed with $NaHCO_3$ (3 x 4 mL) and brine (3 x 4 mL), dried over $MgSO_4$, filtered and concentrated *in vacuo* to a yellow oil, which was purified by flash silica gel column chromatography (3% ethyl acetate in *n*-hexane) to yield

272 as a yellow oil (690 mg, 45%). The proton NMR spectrum matched that given in literature.[107]

^{1}H NMR (400 MHz, $CDCl_3$): δ 7.33 (2H, d, *J* = 8.2 Hz, H-2), 7.24 (2H, d, *J* = 8.2 Hz, H-3), 6.46 (1H, dd, *J* = 17.2, 9.6, H-4), 6.38 (1H, dd, *J* = 17.2, 1.6 Hz, H-5), 5.76 (1H, dd, *J* = 9.6, 1.6 Hz, H-5), 2.39 (3H, s, H-1) ppm.

(2*E*,4*S*,5*S*,6*R*,7*R*,8*E*)-S-p-Tolyl 7-(dimethyl(1,1-dimethylethyl)silyloxy)-5-hydroxy-4,6,8-trimethyl-9-(2-methyloxazol-4-yl)nona-2,8-dienethioate (278)

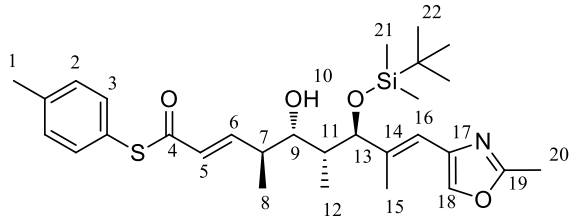

A round bottom flask was charged with (3*S*,4*S*,5*R*,6*R*,*E*)-6-(dimethyl(1,1-dimethylethyl)silyloxy)-3,5,7-trimethyl-8-(2-methyloxazol-4-yl)octa-1,7-dien-4-ol **240** (40 mg, 0.11 mmol), *S*-p-tolyl prop-2-enethioate **272** (56 mg, 0.32 mmol) and dry ether (1 ml) under an atmosphere of N_2. To this, copper (I) iodide (4 mg, 0.02 mmol) and Hoveyda-Grubbs 2nd generation catalyst (13 mg, 0.02 mmol) were then added as solids in one portion. The mixture was refluxed for 3 hours. It was then concentrated in vacuo and purified by flash silica gel column chromatography (10% ethyl acetate in hexanes) to yield **278** as a brown oil (44 mg, 79%).

$[\alpha]^{24}_D$ +26.9 (c = 1.035, $CHCl_3$); **IR** (film, NaCl): υ_{max} 3486, 2956, 2930, 2857, 1682, 1631, 1458, 1383, 1256 cm^{-1}; **^{1}H NMR** (400 MHz, $CDCl_3$): δ 7.48 (1H, s, H-18), 7.30 (2H, d, *J* = 8.1 Hz, H-3), 7.20 (2H, d, *J* = 8.1 Hz, H-2), 7.00 (1H, dd, *J*=15.6 and 8.1, H-6) 6.32 (1H, s, H-16), 6.21 (1H, dd, *J* = 15.6 and 0.9 Hz, H-5), 4.18 (1H, d, *J* = 4.0 Hz, H-13), 3.75 (1H, dd, *J* = 9.2 and 1.1 Hz, H-9), 3.03 (1H, bs, H-10), 2.46 (3H, s, H-20),

2.39 (1H, ddqd, *J* = 9.2, 8.1, 7.0 and 0.9 Hz, H-7), 2.36 (3H, s, H-1), 1.91 (3H, s, H-15), 1.81-1.89 (1H, m, H-11), 0.99 (3H, d, *J*=7.0 Hz, H-8), 0.88-0.96 (12H, m, H-12 + H-22), 0.10 (3H, s, H-21) , 0.01 (3H, s, H-21) ppm; **^{13}C NMR** (100 MHz, $CDCl_3$): δ 188.5, 160.8, 149.8, 139.5, 139.1, 135.6, 134.6, 129.9, 127.7, 124.2, 115.9, 82.3, 73.3, 60.4, 40.5, 36.9, 29.7, 25.9, 21.3, 21.1, 18.1, 15.9, 14.2, 13.9, 10.7, -4.6, -5.2 ppm; **MS** (ESI): m/z 530 ($M+H^+$), 552 ($M+Na^+$); HRMS: found: ($M+H^+$) 530.2757, ($M+Na^+$) 552.2575 $C_{29}H_{44}NO_4SSi$ requires ($M+H^+$) 530.2755, $C_{29}H_{43}NNaO_4SSi$ requires ($M+Na^+$) 552.2574.

(2*E*,4*S*,5*S*,6*R*,7*R*,8*E*)-p-Tolyl 7-((tert-butyldimethylsilyl)oxy)-5-hydroxy-4,6,8-trimethyl-9-(2-methyloxazol-4-yl)nona-2,8-dienoate (296)

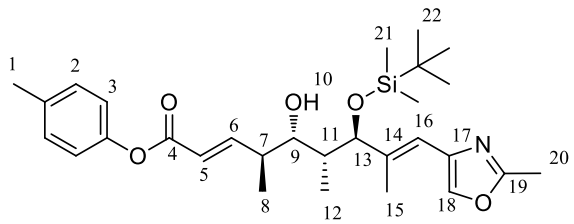

(3*S*,4*S*,5*R*,6*R*,*E*)-6-(dimethyl(1,1-dimethylethyl)silyloxy)-3,5,7-trimethyl-8-(2-methyloxazol-4-yl)octa-1,7-dien-4-ol **240** (35 mg, 0.092 mmol) and *p*-tolyl acrylate **295** (45 mg, 0.28 mmol) were dissolved in dry toluene (1 mL) under an atmosphere of N_2. To this, a solution of Hoveyda-Grubbs 2nd generation catalyst (11.6 mg, 0.019 mmol) in dry toluene (1 mL) was then added. After stirring for 20 hours at 55 °C, the mixture was concentrated *in vacuo* and purified by flash silica gel column chromatography (10% ethyl acetate in hexanes) to yield **296** as a clear oil (28 mg, 60%).

$[\alpha]^{24}_D$ +33.7 (c = 1.050, $CHCl_3$); **IR** (film, NaCl): υ_{max} 3440, 2910, 2885, 2813, 1710, 1624, 1484, 1439, 1232 cm^{-1}; **^{1}H NMR** (400 MHz, $CDCl_3$): δ 7.48 (1H, s, H-18), 7.17 (1H, dd, *J* = 15.7 and 8.2, H-6), 7.15 (2H, d, *J* = 8.4 Hz, H-2), 6.98 (2H, d, *J* = 8.4 Hz, H-3), 6.34 (1H, s, H-16), 6.05 (1H, dd, *J* = 15.7 and 1.1 Hz, H-5), 4.20 (1H, d, *J* = 3.7 Hz,

H-13), 3.78 (1H, dd, *J* = 9.3 and 0.7 Hz, H-9), 3.13 (1H, bs, H-10), 2.49 (1H, ddqd, *J* = 9.3, 8.2, 7.0 and 1.1 Hz, H-7), 2.46 (3H, s, H-20), 2.33 (3H, s, H-1), 1.93 (3H, s, H-15), 1.87 (1H, qdd, *J* = 6.7, 3.7 and 0.7 Hz, H-11), 1.03 (3H, d, *J* = 7.0 Hz, H-8), 0.96 (3H, d, *J* = 6.7 Hz, H-12), 0.94 (9H, s, H-22), 0.10 (3H, s, H-21) , 0.03 (3H, s, H-21) ppm; **^{13}C NMR** (100 MHz, $CDCl_3$): δ 165.1, 160.8, 154.6, 148.5, 139.0, 138.0, 135.6, 135.1, 129.8, 121.3, 120.5, 115.8, 82.3, 73.3, 60.4, 40.5, 36.8, 30.3, 25.9, 20.8, 18.1, 15.9, 13.9, 10.7, -4.7, -5.3 ppm; **MS** (ESI): m/z 514 ($M+H^+$), 536 ($M+Na^+$); HRMS: found: ($M+H^+$) 514.2972, ($M+Na^+$) 536.2788 $C_{29}H_{44}NO_5Si$ requires ($M+H^+$) 514.2983, $C_{29}H_{43}NNaO_5Si$ requires ($M+Na^+$) 536.2803.

_S_-4-Methylphenyl 2'-((2_R_,3_R_,4_S_,5_R_,6_R_)-tetrahydro-4-hydroxy-3,5-dimethyl-6-((_E_)-1-(2-methyloxazol-4-yl)prop-1-en-2-yl)-2H-pyran-2-yl)ethanethioate (322)

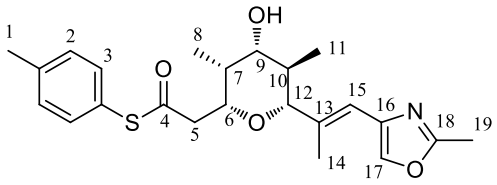

(2*E*,4*S*,5*S*,6*R*,7*R*,8*E*)-*S*-p-Tolyl 7-(dimethyl(1,1-dimethylethyl)silyloxy)-5-hydroxy-4,6,8-trimethyl-9-(2-methyloxazol-4-yl)nona-2,8-dienethioate **278** (30 mg, 0.057 mmol) was dissolved in dichloromethane (1.0 ml) and water (0.1 mL) was added. The mixture was cooled to 0 °C and trifluoroacetic acid was then added over a period of 3 minutes. After stirring for 6 hours at room temperature the reaction was quenched with a saturated aqueous solution of $NaHCO_3$ and diluted with DCM. The phases were separated and the aqueous layer extracted with DCM. The combined organics were dried over $MgSO_4$, filtered, concentrated *in vacuo* and purified by flash silica gel column chromatography (50% diethyl ether in hexanes) to yield **322** as a clear oil (16.7 mg, 71%).

[α]^{24}D +30.6 (c = 0.350, $CHCl_3$) **IR** (film, NaCl): υ_{max} 3348, 3005, 2923, 2879, 2829, 1677, 1560, 1470, 1435, 1363, 1296, 1247 cm^{-1}; **NOE**: H-6 – H-12 7.5%, H-6 – H-7 2.2%, H-7 – H-9 1.6%, H-7 – H-8 1.6%, H-10 – H-8 2.2%, H-10 – H-11 2.2%; **^{1}H NMR** (400 MHz, $CDCl_3$): δ 7.49 (1H, s, H-17), 7.26 (2H, d, *J* = 8.1 Hz, H-2), 7.20 (2H, d, *J* = 8.1 Hz, H-3), 6.18 (1H, s, H-15), 4.02 (1H, ddd, *J* = 6.8, 6.8 and 1.9 Hz, H-6), 3.52 (1H, dd, *J* = 10.3 and 4.6 Hz, H-9), 3.49 (1H, d, *J* = 10.1 Hz, H-12), 2.97 (1H, dd, *J* = 15.2 and 6.8 Hz, H-5), 2.76 (1H, dd, *J* = 15.2 and 6.8, H-5), 2.45 (3H, s, H-19), 2.36 (3H, s, H-1), 1.99 (1H, qdd, *J* = 6.9, 4.6 and 1.9 Hz, H-7), 1.93 (3H, s, H-14), 1.71 (1H, ddq, *J* = 10.3, 10.1 and 6.5 Hz, H-10), 1.02 (3H, d, *J* = 6.9 Hz, H-8), 0.85 (3H, d, *J* = 6.5 Hz, H-11) ppm; **^{13}C NMR** (100 MHz, $CDCl_3$): δ 195.5, 160.7, 139.7, 137.4, 135.7, 134.4, 130.0, 124.0, 118.6, 88.7, 76.2, 74.8, 46.6, 37.9, 34.3, 30.3, 21.3, 14.3, 13.8, 13.3, 5.8 ppm; **MS** (ESI): m/z 416 ($M+H^+$), 438 ($M+Na^+$); HRMS: found: ($M+H^+$) 416.1874, ($M+Na^+$) 438.1690 $C_{23}H_{30}NO_4S$ requires ($M+H^+$) 416.1890, $C_{23}H_{29}NNaO_4S$ requires ($M+Na^+$) 438.1710.

4-Methylphenyl 2'-((2*S*,3*R*,4*S*,5*R*,6*R*)-tetrahydro-4-hydroxy-3,5-dimethyl-6-((*E*)-1-(2-methyloxazol-4-yl)prop-1-en-2-yl)-2H-pyran-2-yl)acetate (324)

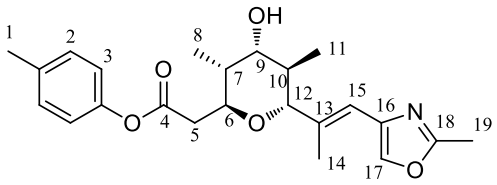

(2*E*,4*S*,5*S*,6*R*,7*R*,8*E*)-*p*-Tolyl-7-((tert-butyldimethylsilyl)oxy)-5-hydroxy-4,6,8-trimethyl-9-(2-methyloxazol-4-yl)nona-2,8-dienoate **296** (10.0 mg, 0.020 mmol) and acetic acid (0.2 μL, 0.004 mmol) were dissolved in THF (1 mL) under an atmosphere of N_2. To this, 1 M solution of tetrabutylammonium fluoride (30 μL, 0.030 mmol) was then added. After stirring for 1 hour at room temperature, 5% aqueous solution of $NaHCO_3$ (1 mL) was

added. The phases were separated and the aqueous extracted with diethyl ether (3 x 2 ml). The combined organics were dried over $MgSO_4$, filtered, concentrated *in vacuo* and purified by flash silica gel column chromatography (50% diethyl ether in hexanes) to yield **324** as a clear oil (5.5 mg, 71%).

$[\alpha]^{24}_D$ -26.9 (c = 0.710, $CHCl_3$) **IR** (film, NaCl): υ_{max} 3357, 2919, 2883, 1727, 1560, 1484, 1434, 1358, 1298, 1223 cm^{-1}; **NOE**: H-6 – H-10 2.4%, H-6 – H-8 2.7%, H-7 – H-12 2.1%, H-7 – H-9 1.2%, H-9 – H-10 3.7%, H-9 – H-11 2.7%, H-11 – H-12 2.6%; **^{1}H NMR** (700 MHz, $CDCl_3$): δ 7.45 (1H, s, H-17), 7.12 (2H, d, *J* = 8.2 Hz, H-2), 6.93 (2H, d, *J* = 8.2 Hz, H-3), 6.23 (1H, s, H-15), 4.43 (1H, ddd, *J* = 9.2, 6.0 and 2.2 Hz, H-6), 3.84 (1H, d, *J* = 9.9 Hz, H-12), 3.76 (1H, dd, *J* = 9.3 and 4.5 Hz, H-9), 3.09 (1H, dd, *J* = 14.3 and 9.2 Hz, H-5), 2.78 (1H, dd, *J* = 14.3 and 6.0, H-5), 2.45 (3H, s, H-19), 2.32 (3H, s, H-1), 2.01 (1H, ddq, *J* = 9.9, 9.3 and 6.5 Hz, H-10), 1.97 (3H, s, H-14), 1.93 (1H, qdd, *J* = 7.0, 4.5 and 2.2 Hz, H-7), 1.21 (3H, d, *J* = 7.0 Hz, H-8), 0.91 (3H, d, *J* = 6.5 Hz, H-11) ppm; **^{13}C NMR** (100 MHz, $CDCl_3$): δ 170.0, 160.7, 148.4, 137.7, 137.4, 135.8, 135.5, 129.9, 121.2, 118.6, 82.1, 75.7, 72.3, 45.2, 37.1, 37.0, 35.3, 20.8, 14.2, 13.8, 12.6 ppm; **MS** (ESI): m/z 400 ($M+H^+$), 422 ($M+Na^+$); HRMS: found: ($M+H^+$) 400.2110, ($M+Na^+$) 422.1929 $C_{23}H_{30}NO_5$ requires ($M+H^+$) 400.2118, $C_{23}H_{29}NNaO_5$ requires ($M+Na^+$) 422.1938.

4-Methylphenyl 2'-((2*S*,3*R*,4*S*,5*R*,6*R*)-tetrahydro-4-hydroxy-3,5-dimethyl-6-((*E*)-1-(2-methyloxazol-4-yl)prop-1-en-2-yl)-2H-pyran-2-yl)acetate (321)

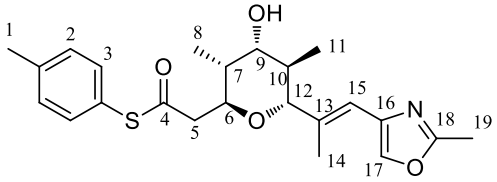

(2*E*,4*S*,5*S*,6*R*,7*R*,8*E*)-S-p-Tolyl 7-(dimethyl(1,1-dimethylethyl)silyloxy)-5-hydroxy-4,6,8-trimethyl-9-(2-methyloxazol-4-yl)nona-2,8-dienethioate **278** (20.0 mg, 0.038 mmol) and acetic acid (0.4 μL, 0.008 mmol) were dissolved in THF (1 ml) under an atmosphere of N_2. To this, 1 M solution of tetrabutylammonium fluoride (60 μL, 0.060 mmol) was then added. After stirring for 1 hour at room temperature, 5% aqueous solution of $NaHCO_3$ (2 mL) was added. The phases were separated and the aqueous layer extracted with diethyl ether (3 × 2 ml). Combined organics were dried over $MgSO_4$, filtered, concentrated *in vacuo* and purified by flash silica gel column chromatography (50% diethyl ether in hexanes) to yield **321** as a clear oil (5.5 mg, 35%).

$[\alpha]^{24}_D$ -42.4 (c = 0.380, $CHCl_3$) **IR** (film, NaCl): υ_{max} 3356, 2919, 2882, 2832, 1674, 1560, 1434, 1358, 1245 cm^{-1}; **NOE**: H-6 – H-10 1.7%, H-6 – H-8 2.4%, H-7 – H-8 2.4%, H-7 – H-11 2.5%, H-9 – H-12 1.8%, H-9 – H-10 2.8%, H-9 – H-11 2.6%, H-12 – H-11 2.2%, H-10 – H-8 2.5%; **^{1}H NMR** (700 MHz, $CDCl_3$): δ 7.49 (1H, s, H-17), 7.27 (2H, d, *J* = 8.0 Hz, H-2), 7.19 (2H, d, *J* = 8.0 Hz, H-3), 6.26 (1H, s, H-15), 4.35 (1H, ddd, *J* = 7.3, 7.3 and 2.0 Hz, H-6), 3.78 (1H, d, *J* = 10.0 Hz, H-12), 3.72 (1H, dd, *J* = 9.2 and 4.2 Hz, H-9), 3.16 (1H, dd, *J* = 14.4 and 7.3 Hz, H-5), 2.92 (1H, dd, *J* = 14.4 and 7.3, H-5), 2.45 (3H, s, H-19), 2.36 (3H, s, H-1), 1.99 (1H, qdd, *J* = 6.9, 4.2 and 2.0 Hz, H-7), 1.94 (3H, s, H-14), 1.89 (1H, ddq, *J* = 10.0, 9.2 and 6.5 Hz, H-10), 1.16 (3H, d, *J* = 6.9 Hz, H-8), 0.90 (3H, d, *J* = 6.5 Hz, H-11) ppm; **^{13}C NMR** (100 MHz, $CDCl_3$): δ 195.3, 160.7, 139.8, 137.7, 137.3, 135.7, 134.4, 130.0, 123.9, 118.9, 82.3, 75.9, 72.2, 45.2, 36.9, 35.2,

21.3, 14.2, 13.8, 13.7, 12.5 ppm; **MS** (ESI): m/z 416 ($M+H^+$), 438 ($M+Na^+$); HRMS: found: ($M+H^+$) 416.1878, ($M+Na^+$) 438.1703 $C_{23}H_{30}NO_4S$ requires ($M+H^+$) 416.1890, $C_{23}H_{29}NNaO_4S$ requires ($M+Na^+$) 438.1710.

1-phenylhex-5-en-1-ol (379a)
(prepared by Ugur Kaya)

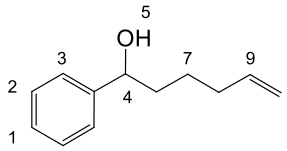

5-Bromo-1-pentene (**380**) (894 mg, 6.00 mmol) in dry THF (2 mL) was added to a suspension of magnesium turnings (146 mg, 6.00 mmol) in dry THF (8.5 mL) over a period of 5 minutes under N_2 atmosphere at 0 °C. After stirring for 1 h at room temperature the Grignard reagent (3.34 mL, 1.2 eq.) was added to a solution of benzaldehyde (160 mg, 1.5 mmol) in dry THF (1 mL) over a period of 5 minutes at 0 °C. After a further 1 h Grignard reagent (1.41 mL, 0.5 eq.) was added over 5 minutes at the same temperature. After stirring for 1.5 h the reaction was quenched with ice water (6 mL) and treated with sulfuric acid (5 M, 1.5 mL) until the magnesium salt dissolved. After seperation of the phases the aqueous layer was extracted with diethyl ether (2 × 4 mL). The combined organic phases were dried over $MgSO_4$, filtered and concentrated *in vacuo* to give a yellow oil, which was further purified by flash silica gel column chromatography (5 to 15 % ethyl acetate in petroleum ether) to yield **379a** as a yellow oil (189 mg, 72 %).

IR (film, NaCl): ν_{max} 3321, 3017, 2888, 2816, 1431, 1047, 1012, 981, 897, 750, 690 cm^{-1}. **^{1}H-NMR** (400 MHz, $CDCl_3$) δ 7.37 – 7.31 (3H, m, H-1 + H-2), 7.30 – 7.27 (2H, m, H-3), 5.78 (1H, dddd, *J* = 17.0, 10.2, 6.7 and 6.7 Hz, H-9), 4.99 (1H, ddd, *J* = 17.0, 3.5 and 1.9 Hz, H-10), 4.94 (1H, dddd, *J* = 10.2, 1.9 and 1.2 Hz, H-10) 4.68 (1H, dd, *J* = 7.5 and 5.8 Hz, H-4), 2.13 – 2.02 (2H, m, H-8), 1.88 – 1.65 (2H, m, H-5), 1.53 (1H, ddddd, *J* =

10.8, 7.4, 7.4, 7.4 and 5.3 Hz, H-7), 1.45 – 1.30 (1H, m, H-7) ppm. **^{13}C-NMR** (101 MHz, $CDCl_3$) δ 144.9, 138.7, 128.5, 127.6, 126.0, 114.8, 74.6, 38.6 , 33.7, 25.2 ppm.

2-methyloct-7-en-3-ol (379b)
(prepared by Ugur Kaya)

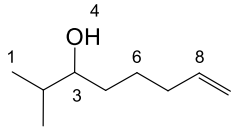

5-Bromo-1-pentene (**380**) (894 mg, 6.00 mmol) in dry THF (2.0 mL) was added over a period of 5 minutes to a suspension of magnesium turnings (146 mg, 6.00 mmol) in dry THF (8.5 mL) under N_2 atmosphere at 0 °C. After stirring for 40 minutes at room temperature the Grignard reagent (5.65 mL, 1.5 eq.) was added over a period of 5 minutes to a solution of isobutyraldeyhde (144 mg, 2.0 mmol) in dry THF (1 mL) at 0 °C. After stirring for 1 h the reaction was quenched with ice water (6 mL) and treated with sulfuric acid (5 M, 1.5 mL) until the magnesium salt dissolved. After seperation of the phases the aqueous layer was extracted with diethyl ether (2 × 5 mL). The combined organic phases were dried over $MgSO_4$, filtered and concentrated *in vacuo* to give a yellow oil, which was further purified by flash silica gel column chromatography (10 % ethyl acetate in petroleum ether) to yield **379b** as a yellow oil (73 mg, 26 %).

IR (film, NaCl): ν_{max} 3345, 3031, 2915, 2830, 1686, 1616, 1446, 1364, 1347, 1250, 979, 896 cm^{-1}. **^{1}H-NMR** (400 MHz, $CDCl_3$) δ 5.82 (1H, dddd, *J* = 17.0, 10.2, 6.7 and 6.7 Hz, H-8), 5.01 (1H, dddd, *J* = 17.0, 2.0, 1.6 and 1.6 Hz, H-9), 4.95 (1H, dddd, *J* = 10.2, 2.0, 1.2 and 1.2 Hz, H-9), 3.37 (1H, ddd, *J* = 8.5, 5.1 and 3.5 Hz, H-3), 2.13 – 2.05 (1H, m, H-2), 1.71 – 1.55 (2H, m, H-7), 1.53 – 1.43 (2H, m, H-5), 1.29 – 1.03 (2H, m, H-6), 0.92 (3H, d, *J* = 4.3 Hz, H-1), 0.90 (3H, d, *J* = 4.3 Hz, H-1) ppm. **^{13}C-NMR** (101 MHz,

$CDCl_3$) δ 138.9, 127.8, 114.7, 76.7, 33.9, 33.6, 25.4, 19.0, 17.2 ppm. **MS** (ESI): m/z 165 ($M+Na^+$); HRMS: found: ($M+Na^+$) 165.1250 $C_9H_{18}NaO$ requires ($M+Na^+$) 165.1255

Tetradec-1-en-6-ol (379c)
(prepared by Ugur Kaya)

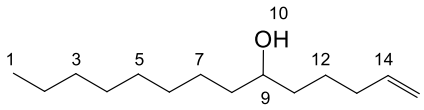

5-Bromo-1-pentene (**380**) (894 mg, 6.00 mmol) in dry THF (2.0 mL) was added over a period of 5 minutes to a suspension of magnesium turnings (146 mg, 6.00 mmol) in dry THF (8.5 mL) under N_2 atmosphere at 0 °C. After stirring for 40 minutes at room temperature the Grignard reagent (5.65 mL, 1.5 eq.) was added over a period of 5 minutes to a solution of nonanal (284 mg, 2.0 mmol) in dry THF (1 mL) at 0 °C. After stirring for 1 h the reaction was quenched with ice water (6 mL) and treated with sulfuric acid (5 M, 1.5 mL) until the magnesium salt dissolved. After separation of the phases the aqueous layer was extracted with diethyl ether (2 × 5 mL). The combined organic phases were dried over $MgSO_4$, filtered and concentrated *in vacuo* to give a yellow oil, which was further purified by flash silica gel column chromatography (10 % ethyl acetate in petroleum ether) to yield **379c** as a yellow oil (224 mg, 53 %).

IR (film, NaCl): ν_{max} 3290, 3030, 2882, 2812, 1689, 1616, 1437, 1356, 1158, 1109, 1051, 978, 895, 815, 711 cm^{-1}. **^{1}H-NMR** (400 MHz, $CDCl_3$) δ 5.81 (1H, dddd, *J* = 17.0, 10.2, 6.7 and 6.7 Hz, H-14), 5.01 (1H, ddd, *J* = 17.0, 3.6 and 1.9 Hz, H-15), 4.95 (1H, dddd, *J* = 10.2, 1.9, 1.2 and 1.2 Hz, H-15) 3.65 – 3.54 (1H, m, H-9), 2.12 – 2.05 (2H, m, H-13), 1.58 – 1.38 (6H, m, H-8 + H-11 + H-12), 1.36 – 1.21 (12H, m, H-2 + H-3 + H-4 + H-5 + H-6 + H-7), 0.88 (3H, t, *J* = 6.8 Hz, m, H-1) ppm **^{13}C-NMR** (101 MHz, $CDCl_3$) δ 138.9, 114.6, 71.9, 37.60, 36.94, 33.86, 31.96, 29.82, 29.71, 29.40, 25.76, 25.03, 22.78,

14.20. **MS** (ESI): m/z 213 ($M+H^+$), 235 ($M+Na^+$); HRMS: found: ($M+H^+$) 213.2213, ($M+Na^+$) 235.2032 $C_{14}H_{29}O$ requires ($M+H^+$) 213.2218, $C_{14}H_{28}NaO$ requires ($M+Na^+$) 235.2038

(*E*)-*S*-*p*-Tolyl 7-hydroxy-7-phenylhept-2-enethioate (328a)
(prepared by Ugur Kaya)

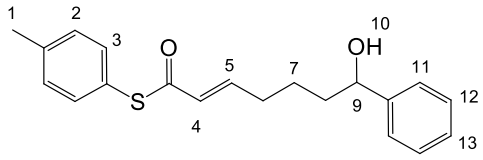

S-p-Tolyl prop-2-enethioate (**272**) (13 mg, 0.073 mmol, 1.1 eq.) and 1-phenylhex-5-en-1-ol (**379a**) (12 mg, 0.068 mmol) were dissolved in dry diethyl ether (1 mL) under an N_2 atmosphere at room temperature. To this, copper (I) iodide (4 mg, 0.021 mmol, 0.3 eq.) and Hoveyda-Grubbs 2nd generation catalyst (10 mg, 0.016 mmol, 20 mol%) were then added as solids in one portion and the reaction mixture was heated under reflux. After 3.5 hours the reaction mixture was concentrated *in vacuo* and purified by flash silica gel column chromatography (10 % to 15 % ethyl acetate in petroleum ether) to yield **328a** as a brown oil (16.9 mg, 67 %).

IR (film, NaCl): ν_{max} 2882, 2812, 1661, 1470, 1429, 1072, 1028, 984, 795, 739, 688 cm^{-1}. **^{1}H-NMR** (400 MHz, $CDCl_3$) δ 7.40 – 7.28 (m, 7H, Ar-H), 7.22 (2H, d, *J* = 8.4 Hz, H-3), 6.94 (ddd, *J* = 15.5, 7.1 and 7.1 Hz, 1H, H-5), 6.16 (1H, ddd, *J* = 15.5, 1.5 and 1.5 Hz, H-4), 4.69 (1H, dd, *J* = 7.4, 5.6 Hz, H-9), 2.38 (3H, s, H-1), 2.25 (2H, m, H-6), 1.90 – 1.71 (2H, m, H-8), 1.56 – 1.44 (2H, m, H-7) ppm. **^{13}C-NMR** (101 MHz, $CDCl_3$) δ 146.1, 134.7, 130.1, 128.7, 128.3, 75.1, 74.5, 50.3, 38.5, 33.2, 32.3, 31.0, 29.9, 24.3, 23.9, 21.5 ppm. **MS** (ESI): m/z 327 ($M+H^+$), 349 ($M+Na^+$); HRMS: found: ($M+H^+$) 327.1413,

(M+Na$^+$) 349.1233 $C_{20}H_{23}O_2S$ requires (M+H$^+$) 327.1419, $C_{20}H_{23}NaO_2S$ requires (M+Na$^+$) 349.1238

(*E*)-*S*-*p*-Tolyl 7-hydroxy-8-methylnon-2-enethioate (328b)
(prepared by Ugur Kaya)

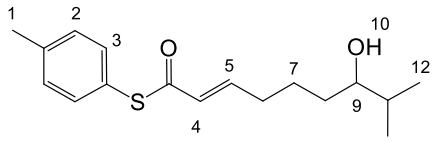

S-p-Tolyl prop-2-enethioate (**272**) (87 mg, 0.489 mmol, 3.0 eq.) and 2-methyloct-7-en-3-ol (**379b**) (24 mg, 0.169 mmol) were dissolved in dry diethyl ether (2 mL) under an N_2 atmosphere at room temperature. To this, copper(I) iodide (5 mg, 0.026 mmol, 0.15 eq.) and Hoveyda-Grubbs 2nd generation catalyst (10 mg, 0.016 mmol, 10 mol%) were then added as solids in one portion and the reaction mixture was heated under reflux. After 2 hours the reaction mixture was concentrated *in vacuo* and purified by flash silica gel column chromatography (10 % to 15 % ethyl acetate in petroleum ether) to yield **328b** as a brown oil (40.8 mg, 88 %).

IR (film, NaCl): ν_{max} 3379, 2889, 2827, 1680, 1056, 1031, 981, 795 cm^{-1}. **^{1}H-NMR** (400 MHz, $CDCl_3$) δ 7.31 (2H, d, *J* = 8.1 Hz, H-2), 7.22 (2H, d, *J* = 8.1 Hz, H-3), 6.97 (1H, ddd, *J* = 15.5, 6.9 and 6.9 Hz, H-5), 6.19 (1H, ddd, *J* = 15.5, 1.5 and 1.5 Hz, H-4), 3.36 (1H, ddd, *J* = 8.5, 5.1, 3.3 Hz, H-9), 2.37 (3H, s, H-1), 2.30 – 2.21 (2H, m, H-6), 1.72 – 1.60 (m, 2H, H-8), 1.55 – 1.32 (3H, m, H-7 + H-11), 0.92 (3H, d, *J* = 3.6 Hz, H-12), 0.90 (3H, d, *J* = 3.5 Hz, H-12) ppm. **^{13}C-NMR** (101 MHz, $CDCl_3$) δ 188.7, 146.5, 139.7, 134.6, 130.1, 128.1, 83.4, 76.6, 33.7, 32.4, 31.4, 24.6, 21.5, 19.0, 17.2 ppm. **MS** (ESI): m/z 293 (M+H$^+$), 315 (M+Na$^+$); HRMS: found: (M+H$^+$) 293.1570, (M+Na$^+$) 315.1389; $C_{17}H_{25}O_2S$ requires (M+H$^+$) 293.1575, $C_{17}H_{24}NaO_2S$ requires (M+Na$^+$) 315.1395

(*E*)-*S*-p-Tolyl 7-hydroxypentadec-2-enethioate (328c)
(prepared by Ugur Kaya)

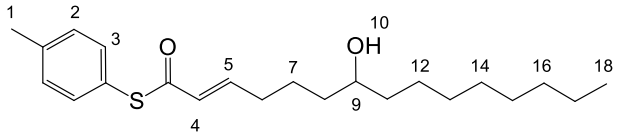

S-p-Tolyl prop-2-enethioate (**272**) (85 mg, 0.478 mmol, 3.0 eq.) and tetradec-1-en-6-ol (**379c**) (34 mg, 0.160 mmol) were dissolved in dry diethyl ether (2 mL) under an N_2 atmosphere at room temperature. To this, copper(I) iodide (4 mg, 0.02 mmol, 0.13 eq.) and Hoveyda-Grubbs 2nd generation catalyst (10 mg, 0.016 mmol, 10 mol%) were then added as solids in one portion and the reaction mixture was heated under reflux. After 2 hours the reaction mixture was concentrated *in vacuo* and purified by flash silica gel column chromatography (10 % to 15 % ethyl acetate in petroleum ether) to yield **328c** as a brown oil (40.9 mg, 71 %).

IR (film, NaCl): ν_{max} 3390, 2882, 2811, 1663, 1607, 1471, 1436, 1355, 1001, 795 cm^{-1}. **^{1}H-NMR** (400 MHz, $CDCl_3$) δ 7.31 (2H, d, *J* = 8.3 Hz, H-2), 7.22 (2H, d, *J* = 8.3 Hz, H-3), 6.97 (1H, ddd, *J* = 15.5, 6.9 and 6.9 Hz, H-5), 6.19 (1H, ddd, *J* = 15.5, 1.5 and 1.5 Hz, 1H, H-4), 3.64 – 3.55 (1H, m, H-9), 2.37 (3H, s, CH_3), 2.29 – 2.21 (2H, m, H-6), 1.73 – 1.59 (2H, m, H-8), 1.58 – 1.50 (2H, m, H-11), 1.31 – 1.24 (14H, m, H-7 + H-12 + H-13 + H-14 + H-15 + H-16 + H-17), 0.88 (3H, t, *J* = 6.9 Hz, H-18) ppm. **^{13}C-NMR** (101 MHz, $CDCl_3$) δ 188.7, 146.4, 139.7, 134.7, 130.1, 128.1, 124.2, 71.8, 60.5, 37.7, 36.9, 32.4, 32.0, 29.8, 29.4, 25.8, 24.2, 22.8, 21.5, 14.3 ppm. **MS** (ESI): m/z 363 (M+H$^+$), 385 (M+Na$^+$); HRMS: found: (M+H$^+$) 363.2352, (M+Na$^+$) 385.2172; $C_{22}H_{35}O_2S$ requires (M+H$^+$) 363.2358, $C_{22}H_{34}NaO_2S$ requires (M+Na$^+$) 385.2177

_S_-_p_-Tolyl 2-((2_R_,6_S_)-6-phenyltetrahydro-2H-pyran-2-yl)ethanethioate (331a)
(prepared by Ugur Kaya)

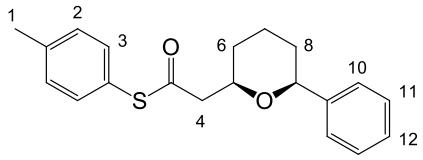

TBAF conditions: (*E*)-*S*-*p*-tolyl 7-hydroxy-7-phenylhept-2-enethioate (**328a**) (7.5 mg, 0.023 mmol) was dissolved in dry THF (0.5 mL, 0.05 M). A solution of acetic acid (0.0010 mmol, 0.06 eq.) and tetrabutylammonium fluoride (0.0070 mmol, 0.3 eq.) in THF (0.5 mL) was added over 3 minutes to the reaction mixture at -10 °C under N_2 atmosphere. After stirring for 45 minutes at -10 °C the reaction was quenched with saturated solution of $NaHCO_3$ (1 mL). The phases were separated and the aqueous layer was extracted with diethyl ether (3 × 1 mL). The combined organics were dried over $MgSO_4$, filtered, concentrated *in vacuo* to yield **331a** (4.0 mg, 0.013 mmol, 53% yield) as a crude yellow oil.

Acidic conditions: (*E*)-*S*-*p*-tolyl 7-hydroxy-7-phenylhept-2-enethioate (**328a**) (7.5 mg, 0.023 mmol) was dissolved in DCM (0.4 mL, 0.06 M) and water (0.4 mL, 0.06 M) was added. The mixture was cooled down to 0 °C and trifluoroacetic acid (0.3 mL, 0.08 M) was added over 3 minutes. After stirring for 4 hours at room temperature the reaction was quenched with saturated aqueous $NaHCO_3$ solution and the aqueous layer was extracted with DCM (2 × 1 mL). The combined organics were dried over $MgSO_4$, filtered, concentrated *in vacuo* and purified by flash silica gel column chromatography (5 % ethyl acetate in petroleum ether) to yield **331a** (4.2 mg, 0.013 mmol, 56% yield) as a yellow oil.

IR (film, NaCl): ν_{max} 2882, 2811, 1680, 1470, 1430, 1241, 1073, 793, 734, 687 cm^{-1}. **^{1}H-NMR** (400 MHz, $CDCl_3$) δ 7.40 – 7.27 (m, 7H, Ar-H), 7.20 (2H, d, *J* = 7.9 Hz, H-3), 4.42 (1H, dd, *J* = 11.3 and 2.1 Hz, H-9), 4.08 – 3.98 (1H, m, H-5), 3.01 (1H, dd, *J* =

14.7, 6.9 Hz, H-4), 2.79 (1H, dd, *J* = 14.7, 5.9 Hz, H-4), 2.37 (3H, s, H-1), 2.00 – 1.84 (2H, m, H-8), 1.80 – 1.72 (2H, m, H-6), 1.71 – 1.63 (2H, m, H-7) ppm. **^{13}C-NMR** (101 MHz, $CDCl_3$) δ 196.0, 139.8, 134.7, 130.1, 128.3, 127.3, 125.9, 124.4, 79.7, 75.1, 50.3, 33.1, 31.0, 29.9, 23.9, 21.5 ppm. **MS** (ESI): m/z 327 ($M+H^+$), 349 ($M+Na^+$); HRMS: found: ($M+H^+$) 327.1413, ($M+Na^+$) 349.1233 $C_{20}H_{23}O_2S$ requires ($M+H^+$) 327.1419, $C_{20}H_{23}NaO_2S$ requires ($M+Na^+$) 349.1238

_S_-_p_-Tolyl 2-((2_R_,6_S_)-6-isopropyltetrahydro-2H-pyran-2-yl)ethanethioate (331b)
(prepared by Ugur Kaya)

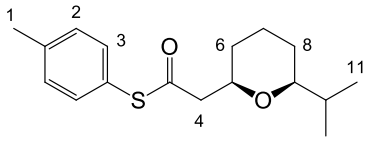

TBAF conditions: (*E*)-*S*-*p*-tolyl 7-hydroxy-8-methylnon-2-enethioate (**328b**) (18.0 mg, 0.062 mmol) was dissolved in dry THF (0.5 mL, 0.1 M). A solution of acetic acid (0.004 mmol, 0.06 eq.) and tetrabutylammonium fluoride (0.019 mmol, 0.3 eq.) was added over 3 minutes to the reaction mixture at -10 °C under N_2 atmosphere. After stirring for 1 hour at -10 °C, the reaction was quenched with saturated aqueous solution of $NaHCO_3$ (3 mL). The phases were separated and the aqueous layer was extracted with diethyl ether (3 × 2 mL). The combined organics were dried over $MgSO_4$, filtered, concentrated *in vacuo* and purified by flash silica gel column chromatography (5 % ethyl acetate in petroleum ether) to yield **331b** (5.0 mg, 0.017 mmol, 27% yield) as a yellow oil.

Acidic conditions: (*E*)-*S*-*p*-tolyl 7-hydroxy-8-methylnon-2-enethioate (**328b**) (17.0 mg, 0.058 mmol) was dissolved in DCM (1.0 mL, 0.05 M) and water (0.1 mL, 0.5 M) was added. The mixture was cooled down to 0 °C and trifluoroacetic acid (0.9 mL, 0.06 M) was added over 3 minutes. After stirring for 5.5 hours at room temperature the reaction

was quenched with saturated aqueous solution of $NaHCO_3$ (2 mL) and diluted with DCM (2 mL). The aqueous layer was extracted with DCM (2 × 2 mL). The combined organics were dried over $MgSO_4$, filtered, concentrated *in vacuo* and purified by flash silica gel column chromatography (5 % ethyl acetate in petroleum ether) to yield **331b** (8.0 mg, 0.027 mmol, 47% yield) as a yellow oil.

IR (film, NaCl): ν_{max} 2887, 2816, 1681, 1471, 1435, 1357, 1056, 1032, 981, 794 cm^{-1}. **^{1}H-NMR** (400 MHz, $CDCl_3$) δ 7.28 (2H, d, *J* = 8.3 Hz, H-2), 7.21 (2H, *J* = 8.3 Hz, H-3), 3.80 (1H, dddd, *J* = 10.9, 8.1, 4.9 and 2.0 Hz, H-5), 2.96 (1H, ddd, *J* = 11.1, 7.0 and 1.8 Hz, H-9), 2.87 (1H, dd, *J* = 14.4 and 8.1 Hz, H-4), 2.65 (1H, dd, *J* = 14.4, 4.9 Hz, H-4), 2.37 (3H, s, H-1), 1.85 (1H, dhept, *J* = 7.0 and 6.8, H-10), 1.68 – 1.41 (6H, m, H-6 + H-7 + H-8), 0.95 (3H, d, *J* = 6.8 Hz, H-11), 0.87 (3H, d, *J* = 6.8 Hz, H-11) **^{13}C-NMR** (101 MHz, $CDCl_3$) δ 196.3, 139.7, 134.6, 130.1, 124.6, 83.4, 75.0, 50.5, 33.5, 31.5, 28.2, 23.7, 21.5, 18.8 ppm. **MS** (ESI): m/z 293 ($M+H^+$), 315 ($M+Na^+$); HRMS: found: ($M+H^+$) 293.1572, ($M+Na^+$) 315.1386; $C_{17}H_{25}O_2S$ requires ($M+H^+$) 293.1575, $C_{17}H_{24}NaO_2S$ requires ($M+Na^+$) 315.1395

_S_-_p_-Tolyl 2-((2_R_,6_R_)-6-octyltetrahydro-2H-pyran-2-yl)ethanethioate (331c)
(prepared by Ugur Kaya)

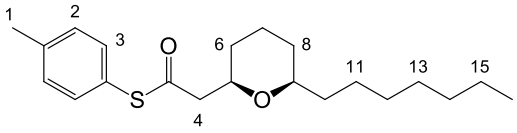

TBAF conditions: (*E*)-*S*-*p*-tolyl 7-hydroxypentadec-2-enethioate (**328c**) (18.6 mg, 0.051 mmol) was dissolved in dry THF (0.5 mL, 0.1 M). A solution of acetic acid (0.003 mmol, 0.06 eq.) and tetrabutylammonium fluoride (0.015 mmol, 0.3 eq.) was added over 3 minutes to the reaction mixture at -10 °C under N_2 atmosphere. After stirring for 1.5 hours

at -10 °C the reaction was quenched with saturated aqueous solution of $NaHCO_3$ (3 mL). The phases were separated and the aqueous layer was extracted with diethyl ether (3 × 2 mL). The combined organics were dried over $MgSO_4$, filtered, concentrated *in vacuo* and purified by flash silica gel column chromatography (5 % ethyl acetate in petroleum ether) to yield **331c** (4.6 mg, 0.018 mmol, 25% yield) as a yellow oil.

Acidic conditions: (*E*)-*S*-*p*-tolyl 7-hydroxypentadec-2-enethioate (**328c**) (19.0 mg, 0.052 mmol) was dissolved in DCM (1.0 mL, 0.05 M) and water (0.1 mL, 0.5 M) was added. The mixture was cooled down to 0 °C and trifluoroacetic acid (0.9 mL, 0.06 M) was added over 3 minutes. After stirring for 5.5 hours at room temperature the reaction was quenched with saturated aqueous solution of $NaHCO_3$ (2 mL) and diluted with DCM (2mL). The aqueous layer was extracted with DCM (2 × 2 mL). The combined organics were dried over $MgSO_4$, filtered, concentrated *in vacuo* to yield **331c** (6.7 mg, 0.019 mol, 36% yield) as a yellow oil.

IR (film, NaCl): ν_{max} 2881, 2811, 1754, 1681, 1434, 1202, 1146, 1071, 1055, 794 cm^{-1}. **^{1}H-NMR** (400 MHz, $CDCl_3$) δ 7.28 (2H, d, *J* = 8.0 Hz, H-2), 7.21 (2H, d, *J* = 8.0 Hz, H-3), 3.87 – 3.75 (1H, m, H-5), 3.33 – 3.21 (1H, m, H-9), 2.88 (1H, dd, *J* = 14.6, 7.8 Hz, H-4), 2.66 (1H, dd, *J* = 14.6, 5.3 Hz, H-4), 2.37 (3H, s, CH_3), 1.70 – 1.49 (6H, m, H-6 + H-8 + H-10), 1.35 – 1.20 (12H, m, H-7 + H-11 + H-12 + H-13 + H-14 + H-15), 0.87 (3H, t, *J* = 6.8 Hz, H-16) ppm. **^{13}C-NMR** (101 MHz, $CDCl_3$) δ 196.1, 139.7, 134.5, 130.0, 124.5, 78.3, 74.8, 50.7, 36.6, 32.0, 31.4, 29.8, 29.4, 25.7, 23.6, 22.8, 22.5 21.4, 14.2 ppm. **MS** (ESI): m/z 363 ($M+H^+$), 385 ($M+Na^+$); HRMS: found: ($M+H^+$) 363.2345, ($M+Na^+$) 385.2175; $C_{22}H_{35}O_2S$ requires ($M+H^+$) 363.2358, $C_{22}H_{34}NaO_2S$ requires ($M+Na^+$) 385.2177

Octa-1,7-diene-4,5-diol (391)

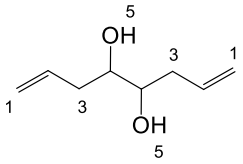

Allyl bromide (7.15 mL, 82.7 mmol, 2.4 eq.) and 40% aqueous glyoxal (3.94 mL, 34.5 mmol) were dissolved in 1:1 THF/H_2O (35 mL). Tin powder (9.82 g, 82.7 mmol, 2.4 eq.) was added and the mixture was sonicated for 6 hours. The reaction was quenched with a 25% KOH solution (28 mL, w:w in H_2O) and diluted with diethyl ether (30 mL). Solid NaCl was added until the aqueous layer was saturated and then the mixture was filtered through celite. The aqueous layer was extracted with diethyl ether (3 x 10 mL) and the combined organics were dried over $MgSO_4$, filtered and concentrated *in vacuo* to give a yellow oil, which was purified by flash silica gel column chromatography (20% to 50% ethyl acetate in petroleum ether) to yield **391** as a yellow oil (3.04 g, 62%). The proton NMR spectrum matched that given in literature.[108]

^{1}H NMR (400 MHz, $CDCl_3$): δ 5.93 – 5.78 (2H, m, H-2), 5.19 (2H, ddd, *J* = 8.1, 3.1, 1.6 Hz, H-1), 5.18 – 5.13 (2H, m, H-1), 3.71 – 3.64 (1H, m, H-4), 3.59 – 3.51 (1H, m, H-4), 2.43 – 2.32 (2H, m, H-3), 2.31 – 2.20 (2H, m, H-3), 2.06 (2H, br m, H-5) ppm.

But-3-enal (387)

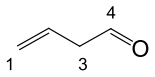

Octa-1,7-diene-4,5-diol **391** (600 mg, 4.22 mmol) was dissolved in DCM (4.5 mL), H_2O (4.5 mL) and cooled to 0 °C. Sodium periodate (1.084 g, 5.07 mmol, 1.2 eq.) was added to the mixture in portions after which it was warmed up to room temperature and stirred for 7 hours. The organic layer was washed with water (2 × 5 mL), brine (2 × 5 mL), dried over $MgSO_4$ and filtered to yield **387** as a colourless solution in DCM (290 mg

by NMR, 4.11 mmol, 49 %). The proton NMR spectrum matched that given in literature.[106]

^{1}H NMR (400 MHz, $CDCl_3$): δ 9.66 (1H, t, *J* = 1.7 Hz, H-4), 5.92 (1H, ddt, *J* = 17.2, 10.3 and 6.8 Hz, H-2), 5.27 (1H, dd, *J* = 10.3 and 1.5 Hz, H-1), 5.22 (1H, ddd, *J* = 17.2, 3.0 and 1.5 Hz, H-1), 3.17 (2H, ddd, *J* = 6.8, 3.0 and 1.7 Hz, H-3) ppm.

Trimethyl((1-phenylvinyl)oxy)silane (392)
(prepared by Alan Jeuken)

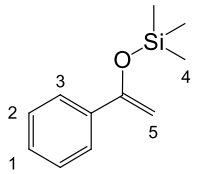

To a solution of acetophenone (0.63 g, 5.2 mmol) in dry MeCN (2.5 mL) under N_2 was added triethylamine (3.63 mL, 25.9 mmol, 5 eq.) over a period of 5 minutes. The mixture was stirred and heated to 30-35 ºC, after which trimethylsilyl chloride (1.33 mL, 10.4 mmol, 2 eq.) was added over 3 minutes. After the mixture was stirred for 30 minutes at the same temperature, a solution of NaI (1.56 g, 10.4 mmol, 2 eq.) in dry MeCN (8.75 mL) was added over 5 minutes. The reaction temperature was raised to 40-45 ºC and left stirring for 3 hours, after which the reaction was left to cool to room temperature. The reaction mixture was filtered through celite, extracted with pentane, concentrated *in vacuo*, filtered through celite again and extracted with pentane. The filtrate was concentrated in vacuo to yield **392** as a yellow oil (0.99 g, 99%). The proton NMR spectrum matched that given in literature.[109]

^{1}H NMR (400 MHz, $CDCl_3$): δ 7.70 – 7.65 (2H, m, H-3), 7.15 – 7.06 (3H, m, H-1 + H-2), 4.92 (1H, d, *J* = 1.7 Hz, H-5), 4.47 (1H, d, *J* = 1.7 Hz, H-5), 0.20 – 0.16 (9H, s, H-4) ppm.

3-hydroxy-1-phenylhex-5-en-1-one (393)

(prepared by Alan Jeuken)

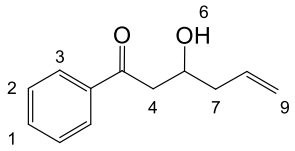

To a solution of silyl enol ether **392** (273 mg, 1.44 mmol) in dry DCM (10 mL) was added a but-3-enal **387** (100 mg, 1.43 mmol) solution in dry DCM over 3 minutes at -78 ºC under N_2. After stirring for 15 minutes at the same temperature, a solution of $TiCl_4$ in dry DCM was added over 3 minutes to the reaction mixture. After leaving the reaction to stir for 4 hours at -78 ºC, it was quenched with cold water (7 mL). Saturated $NaHCO_3$ solution (5 mL) was added and the layers separated. The aqueous layer was extracted with DCM (2 x 5 mL) and the combined organic layers were dried over $MgSO_4$, filtered and concentrated *in vacuo* to give a yellow oil, which was purified by flash silica gel column chromatography (10% ethyl acetate in petroleum ether) to yield **393** as a yellow oil (73 mg, 27%). The proton NMR spectrum matched that given in literature.[110]

^{1}H NMR (400 MHz, $CDCl_3$): δ 7.98 - 7.94 (2H, m, H-3), 7.62 – 7.56 (1H, m, H-1), 7.51 – 7.45 (2H, m, H-2), 5.89 (1H, dddd, *J* = 17.2, 10.2, 7.1 and 7.1 Hz, H-8), 5.21 – 5.12 (2H, m, H-9), 4.36 – 4.26 (1H, m, H-5), 3.20 (1H, dd, *J* = 18.2, 3.1 Hz, H-4), 3.07 (1H, dd, *J* = 18.2 and 8.9 Hz, H-4), 2.38 (2H, m, H-7) ppm.

(±)-(1*S*,3*R*)-1-phenylhex-5-ene-1,3-diol (386a)

(prepared by Alan Jeuken)

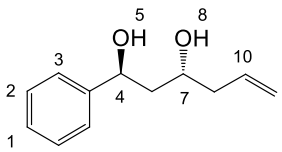

To a solution of $NMe_4BH(OAc)_3$ (1.09 g, 4.12 mmol, 7 eq.) in dry MeCN (4.4 mL) and AcOH (4.5 mL) at -35 ºC under an N_2 atmosphere was added a solution of β-

hydroxy ketone **399a** (112 mg, 0.59 mmol) in dry MeCN (4.4 mL) over a period of 3 minutes. The reaction mixture was stirred for 6 hours at -35 ºC and 18 hours at -20 ºC. The reaction was quenched with 10% Rochelles salt (7 mL) and warmed to room temperature. The mixture was partitioned between ethyl acetate (40 mL) and a saturated aqueous solution of $NaHCO_3$ (40 mL) and the aqueous layer was extracted with ethyl acetate (2 × 40 mL). The combined organics were dried over $MgSO_4$, filtered and concentrated *in vacuo* to give a yellow oil, which was purified by flash silica gel column chromatography (20% to 50% ethyl acetate in petroleum ether) to yield **386a** as a yellow oil (68 mg, 61%). The proton NMR spectrum matched that given in literature.[111]

^{1}H NMR (400 MHz, $CDCl_3$): δ 7.40 – 7.32 (4H, m, H-2 + H-3), 7.30 – 7.27 (1H, m, H-1), 5.85 – 5.71 (1H, m, H-10), 5.19 – 5.10 (2H, m, H-11), 5.08 (1H, dd, *J* = 7.8, 3.6 Hz, H-4), 3.92 (1H, dddd, *J* = 8.3, 8.3, 5.1, and 3.2 Hz, H-7), 2.88 (2H, br, H-5 + H-8), 2.38 – 2.20 (2H, m, H-8), 1.99 – 1.84 (2H, m, H-6) ppm.

(±)-(1*S*,3*S*)-1-phenylhex-5-ene-1,3-diol (400a)

(prepared by Alan Jeuken)

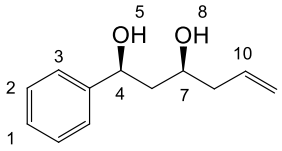

1 M Triethyl borane solution in hexanes (0.75 mL, 0.75 mmol, 1.1 eq.) was added to a mixture of dry THF (6 mL) and methanol (1.5 mL) at room temperature under a N_2 atmosphere. After stirring the mixture for 1 hour and 45 minutes it was cooled down to -78 ºC, followed by addition of β-hydroxy ketone **399a** (130 mg, 0.68 mmol) solution in dry THF (1 mL) over a period of 3 minutes. After stirring for 30 minutes $NaBH_4$ (29 mg, 0.75 mmol, 1.1 eq.) was added in one portion. After stirring the reaction for another 4 hours the reaction mixture was quenched with saturated aqueous NH_4Cl (6 mL) and diluted with

ethyl acetate (7 mL). The aqueous layer was extracted with ethyl acetate (2 × 4 mL) and the combined organics were dried over $MgSO_4$, filtered and concentrated *in vacuo* to give a yellow oil, which was azeotroped with methanol (8 × 5 mL). The oil was then purified by flash silica gel column chromatography (20% to 40% ethyl acetate in petroleum ether) to yield **400a** as a yellow oil (76 mg, 58%) The proton NMR spectrum matched that given in literature.[112]

^{1}H NMR (400 MHz, $CDCl_3$): δ 7.40 – 7.32 (4H, m, H-2 + H-3), 7.31 – 7.27 (1H, m, H-1), 5.81 (1H, dddd, *J* = 11.7, 9.2, 7.5 and 6.9 Hz, H-10), 5.18 – 5.13 (1H, m, H-11), 5.13 – 5.10 (1H, m, H-11), 4.96 (1H, dd, *J* = 9.2 and 3.8 Hz, H-4), 4.05 – 3.95 (1H, m, H-7), 2.48 (2H, br, H-5 + H-8), 2.35 – 2.19 (2H, m, H-9), 1.92 – 1.78 (2H, m, H-6) ppm.

(±)- (5*R*,7*S*,*E*)-*S*-*p*-Tolyl 5,7-dihydroxy-7-phenylhept-2-enethioate (385a)

(prepared by Alan Jeuken)

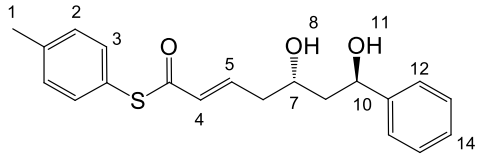

S-*p*-Tolyl prop-2-enethioate **272** (111 mg, 0.63 mmol, 3 eq.) and diol **386a** (40 mg, 0.21 mmol) were dissolved in dry diethyl ether (5 mL) under an N_2 atmosphere. Copper (I) iodide (5 mg, 0.021 mmol, 10 mol %) and Hoveyda-Grubbs 2nd generation catalyst (13.2 mg, 0.021 mmol, 10 mol %) were added as solids in a single portion, and the mixture was left to stir under reflux for 3 hours. The mixture was then concentrated *in vacuo* and purified by flash silica gel column chromatography (30% to 70% ethyl acetate in petroleum ether) to yield **385a** as a colourless oil (44 mg, 62%).

IR (film): ν_{max} 3390, 2923, 2867, 1676, 1630, 1494, 1454, 1304 cm^{-1}. **^{1}H NMR** (400 MHz, $CDCl_3$): δ 7.38 – 7.27 (7H, m, Ar-H), 7.21 (2H, d, *J* = 7.9 Hz, H-3), 6.94 (1H, ddd, *J* = 15.3, 7.1 and 7.1 Hz, H-5), 6.23 (1H, d, *J* = 15.3 Hz, H-4), 5.05 (1H, dd, *J* = 6.0

and 6.0 Hz, H-10), 4.09 – 4.00 (1H, m, H-7), 2.94, (2H, br, H-8 + H-11), 2.43 – 2.38 (2H, m, H-6), 2.37 (3H, s, H-1), 1.95 – 1.83 (2H, m, H-9) ppm. **^{13}C-NMR** (101 MHz, $CDCl_3$): δ 188.5, 144.0, 142.0, 139.7, 134.5, 130.1, 130.0, 128.6, 127.6, 125.5, 123.8, 71.6, 67.6, 44.3, 40.2, 21.3 ppm. **MS** (ESI): m/z 365 ($M+Na^+$); HRMS: found: ($M+Na^+$) 365.1182; $C_{20}H_{22}NaO_3S$ requires ($M+Na^+$) 365.1187

(±)-(5*S*,7*S*,*E*)-*S*-*p*-Tolyl 5,7-dihydroxy-7-phenylhept-2-enethioate (401a)

(prepared by Alan Jeuken)

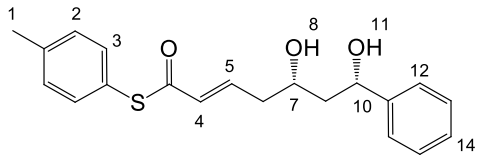

S-*p*-Tolyl prop-2-enethioate **272** (111 mg, 0.63 mmol, 3 eq.) and diol **400a** (40 mg, 0.21 mmol) were dissolved in dry diethyl ether (5 mL) under an N_2 atmosphere. Copper (I) iodide (5 mg, 0.021 mmol, 10 mol %) and Hoveyda-Grubbs 2nd generation catalyst (13.2 mg, 0.021 mmol, 10 mol %) were added as solids in a single portion, and the mixture was left to stir under reflux for 3 hours. The mixture was then concentrated *in vacuo* and purified by flash silica gel column chromatography (30% to 70% ethyl acetate in petroleum ether) to yield **401a** as a colourless oil (67 mg, 94%).

IR (film): ν_{max} 3374, 2928, 2872, 1679, 1630, 1493, 1455, 1307 cm^{-1}. **^{1}H NMR** (400 MHz, $CDCl_3$): δ 7.38 – 7.27 (7H, m, Ar-H), 7.21 (2H, d, *J* = 8.0 Hz, H-3), 6.95 (1H, ddd, *J* = 15.2, 7.4 and 7.4 Hz, H-5), 6.22 (1H, ddd, *J* = 15.2, 1.2 and 1.2 Hz, H-4), 4.93 (1H, dd, *J* = 9.1 and 8.0 Hz, H-10), 4.11 (1H, m, H-7), 3.64 (1H, br, H-11), 3.10 (1H, br, H-8), 2.48 – 2.33 (5H, m, H-1 + H-6), 1.86 (1H, ddd, *J* = 14.5, 10.0 and 9.1 Hz, H-9), 1.75 (1H, ddd, *J* = 14.5, 8.0 and 2.6 Hz, H-9) ppm. **^{13}C-NMR** (101 MHz, $CDCl_3$): δ 188.4, 144.0, 141.7, 139.7, 134.5, 130.2, 130.0, 128.6, 127.9, 125.6, 123.8, 75.3, 71.0, 44.8, 40.6, 21.3 ppm. **MS** (ESI): m/z 343 ($M+H^+$), 365 ($M+Na^+$); HRMS: found: ($M+H^+$) 343.1358,

(M+Na$^+$) 365.1180; $C_{20}H_{23}O_3S$ requires (M+H$^+$) 343.1368, $C_{20}H_{22}NaO_3S$ requires (M+Na$^+$) 365.1187

(±)-*S*-(*p*-Tolyl) 2-((2*S*,4*R*,6*S*)-4-hydroxy-6-phenyltetrahydro-2H-pyran-2-yl)ethanethioate (402a)

(prepared by Alan Jeuken)

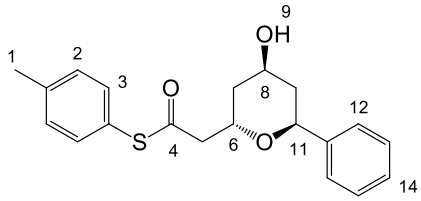

(5*S*,7*S*,*E*)-*S*-*p*-Tolyl 5,7-dihydroxy-7-phenylhept-2-enethioate (**385a**) (17.0 mg, 0.050 mmol) was dissolved in dry THF (1.3 mL, 0.04 M). A solution of acetic acid (0.0030 mmol, 0.06 eq.) and tetrabutylammonium fluoride (0.015 mmol, 0.3 eq.) was added over a period of 3 minutes to the reaction mixture at -10 °C under N_2 atmosphere. The reaction mixture was treated after 1.5 and 2 hours with additional solution (0.1 mL) of acetic acid and tetrabutylammonium fluoride. After stirring for 3 hours at -10 °C the reaction was quenched with saturated aqueous solution of $NaHCO_3$ (3 mL). The phases were separated and the aqueous layer was extracted with diethyl ether (3 × 3 mL). The combined organics were dried over $MgSO_4$, filtered, concentrated *in vacuo* and purified by flash silica gel column chromatography (20 to 50 % ethyl acetate in petroleum ether) to yield **402a** (6.8 mg, 0.020 mmol, 40 % yield) as a yellow oil.

IR (film): ν_{max} 3437, 2964, 2923, 2852, 1735, 1630, 1489, 1452, 1253, 1073 cm^{-1}. **^{1}H-NMR** (400 MHz, $CDCl_3$): δ = 7.39 – 7.31 (7H, m, Ar-H), 7.15 (2H, d, *J* = 7.8 Hz, H-3), 5.06 (1H, dd, *J* = 7.8 and 5.3 Hz, H-11), 4.64 (1H, dddd, *J* = 11.9, 10.6, 5.8 and 2.9 Hz, H-6), 3.46 – 3.35 (1H, m, H-8), 2.92 (1H, dd, *J* = 17.7 and 5.8 Hz, H-5), 2.44 (1H, dd, *J* = 17.7 and 10.6 Hz, H-5), 2.35 (3H, s, H-1), 2.09 (1H, br, H-9), 1.92 (2H, m, H-10), 1.57 (2H, m, H-7) ppm. **^{13}C-NMR** (101 MHz, $CDCl_3$): δ 169.6, 144.2, 139.0, 134.6,

130.2, 128.7, 127.9, 127.8, 125.6, 77.3, 76.4, 69.6, 45.2, 39.6, 36.6, 21.2 ppm. **MS (ESI)**: m/z 343 ($M+H^+$); HRMS: found: ($M+H^+$) 343.1341, $C_{20}H_{23}O_3S$ requires ($M+H^+$) 343.1362

(±)-*S*-(*p*-Tolyl) 2-((2*R*,4*R*,6*R*)-4-hydroxy-6-phenyltetrahydro-2H-pyran-2-yl)ethanethioate (404a)

(prepared by Alan Jeuken)

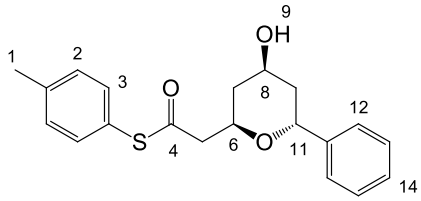

(5*R*,7*S*,E)-*S*-*p*-Tolyl 5,7-dihydroxy-7-phenylhept-2-enethioate (**401a**) (20.0 mg, 0.058 mmol) was dissolved in dry THF (1.5 mL, 0.04 M). A solution of acetic acid (0.004 mmol, 0.06 eq.) and tetrabutylammonium fluoride (0.017 mmol, 0.3 eq.) was added to the reaction mixture over a period of 3 minutes at -10 °C under N_2 atmosphere. The reaction mixture was treated after 1.5 and 2 hours with additional solution (0.12 mL) of acetic acid and tetrabutylammonium fluoride. After stirring for 3 hours at -10 °C the reaction was quenched with saturated aqueous solution of $NaHCO_3$ (3 mL). The phases were separated and the aqueous layer was extracted with diethyl ether (3 × 3 mL). The combined organics were dried over $MgSO_4$, filtered, concentrated *in vacuo* and purified by flash silica gel column chromatography (20 to 50 % ethyl acetate in petroleum ether) to yield **404a** (7.9 mg, 0.023 mmol, 40% yield) as a yellow oil.

IR (film): ν_{max} 3448, 2954, 2924, 2852, 1734, 1630, 1495, 1391, 1243, 1065 cm^{-1}. **^{1}H-NMR** (400 MHz, $CDCl_3$): δ = 7.40 – 7.27 (m, 7H, Ar-H), 7.14 (2H, d, *J* = 7.7 Hz, H-3), 4.96 (1H, dd, *J* = 6.9 and 6.9 Hz, H-11), 4.24 – 4.12 (1H, m, H-6), 3.35 – 3.23 (1H, m, H-8), 2.87 (1H, dd, *J* = 17.8 and 5.8 Hz, H-5), 2.42 (1H, dd, *J* = 17.8 and 10.9 Hz, H-5), 2.34 (3H, s, H-1), 2.30 – 2.13 (2H, m, H-10), 1.91 (1H, ddd, *J* = 13.9, 6.6 and 4.3 Hz, H-7) 1.63 (1H, ddd, *J* = 13.9, 11.7 and 11.7 Hz, H-7) ppm. **^{13}C-NMR** (101 MHz,

$CDCl_3$): δ 169.1, 143.3, 138.9, 134.5, 130.0, 128.7, 128.5, 127.6, 126.0, 77.7, 77.2, 71.2, 44.6, 39.3, 36.6, 21.2 ppm. **MS (ESI)**: m/z 365 ($M+Na^+$); HRMS: found: ($M+Na^+$) 365.1198, $C_{20}H_{22}NaO_3S$ requires ($M+Na^+$) 365.1182

(±)-*S*-(*p*-Tolyl) 2-((2*S*,4*R*,6*R*)-4-hydroxy-6-phenyltetrahydro-2H-pyran-2-yl) ethanethioate (403a)

(prepared by Alan Jeuken)

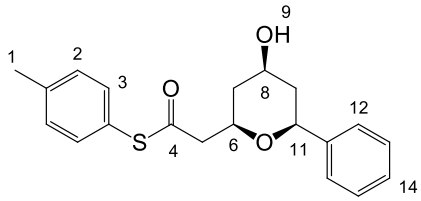

Diol **385a** (10 mg, 0.029 mmol) was dissolved in DCE (2.0 mL) and CSA (3.4 mg, 0.014 mmol, 50 mol %) was added in one portion. The reaction was heated to 60 ºC and left to stir for 24 hours. Another portion of CSA (3.4 mg, 0.014 mmol, 50 mol %) was added and the reaction was stirred for another 24 hours. A final portion of CSA (13..6 mg, 0.58 mmol, 2 eq.) was added and the reaction mixture was heated to 80 ºC and left to stir for 24 hours. The reaction was quenched with Et_3N, washed with $NaHCO_3$ (2 × 5 mL) and brine (2 × 5 mL), dried over $MgSO_4$, filtered and concentrated *in vacuo*. The residue was purified by flash silica gel column chromatography (50% diethyl ether in petroleum ether) to yield **403a** as a colourless oil (5.8 mg, 58%).

IR (film): ν_{max} 3396, 2922, 2855, 1703, 1495, 1454, 1368, 1064 cm^{-1}. **^{1}H NMR** (400 MHz, $CDCl_3$): δ 7.39 – 7.27 (7H, m, Ar-H), 7.20 (2H, d, *J* = 8.0 Hz, H-3), 4.42 (1H, dd, *J* = 11.5, 2.0 Hz, H-11), 4.08 – 3.95 (2H, m, H-6 + H-8), 3.06 (1H, dd, *J* = 14.9 and 7.0 Hz, H-5), 2.83 (1H, dd, *J* = 14.9, 5.9 Hz, H-5), 2.37 (3H, s, H-1), 2.28 – 2.10 (2H, m, H-10), 1.55 – 1.32 (2H, m, H-7) ppm. **^{13}C-NMR** (101 MHz, $CDCl_3$): δ 195.6, 142.5, 139.7,

134.4, 130.0, 128.3, 127.2, 125.7, 124.2, 73.5, 69.1, 64.6, 49.7, 39.9, 37.9, 21.3 ppm. **MS (ESI)**: m/z 365 ($M+Na^+$); HRMS: found: ($M+Na^+$) 365.1151, $C_{20}H_{22}NaO_3S$ requires ($M+Na^+$) 365.1182

(±)-*S*-(*p*-Tolyl) 2-((2*R*,4*R*,6*S*)-4-hydroxy-6-phenyltetrahydro-2H-pyran-2-yl) ethanethioate (405a)

(prepared by Alan Jeuken)

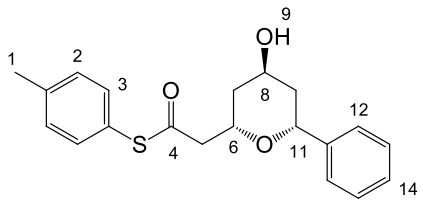

Diol **401a** (10 mg, 0.029 mmol) was dissolved in DCE (2.0 mL) and CSA (20.4 mg, 0.086 mmol, 3 eq.) was added in one portion. The reaction was heated to 80 ºC and left to stir for 20 hours. The reaction was quenched with Et_3N, washed with $NaHCO_3$ (2 × 5 mL) and brine (2 × 5 mL), dried over $MgSO_4$, filtered and concentrated *in vacuo*. The residue was purified by flash silica gel column chromatography (50% diethyl ether in petroleum ether) to yield **405a** as a colourless oil (7.4 mg, 74%).

IR (film): ν_{max} 3435, 2924, 2876, 1705, 1495, 1452, 1381, 1217, 1062 cm^{-1}. **^{1}H NMR** (400 MHz, $CDCl_3$): δ 7.40 – 7.22 (7H, m, Ar-H), 7.22 – 7.16 (2H, d, *J* = 8.0 Hz, H-3), 4.91 (1H, dd, *J* = 11.8, 2.2 Hz, H-11), 4.50 (1H, dddd, *J* = 7.2, 6.9, 6.0 and 2.2 Hz, H-6), 4.40 – 4.32 (1H, m, H-8), 2.99 (1H, dd, *J* = 14.8 and 6.9 Hz, H-5), 2.78 (1H, dd, *J* = 14.8 and 6.0 Hz, H-5), 2.36 (3H, s, H-1), 1.95 (1H, ddd, *J* = 13.9, 7.2 and 2.3 Hz, H-7), 1.84 (1H, ddd, *J* = 13.9, 5.2 and 2.2 Hz, H-7), 1.71 (2H, m, H-10) ppm. **^{13}C-NMR** (101 MHz, $CDCl_3$): δ 195.7, 142.6, 139.7, 134.5, 130.1, 128.4, 127.4, 125.8, 124.3, 73.6, 69.2, 64.7, 49.8, 40.0, 38.0, 21.4 ppm. **MS (ESI)**: m/z 365 ($M+Na^+$); HRMS: found: ($M+Na^+$) 365.1164, $C_{20}H_{22}NaO_3S$ requires ($M+Na^+$) 365.1182

5-hydroxy-2-methyloct-7-en-3-one (399b)

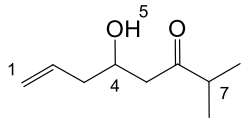

To a solution of silyl enol ether **392b** (1.0 g, 6.3 mmol) in dry DCM (20 mL) was added a 2M solution of butenal **387** (3.2 mL, 6.3 mmol) in dry DCM over a period of 3 minutes at -78 ºC and stirred under N_2 for 15 minutes. A solution of $TiCl_4$ (760 µL, 6.9 mmol) in dry DCM (5 mL) was then added to the reaction mixture over a period of 3 minutes. After leaving the reaction to stir for 2 hours at -78 ºC, it was quenched with cold water (10 mL). Saturated $NaHCO_3$ solution (5 mL) was added and the layers separated. The aqueous layer was extracted with DCM (2 × 10 mL) and the combined organic layers were dried over $MgSO_4$, filtered and concentrated *in vacuo* to give a yellow oil. The crude reaction mixture was purified by flash chromatography (10% ethyl acetate in petroleum ether) on a silica gel column (deadened with 0.5% Et_3N solution) to yield **399b** as a yellow oil (890 mg, 91%).

IR (film): υ_{max} 3428, 3078, 2976, 2934, 1703, 1639, 1467, 1382, 1292, 1035 cm^{-1}; **^{1}H NMR** (400 MHz, $CDCl_3$): δ 5.82 (1H, dddd, *J* = 16.4, 10.6, 7.1 and 7.1 Hz, H-2), 5.16 – 5.09 (2H, m, H-1), 4.10 (1H, ddddd, *J* = 12.2, 7.6, 3.2, 3.1 and 3.1 Hz, H-4), 3.10 (1H, d, *J* = 3.2 Hz, H-5), 2.66 (1H, dd, *J* = 17.7, 3.1 Hz, H-6), 2.60 (1H, hept, *J* = 6.9 Hz, H-7), 2.55 (1H, dd, *J* = 17.7, 7.6 Hz, H-6), 2.26 (2H, m, H-3) 1.10 (3H, d, *J* = 6.9 Hz, H-8), 1.10 (3H, d, *J* = 6.9 Hz, H-8) ppm. **^{13}C-NMR** (101 MHz, $CDCl_3$): δ 171.4, 134.4, 118.0, 67.2, 45.8, 41.6, 41.0, 18.1, 29.2, 29.1, 23.7, 22.7, 14.1 ppm. **MS (ESI)**: m/z 179 ($M+Na^+$); HRMS: found: ($M+Na^+$) 179.1053, $C_9H_{16}O_2Na$ requires ($M+Na^+$) 179.1043

4-hydroxytridec-1-en-6-one (399c)

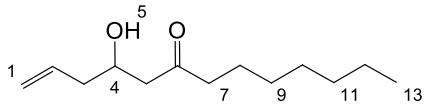

To a solution of silyl enol ether **392c** (850 mg, 4.0 mmol) in dry DCM (20 mL) was added a 2 M solution of butenal **387** (2.0 mL, 4.0 mmol) in dry DCM over a period of 3 minutes at -78 ºC and stirred under N_2 for 15 minutes. A solution of $TiCl_4$ (530 μL) in dry DCM (3 mL) was then added over a period of 3 minutes to the reaction mixture. After leaving the reaction to stir for 2 hours at -78 ºC, it was quenched with cold water (10 mL). Saturated $NaHCO_3$ solution (5 mL) was added and the layers separated. The aqueous layer was extracted with DCM (2 × 10 mL) and the combined organic layers were dried over $MgSO_4$, filtered and concentrated *in vacuo* to give a yellow oil. The crude reaction mixture was purified by flash chromatography (10% ethyl acetate in petroleum ether) on a silica gel column (deadened with 0.5% Et_3N solution) to yield **399c** as a yellow oil (290 mg, 34%).

IR (film): υ_{max} 3422, 3075, 2928, 2857, 1704, 1640, 1461, 1407, 1375, 1045 cm^{-1}; **^{1}H NMR** (400 MHz, $CDCl_3$): δ 5.81 (1H, dddd, 18.3, 9.3, 7.1 and 7.1 Hz, H-2), 5.16 – 5.09 (2H, m, H-1), 4.05-4.16 (1H, m, H-4), 3.07 (1H, br s, H-5), 2.61 (1H, dd, *J* = 17.6 and 3.1 Hz, H-6), 2.51 (1H, dd, *J* = 17.6 and 8.9 Hz, H-6), 2.41 (1H, t, *J* = 7.4 Hz, H-7), 2.17-2.31 (2H, m, H-3) 1.34 - 1.18 (10H, m, H-8 + H-9 + H-10 + H-11 + H-12), 0.87 (3H, t, *J* = 6.8, H-13) ppm. **^{13}C-NMR** (101 MHz, $CDCl_3$): δ 212.3, 134.3, 118.0, 67.1, 48.2, 43.4, 41.0, 31.7, 29.2, 29.1, 23.7, 22.7, 14.1 ppm. **MS (ESI)**: m/z 235 ($M+Na^+$); HRMS: found: ($M+Na^+$) 235.1666, $C_{13}H_{24}O_2Na$ requires ($M+Na^+$) 235.1669

(±)-(4*S*,6*R*)-tridec-1-ene-4,6-diol (400c)

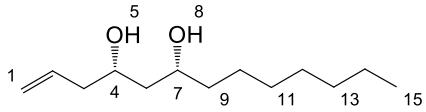

1 M Triethyl borane solution in hexanes (0.23 mL, 0.23 mmol, 1.1 eq.) was added to a mixture of dry THF (2 mL) and methanol (0.5 mL) at room temperature under a N_2 atmosphere. After stirring the mixture for 1 hour and 30 minutes it was cooled down to -78 ºC, followed by addition of β-hydroxy ketone **399c** (45 mg, 0.21 mmol) solution in dry THF (1 mL) over a period of 3 minutes. After stirring for 30 minutes $NaBH_4$ (10 mg, 0.40 mmol, 1.1 eq.) was added in one portion. After stirring the reaction for another 3 hours the reaction mixture was quenched with saturated aqueous NH_4Cl (3 mL) and diluted with ethyl acetate (3 mL). The aqueous layer was extracted with ethyl acetate (2 × 3 mL) and the combined organics were dried over $MgSO_4$, filtered and concentrated *in vacuo* to give a yellow oil, which was azeotroped with methanol (8 × 2 mL). The oil was then purified by flash chromatography (30% ethyl acetate in petroleum ether) on a silica gel column to yield **400c** as a yellow oil (35 mg, 78%)

IR (film): υ_{max} 3344, 3079, 2928, 2857, 1643, 1461, 1325, 1085 cm^{-1}; **^{1}H NMR** (400 MHz, $CDCl_3$): δ 5.80 (1H, dddd, *J* = 14.1, 9.5, 7.2 and 7.2 Hz, H-2), 5.17 – 5.06 (2H, m, H-1), 3.95 – 3.77 (2H, m, H-4 + H-7), 3.15 (2H, br s, H-5 + H-8), 2.30 – 2.15 (2H, m, H-3), 1.62 (1H, ddd, *J* = 14.5, 2.2 Hz, H-6), 1.52 – 1.17 (13H, m, H-6 + H-9 + H-10 + H-11 + H-12 + H-13 + H-14), 0.87 (3H, t, *J* = 6.8 Hz, H-15) ppm. **^{13}C-NMR** (101 MHz, $CDCl_3$): δ 134.4, 118.3, 73.0, 72.1, 42.3, 42.4, 38.2, 31.9, 29.7, 29.4, 25.5, 22.7, 14.2 ppm. **MS (ESI)**: m/z 215 ($M+H^+$) 237 ($M+Na^+$); HRMS: found: ($M+H^+$) 215.2007, ($M+Na^+$) 237.1834, $C_{13}H_{27}O_2$ requires ($M+H^+$) 215.2011, $C_{13}H_{26}O_2Na$ requires ($M+Na^+$) 237.1825

(±)-(4*S*,6*S*)-tridec-1-ene-4,6-diol (386c)

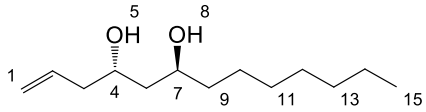

To a solution of $NMe_4BH(OAc)_3$ (1.04 g, 3.95 mmol, 7 eq.) in dry MeCN (5 mL) and AcOH (6 mL) at -35 ºC under an N_2 atmosphere was added a solution of β-hydroxy ketone **399c** (120 mg, 0.56 mmol) in dry MeCN (5 mL) over a period of 3 minutes. The reaction mixture was stirred for 3 hours at -35 ºC. The reaction was quenched with 10% Rochelle's salt (7 mL) and warmed to room temperature. The mixture was partitioned between ethyl acetate (20 mL) and a saturated aqueous solution of $NaHCO_3$ (20 mL) and the aqueous layer was extracted with ethyl acetate (2 × 20 mL). The combined organics were dried over $MgSO_4$, filtered and concentrated *in vacuo* to give a yellow oil. The oil was then purified by flash chromatography (30% ethyl acetate in petroleum ether) on a silica gel column to yield **386c** as a yellow oil (103 mg, 86%).

IR (film): υ_{max} 3378, 3078, 2925, 2855, 1642, 1404, 1334, 1143, 1073 cm^{-1}; **^{1}H NMR** (400 MHz, $CDCl_3$): δ 5.82 (1H, dddd, *J* = 16.6, 9.5, 7.2 and 7.2 Hz, H-2), 5.18 – 4.96 (2H, m, H-1), 4.39 – 3.60 (3H, m, H-5 + H-8 + H-4), 2.61 – 2.17 (4H, m, H-7 + H-3), 1.64 – 1.20 (14H, m, H-6 + H-9 + H-10 + H-11 + H-12 + H-13 + H-14), 0.87 (3H, t, *J* = 6.8 Hz, H-15) ppm. **^{13}C-NMR** (101 MHz, $CDCl_3$): δ 134.8, 118.3, 69.4, 68.3, 42.1, 41.9, 37.6, 31.9, 29.7, 29.4, 25.9, 22.7, 14.2 ppm. **MS (ESI)**: m/z 237 ($M+Na^+$); HRMS: found: ($M+H^+$) 215.2006, ($M+Na^+$) 237.1826, $C_{13}H_{27}O_2$ requires ($M+H^+$) 215.2011, $C_{13}H_{26}O_2Na$ requires ($M+Na^+$) 237.1825

(±)-(3*S*,5*S*)-2-methyloct-7-ene-3,5-diol (400b)

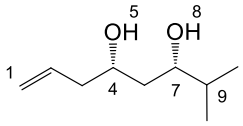

1 M Triethyl borane solution in hexanes (0.46 mL, 0.46 mmol, 1.1 eq.) was added to a mixture of dry THF (4 mL) and methanol (1 mL) at room temperature under a N_2 atmosphere. After stirring the mixture for 1 hour and 30 minutes it was cooled down to -78 ºC, followed by addition of β-hydroxy ketone **399b** (70 mg, 0.44 mmol) solution in dry THF (1.5 mL) over a period of 3 minutes. After stirring for 30 minutes $NaBH_4$ (20 mg, 0.54 mmol, 1.1 eq.) was added in one portion. After stirring the reaction for another 3 hours the reaction mixture was quenched with saturated aqueous NH_4Cl (5 mL) and diluted with ethyl acetate (5 mL). The aqueous layer was extracted with ethyl acetate (2 × 5 mL) and the combined organics were dried over $MgSO_4$, filtered and concentrated *in vacuo* to give a yellow oil, which was azeotroped with methanol (8 × 2 mL). The oil was then purified by flash chromatography (30% ethyl acetate in petroleum ether) on a silica gel column to yield **400b** as a yellow oil (31 mg, 43%)

IR (film): υ_{max} 3357, 3080, 2959, 2878, 1645, 1464, 1435, 1330, 1146, 1072 cm^{-1}; **^{1}H NMR** (400 MHz, $CDCl_3$): δ 5.88 – 5.77 (1H, m, H-2), 5.17 – 5.08 (2H, m, H-1), 3.94 – 3.85 (1H, m, H-4), 3.64 (1H, ddd, *J* = 10.4, 5.8, 2.1 Hz, H-7), 2.99 (2H, br s, H-5 + H-8), 2.33 – 2.18 (2H, m, H-3), 1.67 (1H, ddd, *J* = 14.0, 5.8 and 1.9 Hz, H-6), 1.62 (1H, ddd, *J* = 14.0, 2.1 and 2.1 Hz, H-6), 1.46 (1H, heptd, *J* = 10.4 and 6.8 Hz, H-9), 0.92 (3H, d, *J* = 6.8 Hz, H-10), 0.92 (3H, d, *J* = 6.8 Hz, H-10) ppm. **^{13}C-NMR** (101 MHz, $CDCl_3$): δ 134.5, 118.4, 77.8, 72.2, 42.7, 39.0, 34.2, 18.3, 17.5 ppm. **MS (ESI)**: m/z 181 ($M+Na^+$); HRMS: found: ($M+Na^+$) 181.1192, $C_9H_{18}O_2Na$ requires ($M+Na^+$) 181.1199

(±)-(3R,5S)-2-methyloct-7-ene-3,5-diol (386b)

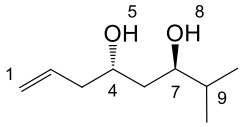

To a solution of $NMe_4BH(OAc)_3$ (412 mg, 1.6 mmol, 7 eq.) in dry MeCN (1 mL) and AcOH (1.2 mL) at -35 ºC under an N_2 atmosphere was added a solution of β-hydroxy ketone **399b** (35 mg, 0.22 mmol) in dry MeCN (1 mL) over a period of 3 minutes. The reaction mixture was stirred for 4 hours at -35 ºC. The reaction was quenched with 10% Rochelle's salt (5 mL) and warmed to room temperature. The mixture was partitioned between ethyl acetate (10 mL) and a saturated aqueous solution of $NaHCO_3$ (10 mL) and the aqueous layer was extracted with ethyl acetate (2 x 10 mL). The combined organics were dried over $MgSO_4$, filtered and concentrated *in vacuo* to give a yellow oil. The oil was then purified by flash chromatography (30% ethyl acetate in petroleum ether) on a silica gel column to yield **386b** as a yellow oil (29 mg, 83%).

IR (film): υ_{max} 3390, 3081, 2959, 2928, 2875, 1642, 1405, 1333, 1288, 1143, 1051 cm^{-1}; **^{1}H NMR** (400 MHz, $CDCl_3$): δ 5.89 – 5.73 (1H, m, H-2), 5.19 – 5.01 (2H, m, H-1), 3.99 (1H, dddd, *J* = 7.7, 7.4, 5.5 and 3.3 Hz, H-4), 3.68 (1H, ddd, *J* = 8.9, 6.1 and 2.8 Hz, H-7), 2.36 – 2.16 (2H, m, H-3), 1.76 – 1.62 (2H, m, H-6 + H-9), 1.58 (1H, ddd, *J* =14.5, 7.7, 2.8 Hz, H-6), 0.95 (3H, d, *J* = 6.7 Hz, H-10), 0.90 (3H, d, *J* = 6.8 Hz, H-10) ppm. **^{13}C-NMR** (101 MHz, $CDCl_3$): δ 134.7, 118.3, 73.9, 68.3, 42.0, 38.9, 33.4, 18.6, 17.9 ppm. **MS (ESI)**: m/z 181 ($M+Na^+$); HRMS: found: ($M+Na^+$) 181.1202, $C_9H_{18}O_2Na$ requires ($M+Na^+$) 181.1199

(±)-(5*S*,7*R*,*E*)-*S*-*p*-Tolyl 5,7-dihydroxytetradec-2-enethioate (401c)

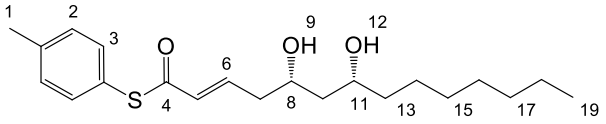

S-*p*-Tolyl prop-2-enethioate **272** (50 mg, 0.28 mmol, 3 eq.) and diol **400c** (20 mg, 0.09 mmol) were dissolved in dry diethyl ether (0.5 mL) under an N_2 atmosphere. Copper (I) iodide (2.7 mg, 0.014 mmol, 15 mol%) and Hoveyda-Grubbs 2nd generation catalyst (5.8 mg, 0.009 mmol, 10 mol %) were added as solids in a single portion, and the mixture was left to stir under reflux for 3 hours. The mixture was then concentrated *in vacuo* and purified by flash chromatography (40% ethyl acetate in petroleum ether) on a silica gel column to yield **401c** as a colourless oil (28 mg, 86%).

IR (film): υ_{max} 3372, 2924, 2930, 2853, 1679, 1632, 1500, 1457, 1303, 1138, 1024 cm^{-1}; **^{1}H NMR** (400 MHz, $CDCl_3$): δ 7.31 (2H, d, *J* = 8.1 Hz, H-2), 7.22 (2H, d, *J* = 8.1 Hz, H-3), 6.97 (1H, ddd, *J* = 15.5, 7.5 and 7.5 Hz, H-6), 6.25 (1H, d, *J* = 15.5 Hz, H-5), 4.08 – 3.99 (1H, m, H-8), 3.91 – 3.82 (1H, m, H-11), 2.46 – 2.27 (5H, m, H-1 + H-7), 1.65 – 1.18 (14H, m, H-10 + H-13 + H-14 + H-15 + H-16 + H-17 + H-18), 0.88 (3H, t, *J* = 6.4 Hz, H-19) ppm. **^{13}C-NMR** (101 MHz, $CDCl_3$): δ 188.5, 142.0, 139.7, 134.6, 130.1, 130.0, 123.9, 73.2, 71.3, 42.4, 40.1, 38.3, 31.8, 29.5, 29.2, 25.2, 22.6, 21.3, 14.1 ppm. **MS (ESI)**: m/z 365 ($M+H^+$) 387 ($M+Na^+$); HRMS: found: ($M+H^+$) 365.2141, ($M+Na^+$) 387.1962, $C_{21}H_{33}O_3S$ requires ($M+H^+$) 365.2145, $C_{21}H_{32}NaO_3S$ requires ($M+Na^+$) 387.1964

(±)-(5*S*,7*S*,*E*)-*S*-*p*-Tolyl 5,7-dihydroxytetradec-2-enethioate (385c)

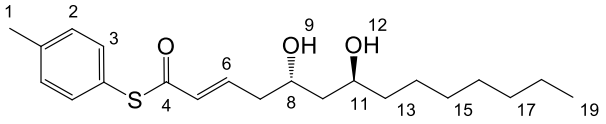

S-*p*-Tolyl prop-2-enethioate **272** (100 mg, 0.56 mmol, 3 eq.) and diol **386c** (40 mg, 0.19 mmol) were dissolved in dry diethyl ether (2 mL) under an N_2 atmosphere. Copper (I) iodide (5.3 mg, 0.028 mmol, 15 mol %) and Hoveyda-Grubbs 2nd generation catalyst (11.7 mg, 0.019 mmol, 10 mol %) were added as solids in a single portion, and the mixture was left to stir under reflux for 3 hours. The mixture was then concentrated *in vacuo* and purified by flash chromatography (40% ethyl acetate in petroleum ether) on a silica gel column to yield **385c** as a colourless oil (36 mg, 53%).

IR (film): υ_{max} 3387, 2925, 2856, 1683, 1629, 1500, 1464, 1138, 1013 cm^{-1}; **^{1}H NMR** (400 MHz, $CDCl_3$): δ 7.31 (2H, d, *J* = 8.1 Hz, H-2), 7.23 (2H, d, *J* = 8.1 Hz, H-3), 6.98 (1H, ddd, *J* = 15.5, 7.3 and 7.3 Hz, H-6), 6.27 (1H, d, *J* = 15.5 Hz, H-5), 4.18 – 4.10 (1H, m, H-8), 3.99 – 3.92 (1H, m, H-11), 2.50 – 2.29 (5H, m, H-1 + H-7), 1.72 – 1.18 (14H, m, H-10 + H-13 + H-14 + H-15 + H-16 + H-17 + H-18), 0.88 (3H, t, *J* = 6.8 Hz, H-19) ppm. **^{13}C-NMR** (101 MHz, $CDCl_3$): δ 188.4, 142.2, 139.7, 134.6, 130.1, 130.0, 123.9, 69.5, 67.9, 42.1, 40.3, 37.4, 31.8, 29.5, 29.2, 25.7, 22.6, 21.3, 14.1 ppm. **MS (ESI)**: m/z 387 ($M+Na^+$); HRMS: found: ($M+Na^+$) 387.1961, $C_{21}H_{32}NaO_3S$ requires ($M+Na^+$) 387.1964

(±)-(5*S*,7*S*,*E*)-*S*-*p*-Tolyl 5,7-dihydroxy-8-methylnon-2-enethioate (401b)

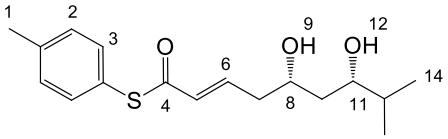

S-*p*-Tolyl prop-2-enethioate **272** (75 mg, 0.42 mmol, 3 eq.) and diol **400b** (30 mg, 0.14 mmol) were dissolved in dry diethyl ether (2 mL) under an N_2 atmosphere.

Copper (I) iodide (4 mg, 0.021 mmol, 15 mol %) and Hoveyda-Grubbs 2nd generation catalyst (8.8 mg, 0.014 mmol, 10 mol %) were added as solids in a single portion, and the mixture was left to stir under reflux for 3 hours. The mixture was then concentrated *in vacuo* and purified by flash chromatography (40% ethyl acetate in petroleum ether) on a silica gel column to yield **401b** as a colourless oil (44 mg, 75%).

IR (film): υ_{max} 3383, 2957, 2921, 2871, 1686, 1633, 1496, 1435, 1303, 1142, 1018 cm^{-1}; **^{1}H NMR** (400 MHz, $CDCl_3$): δ 7.31 (2H, d, *J* = 8.1 Hz, H-2), 7.22 (1H, d, *J* = 8.1 Hz, H-3), 6.99 (1H, ddd, *J* = 15.5, 7.4 and 7.4 Hz, H-6), 6.26 (1H, ddd, *J* = 15.5, 1.4 and 1.4 Hz, H-5), 4.31 – 4.22 (1H, br m, H-9), 4.07 – 3.97 (1H, m, H-8), 3.78 – 3.71 (1H, br m, H-12), 3.67 (1H, ddd, *J* = 10.2, 5.0 and 2.2 Hz, H-11), 2.45 – 2.30 (5H, m, H-1 + H-7), 1.71 – 1.56 (3H, m, H-10 + H-13), 0.92 (3H, d, *J* = 6.8 Hz, H-14), 0.92 (3H, d, *J* = 6.8 Hz, H-14) ppm. **^{13}C-NMR** (101 MHz, $CDCl_3$): δ 188.4, 142.1, 139.7, 134.6, 130.1, 130.0, 123.9, 77.9, 71.5, 40.7, 39.0, 34.3, 21.3, 18.2, 17.2 ppm. **MS (ESI)**: m/z 309 ($M+H^+$), 331 ($M+Na^+$); HRMS: found: ($M+H^+$) 309.1532, ($M+Na^+$) 331.1327, $C_{17}H_{25}O_3S$ requires ($M+H^+$) 309.1519, $C_{17}H_{24}NaO_3S$ requires ($M+Na^+$) 331.1338

(±)-(5*S*,7*R*,*E*)-*S*-*p*-Tolyl 5,7-dihydroxy-8-methylnon-2-enethioate (385b)

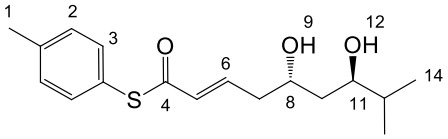

S-*p*-Tolyl prop-2-enethioate **272** (135 mg, 0.75 mmol, 3 eq.) and diol **386b** (40 mg, 0.25 mmol) were dissolved in dry diethyl ether (2 mL) under an N_2 atmosphere. Copper (I) iodide (7.2 mg, 0.038 mmol, 15 mol %) and Hoveyda-Grubbs 2nd generation catalyst (16.0 mg, 0.025 mmol, 10 mol %) were added as solids in a single portion, and the mixture was left to stir at reflux for 3 hours. The mixture was then concentrated *in vacuo*

and purified by flash chromatography (40% ethyl acetate in petroleum ether) on a silica gel column to yield **385b** as a colourless oil (41 mg, 54%).

IR (film): υ_{max} 3401, 2960, 2921, 2871, 1683, 1629, 1493, 1464, 1400, 1142, 1013 cm^{-1}; **^{1}H NMR** (400 MHz, $CDCl_3$): δ 7.31 (2H, d, *J* = 8.1 Hz, H-2), 7.22 (1H, d, *J* = 8.1 Hz, H-3), 6.98 (1H, ddd, *J* = 15.5, 7.3 and 7.3 Hz, H-6), 6.27 (1H, ddd, *J* = 15.5, 1.4 and 1.4 Hz, H-5), 4.16 – 4.08 (1H, m, H-8), 3.85 – 3.72 (2H, br m, H-9 + H-12), 3.68 (1H, ddd, *J* = 9.0, 6.1 and 3.2 Hz, H-11), 2.49 – 2.34 (5H, m, H-1 + H-7), 1.99 (1H, heptd, *J* = 6.8 and 6.1 Hz, H-13), 1.71 – 1.60 (2H, m, H-10), 0.95 (3H, d, *J* = 6.8 Hz, H-14), 0.91 (3H, d, *J* = 6.8 Hz, H-14) ppm. **^{13}C-NMR** (101 MHz, $CDCl_3$): δ 188.4, 142.3, 139.7, 134.6, 130.1, 130.0, 123.9, 73.9, 68.1, 40.3, 39.2, 33.4, 21.3, 18.6, 17.9 ppm. **MS (ESI)**: m/z 331 ($M+Na^+$); HRMS: found: ($M+Na^+$) 331.1344, $C_{17}H_{24}NaO_3S$ requires ($M+Na^+$) 331.1338

(±)-*S*-*p*-Tolyl 2-((2*R*,4*R*,6*R*)-6-heptyl-4-hydroxytetrahydro-2H-pyran-2-yl)ethanethioate (405c)

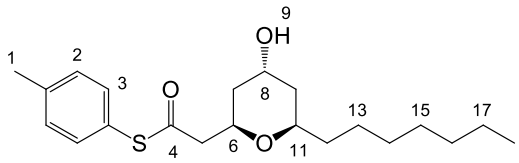

Thioester **401c** (10.0 mg, 0.028 mmol) was dissolved in DCM (0.5 mL) and water (0.05 mL) was added. The mixture was cooled down to 0 °C and trifluoroacetic acid (0.45 mL) was added over a period of 3 minutes. After stirring for 5.5 hours at room temperature the reaction was quenched with saturated aqueous solution of $NaHCO_3$ (2 mL) and diluted with DCM (2mL). The aqueous layer was extracted with DCM (2 × 2 mL). The combined organics were dried over $MgSO_4$, filtered, concentrated *in vacuo* and purified by flash chromatography (20% ethyl acetate in petroleum ether) on a silica gel column to yield **405c** as a colourless oil (6.5 mg, 65%).

IR (film): υ_{max} 3419, 2921, 2857, 1708, 1468, 1375, 1099, 1070 cm^{-1}; **^{1}H-NMR** (400 MHz, $CDCl_3$) δ 7.28 (2H, d, *J* = 8.1 Hz, H-2), 7.21 (2H, d, *J* = 8.1 Hz, H-3), 4.33 – 4.24 (2H, m, H-6 + H-8), 3.80 – 3.71 (1H, m, H-11), 2.87 (1H, dd, *J* = 14.6, 8.1 Hz, H-5), 2.64 (1H, dd, *J* = 14.6, 5.3 Hz, H-5), 2.37 (3H, s, H-1), 1.73 (1H, ddd, *J* = 13.7, 4.9, 2.2 Hz, H-7), 1.65 (1H, ddd, *J* = 14.0, 4.9, 2.2 Hz, H-10), 1.57 – 1.41 (4H, m, H-7 + H-10 + H-12), 1.33 – 1.18 (10H, m, H-13 + H-14 + H-15 + H-16 + H-17), 0.87 (3H, t, *J* = 6.9 Hz, H-18) ppm. **^{13}C-NMR** (101 MHz, $CDCl_3$): δ 195.7, 139.6, 134.4, 130.0, 124.3, 71.9, 68.9, 64.6, 49.9, 38.4, 36.4, 31.8, 29.6, 29.3, 25.5, 22.7, 21.2, 14.1 ppm. **MS (ESI)**: m/z 365 ($M+H^+$) 387 ($M+Na^+$); HRMS: found: ($M+H^+$) 365.2147, ($M+Na^+$) 387.1967, $C_{21}H_{33}O_3S$ requires ($M+H^+$) 365.2145, $C_{21}H_{32}NaO_3S$ requires ($M+Na^+$) 387.1964

(±)-*S*-*p*-Tolyl 2-((2*S*,4*R*,6*R*)-6-heptyl-4-hydroxytetrahydro-2H-pyran-2-yl)ethanethioate (404c)

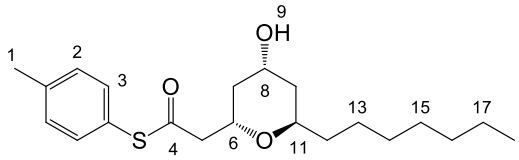

Thioester **401c** (10.0 mg, 0.028 mmol) was dissolved in dry THF (0.3 mL). A solution of acetic acid (0.002 mmol, 6 mol%) and tetrabutylammonium fluoride (0.008 mmol, 30 mol%) was added to the reaction mixture over a period of 3 minutes at 0 °C under N_2 atmosphere. After stirring for 5 hours at 0 °C the reaction was quenched with saturated aqueous solution of $NaHCO_3$ (2 mL). The phases were separated and the aqueous layer was extracted with diethyl ether (3 × 2 mL). The combined organics were dried over $MgSO_4$, filtered, concentrated *in vacuo* and purified by flash chromatography (20% ethyl acetate in petroleum ether) on a silica gel column to yield **404c** as a colourless oil (4.8 mg, 48%).

IR (film): υ_{max} 3433, 2928, 2853, 1732, 1460, 1378, 1246, 1052 cm^{-1}; **^{1}H-NMR** (400 MHz, $CDCl_3$) δ 7.35 (2H, d, *J* = 8.0 Hz, H-2), 7.15 (2H, d, *J* = 8.0 Hz, H-3), 4.46 (1H, dddd, *J* = 11.3, 7.5, 5.8 and 2.7 Hz, H-6), 3.83 – 3.76 (1H, m, H-8), 3.32 – 3.42 (1H, m, H-11), 2.89 (1H, dd, *J* = 17.8 and 5.8 Hz, H-5), 2.43 (1H, dd, *J* = 17.8, 11.3 Hz, H-5), 2.35 (3H, s, H-1), 1.87 (1H, ddd, *J* = 14.6, 8.6 and 7.5 Hz, H-7), 1.72 (1H, ddd, *J* = 14.5, 5.6 and 3.6 Hz, H-10), 1.59 (1H, ddd, *J* = 13.7, 11.7 and 11.7 Hz, H-12), 1.59 (1H, ddd, *J* = 13.7, 11.7 and 11.7 Hz, H-12), 1.48 – 1.41 (2H, m, H-7 + H-10), 1.34 – 1.20 (10H, m, H-13 + H-14 + H-15 + H-16 + H-17), 0.88 (3H, t, *J* = 6.6 Hz, H-18) ppm. **^{13}C-NMR** (101 MHz, $CDCl_3$): δ 193.3, 138.9, 134.5, 130.1, 127.7, 78.6, 77.2, 69.1, 42.9, 37.7, 36.7, 35.5, 31.7, 29.5, 29.2, 25.4, 22.6, 21.2, 14.1 ppm. **MS (ESI)**: 387 ($M+Na^+$); HRMS: found: ($M+Na^+$) 387.1963, $C_{21}H_{32}NaO_3S$ requires ($M+Na^+$) 387.1964

(±)-*S*-*p*-Tolyl 2-((2*S*,4*R*,6*S*)-6-heptyl-4-hydroxytetrahydro-2H-pyran-2-yl)ethanethioate (403c)

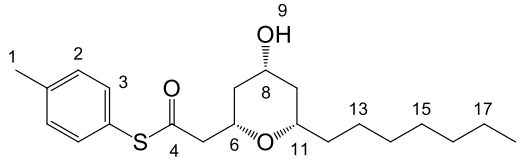

Thioester **385c** (15.0 mg, 0.041 mmol) was dissolved in DCM (0.5 mL) and water (0.05 mL) was added. The mixture was cooled down to 0 °C and trifluoroacetic acid (0.45 mL) was added dropwise. After stirring for 5.5 hours at room temperature the reaction was quenched with saturated aqueous solution of $NaHCO_3$ (2 mL) and diluted with DCM (2 mL). The aqueous layer was extracted with DCM (2 × 2 mL). The combined organics were dried over $MgSO_4$, filtered, concentrated *in vacuo* and purified by flash chromatography (20% ethyl acetate in petroleum ether) on a silica gel column to yield **403c** as a colourless oil (7.1 mg, 47%).

IR (film): υ_{max} 3394, 2925, 2850, 1704, 1464, 1371, 1085, 1035 cm^{-1}; **^{1}H-NMR** (400 MHz, $CDCl_3$) δ 7.28 (2H, d, *J* = 8.0 Hz, H-2), 7.21 (2H, d, *J* = 8.0 Hz, H-3), 3.86 – 3.76 (2H, m, H-6 + H-8), 3.33 – 3.25 (1H, m, H-11), 2.94 (1H, dd, *J* = 14.7, 7.8 Hz, H-5), 2.70 (1H, dd, *J* = 14.7, 5.2 Hz, H-5), 2.37 (3H, s, H-1), 2.05-1.90 (2H, m, H-7 + H-10), 1.64 – 1.39 (4H, m, H-7 + H-10 + H-12), 1.33 – 1.17 (10H, m, H-13 + H-14 + H-15 + H-16 + H-17), 0.87 (3H, t, *J* = 6.6 Hz, H-18) ppm. **^{13}C-NMR** (101 MHz, $CDCl_3$): δ 195.7, 139.7, 134.4, 130.0, 124.2, 75.8, 72.2, 68.0, 49.6, 41.0, 40.7, 36.0, 31.8, 29.5, 29.3, 25.6, 22.7, 21.3, 14.1 ppm. **MS (ESI)**: m/z 365 ($M+H^+$) 387 ($M+Na^+$); HRMS: found: ($M+H^+$) 365.2142, ($M+Na^+$) 387.1958, $C_{21}H_{33}O_3S$ requires ($M+H^+$) 365.2145, $C_{21}H_{32}NaO_3S$ requires ($M+Na^+$) 387.1964

(±)-*S*-*p*-Tolyl 2-((2*R*,4*R*,6*S*)-6-heptyl-4-hydroxytetrahydro-2H-pyran-2-yl)ethanethioate (402c)

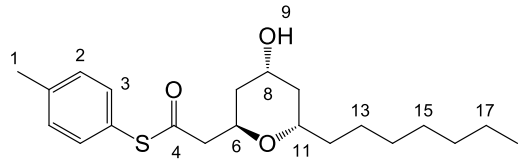

Thioester **385c** (15.0 mg, 0.041 mmol) was dissolved in dry THF (0.3 mL). A solution of acetic acid (0.002 mmol, 6 mol%) and tetrabutylammonium fluoride (0.012 mmol, 30 mol%) was added to the reaction mixture over a period of 3 minutes at 0 °C under N_2 atmosphere. After stirring for 5 hours at 0 °C the reaction was quenched with saturated aqueous solution of $NaHCO_3$ (2 mL). The phases were separated and the aqueous layer was extracted with diethyl ether (3 × 2 mL). The combined organics were dried over $MgSO_4$, filtered, concentrated *in vacuo* and purified by flash chromatography (20% ethyl acetate in petroleum ether) on a silica gel column to yield **402c** as a colourless oil (6.2 mg, 41%).

. **IR** (film): υ_{max} 3424, 2924, 2854, 1715, 1489, 1464, 1378, 1250, 1060 cm^{-1}; **^{1}H-NMR** (400 MHz, $CDCl_3$) δ 7.35 (2H, d, *J* = 8.1 Hz, H-2), 7.15 (2H, d, *J* = 8.1 Hz, H-3), 4.56 (1H, dddd, *J* = 12.3, 10.3, 5.9 and 2.4 Hz, H-6), 3.99 – 3.91 (1H, m, H-8), 4.39 (1H, dddd, *J* = 10.6, 10.6, 5.9 and 4.5 Hz, H-11), 2.91 (1H, dd, *J* = 17.7 and 5.9 Hz, H-5), 2.43 (1H, dd, *J* = 17.7 and 10.3 Hz, H-5), 2.35 (3H, s, H-1), 2.22 – 2.15 (1H, m, H-10), 1.74 (1H, ddd, *J* = 14.5, 9.8 and 2.4 Hz, H-7), 1.64 – 1.39 (4H, m, H-7 + H-10 + H-12), 1.33 – 1.17 (10H, m, H-13 + H-14 + H-15 + H-16 + H-17), 0.88 (3H, t, *J* = 6.6 Hz) ppm. **^{13}C-NMR** (101 MHz, $CDCl_3$): δ 193.3, 138.9, 134.4, 130.0, 124.2, 77.2, 68.0, 67.3, 43.1, 38.0, 36.5, 36.1, 31.8, 29.5, 29.3, 29.2, 25.5, 22.6, 21.2, 14.1 ppm **MS (ESI)**: m/z 365 ($M+H^+$) 387 ($M+Na^+$); HRMS: found: ($M+H^+$) 365.2149, ($M+Na^+$) 387.1969, $C_{21}H_{33}O_3S$ requires ($M+H^+$) 365.2145, $C_{21}H_{32}NaO_3S$ requires ($M+Na^+$) 387.1964

(±)-*S*-*p*-Tolyl 2-((2*R*,4*S*,6S)-4-hydroxy-6-isopropyltetrahydro-2H-pyran-2-yl)ethanethioate (405b)

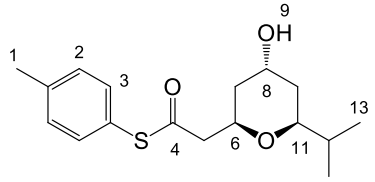

Thioester **401b** (8.0 mg, 0.026 mmol) was dissolved in DCM (0.5 mL) and water (0.05 mL) was added. The mixture was cooled down to 0 °C and trifluoroacetic acid (0.45 mL) was added dropwise. After stirring for 5.5 hours at room temperature the reaction was quenched with saturated aqueous solution of $NaHCO_3$ (2 mL) and diluted with DCM (2 mL). The aqueous layer was extracted with DCM (2 × 2 mL). The combined organics were dried over $MgSO_4$, filtered, concentrated *in vacuo* and purified by flash chromatography (20% ethyl acetate in petroleum ether) on a silica gel column to yield **405b** as a colourless oil (5.3 mg, 66%).

IR (film): υ_{max} 3446, 2959, 2924, 2877, 2851, 1706, 1467, 1435, 1381, 1066 cm^{-1}; **^{1}H-NMR** (400 MHz, $CDCl_3$) δ 7.28 (2H, d, *J* = 8.1 Hz, H-2), 7.21 (2H, d, *J* = 8.1 Hz, H-3), 4.32 – 4.22 (2H, m, H-6 + H-8), 3.45 (1H, ddd, *J* = 11.9, 7.0 and 1.9 Hz, H-11), 2.86 (1H, dd, *J* = 14.5 and 8.2 Hz, H-5), 2.65 (1H, dd, *J* = 14.5 and 4.9 Hz, H-5), 2.37 (3H, s, H-1), 1.73 –1.68 (1H, m, H-7), 1.66 - 1.58 (1H, m, H-10), 1.54 – 1.41 (3H, m, H-7 + H-10 + H-12), 0.96 (3H, d, *J* = 6.7 Hz, H-13), 0.88 (3H, d, *J* = 6.8 Hz, H-13) ppm. **^{13}C-NMR** (101 MHz, $CDCl_3$): δ 193.4, 139.6, 134.4, 130.0, 124.4, 77.2, 69.0, 64.7, 49.9, 38.3, 35.3, 33.1, 30.3, 21.3, 18.5 ppm. **MS (ESI)**: 331 ($M+Na^+$); HRMS: found: ($M+Na^+$) 331.1333, $C_{17}H_{24}NaO_3S$ requires ($M+Na^+$) 331.1338

(±)-*S*-*p*-Tolyl 2-((2*S*,4*S*,6*S*)-4-hydroxy-6-isopropyltetrahydro-2H-pyran-2-yl)ethanethioate (404b)

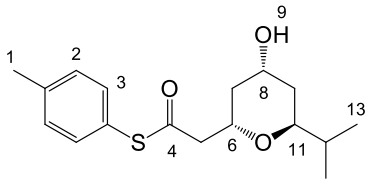

Thioester **401b** (8.0 mg, 0.026 mmol) was dissolved in dry THF (0.3 mL). A solution of acetic acid (0.002 mmol, 6 mol%) and tetrabutylammonium fluoride (0.008 mmol, 30 mol%) was added to the reaction mixture over a period of 3 minutes at 0 °C under N_2 atmosphere. After 5 hours TLC still showed starting material, therefore solution containing acetic acid (0.004 mmol, 12 mol%) and tetrabutylammonium fluoride (0.016 mmol, 60 mol%) was added and the reaction warmed to room temperature. After stirring for another 1 hour the reaction was quenched with saturated aqueous solution of $NaHCO_3$ (2 mL). The phases were separated and the aqueous layer was extracted with diethyl ether (3 × 2 mL). The combined organics were dried over $MgSO_4$, filtered, concentrated *in vacuo* and purified by flash chromatography (20% ethyl acetate in petroleum ether) on a silica gel column to yield **404b** as a colourless oil (5.5 mg, 69%).

IR (film): υ_{max} 3448, 2957, 2925, 2853, 1736, 1467, 1439, 1385, 1246, 1053 cm^{-1}; **^{1}H-NMR** (400 MHz, $CDCl_3$) δ 7.35 (2H, d, *J* = 8.0 Hz, H-2), 7.11 (2H, d, *J* = 8.0 Hz, H-3), 4.49 (1H, dddd, *J* = 11.8, 6.7, 6.6 and 2.8 Hz, H-8), 3.65 (1H, ddd, *J* = 9.5, 4.8 and 2.6 Hz, H-11), 3.37 (1H, dddd, *J* = 11.2, 11.0, 5.9 and 4.3 Hz, H-6), 2.90 (1H, dd, *J* = 17.7 and 5.9 Hz, H-5), 2.43 (1H, dd, *J* = 17.7 and 11.0 Hz, H-5), 2.35 (3H, s, H-1), 2.34 - 2.26 (2H, m, H-7), 1.85 (1H, ddd, *J* = 14.3, 9.5 and 6.7 Hz, H-10), 1.72 (1H, ddd, *J* = 14.3, 6.6 and 2.6 Hz, H-10), 1.66 (1H, heptd, *J* = 6.5 and 4.8 Hz, H-12), 0.92 (3H, d, *J* = 6.5 Hz, H-13), 0.90 (3H, d, *J* = 6.5 Hz, H-13) ppm. **^{13}C-NMR** (101 MHz, $CDCl_3$): δ 193.4, 139.0, 134.5, 130.2, 125.6, 79.2, 77.3, 73.8, 39.7, 39.5, 35.5, 33.9, 30.4, 21.3, 18.4, 17.2 ppm. **MS (ESI)**: m/z 309 ($M+H^+$), 331 ($M+Na^+$); HRMS: found: ($M+H^+$) 309.1548, ($M+Na^+$) 331.1338, $C_{17}H_{25}O_3S$ requires ($M+H^+$) 309.1519, $C_{17}H_{24}NaO_3S$ requires ($M+Na^+$) 331.1338

(±)-*S*-*p*-Tolyl 2-((2*S*,4*S*,6*R*)-4-hydroxy-6-isopropyltetrahydro-2H-pyran-2-yl)ethanethioate (403b)

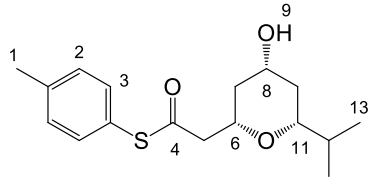

Thioester **385b** (15.0 mg, 0.049 mmol) was dissolved in DCM (0.5 mL) and water (0.05 mL) was added. The mixture was cooled down to 0 °C and trifluoroacetic acid (0.45 mL) was added dropwise. After stirring for 5.5 hours at room temperature the reaction was quenched with saturated aqueous solution of $NaHCO_3$ (2 mL) and diluted with DCM (2 mL). The aqueous layer was extracted with DCM (2 × 2 mL). The combined organics were dried over $MgSO_4$, filtered, concentrated *in vacuo* and purified by flash chromatography (20% ethyl acetate in petroleum ether) on a silica gel column to yield **403b** as a colourless oil (9.9 mg, 66%).

IR (film): υ_{max} 3419, 2925, 2850, 1704, 1464, 1364, 1221, 1020 cm^{-1}; **^{1}H-NMR** (400 MHz, $CDCl_3$) δ 7.28 (2H, d, *J* = 8.1 Hz, H-2), 7.21 (2H, d, *J* = 8.1 Hz, H-3), 3.86 – 3.75 (2H, m, H-6 + H-8), 3.00 (1H, ddd, *J* = 11.1, 6.7 and 1.7 Hz, H-11), 2.92 (1H, dd, *J* = 14.6 and 8.1 Hz, H-5), 2.69 (1H, dd, *J* = 14.6 and 4.9 Hz, H-5), 2.37 (3H, s, H-1), 2.04 – 1.95 (2H, m, H-7), 1.85 (1H, ddd, *J* = 15.2, 7.0 and 6.7 Hz, H-10), 1.75 – 1.65 (1H, m, H-10), 1.43 (1H, septd, *J* = 6.7 and 1.7 Hz, H-12), 0.96 (3H, d, *J* = 6.7 Hz, H-13), 0.90 (3H, d, *J* = 6.7 Hz, H-13) ppm. **^{13}C-NMR** (101 MHz, $CDCl_3$): δ 193.4, 139.7, 134.4, 130.0, 123.8, 80.8, 72.3, 68.3, 49.6, 37.8, 34.1, 33.0, 29.7, 21.3, 18.6 ppm. **MS (ESI)**: m/z 331 ($M+Na^+$); HRMS: found: ($M+Na^+$) 331.1343, $C_{17}H_{24}NaO_3S$ requires ($M+Na^+$) 331.1338

(±)-S-p-tolyl 2-((2R,4S,6R)-4-hydroxy-6-isopropyltetrahydro-2H-pyran-2-yl)ethanethioate (402b)

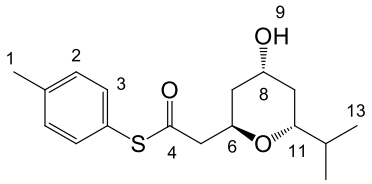

Thioester **385b** (7.5 mg, 0.024 mmol) was dissolved in dry THF (0.3 mL). A solution of acetic acid (0.002 mmol, 6 mol%) and tetrabutylammonium fluoride (0.008 mmol, 30 mol%) was added dropwise to the reaction mixture at 0 °C under N_2 atmosphere. After stirring for 2 hours at 0 °C and 1 hour at room temperature the reaction was quenched with saturated aqueous solution of $NaHCO_3$ (2 mL). The phases were separated and the aqueous layer was extracted with diethyl ether (3x2 mL). The combined organics were dried over $MgSO_4$, filtered, concentrated *in vacuo* and purified by flash chromatography (20% ethyl acetate in petroleum ether) on a silica gel column to yield **402b** as a colourless oil (5.2 mg, 69%).

IR (film): υ_{max} 3450, 2959, 2918, 1730, 1467, 1368, 1247, 1057 cm^{-1}; **^{1}H-NMR** (400 MHz, $CDCl_3$) δ 7.35 (2H, d, *J* = 8.0 Hz, H-2), 7.15 (2H, d, *J* = 8.0 Hz, H-3), 4.55

(1H, dddd, *J* = 12.4, 9.8, 2.6 and 2.6 Hz, H-8), 3.77 (1H, ddd, *J* = 10.6, 5.2 and 2.1 Hz, H-11), 3.44 – 3.36 (1H, m, H-6), 2.91 (1H, dd, *J* = 17.7 and 6.0 Hz, H-5), 2.43 (1H, dd, *J* = 17.7 and 10.7 Hz, H-5), 2.35 (3H, s, H-1), 2.20 (1H, ddd, *J* = 13.8, 4.4 and 2.6 Hz, H-7), 1.72 (1H, ddd, *J* = 14.4, 9.8 and 2.1 Hz, H-10), 1.65 – 1.50 (3H, m, H-7 + H-10 + H-12), 0.90 (3H, d, *J* = 6.8 Hz, H-13), 0.90 (3H, d, *J* = 6.8 Hz, H-13) ppm. **^{13}C-NMR** (101 MHz, $CDCl_3$): δ 193.3, 138.8, 134.4, 130.0, 125.0, 77.5, 77.2, 71.6, 39.6, 39.4, 36.2, 34.0, 29.7, 21.2, 18.5, 17.1 ppm. **MS (ESI)**: m/z 331 ($M+Na^+$); HRMS: found: ($M+Na^+$) 331.1726, $C_{17}H_{24}NaO_3S$ requires ($M+Na^+$) 331.1338

5-methoxy-2-methyloct-7-en-3-one (407)

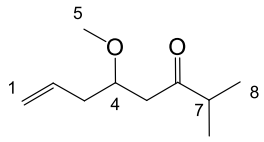

Methyl iodide (5 mL) and silver (I) oxide (460 mg, 2.0 mmol) were added to a solution of β-hydroxyketone **406** (156 mg, 1.0 mmol) in MeCN (5 ml). The mixture was heated under reflux for 18 hours. Another portion of silver (I) oxide (460 mg, 2.0 mmol) was added and heating continued for another 5 hours. The solids were filtered off and the reaction quenched with saturated aqueous solution of $NaHCO_3$ (15 ml) and extracted with diethyl ether (3 × 10 ml). The organic fraction was dried with $MgSO_4$, filtered and concentrated *in vacuo* and purified by flash chromatography (10% diethyl ether in pentane) on a silica gel column to yield **407** as a colourless oil (100 mg, 64%).

IR (film): υ_{max} 2966, 2931, 1709, 1461, 1365, 1260, 1098 cm^{-1}; **^{1}H NMR** (400 MHz, $CDCl_3$): δ 5.76 (1H, dddd, *J* = 19.1, 9.5 and 7.1 Hz, H-2), 5.09 – 5.02 (2H, m, H-1), 3.77 (1H, m, H-4), 3.30 (3H, s, H-5), 2.68 (1H, dd, *J* = 16.6 and 7.4 Hz, H-6), 2.57 (1H, hept, *J* = 6.9 Hz, H-7), 2.56 (1H, dd, *J* = 16.6 and 5.2 Hz, H-6), 2.30 - 2.24 (2H, m, H-3), 1.06 (3H, d, *J* = 6.9 Hz, H-8), 1.06 (3H, d, *J* = 6.9 Hz, H-8) ppm. **^{13}C-NMR** (101 MHz,

$CDCl_3$): δ 213.3, 134.0, 117.7, 76.4, 57.1, 44.5, 41.6, 37.9, 17.9, 17.8 ppm. **MS (ESI)**: m/z 193 ($M+Na^+$); HRMS: found: ($M+Na^+$) 193.1202, $C_{10}H_{18}NaO_2$ requires ($M+Na^+$) 193.1199

(±)-(5*S*,7*R*,*E*)-*S*-*p*-Tolyl 7-hydroxy-5-methoxy-8-methylnon-2-enethioate (408)

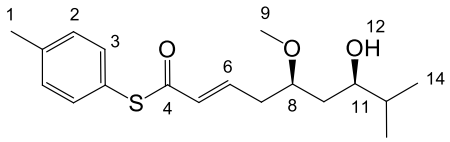

To a solution of β-methoxyketone **407** (80 mg, 0.47 mmol) in methanol (10 ml) $NaBH_4$ (18 mg, 0.47 mmol) was added in one portion. The mixture was stirred for 1 hour at room temperature and then quenched with saturated aqueous solution of NH_4Cl. The solvents were removed *in vacuo* and the resultant brown oil was dissolved in ethyl acetate (15 mL) and H_2O (15 mL) added. The layers were separated and the organic layer was washed with brine (15 mL), dried ($MgSO_4$) and concentrated *in vacuo* to give the methoxy alcohol as a mixture of diastereomers.

S-*p*-Tolyl prop-2-enethioate **272** (250 mg, 1.4 mmol, 3 eq.) and mixture of diasatereomers of methoxy alcohol (80 mg, 0.46 mmol) were dissolved in dry diethyl ether (8 ml) under an N_2 atmosphere. Copper (I) iodide (13 mg, 0.070 mmol, 15 mol %) and Hoveyda-Grubbs 2nd generation catalyst (30 mg, 0.046 mmol, 10 mol %) were added as solids in a single portion, and the mixture was left to stir at reflux for 3 hours. The mixture was then concentrated *in vacuo* and purified by repeated preparative thin layer chromatography (0.5% methanol in DCM) on a silica gel plate to yield the 1,3-*syn* methoxy alcohol ***syn*-408** (50 mg, 34%) and 1,3-*anti* methoxy alcohol ***anti*-408** (45 mg, 30%) as colorless oils.

IR (film): υ_{max} 3487, 2960, 2928, 2871, 1679, 1632, 1489, 1464, 1364, 1181, 1092, 1018 cm^{-1}; **^{1}H NMR** (400 MHz, $CDCl_3$): δ 7.32 (2H, d, *J* = 8.1 Hz, H-2), 7.23 (1H,

d, *J* = 8.1 Hz, H-3), 6.93 (1H, ddd, *J* = 15.3, 7.4 and 7.4 Hz, H-6), 6.27 (1H, d, *J* = 15.3 Hz, H-5), 3.65 –3.52 (2H, m, H-8 + H-11), 3.41 (3H, s, H-9), 3.35 – 3.29 (1H, br s, H-12), 2.54 – 2.45 (2H, m, H-7), 2.38 (3H, s, H-1), 1.65 (1H, ddd, *J* = 13.4, 11.9 and 6.7 Hz, H-10), 1.62 – 1.54 (1H, m, H-12), 1.39 (1H, m, H-10), 0.91 (3H, d, *J* = 6.8 Hz, H-14), 0.91 (3H, d, *J* = 6.8 Hz, H-14) ppm. **^{13}C-NMR** (101 MHz, $CDCl_3$): δ 188.2, 141.2, 139.7, 134.6, 130.3, 130.0, 80.9, 76.1, 56.7, 37.6, 36.2, 33.8, 21.3, 18.4, 17.4 ppm. **MS (ESI)**: m/z 323 ($M+H^+$), 345 ($M+Na^+$); HRMS: found: ($M+H^+$) 323.1679, ($M+Na^+$) 345.1491, $C_{18}H_{27}O_3S$ requires ($M+H^+$) 323.1675, $C_{18}H_{26}NaO_3S$ requires ($M+Na^+$) 345.1495

(±)-*S*-*p*-Tolyl 2-((2*S*,4*S*,6*R*)-6-isopropyl-4-methoxytetrahydro-2H-pyran-2-yl)ethanethioate (409)

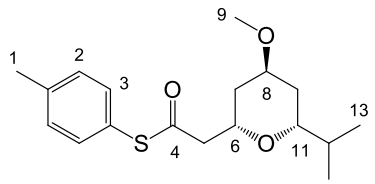

Thioester **408** (5.0 mg, 0.015 mmol) was dissolved in DCM (0.5 mL) and water (0.05 mL) was added. The mixture was cooled down to 0 °C and trifluoroacetic acid (0.45 mL) was added over a period of 3 minutes. After stirring for 5.5 hours at room temperature the reaction was quenched with saturated aqueous solution of $NaHCO_3$ (2 mL) and diluted with DCM (2mL). The aqueous layer was extracted with DCM (2 × 2 mL). The combined organics were dried over $MgSO_4$, filtered, concentrated *in vacuo* and purified by flash chromatography (10% ethyl acetate in petroleum ether) on a silica gel column to yield **409** as a colourless oil (2.4 mg, 48%).

IR (film): υ_{max} 2954, 2929, 2875, 2853, 1708, 1464, 1381, 1347, 1222, 1170, 1094 cm^{-1}; **^{1}H-NMR** (400 MHz, $CDCl_3$) δ 7.30 (2H, d, *J* = 7.9 Hz, H-2), 7.21 (2H, d, *J* = 7.9 Hz, H-3), 4.21 – 4.13 (1H, m, H-6), 3.69 – 3.64 (1H, m, H-8), 3.42 – 3.28 (4H, m, H-11 + H-9), 2.84 (1H, dd, *J* = 14.4 and 8.2 Hz, H-5), 2.64 (1H, dd, *J* = 14.4 and 5.0 Hz, H-

5), 2.36 (3H, s, H-1), 1.92 – 1.90 (1H, m, H-7), 1.88 (1H, ddd, *J* = 7.2, 2.3 and 2.3 Hz, H-10), 1.85 – 1.82 (1H, m, H-7), 1.65 – 1.55 (2H, m, H-10 + H-12), 0.95 (3H, d, *J* = 6.6 Hz, H-13), 0.88 (3H, d, *J* = 6.8 Hz, H-13) ppm. **^{13}C-NMR** (101 MHz, $CDCl_3$): δ 193.2, 139.5, 134.4, 130.0, 123.6, 77.2, 73.5, 69.3, 56.0, 50.0, 34.6, 33.1, 32.3, 22.7, 21.3, 18.5 ppm. **MS (ESI)**: m/z 323 ($M+H^+$), 345 ($M+Na^+$); HRMS: found: ($M+H^+$) 323.1678, ($M+Na^+$) 345.1473, $C_{18}H_{27}O_3S$ requires ($M+H^+$) 323.1675, $C_{18}H_{26}NaO_3S$ requires ($M+Na^+$) 345.1495

9.3 Computational studies

All of the molecular mechanics conformation analyses were done using MMFF forcefield. The geometries were fully optimized at the B3LYP^x/6-31G(d) level of theory and all of the optimized geometries were verified by frequency analysis as minima (zero imaginary frequencies) of transition structures (a single imaginary frequency). All of the molecular mechanics and quantum chemical computations were done using Spartan '08 v1.2. All of the structural representations were generated with jmol-14.2.4.

Thioester alkoxide low energy pseudo-2,6-*trans* conformation (348)

Cartesian Coordinates (Angstroms)

Atom	X	Y	Z
1 C	C	1.9786926	1.8724460	4.6560388
2 C	C1	1.6441302	0.5186188	4.7353062
3 C	C2	1.4688509	-0.2273124	3.5672502
4 C	C3	1.6262591	0.3820429	2.3119578
5 C	C4	1.9459854	1.7376504	2.2558576
6 C	C5	2.1293372	2.5035923	3.4169061
7 C	C6	2.4682789	3.9740911	3.3224452
8 H	H	2.1132057	2.4464460	5.5716604
9 H	H1	1.5133941	0.0408000	5.7019314
10 S	S1	1.0838394	-1.9803331	3.6459998
11 H	H2	1.4899674	-0.1958872	1.3887274
12 H	H3	2.0549006	2.2093416	1.2806029
13 H	H4	3.3519580	4.1438280	2.6938908
14 H	H5	1.6452695	4.5468259	2.8745519
15 H	H6	2.6720059	4.4044078	4.3095397
16 C	C7	-0.7425842	-1.8885844	3.2230056
17 O	O	-1.4771612	-1.1635069	3.8594786
18 C	C8	-1.1866297	-2.7339249	2.1148894
19 C	C9	-0.3761597	-3.2629717	1.1749344
20 H	H7	-2.2710460	-2.7976904	2.0240899
21 H	H8	0.6956130	-3.1254065	1.2535802
22 C	C10	-0.8481931	-4.0418929	-0.0147674
23 C	C11	-0.4912893	-5.5310511	0.1944922
24 C	C12	-0.1851481	-3.5587856	-1.3533927
25 H	H9	-1.9407077	-3.9553513	-0.1005828
26 H	H10	-0.5177651	-4.2962729	-2.1075761
27 O	O1	1.2173024	-3.6301305	-1.2700791
28 C	C13	-0.6146714	-2.1594540	-1.8751620
29 H	H11	0.5964899	-5.6463809	0.2079787
30 H	H12	-0.8876123	-6.1366009	-0.6311284
31 H	H13	-0.9034520	-5.9179591	1.1340019
32 C	C14	-2.1147995	-2.0634464	-2.1764340
33 H	H14	-0.0736028	-2.0739755	-2.8303572
34 C	C15	-0.1001336	-0.9926845	-0.9404879
35 H	H15	1.4247895	-2.7029017	-0.8682624
36 O	O2	1.0946000	-1.2994582	-0.3346323
37 H	H16	-2.4515618	-2.8893621	-2.8196771
38 H	H17	-2.3531051	-1.1232200	-2.6869769
39 H	H18	-2.7144932	-2.0921883	-1.2577847
40 C	C16	0.0279546	0.2995187	-1.7680441
41 H	H19	-0.9148334	-0.8050844	-0.2036490
42 C	C17	1.2540970	0.3786957	-2.6399160
43 C	C18	-0.8816512	1.2922189	-1.6651695
44 H	H20	1.0059527	0.3103840	-3.7102226
45 H	H21	1.9240566	-0.4398428	-2.3641778
46 H	H22	1.7952174	1.3241102	-2.4955200
47 H	H23	-1.7153854	1.1665928	-0.9765422
48 C	C19	-0.8966766	2.5691169	-2.3624737
49 C	C20	-0.1040622	3.1060981	-3.3409753
50 N	N	-1.8869699	3.5238410	-2.0565691

51 O O3 -0.5713626 4.3691786 -3.6458691
52 H H24 0.7462950 2.7701519 -3.9074108
53 C C21 -1.6444979 4.5359892 -2.8253496
54 C C22 -2.3818614 5.8279855 -2.9087947
55 H H25 -3.2284416 5.7933118 -2.2203687
56 H H26 -2.7540960 6.0105825 -3.9241789
57 H H27 -1.7384889 6.6737937 -2.6365847
Electronic energy: -1647.14402 au

Thioester alkoxide low energy pseudo-2,6-*cis* conformation (347)

Cartesian Coordinates (Angstroms)
Atom X Y Z
--------- ------------ ------------ ------------
1 C C 2.0547161 2.5610644 -1.5119298
2 C C1 0.9274560 1.9419415 -2.0458522
3 C C2 0.8218383 1.8055870 -3.4400745
4 C C3 1.8303330 2.2989502 -4.2699978
5 C C4 2.9427512 2.9362167 -3.7140083
6 C C5 3.0753518 3.0726722 -2.3289767
7 C C6 4.2802076 3.7552320 -1.7211217
8 H H 2.1394877 2.6523418 -0.4302991
9 H H1 0.1314913 1.5624810 -1.3939959
10 S S1 -0.6548786 1.0740864 -4.1425877
11 H H2 1.7496202 2.1787410 -5.3470522
12 H H3 3.7242254 3.3191079 -4.3689138
13 H H4 4.7705914 3.1153451 -0.9766468
14 H H5 5.0235322 4.0094089 -2.4850445
15 H H6 4.0015676 4.6852551 -1.2069969
16 C C7 -0.6226523 -0.5794316 -3.2842128
17 O O 0.4220691 -1.1471112 -3.0546278
18 C C8 -1.9661419 -1.0206484 -2.9020041
19 C C9 -2.1110821 -2.0657670 -2.0661607
20 H H7 -2.7944994 -0.3618630 -3.1330728
21 H H8 -1.2155375 -2.6339085 -1.8209361
22 C C10 -3.3662386 -2.3688952 -1.3076400
23 C C11 -4.6140290 -2.4550442 -2.2030603
24 C C12 -3.6298373 -1.2647030 -0.1909291
25 H H9 -3.2437152 -3.3322992 -0.7945503
26 H H10 -4.5547102 -1.6273020 0.3006584
27 O O1 -3.8943554 -0.0192652 -0.7658525
28 C C13 -2.5517778 -1.1408209 0.9220834
29 H H11 -4.8535942 -1.4695098 -2.6109168
30 H H12 -5.4794479 -2.7905404 -1.6168311
31 H H13 -4.4688169 -3.1579794 -3.0323381
32 C C14 -2.2649493 -2.4806293 1.6094757
33 H H14 -3.0216274 -0.4729075 1.6603164
34 C C15 -1.2476750 -0.3973561 0.4258720
35 H H15 -2.9687506 0.4597310 -0.7043383
36 O O2 -1.5310441 0.7053597 -0.3346902
37 H H16 -3.1956484 -2.9909969 1.8975866
38 H H17 -1.6639628 -2.3432837 2.5149252

39 H H18 -1.7053145 -3.1616957 0.9546910
40 C C16 -0.3930513 0.0022090 1.6462624
41 H H19 -0.6524929 -1.1640236 -0.1282229
42 C C17 -0.8671243 1.2362994 2.3689593
43 C C18 0.7193853 -0.6831524 1.9860834
44 H H20 -1.3226143 0.9987808 3.3428247
45 H H21 -1.5986709 1.7352103 1.7275635
46 H H22 -0.0433274 1.9372617 2.5611197
47 H H23 1.0138823 -1.5353299 1.3764940
48 C C19 1.6285600 -0.4220035 3.0915944
49 C C20 1.5974513 0.4609151 4.1378491
50 N N 2.8107348 -1.1779866 3.2188252
51 O O3 2.7307476 0.2784141 4.9050325
52 H H24 0.9096072 1.2110462 4.4857832
53 C C21 3.4017031 -0.7261649 4.2774898
54 C C22 4.6971316 -1.1645425 4.8688912
55 H H25 5.1059342 -1.9713490 4.2576471
56 H H26 4.5664073 -1.5263962 5.8962154
57 H H27 5.4207842 -0.3407517 4.8996380
Electronic energy: -1647.13966 au

Thioester alkoxide cyclization transition state leading to 2,6-*trans* product

(350)

Cartesian Coordinates (Angstroms)
Atom X Y Z
--- --- --- ---
1 C C -2.7214893 -4.8280310 -0.3117213
2 C C1 -3.5887538 -3.7486588 -0.1266495
3 C C2 -3.1044162 -2.4372228 -0.1703445
4 C C3 -1.7346075 -2.2187973 -0.3962575
5 C C4 -0.8797784 -3.3067424 -0.5568387
6 C C5 -1.3539239 -4.6273567 -0.5238882
7 C C6 -0.4125096 -5.7935188 -0.7246509
8 H H -3.1146628 -5.8433305 -0.2756385
9 H H1 -4.6445396 -3.9208299 0.0631413
10 S S1 -4.2269348 -1.0528942 0.0063197
11 H H2 -1.3516749 -1.1982532 -0.4461827
12 H H3 0.1813073 -3.1227556 -0.7194853
13 H H4 -0.9107194 -6.7487943 -0.5234061
14 H H5 -0.0283444 -5.8328017 -1.7535264
15 H H6 0.4605422 -5.7266076 -0.0628670
16 C C7 -3.4641958 -0.2703601 1.5935923
17 O O1 -3.5304016 -0.9181435 2.6215986
18 C C8 -2.9208815 1.0425999 1.4415900
19 C C9 -2.6725304 1.7146460 0.2615091
20 H H7 -2.5832380 1.4753885 2.3834406
21 H H8 -3.1187777 1.3454452 -0.6529411
22 C C10 -2.3512791 3.1980075 0.2986472
23 C C11 -3.6124699 3.9853654 -0.1107854
24 C C12 -1.1567922 3.6123396 -0.6011704

```
25 H H9 -2.1034807 3.4704391 1.3346905
26 H H10 -1.1242649 4.7137395 -0.6140474
27 O O2 -1.3659713 3.1964600 -1.9428724
28 C C13 0.2137061 3.0916861 -0.1012082
29 H H11 -3.8240497 3.8176414 -1.1719352
30 H H12 -3.4633411 5.0631106 0.0389407
31 H H13 -4.4836582 3.6739341 0.4767086
32 C C14 0.7385951 3.8145362 1.1445464
33 H H14 0.9030163 3.3091840 -0.9290318
34 C C15 0.1275465 1.5304802 0.0990515
35 H H15 -1.2255873 2.2141419 -1.8378319
36 O O3 -0.8982791 0.9947642 -0.6608090
37 H H16 0.8193805 4.8981163 0.9807833
38 H H17 1.7351049 3.4432625 1.4142600
39 H H18 0.0863724 3.6554651 2.0129627
40 C C16 1.4653953 0.8580594 -0.2271151
41 H H19 -0.0591147 1.3593596 1.1817326
42 C C17 1.7570357 0.6857487 -1.6929789
43 C C18 2.2512661 0.4298858 0.7843585
44 H H20 0.9362726 0.1130145 -2.1391010
45 H H21 2.7090256 0.1893575 -1.8782601
46 H H22 1.7564979 1.6580990 -2.2047097
47 H H23 1.8675326 0.5733466 1.7951321
48 C C19 3.5476662 -0.2338510 0.7690906
49 C C20 4.2317127 -0.6840926 1.8633607
50 N N 4.3280435 -0.5302603 -0.3617349
51 O O4 5.4149835 -1.2538986 1.4474654
52 H H24 4.0409480 -0.6891770 2.9245452
53 C C21 5.3881831 -1.1189030 0.0926117
54 C C22 6.5460377 -1.6529973 -0.6773481
55 H H25 6.3828190 -1.4558096 -1.7385255
56 H H26 6.6567539 -2.7342101 -0.5299891
57 H H27 7.4849234 -1.1793263 -0.3662276
Electronic energy: -1647.14020 au
```

Thioester alkoxide cyclization transition state leading to 2,6-*cis* product (349)

```
Cartesian Coordinates (Angstroms)
Atom X Y Z
--------- ------------ ------------ ------------
1 C C 1.7478453 -2.9514927 -0.3516700
2 C C 2.0913552 -1.6307273 -0.6296822
3 C C 3.0217535 -1.3504077 -1.6456936
4 C C 3.5803915 -2.4123048 -2.3661758
5 C C 3.2111198 -3.7300568 -2.0870168
6 C C 2.2941943 -4.0242379 -1.0730120
7 C C 1.9109266 -5.4507786 -0.7498414
8 H H 1.0224646 -3.1511828 0.4358281
9 H H 1.6356987 -0.8114467 -0.0718197
10 S S1 3.4234167 0.3366461 -2.0831915
11 H H 4.3068270 -2.2027417 -3.1466479
12 H H 3.6532444 -4.5424179 -2.6628594
```

13 H H 0.8240339 -5.5628317 -0.6474969
14 H H 2.2462344 -6.1425256 -1.5313915
15 H H 2.3559519 -5.7867259 0.1974753
16 C C 4.0631328 0.9824912 -0.3696078
17 O O 5.0795863 0.4754986 0.0653815
18 C C 3.3206159 2.0657507 0.1862886
19 C C 2.0367530 2.4373233 -0.1715217
20 H H 3.7935524 2.4993682 1.0645803
21 H H 1.6598373 2.0212053 -1.0987290
22 C C 1.4181472 3.7765964 0.2293537
23 C C 2.3834133 4.7131439 0.9733548
24 C C 0.1004148 3.6527091 1.0500587
25 H H 1.1493244 4.2714236 -0.7185926
26 H H -0.2727631 4.6776396 1.2035202
27 O O 0.3593406 3.1253664 2.3430880
28 C C -1.0157453 2.8285762 0.3708030
29 H H 2.6165624 4.3133586 1.9639359
30 H H 1.9162451 5.6965079 1.1159373
31 H H 3.3168189 4.8518597 0.4180476
32 C C -1.5875673 3.4698300 -0.8987469
33 H H -1.8227650 2.7976643 1.1156923
34 C C -0.4979819 1.3562572 0.1117234
35 H H 0.6208986 2.1938222 2.1023512
36 O O 0.7137938 1.1279748 0.7458776
37 H H -1.9698384 4.4820179 -0.7077834
38 H H -2.4184019 2.8678656 -1.2874834
39 H H -0.8360172 3.5400911 -1.6953309
40 C C -1.5516083 0.3382568 0.5509416
41 H H -0.3873672 1.2475037 -0.9897744
42 C C -1.6178975 0.0862850 2.0330661
43 C C -2.3058797 -0.2742389 -0.3868650
44 H H -0.7033839 -0.4372444 2.3374078
45 H H -2.4865643 -0.5050372 2.3212491
46 H H -1.6101434 1.0359418 2.5824148
47 H H -2.0902041 -0.0265744 -1.4268449
48 C C -3.3755353 -1.2535850 -0.2582375
49 C C -4.0460423 -1.8483210 -1.2899034
50 N N -3.9144589 -1.7594129 0.9370421
51 O O -4.9860693 -2.7123206 -0.7727012
52 H H -3.9876119 -1.7867419 -2.3647844
53 C C -4.8356255 -2.5949184 0.5758320
54 C C -5.7199064 -3.4216349 1.4436540
55 H H -5.4929327 -3.1998472 2.4880571
56 H H -5.5631119 -4.4925283 1.2659623
57 H H -6.7784714 -3.2066924 1.2544811
Electronic energy: -1647.13467 au

Cyclised 2,6-cis Thioester E-enolate (352)

Cartesian Coordinates (Angstroms)

Atom	X	Y	Z
1 C	C	0.3353579	3.7853384	-0.0703447
2 C	C1	0.0799336	3.1289269	1.3257630
3 C	C2	-0.6209021	1.7554777	1.1805749
4 O	O	1.2314794	3.0154797	2.1386829
5 H	H	-0.5951647	3.7974275	1.8821056
6 C	C3	-1.6796466	1.7947591	0.0576435
7 H	H1	0.1572515	1.0416489	0.8907041
8 C	C4	-1.2119732	1.3101207	2.5227044
9 O	O1	-1.1663317	2.2324137	-1.2018221
10 C	C5	-2.3392885	0.4471052	-0.1846316
11 H	H2	-2.4661882	2.5049073	0.3747425
12 C	C6	0.1933180	2.7975752	-1.2456681
13 C	C7	1.2359001	1.7488252	-1.5278401
14 H	H3	0.1177961	3.4134338	-2.1539260
15 H	H4	-0.5039256	4.4803348	-0.2263610
16 C	C8	1.6247504	4.6120164	-0.1304320
17 C	C9	-3.6568907	0.2920071	0.0578556
18 C	C10	-1.4534500	-0.6498636	-0.7187671
19 C	C11	2.2845660	1.3137198	-0.7591595
20 H	H5	1.1160682	1.2800304	-2.5000207
21 H	H6	-0.4546449	-0.2702642	-0.9488907
22 H	H7	-1.8674017	-1.0773351	-1.6423487
23 H	H8	-1.3557972	-1.4734658	0.0034824
24 H	H9	-4.2303382	1.1441295	0.4164066
25 C	C12	-4.4622505	-0.9074742	-0.1114916
26 H	H10	-1.5567792	0.2705966	2.4979453
27 H	H11	-2.0701062	1.9359175	2.8071830
28 H	H12	-0.4472358	1.4095890	3.2992033
29 H	H13	1.7028424	5.1189970	-1.1013472
30 H	H14	2.5070372	3.9833094	0.0044949
31 H	H15	1.6310567	5.3754798	0.6560890
32 H	H16	1.8629633	2.4696396	1.6036998
33 C	C13	-4.1589717	-2.1894674	-0.4813128
34 N	N	-5.8484921	-0.8532349	0.1258972
35 O	O2	-5.3196542	-2.9310261	-0.4820858
36 H	H17	-3.2606810	-2.7177906	-0.7474983
37 C	C14	-6.2863696	-2.0490182	-0.1051360
38 C	C15	-7.6838107	-2.5565639	-0.0132813
39 H	H18	-8.0277755	-2.9485211	-0.9778645
40 H	H19	-8.3367289	-1.7359636	0.2899333
41 H	H20	-7.7661191	-3.3672001	0.7207251
42 O	O3	2.6937511	1.5876837	0.4002640
43 S	S	3.3879927	0.1265403	-1.7941422
44 C	C16	3.7718995	-1.2502833	-0.7279752
45 C	C17	3.5297403	-1.2853360	0.6572043
46 H	H21	3.1003318	-0.4123986	1.1340515
47 C	C18	3.8604811	-2.4175105	1.3990788
48 H	H22	3.6596897	-2.4184798	2.4702435
49 C	C19	4.4501309	-3.5456939	0.8128002
50 C	C20	4.7790936	-4.7724138	1.6330953

51 C C21 4.7025887 -3.4966841 -0.5630037
52 H H23 5.1620133 -4.3543647 -1.0534561
53 C C22 4.3687796 -2.3759655 -1.3217203
54 H H24 4.5657752 -2.3712220 -2.3913655
55 H H25 3.8784660 -5.3500562 1.8873791
56 H H26 5.2636689 -4.5080409 2.5817368
57 H H27 5.4536127 -5.4463305 1.0918995
Electronic energy: -1647.16073 au

Cyclised 2,6-*trans* Thioester E-enolate (351)

Cartesian Coordinates (Angstroms)
Atom X Y Z
--------- ------------ ------------ ------------
1 C C -1.2748098 2.6335025 4.7876216
2 C C1 -1.6669106 1.7821831 3.7560171
3 C C2 -2.3331893 0.5751123 4.0412736
4 C C3 -2.5911596 0.2772463 5.3930822
5 C C4 -2.1841490 1.1344244 6.4128824
6 C C5 -1.5133761 2.3320683 6.1347579
7 C C6 -1.0453353 3.2495588 7.2413642
8 H H -0.7658130 3.5632766 4.5330504
9 H H1 -1.4976270 2.0576056 2.7226568
10 S S1 -2.8456044 -0.6109390 2.8235089
11 H H2 -3.1197540 -0.6404431 5.6410721
12 H H3 -2.3991658 0.8681116 7.4478353
13 H H4 -1.0926036 4.3028140 6.9379097
14 H H5 -1.6582877 3.1353247 8.1438738
15 H H6 -0.0034826 3.0487826 7.5333979
16 C C7 -2.6397562 0.2720171 1.0656156
17 O O -2.8179436 1.5011218 1.0250641
18 C C8 -2.3815834 -0.7037513 0.1335716
19 C C9 -2.3700572 -0.5332912 -1.3566546
20 H H7 -2.2567293 -1.7253601 0.4804040
21 H H8 -3.1680325 -1.1389592 -1.8146200
22 C C10 -2.4904930 0.9113400 -1.8869452
23 C C11 -2.8694671 0.9313843 -3.3749429
24 C C12 -1.1785607 1.6645387 -1.5873733
25 H H9 -3.2746841 1.4124777 -1.3071412
26 H H10 -1.0838360 1.7225703 -0.4971944
27 O O1 -1.2077753 3.0052474 -2.1177939
28 C C13 0.0590700 0.9539119 -2.1480112
29 H H11 -2.2092435 0.2838881 -3.9619784
30 H H12 -2.8042790 1.9473958 -3.7774257
31 H H13 -3.8965140 0.5696169 -3.5137450
32 C C14 1.3475606 1.6895174 -1.7581446
33 H H14 -0.0227719 0.9376807 -3.2433093
34 C C15 0.0364305 -0.5116346 -1.6331147
35 H H15 -1.8696078 3.4742793 -1.5851066
36 O O2 -1.1867235 -1.1515232 -1.9780356
37 H H16 1.2851674 2.7386275 -2.0600944

```
38 H H17 2.2297693 1.2374498 -2.2253962
39 H H18 1.4967968 1.6611081 -0.6701911
40 C C16 1.1607893 -1.3676717 -2.1941479
41 H H19 0.1244884 -0.4759021 -0.5356490
42 C C17 1.0651807 -1.7100478 -3.6572258
43 C C18 2.1426986 -1.7642638 -1.3586581
44 H H20 1.8814514 -2.3510688 -3.9879487
45 H H21 1.0674604 -0.7952407 -4.2658792
46 H H22 0.1028995 -2.2003736 -3.8434381
47 H H23 2.0499947 -1.4669287 -0.3146378
48 C C19 3.3436134 -2.5488246 -1.6110544
49 C C20 4.2572762 -2.9337950 -0.6712333
50 N N 3.7832739 -3.0406033 -2.8509240
51 O O3 5.2539900 -3.6521594 -1.2893414
52 H H24 4.3483865 -2.7979763 0.3946158
53 C C21 4.8881672 -3.6686028 -2.6017121
54 C C22 5.7788310 -4.3840280 -3.5569888
55 H H25 5.3569669 -4.3016165 -4.5603248
56 H H26 5.8714273 -5.4449240 -3.2954748
57 H H27 6.7876357 -3.9542553 -3.5577185

Electronic energy: -1647.15728 au
```

Oxoester alkoxide low energy pseudo-2,6-*trans* conformation (353)

```
Cartesian Coordinates (Angstroms)
Atom X Y Z
--------- ------------ ------------ ------------
1 C C -0.8795054 -3.1240729 -1.9512837
2 C C1 0.0750790 -2.6542240 -1.0513014
3 C C2 1.4236140 -2.8912059 -1.3309135
4 C C3 1.8218338 -3.5706104 -2.4795753
5 C C4 0.8427723 -4.0267157 -3.3657454
6 C C5 -0.5183967 -3.8180200 -3.1162721
7 C C6 -1.5759133 -4.3390839 -4.0640360
8 H H -1.9323464 -2.9370239 -1.7464945
9 H H1 -0.1908995 -2.0899834 -0.1493645
10 O O4 2.3281963 -2.4589251 -0.3685198
11 H H2 2.8764127 -3.7208773 -2.6779787
12 H H3 1.1479446 -4.5526096 -4.2691121
13 H H4 -2.0134829 -5.2826604 -3.7073696
14 H H5 -2.4011272 -3.6253605 -4.1729153
15 H H6 -1.1632947 -4.5294612 -5.0615241
16 C C7 3.2740831 -1.4970773 -0.6581556
17 O O 3.7824951 -1.3701915 -1.7549066
18 C C8 3.5551941 -0.6610150 0.5168651
19 C C9 2.7944175 -0.7042372 1.6259821
20 H H7 4.3571057 0.0612337 0.3791736
21 H H8 1.9726034 -1.4137500 1.6617396
22 C C10 2.9089381 0.1944684 2.8195834
23 C C11 3.7551312 -0.4996002 3.9098620
```

24 C C12 1.4972046 0.5250943 3.4215637
25 H H9 3.4173297 1.1279457 2.5361786
26 H H10 1.7158758 1.1505811 4.3086377
27 O O1 0.8600220 -0.6484393 3.8637919
28 C C13 0.5315038 1.3508737 2.5251207
29 H H11 3.2460220 -1.4068084 4.2464615
30 H H12 3.8750819 0.1632752 4.7772573
31 H H13 4.7512928 -0.7630555 3.5350289
32 C C14 1.1262416 2.7009993 2.1067906
33 H H14 -0.3223939 1.5485130 3.1913247
34 C C15 -0.0271571 0.5197229 1.2992303
35 H H15 0.3169143 -0.9179583 3.0256271
36 O O2 -0.2404840 -0.8035535 1.6048074
37 H H16 1.5295204 3.2489158 2.9710412
38 H H17 0.3685858 3.3345193 1.6320748
39 H H18 1.9421308 2.5759318 1.3832475
40 C C16 -1.3321583 1.1698976 0.8024036
41 H H19 0.7129317 0.6560155 0.4769167
42 C C17 -2.5549844 0.8460685 1.6211195
43 C C18 -1.3640424 1.9238087 -0.3173774
44 H H20 -2.2903577 0.0673596 2.3410316
45 H H21 -3.3704692 0.4609420 0.9927443
46 H H22 -2.9459862 1.7294797 2.1487469
47 H H23 -0.4398047 2.0749579 -0.8722070
48 C C19 -2.5127282 2.5791955 -0.9230480
49 C C20 -3.8250036 2.6955139 -0.5497553
50 N N -2.3627888 3.2708437 -2.1417475
51 O O3 -4.4937973 3.4337059 -1.5063349
52 H H24 -4.4146083 2.3659704 0.2871434
53 C C21 -3.5360672 3.7372015 -2.4246780
54 C C22 -3.9477569 4.5432444 -3.6082669
55 H H25 -4.7149566 4.0250613 -4.1966721
56 H H26 -3.0730256 4.7125035 -4.2392386
57 H H27 -4.3629416 5.5126766 -3.3067017
Electronic energy: -1324.18528 au

Oxoester alkoxide low energy pseudo-2,6-cis conformation (355)

Cartesian Coordinates (Angstroms)
Atom X Y Z
--------- ------------ ------------ ------------
1 C C -3.0842649 -3.7287287 -2.6561388
2 C C -1.8500195 -3.3167906 -3.1624205
3 C C -1.0320599 -2.5105083 -2.3763881
4 C C -1.4132884 -2.1104164 -1.0939719
5 C C -2.6510336 -2.5358398 -0.6122778
6 C C -3.5036537 -3.3471862 -1.3757572
7 C C -4.8287183 -3.8186585 -0.8186661
8 H H -3.7299544 -4.3564511 -3.2686959
9 H H -1.5200215 -3.6092805 -4.1540702
10 O O 0.1646394 -2.0027244 -2.8735526

```
11 H H -0.7349094 -1.4780279 -0.5053473
12 H H -2.9617027 -2.2246534 0.3838351
13 H H -5.2769190 -3.0654204 -0.1601446
14 H H -4.7163806 -4.7374505 -0.2254021
15 H H -5.5468334 -4.0363947 -1.6180755
16 C C 1.3027689 -2.7913604 -2.8098964
17 O O 1.2670221 -3.9981366 -2.9437158
18 C C 2.5064085 -1.9958589 -2.5561054
19 C C 2.4445998 -0.7208844 -2.1275517
20 H H 3.4333288 -2.5582176 -2.6024002
21 H H 1.4654227 -0.2641625 -2.0810690
22 C C 3.5917462 0.1275710 -1.6632618
23 C C 4.9663286 -0.4791189 -1.9725939
24 C C 3.4997770 0.4226178 -0.1104498
25 H H 3.5109009 1.0967668 -2.1822050
26 H H 4.4792541 0.8716059 0.1359987
27 O O 3.3816511 -0.7663449 0.6223730
28 C C 2.4280082 1.4576639 0.3433484
29 H H 5.1257501 -1.3738442 -1.3612075
30 H H 5.7624127 0.2362118 -1.7324664
31 H H 5.0660063 -0.7544237 -3.0297535
32 C C 2.7291948 2.8590147 -0.2092846
33 H H 2.5585599 1.4889762 1.4344338
34 C C 0.9554581 0.9259771 0.0989289
35 H H 2.3633097 -0.8810633 0.6141478
36 O O 0.8866260 -0.4177306 0.3202980
37 H H 3.8079228 3.0716632 -0.1775985
38 H H 2.2311968 3.6424580 0.3720185
39 H H 2.4041188 2.9689883 -1.2531120
40 C C -0.0558556 1.7386869 0.9487786
41 H H 0.7084474 1.2081164 -0.9628430
42 C C -0.6355890 2.9939649 0.3466962
43 C C -0.4162723 1.2081867 2.1341802
44 H H -1.3491848 2.7169053 -0.4450915
45 H H 0.1322958 3.6023253 -0.1442176
46 H H -1.1681026 3.6058042 1.0766741
47 H H 0.0307369 0.2350854 2.3372289
48 C C -1.3206897 1.6975607 3.1589314
49 C C -1.6308802 1.0624222 4.3293756
50 N N -2.0336368 2.9127618 3.1460004
51 O O -2.5144528 1.8439351 5.0450912
52 H H -1.3407908 0.1268042 4.7795206
53 C C -2.7000945 2.9370142 4.2558830
54 C C -3.6201981 3.9986835 4.7523357
55 H H -3.2653977 4.4257293 5.6985232
56 H H -4.6285233 3.6038521 4.9264805
57 H H -3.6744649 4.7923244 4.0046505
Electronic energy: -1324.17674 au
```

Oxoester alkoxide low energy linear conformation (354)

Cartesian Coordinates (Angstroms)

Atom	X	Y	Z
1 C	C	6.6584288	-0.1198872	1.6482371
2 C	C1	5.7095189	-0.5509636	0.7209649
3 C	C2	4.3753399	-0.6643581	1.1168502
4 C	C3	4.0022083	-0.3466836	2.4237726
5 C	C4	4.9642562	0.0857051	3.3335618
6 C	C5	6.3100712	0.2088819	2.9641146
7 C	C6	7.3455683	0.7073058	3.9463733
8 H	H	7.6975820	-0.0376729	1.3350839
9 H	H1	5.9999532	-0.8101620	-0.2888369
10 O	O4	3.3472968	-0.9987335	0.2546187
11 H	H2	2.9589152	-0.4437272	2.7078912
12 H	H3	4.6604703	0.3294289	4.3497679
13 H	H4	7.3792561	1.8053957	3.9767561
14 H	H5	7.1306627	0.3643753	4.9650588
15 H	H6	8.3498829	0.3594038	3.6803151
16 C	C7	3.4638359	-2.0546629	-0.6366210
17 O	O	4.4587180	-2.7479552	-0.7075183
18 C	C8	2.2657487	-2.2106407	-1.4636547
19 C	C9	1.1846596	-1.4125825	-1.4216321
20 H	H7	2.3195916	-3.0531487	-2.1478629
21 H	H8	1.1746434	-0.5862909	-0.7118765
22 C	C10	-0.0135530	-1.5147470	-2.3194151
23 C	C11	0.0753523	-0.4212768	-3.4055765
24 C	C12	-1.2924206	-1.3938524	-1.4495351
25 H	H9	-0.0055088	-2.4998362	-2.8032266
26 H	H10	-1.2581794	-0.3732949	-1.0078922
27 O	O1	-1.2146349	-2.3729297	-0.4456122
28 C	C13	-2.6403666	-1.4978495	-2.2081435
29 H	H11	0.0370765	0.5805525	-2.9587977
30 H	H12	-0.7616506	-0.5054592	-4.1060271
31 H	H13	1.0093967	-0.5015078	-3.9743319
32 C	C14	-2.8252220	-2.8607879	-2.8854963
33 H	H14	-2.6916592	-0.7075654	-2.9720512
34 C	C15	-3.8025696	-1.2925722	-1.1462261
35 H	H15	-2.2101053	-2.4035946	-0.1122367
36 O	O2	-3.6963540	-2.1718515	-0.1238166
37 H	H16	-2.0472677	-3.0727506	-3.6322470
38 H	H17	-3.7968082	-2.9032771	-3.3959224
39 H	H18	-2.8048947	-3.6446624	-2.1247779
40 C	C16	-3.8736542	0.1989692	-0.7207819
41 H	H19	-4.7513024	-1.4250462	-1.7446012
42 C	C17	-4.1006501	1.2246888	-1.8022581
43 C	C18	-3.7661611	0.4586341	0.5963561
44 H	H20	-4.7132463	0.7956984	-2.6077292
45 H	H21	-3.1510159	1.5366711	-2.2624834
46 H	H22	-4.5827920	2.1291958	-1.4255412
47 H	H23	-3.6306466	-0.4397971	1.2008370
48 C	C19	-3.8157020	1.7178421	1.3148296
49 C	C20	-3.7150780	1.8847074	2.6683772
50 N	N	-3.9706266	3.0005384	0.7502851

```
51 O O3 -3.8016152 3.2302653 2.9645414
52 H H24 -3.5858424 1.2149284 3.5030947
53 C C21 -3.9549070 3.8240149 1.7493937
54 C C22 -4.0774477 5.3089904 1.7193915
55 H H25 -4.9464330 5.6513861 2.2948721
56 H H26 -4.1907570 5.6303602 0.6821337
57 H H27 -3.1893610 5.7921877 2.1452514
Electronic energy: -1324.17710 au
```

Oxoester alkoxide cyclization transition state leading to 2,6-*trans* (356)

```
Cartesian Coordinates (Angstroms)
Atom X Y Z
--------- ------------ ------------ ------------
1 C C -3.1277299 -4.7463811 -0.0207559
2 C C1 -3.6276134 -3.4941190 0.3415946
3 C C2 -2.9183494 -2.3429290 -0.0025452
4 C C3 -1.7025808 -2.4454108 -0.6876834
5 C C4 -1.2199810 -3.7030788 -1.0432525
6 C C5 -1.9235156 -4.8742907 -0.7235579
7 C C6 -1.4034843 -6.2319809 -1.1411989
8 H H -3.6828342 -5.6422218 0.2556816
9 H H1 -4.5535241 -3.3942991 0.8984962
10 O O -3.4087096 -1.0899908 0.2770702
11 H H2 -1.1577579 -1.5279447 -0.9027644
12 H H3 -0.2725840 -3.7773038 -1.5754005
13 H H4 -1.8050405 -7.0279280 -0.5024585
14 H H5 -1.6805812 -6.4776031 -2.1773648
15 H H6 -0.3088282 -6.2780355 -1.0845176
16 C C7 -3.0545143 -0.5277958 1.5491371
17 O O1 -3.1286579 -1.2235655 2.5502297
18 C C8 -2.6791086 0.8411310 1.4366227
19 C C9 -2.4645036 1.5056908 0.2345415
20 H H7 -2.4304854 1.3213439 2.3798585
21 H H8 -2.9264663 1.0956782 -0.6557061
22 C C10 -2.3175385 3.0225764 0.2576718
23 C C11 -3.6583023 3.6620130 -0.1484632
24 C C12 -1.1740125 3.5567626 -0.6425993
25 H H9 -2.0979758 3.3257756 1.2922308
26 H H10 -1.2419534 4.6559725 -0.6581574
27 O O2 -1.3430255 3.1246804 -1.9879789
28 C C13 0.2347973 3.1540984 -0.1393267
29 H H11 -3.8514709 3.4748180 -1.2101028
30 H H12 -3.6391023 4.7496227 0.0052363
31 H H13 -4.4841610 3.2450538 0.4386556
32 C C14 0.7161703 3.9610561 1.0726333
33 H H14 0.9056849 3.3811062 -0.9795624
34 C C15 0.2412625 1.6021773 0.1233158
35 H H15 -1.1466848 2.1563903 -1.8799545
36 O O3 -0.7456675 0.9794649 -0.6276116
37 H H16 0.7507916 5.0371201 0.8524000
```

38 H H17 1.7250789 3.6495999 1.3704434
39 H H18 0.0613950 3.8200332 1.9422302
40 C C16 1.6132281 0.9923784 -0.1608379
41 H H19 0.0416509 1.4611222 1.2063680
42 C C17 1.9296898 0.7711259 -1.6150490
43 C C18 2.4108998 0.6563828 0.8755112
44 H H20 1.1986343 0.0623269 -2.0216512
45 H H21 2.9397918 0.3948557 -1.7740027
46 H H22 1.7941250 1.6993985 -2.1864689
47 H H23 2.0071625 0.8177739 1.8755310
48 C C19 3.7453590 0.0747563 0.9006716
49 C C20 4.4440696 -0.2812428 2.0199968
50 N N 4.5558067 -0.2199716 -0.2090123
51 O O4 5.6663479 -0.7908249 1.6401298
52 H H24 4.2413291 -0.2523817 3.0786216
53 C C21 5.6466069 -0.7171731 0.2804512
54 C C22 6.8469444 -1.2032634 -0.4551896
55 H H25 6.6724061 -1.0865480 -1.5265327
56 H H26 7.0444753 -2.2603296 -0.2396992
57 H H27 7.7430370 -0.6356725 -0.1759244
Electronic energy: -1324.17657 au

Oxoester alkoxide cyclization transition state leading to 2,6-*cis* (357)

Cartesian Coordinates (Angstroms)
Atom X Y Z
--------- ------------ ------------ ------------
1 C C1 5.3852154 -3.0509749 0.1277449
2 C C2 4.4344973 -2.0331337 0.0985727
3 C C3 4.8417084 -0.7032586 0.2903075
4 C C4 6.1965580 -0.4300857 0.5119311
5 C C5 7.1305893 -1.4644696 0.5449429
6 C C6 6.7458250 -2.7958624 0.3514818
7 C C7 7.7534375 -3.9227602 0.3966698
8 H H8 5.0546194 -4.0774802 -0.0258618
9 H H9 3.3916316 -2.2509443 -0.0856879
10 O O10 3.9950881 0.3670117 0.3621237
11 H H11 6.4970060 0.6031204 0.6606972
12 H H12 8.1791108 -1.2296391 0.7225600
13 H H13 7.6597916 -4.5853420 -0.4733142
14 H H14 8.7795535 -3.5380187 0.4118889
15 H H15 7.6262714 -4.5504065 1.2900372
16 C C16 2.7989384 0.4424383 -0.4173510
17 O O17 2.5488930 -0.4021438 -1.2610189
18 C C18 2.0841155 1.6292518 -0.0616217
19 C C19 0.8508445 1.8911165 -0.6109120
20 H H20 2.5181761 2.2588678 0.7052587
21 H H21 0.5545491 1.2524341 -1.4365221
22 C C22 0.1851853 3.2659057 -0.5560502
23 C C23 1.1414315 4.3844864 -0.1076546
24 C C24 -1.0952801 3.3229895 0.3350325

25 H H25 -0.1276285 3.4951697 -1.5874753
26 H H26 -1.4282741 4.3737154 0.3402499
27 O O27 -0.7807312 2.9846591 1.6737922
28 C C28 -2.2694809 2.4492921 -0.1609912
29 H H29 1.3583038 4.2865245 0.9600748
30 H H30 0.6742957 5.3659159 -0.2638221
31 H H31 2.0843073 4.3577758 -0.6634951
32 C C32 -2.9297570 2.9569399 -1.4472396
33 H H33 -3.0145756 2.5150148 0.6445980
34 C C34 -1.7767415 0.9529084 -0.2831525
35 H H35 -0.6040357 2.0034773 1.5545933
36 O O36 -0.6257965 0.7410977 0.4408339
37 H H37 -3.2952001 3.9878607 -1.3399496
38 H H38 -3.7866428 2.3260304 -1.7148568
39 H H39 -2.2335757 2.9367686 -2.2962114
40 C C40 -2.8922015 -0.0121413 0.1368965
41 H H41 -1.6042262 0.7772083 -1.3725037
42 C C42 -3.0308304 -0.2076980 1.6214536
43 C C43 -3.6220458 -0.6389009 -0.8115645
44 H H44 -2.0872103 -0.6224450 1.9941729
45 H H45 -3.8618727 -0.8602108 1.8874770
46 H H46 -3.1484106 0.7607588 2.1260833
47 H H47 -3.3510792 -0.4375754 -1.8491443
48 C C48 -4.7270957 -1.5804556 -0.6994895
49 C C49 -5.3684523 -2.1927859 -1.7399176
50 N N50 -5.3369451 -2.0271331 0.4859721
51 O O51 -6.3583717 -3.0102217 -1.2375963
52 H H52 -5.2604329 -2.1713104 -2.8125098
53 C C53 -6.2657487 -2.8479045 0.1111923
54 C C54 -7.2153636 -3.6144781 0.9654153
55 H H55 -7.0198015 -3.3720744 2.0116239
56 H H56 -7.0955332 -4.6953576 0.8227007
57 H H57 -8.2566021 -3.3635273 0.7295351
Electronic energy: -1324.17217 au

Cyclised 2,6-*cis* Oxoester *E*-enolate (359)

Cartesian Coordinates (Angstroms)
Atom X Y Z
--------- ------------ ------------ ------------
1 C C -0.4022654 -2.9959084 1.7039026
2 C C1 -0.9203449 -3.1762086 0.2419606
3 C C2 -1.6614282 -1.9056937 -0.2488099
4 O O 0.0732124 -3.5632103 -0.6861374
5 H H -1.6413385 -4.0091805 0.2502891
6 C C3 -2.5125997 -1.2890347 0.8844521
7 H H1 -0.8907655 -1.1711047 -0.5067417
8 C C4 -2.4537700 -2.2258965 -1.5204045
9 O O1 -1.7520672 -0.9900749 2.0499272
10 C C5 -3.2461264 -0.0199602 0.4363100
11 H H2 -3.2886849 -2.0331384 1.1579461

12 C C6 -0.3762687 -1.5264200 2.1707083
13 C C7 0.6730878 -0.5699982 1.6972659
14 H H3 -0.2886607 -1.5616314 3.2661785
15 H H4 -1.1701906 -3.4526811 2.3467242
16 C C8 0.9148536 -3.7306640 1.9752766
17 C C9 -2.5521849 1.1339258 0.4090270
18 C C10 -4.7014879 -0.1818858 0.0818090
19 C C11 1.4741618 -0.6071529 0.5844935
20 H H5 0.7913921 0.3063177 2.3280783
21 H H6 -4.8380183 -0.9655899 -0.6751274
22 H H7 -5.1436211 0.7449413 -0.2843700
23 H H8 -5.2640887 -0.5129173 0.9681140
24 H H9 -1.5169561 1.0743156 0.7422719
25 C C12 -2.9567888 2.4701460 0.0040870
26 H H10 -2.8334399 -1.3229801 -2.0114686
27 H H11 -3.3071339 -2.8869931 -1.3096529
28 H H12 -1.7915441 -2.7480289 -2.2176246
29 H H13 1.1944638 -3.6302269 3.0323860
30 H H14 1.7238236 -3.3268023 1.3636509
31 H H15 0.8196928 -4.7986362 1.7454544
32 H H16 0.7346469 -2.8223209 -0.6655672
33 C C13 -2.1481846 3.5710621 -0.0188860
34 N N -4.2287847 2.8730351 -0.4405639
35 O O2 -2.8778751 4.6484265 -0.4671513
36 H H17 -1.1118028 3.7487461 0.2197127
37 C C14 -4.1191942 4.1378087 -0.6971095
38 C C15 -5.1641169 5.0706796 -1.2039510
39 H H18 -5.3232061 5.9052937 -0.5106474
40 H H19 -6.1003281 4.5212219 -1.3195244
41 H H20 -4.8800580 5.4968279 -2.1738239
42 O O3 1.6398674 -1.4266369 -0.3560169
43 O O4 2.2705119 0.6186569 0.5167403
44 C C16 3.4985085 0.6534143 -0.0462427
45 C C17 4.0111026 1.9356433 -0.3116623
46 H H21 3.3788227 2.7926565 -0.0960211
47 C C18 5.2964348 2.1019969 -0.8185887
48 H H22 5.6667621 3.1098600 -1.0051201
49 C C19 6.1200515 1.0024072 -1.0930733
50 C C20 7.5029160 1.1806787 -1.6780370
51 C C21 5.5976117 -0.2701635 -0.8277254
52 H H23 6.2132618 -1.1474686 -1.0258426
53 C C22 4.3158021 -0.4605787 -0.3141947
54 H H24 3.9290324 -1.4549438 -0.1394450
55 H H25 8.1941236 0.4068100 -1.3214621
56 H H26 7.9283724 2.1552558 -1.4088380
57 H H27 7.5008093 1.1240040 -2.7769349
Electronic energy: -1324.18793 au

Cyclised 2,6-*trans* Oxoester *E*-enolate (358)

Cartesian Coordinates (Angstroms)

Atom	X	Y	Z
1 C	C	-3.2039493	-2.4341800	3.7302978
2 C	C1	-2.7477835	-2.1916973	2.4359617
3 C	C2	-2.2466500	-3.2536588	1.6573122
4 C	C3	-2.2273147	-4.5406104	2.2284427
5 C	C4	-2.6824474	-4.7582304	3.5256119
6 C	C5	-3.1871595	-3.7108431	4.3075537
7 C	C6	-3.7212498	-3.9522297	5.7013200
8 H	H	-3.5852315	-1.5950056	4.3125840
9 H	H1	-2.7943772	-1.2006215	2.0068644
10 O	O	-1.7122766	-3.1425466	0.4260151
11 H	H2	-1.8329340	-5.3572181	1.6295605
12 H	H3	-2.6440997	-5.7660903	3.9392343
13 H	H4	-3.6046556	-3.0639879	6.3346056
14 H	H5	-4.7927715	-4.2040172	5.7002737
15 H	H6	-3.2005549	-4.7821633	6.1957604
16 C	C7	-1.9702839	-1.9569511	-0.4329514
17 O	O1	-3.0542778	-1.3636794	-0.2678741
18 C	C8	-0.9080676	-1.7990138	-1.2958087
19 C	C9	-0.8132712	-0.8329981	-2.4290905
20 H	H7	-0.0979055	-2.5182126	-1.2222229
21 H	H8	-0.6770546	-1.3679103	-3.3826503
22 C	C10	-1.9807758	0.1634642	-2.5934233
23 C	C11	-1.9857637	0.7965694	-3.9924634
24 C	C12	-1.9158390	1.2060138	-1.4593001
25 H	H9	-2.9137766	-0.3927042	-2.4427298
26 H	H10	-2.0784331	0.6639170	-0.5214750
27 O	O2	-2.9546994	2.1992455	-1.5969176
28 C	C13	-0.5661550	1.9286853	-1.3770615
29 H	H11	-0.9991246	1.1969073	-4.2505080
30 H	H12	-2.7150164	1.6117217	-4.0458226
31 H	H13	-2.2477370	0.0484731	-4.7521881
32 C	C14	-0.5218750	2.8869995	-0.1798942
33 H	H14	-0.4230549	2.5087031	-2.2993199
34 C	C15	0.5392290	0.8393563	-1.3034115
35 H	H15	-3.7808450	1.7222442	-1.4191778
36 O	O3	0.4447971	-0.0468828	-2.4091890
37 H	H16	-1.3693412	3.5770281	-0.2187467
38 H	H17	0.4078320	3.4672501	-0.1597757
39 H	H18	-0.5856757	2.3303987	0.7649342
40 C	C16	1.9537948	1.3985064	-1.3017431
41 H	H19	0.3758035	0.2698698	-0.3743685
42 C	C17	2.4205101	2.0235950	-2.5894644
43 C	C18	2.6893978	1.2796673	-0.1773668
44 H	H20	2.2660884	1.3067194	-3.4034261
45 H	H21	3.4658538	2.3275030	-2.5485741
46 H	H22	1.8093291	2.9041888	-2.8326578
47 H	H23	2.2203168	0.7699767	0.6636172
48 C	C19	4.0477554	1.7137042	0.1193641
49 C	C20	4.7114270	1.5111860	1.2962850
50 N	N	4.9170711	2.4076691	-0.7385408

51 O O4 5.9704342 2.0568582 1.1963669
52 H H24 4.4639893 1.0342981 2.2311694
53 C C21 6.0093466 2.5748890 -0.0631118
54 C C22 7.2662396 3.2468365 -0.4947649
55 H H25 7.1394890 3.6042714 -1.5183251
56 H H26 8.1174542 2.5562395 -0.4618754
57 H H27 7.5062698 4.0984965 0.1530861
Electronic energy: -1324.18633 au

Low energy protonated thioester conformation (365)

Cartesian Coordinates (Angstroms)
Atom X Y Z
--------- ------------ ------------ ------------
1 C C 3.9104401 2.4137723 -0.6654332
2 C C1 2.7408963 1.7989680 -1.1033078
3 C C2 1.7151846 2.5978099 -1.6230030
4 C C3 1.8568759 3.9838425 -1.7217987
5 C C4 3.0408720 4.5748172 -1.2840946
6 C C5 4.0837958 3.8045896 -0.7518549
7 C C6 5.3734127 4.4478873 -0.3060722
8 H H 4.7075855 1.8010261 -0.2520105
9 H H1 2.6227322 0.7203798 -1.0386605
10 S S 0.2277383 1.8236775 -2.2596181
11 H H2 1.0571143 4.5940635 -2.1301228
12 H H3 3.1534215 5.6531114 -1.3562862
13 H H4 5.7687712 3.9699469 0.5962721
14 H H5 6.1421990 4.3567885 -1.0842535
15 H H6 5.2406797 5.5137181 -0.0990651
16 C C7 -0.6557409 1.3893368 -0.8495548
17 O O -0.2657323 1.7988773 0.3128065
18 C C8 -1.7977157 0.5072372 -0.9752962
19 C C9 -2.7581985 0.5361869 -0.0292975
20 H H7 -1.7822567 -0.2266572 -1.7752237
21 H H8 -2.7862276 1.3793153 0.6545013
22 C C10 -3.7892977 -0.5074017 0.2416400
23 C C11 -5.2020128 0.0014129 -0.1234396
24 C C12 -3.7296641 -0.8813303 1.7561881
25 H H9 -3.5737313 -1.4095921 -0.3431352
26 H H10 -4.6309649 -1.4776431 1.9490584
27 O O1 -3.8334262 0.3646166 2.4919542
28 C C13 -2.5486065 -1.7136187 2.3383928
29 H H11 -5.9473639 -0.7758819 0.0760461
30 H H12 -5.2591391 0.2605662 -1.1845826
31 H H13 -5.4584912 0.8871856 0.4644227
32 C C14 -2.6478187 -3.2075754 1.9754474
33 H H14 -2.7838495 -1.6740182 3.4121346
34 C C15 -1.0939671 -1.1168954 2.2998043
35 H H15 -4.3914036 0.2295866 3.2731454
36 O O2 -1.1385665 0.3533679 2.3221421
37 H H16 -3.5485340 -3.6394075 2.4246812

38 H H17 -1.7879329 -3.7628475 2.3612335
39 H H18 -2.7014648 -3.3917776 0.8998264
40 C C16 -0.0358340 -1.4874416 1.2681370
41 H H19 -0.6595373 -1.4080551 3.2655291
42 C C17 1.3583155 -1.1303799 1.7311362
43 C C18 -0.3208486 -2.0640751 0.0842954
44 H H20 1.5826966 -1.6534048 2.6707983
45 H H21 1.4435111 -0.0578026 1.9469779
46 H H22 2.1134274 -1.3935991 0.9926163
47 H H23 -1.3531649 -2.3264727 -0.1201513
48 C C19 0.5692881 -2.4126842 -1.0173992
49 C C20 0.2762034 -3.2629237 -2.0453471
50 N N 1.8575474 -1.9044861 -1.2355600
51 O O3 1.3493292 -3.3093410 -2.8855123
52 H H24 -0.5670798 -3.8855786 -2.3010122
53 C C21 2.2664190 -2.4645814 -2.3341505
54 C C22 3.5641486 -2.3003410 -3.0409730
55 H H25 4.0826620 -3.2612487 -3.1285860
56 H H26 4.1944200 -1.6072576 -2.4817312
57 H H27 3.4129044 -1.9119913 -4.0541778
58 H H28 -2.0040723 0.6192452 2.7030977
59 H H29 -0.6599478 1.2449781 1.0884265
Electronic energy: -1648.07179 au

Trifluoroacetate mediated cyclisation transition state leading to 2,6-*cis* (368)

Cartesian Coordinates (Angstroms)
Atom X Y Z
--------- ------------- ------------- -------------
1 C C1 -0.2419325 -3.6490605 0.1632554
2 C C2 -1.5259790 -3.5770717 1.0223577
3 C C3 -2.5956128 -2.6021826 0.5158013
4 O O4 -2.1362524 -4.8751766 1.1217606
5 H H5 -1.2276485 -3.2478455 2.0351284
6 C C6 -1.9808581 -1.1856889 0.4146314
7 H H7 -2.8909829 -2.9238782 -0.4901217
8 C C8 -3.8325335 -2.6219903 1.4250506
9 O O9 -0.8373647 -1.2086505 -0.4112979
10 C C10 -2.9500087 -0.1428680 -0.1365894
11 H H11 -1.7163197 -0.8817411 1.4429528
12 C C12 0.5444295 -2.3502253 0.2142101
13 C C13 1.6992882 -2.1797713 -0.5517895
14 H H14 0.3991353 -4.3956740 0.6707892
15 C C15 -0.5029624 -4.1534560 -1.2631177
16 C C16 -3.1724292 0.9701564 0.5908795
17 C C17 -3.4945720 -0.4019539 -1.5165978
18 C C18 2.6489524 -1.1834362 -0.2118477
19 H H19 -2.6597574 -0.6447707 -2.1839669
20 H H20 -4.0453126 0.4528789 -1.9083282
21 H H21 -4.1704534 -1.2689360 -1.5197792
22 H H22 -2.6450443 1.0584327 1.5384923

23 C C23 -3.9688642 2.1499656 0.2802206
24 H H24 -4.6109517 -1.9519446 1.0449506
25 H H25 -3.5769791 -2.2837651 2.4387577
26 H H26 -4.2419586 -3.6327466 1.5019098
27 H H27 0.4287335 -4.4706032 -1.7426167
28 H H28 -1.1854784 -5.0097160 -1.2429729
29 H H29 -0.9424471 -3.3580211 -1.8693795
30 H H30 -1.4303300 -5.4930769 1.3697734
31 C C31 -3.8782654 3.3592318 0.9068156
32 N N32 -4.9697119 2.2523171 -0.6992632
33 O O33 -4.7937407 4.2167207 0.3446202
34 H H34 -3.2446302 3.7598083 1.6814699
35 C C35 -5.4066700 3.4691451 -0.6158255
36 C C36 -6.4737984 4.1235483 -1.4223633
37 H H37 -6.0827327 4.9907484 -1.9676222
38 H H38 -7.2951772 4.4753400 -0.7864281
39 H H39 -6.8649064 3.4002066 -2.1402974
40 O O40 2.6387307 -0.3652779 0.6971754
41 S S41 4.1352991 -1.2560266 -1.3999709
42 C C42 5.1855399 0.0442963 -0.7820626
43 C C43 4.7174171 1.3529508 -0.5831378
44 H H44 3.6795027 1.5994987 -0.7722961
45 C C45 5.5914665 2.3447091 -0.1445396
46 H H46 5.2055779 3.3510344 0.0082696
47 C C47 6.9484402 2.0798200 0.0901612
48 C C48 7.8774655 3.1689928 0.5765319
49 C C49 7.4069723 0.7757573 -0.1238441
50 H H50 8.4561895 0.5395946 0.0492394
51 C C51 6.5371291 -0.2329807 -0.5407519
52 H H52 6.9052592 -1.2459098 -0.6809089
53 H H53 7.7438068 4.0972716 0.0069167
54 H H54 8.9278602 2.8692439 0.4867724
55 H H55 7.6953619 3.4145854 1.6321236
56 H H56 0.5746417 -1.8758221 1.1937927
57 C C57 0.7877960 1.8431334 -0.2960011
58 O O58 1.4738302 2.7640758 -0.7041805
59 C C59 0.4740806 1.8500254 1.2259192
60 F F60 1.5256611 2.2576916 1.9438543
61 F F61 -0.5393620 2.7388812 1.4567990
62 F F62 0.0618693 0.6673067 1.7285205
63 O O63 0.2245178 0.9375103 -1.0355193
64 H H64 1.8633211 -2.7510311 -1.4595889
65 H H65 -0.2262475 0.0464201 -0.6168962
Electronic energy: -2173.96125 au

Low energy thio-ester - trifluoroacetate - hydroxonium ion complex conformation

Cartesian Coordinates (Angstroms)
Atom X Y Z
--------- ------------- ------------- -------------
1 C C -1.9558261 -2.7832086 -1.6307502
2 C C1 -1.3869749 -1.6777133 -2.5624201
3 C C2 -1.4010450 -0.1959039 -2.0663351

4 O O -0.0940840 -2.0984334 -3.0184050
5 H H -2.0536406 -1.6825656 -3.4388830
6 C C3 -0.8109057 0.1553355 -0.6677948
7 H H1 -0.7984428 0.3361985 -2.8133227
8 C C4 -2.8281219 0.3766065 -2.1597340
9 O O1 0.4316438 -0.5370043 -0.4363458
10 C C5 -0.6135431 1.6665403 -0.4952194
11 H H2 -1.5274235 -0.1824593 0.0897030
12 C C6 -1.1718493 -2.8931629 -0.3581053
13 H H3 -2.9858118 -2.4927818 -1.3829905
14 C C7 -1.9998235 -4.1363740 -2.3726366
15 C C8 0.2893327 2.2813618 -1.2833883
16 C C9 -1.4265053 2.3226206 0.5896622
17 C C10 -0.8100544 -2.7175135 2.0506056
18 H H4 -1.1639909 1.8956548 1.5691968
19 H H5 -2.4993465 2.1288727 0.4484810
20 H H6 -1.2634232 3.3994154 0.6294660
21 H H7 0.8248453 1.6605775 -2.0008546
22 C C11 0.7034958 3.6734326 -1.3430664
23 H H8 -3.2498916 0.2104547 -3.1570066
24 H H9 -2.8280819 1.4547348 -1.9745946
25 H H10 -3.5030188 -0.0870869 -1.4291565
26 H H11 -2.4656376 -4.9039185 -1.7460960
27 H H12 -2.5839790 -4.0465450 -3.2958389
28 H H13 -0.9928537 -4.4652020 -2.6408295
29 H H14 0.1215722 -1.5703959 -3.8164846
30 C C12 1.5995234 4.1966931 -2.2309651
31 N N 0.2545074 4.7140425 -0.5188881
32 O O2 1.7208816 5.5370270 -1.9828288
33 H H15 2.1752816 3.7925890 -3.0480890
34 C C13 0.8784704 5.7710959 -0.9349855
35 C C14 0.7874314 7.1651180 -0.4228376
36 H H16 0.4380257 7.8497643 -1.2042043
37 H H17 1.7649262 7.5238526 -0.0809700
38 H H18 0.0860442 7.1907212 0.4128386
39 O O3 0.2949717 -2.1949633 1.9956606
40 S S -1.5387428 -3.3347391 3.5829404
41 C C15 -0.3844703 -2.7592068 4.8260703
42 C C16 0.9518670 -3.1745487 4.8326415
43 H H19 1.3191549 -3.8343080 4.0542347
44 C C17 1.8102999 -2.7220075 5.8314151
45 H H20 2.8505303 -3.0394220 5.8201741
46 C C18 1.3590305 -1.8704510 6.8501678
47 C C19 2.2916367 -1.4137995 7.9470600
48 C C20 0.0165593 -1.4733812 6.8326358
49 H H21 -0.3555738 -0.8076691 7.6078418
50 C C21 -0.8510854 -1.9050748 5.8298974
51 H H22 -1.8854056 -1.5740870 5.8228925
52 H H23 1.9306394 -0.4962972 8.4226583
53 H H24 3.2994647 -1.2234789 7.5626273
54 H H25 2.3828592 -2.1762773 8.7321178
55 H H26 -0.0930907 -2.9417853 -0.4653906
56 C C22 1.6705783 0.5221269 -4.9004655
57 O O4 0.7576366 -0.2814262 -5.0160915
58 C C23 1.8390461 1.6661290 -5.9277066
59 F F 3.0634522 1.6366146 -6.4776692

60 F F1 0.9283383 1.5802161 -6.8997344
61 F F2 1.6857559 2.8604483 -5.3113609
62 O O5 2.5865468 0.5891224 -3.9768546
63 H H27 -2.7693077 -2.8901080 1.0497694
64 H H28 0.4510747 -0.8922989 0.4745222
65 O O6 2.3641011 -1.1701926 -2.1780584
66 H H29 1.9628826 -0.7148409 -1.4040222
67 H H30 2.4891464 -0.1728971 -3.2499729
68 H H31 1.6049599 -1.7487342 -2.4234399
69 C C24 -1.6945626 -2.8751036 0.8795132
Electronic energy: -2250.95162 au

Trifluoroacetate - hydroxonium ion mediated cyclisation chair-like transition state leading to 2,6-*cis* (373)

Cartesian Coordinates (Angstroms)
Atom X Y Z
--------- ------------ ------------ ------------
1 C C1 -0.3898949 -3.7157947 0.1830425
2 C C2 -1.6635212 -3.6276082 1.0642806
3 C C3 -2.7547502 -2.6839770 0.5317819
4 O O4 -2.2589913 -4.9183507 1.1937756
5 H H5 -1.3574925 -3.2621437 2.0614413
6 C C6 -2.2240728 -1.2468900 0.4308661
7 H H7 -3.0321347 -3.0261208 -0.4716528
8 C C8 -4.0007583 -2.7233925 1.4291564
9 O O9 -0.9993713 -1.2764073 -0.3646294
10 C C10 -3.1718342 -0.2551667 -0.2174165
11 H H11 -1.9685502 -0.8966327 1.4371839
12 C C12 0.3992842 -2.4262683 0.2045720
13 C C13 1.4585237 -2.1926274 -0.6936674
14 H H14 0.2727031 -4.4328407 0.7015110
15 C C15 -0.6629354 -4.2681490 -1.2228266
16 C C16 -3.3858539 0.9075167 0.4310660
17 C C17 -3.7311820 -0.6255195 -1.5667876
18 C C18 2.4796897 -1.2929632 -0.4223738
19 H H19 -2.9241235 -0.9761028 -2.2211262
20 H H20 -4.2351838 0.2195128 -2.0339151
21 H H21 -4.4594828 -1.4441514 -1.4857988
22 H H22 -2.8681940 1.0574843 1.3756875
23 C C23 -4.1852188 2.0594174 0.0467909
24 H H24 -4.7814813 -2.0612959 1.0432556
25 H H25 -3.7605519 -2.3922459 2.4480822
26 H H26 -4.3947397 -3.7394968 1.4893699
27 H H27 0.2630044 -4.5962975 -1.7055895
28 H H28 -1.3310041 -5.1307165 -1.1539748
29 H H29 -1.1291774 -3.5131438 -1.8612715
30 H H30 -1.6212226 -5.4987421 1.6379730
31 C C31 -4.1842081 3.2700417 0.6785414
32 N N32 -5.0823297 2.1348441 -1.0262166

33 O O33 -5.0532259 4.1005996 0.0267399
34 H H34 -3.6523655 3.6806969 1.5221454
35 C C35 -5.5554087 3.3406535 -0.9912335
36 C C36 -6.5475898 3.9763953 -1.8994283
37 H H37 -6.1023833 4.8191460 -2.4406884
38 H H38 -7.4068665 4.3591546 -1.3378200
39 H H39 -6.8935389 3.2348414 -2.6214963
40 O O40 2.6048209 -0.7655898 0.7686170
41 S S41 3.6085478 -0.9987081 -1.7619548
42 C C42 4.7653905 0.2295458 -1.1639038
43 C C43 4.4926068 1.5900060 -1.3591113
44 H H44 3.5336851 1.9036523 -1.7568128
45 C C45 5.4427044 2.5369678 -0.9864751
46 H H46 5.2213118 3.5918483 -1.1281267
47 C C47 6.6695839 2.1573383 -0.4247594
48 C C48 7.6719129 3.2008219 0.0064935
49 C C49 6.9283357 0.7919053 -0.2495495
50 H H50 7.8767955 0.4762801 0.1784093
51 C C51 5.9898714 -0.1699737 -0.6170644
52 H H52 6.2062492 -1.2262346 -0.4865227
53 H H53 7.7336965 4.0204019 -0.7177513
54 H H54 8.6727937 2.7741001 0.1254202
55 H H55 7.3836652 3.6410464 0.9700952
56 H H56 0.5110429 -1.9697631 1.1855511
57 C C57 0.7980981 1.7044439 0.3808683
58 O O58 1.7692770 2.4695593 0.2190007
59 C C59 0.2559113 1.6103398 1.8469364
60 F F60 1.1572644 2.0054312 2.7769375
61 F F61 -0.8411773 2.3856451 2.0119780
62 F F62 -0.1060810 0.3421914 2.1850629
63 O O63 0.1700202 1.0270798 -0.4652167
64 H H64 1.4406652 -2.6507915 -1.6753307
65 H H65 -0.5717482 -0.3444779 -0.3557021
66 O O 3.7527748 1.3611348 1.6517784
67 H H 3.3709835 1.3470903 2.5441551
68 H H1 3.2305832 0.0288776 0.9309158
69 H H2 3.1568487 1.9925721 1.1667117
Electronic energy: -2250.90998 au

Trifluoroacetate - hydroxonium ion mediated cyclisation chair-like transition state leading to 2,6-*trans* (374)

Cartesian Coordinates (Angstroms)
Atom X Y Z
--------- ------------ ------------ ------------
1 C C1 -0.9480372 -2.7029609 -2.7194613
2 C C2 -2.4093485 -2.3084311 -2.3964785
3 C C3 -2.6539350 -0.7937895 -2.4308938
4 O O4 -3.2970778 -2.8950790 -3.3466637
5 H H5 -2.6586697 -2.6707852 -1.3849093

```
6 C C6 -1.7743054 -0.0658345 -1.4041004
7 H H7 -2.3987796 -0.4396571 -3.4357390
8 C C8 -4.1316096 -0.4670163 -2.1643703
9 O O9 -0.3596173 -0.4752903 -1.5531852
10 C C10 -1.8059270 1.4457619 -1.5183872
11 H H11 -2.0773200 -0.3698676 -0.3954598
12 C C12 0.0254877 -2.2518654 -1.6452969
13 C C13 0.0034397 -2.8419049 -0.3530223
14 H H14 -0.9150453 -3.8036009 -2.6799682
15 C C15 -0.4981715 -2.2729738 -4.1231851
16 C C16 -2.0276743 2.1558545 -0.3925793
17 C C17 -1.5385414 2.0313309 -2.8824178
18 C C18 1.1102906 -2.8528101 0.4749316
19 H H19 -2.3877776 1.8749854 -3.5617379
20 H H20 -0.6680655 1.5449039 -3.3401899
21 H H21 -1.3610322 3.1044122 -2.8258380
22 H H22 -2.1456446 1.5966585 0.5336708
23 C C23 -2.0920350 3.5952711 -0.2023683
24 H H24 -4.3096064 0.6113837 -2.2110176
25 H H25 -4.4380793 -0.8115476 -1.1680084
26 H H26 -4.7646790 -0.9623397 -2.9027391
27 H H27 0.4335851 -2.7805231 -4.3963497
28 H H28 -1.2604090 -2.5334282 -4.8621491
29 H H29 -0.3192006 -1.1949977 -4.1767553
30 H H30 -3.2473520 -3.8587621 -3.2490660
31 C C31 -2.1348801 4.2384883 1.0015546
32 N N32 -2.1105526 4.5676709 -1.2111390
33 O O33 -2.1739676 5.5838516 0.7719460
34 H H34 -2.1029644 3.9174672 2.0301274
35 C C35 -2.1559749 5.7032950 -0.5893819
36 C C36 -2.1912632 7.0762800 -1.1608480
37 H H37 -2.1790056 7.0070839 -2.2498397
38 H H38 -1.3258104 7.6617060 -0.8302147
39 H H39 -3.0940123 7.6116474 -0.8458179
40 O O40 2.2693360 -2.2815633 0.2655403
41 S S41 1.0014169 -3.8178762 1.9658487
42 C C42 2.2552667 -3.0620622 3.0018598
43 C C43 3.3909146 -3.7883668 3.3638852
44 H H44 3.5356912 -4.7954260 2.9848117
45 C C45 4.3434999 -3.2056426 4.2013722
46 H H46 5.2273483 -3.7751465 4.4794316
47 C C47 4.1919813 -1.8951790 4.6701062
48 C C48 5.2233043 -1.2645011 5.5752687
49 C C49 3.0462612 -1.1804361 4.2889794
50 H H50 2.9125618 -0.1539301 4.6198375
51 C C51 2.0749752 -1.7579814 3.4773330
52 H H52 1.1919043 -1.1947669 3.1967906
53 H H53 4.8913313 -1.2750908 6.6219565
54 H H54 5.4027101 -0.2181069 5.3048236
55 H H55 6.1788461 -1.7962369 5.5277281
56 H H56 1.0198959 -2.0540665 -2.0348061
57 C C57 1.2284813 1.0923765 1.0993677
58 O O58 2.2410705 1.4789972 0.4930051
59 C C59 0.9818231 1.7543386 2.4836526
60 F F60 2.1299004 1.9559839 3.1563710
61 F F61 0.3836073 2.9593511 2.3251106
```

62 F F62 0.1767856 1.0124325 3.2748281
63 O O63 0.3420696 0.2558124 0.7558796
64 H H64 -0.9068399 -3.2969273 0.0219782
65 H H65 0.0770760 -0.1677760 -0.6422334
66 O O 2.6589183 -0.3141492 -1.4124491
67 H H 2.6127706 0.4331562 -0.7410728
68 H H1 2.3047794 -1.5610775 -0.4544124
69 H H2 1.9958814 -0.0607265 -2.0734439
Electronic energy: -2250.91430 au

Trifluoroacetate - hydroxonium ion mediated cyclisation boat-like transition state leading to 2,6-*cis* (375)

Cartesian Coordinates (Angstroms)
Atom X Y Z
---
1 C -3.014801 -1.121900 1.234204
2 C -3.831663 -0.480821 0.085931
3 C -3.605199 1.050876 0.003120
4 O -3.588621 -1.122683 -1.161487
5 H -4.894128 -0.658020 0.288026
6 C -2.123098 1.409810 0.263195
7 H -3.863308 1.328509 -1.025116
8 C -4.517069 1.838701 0.952414
9 O -1.333470 0.239748 -0.139703
10 C -1.639809 2.642326 -0.471729
11 H -1.965752 1.547622 1.340610
12 C -1.511946 -1.171878 0.916588
13 H -3.137880 -0.475195 2.112916
14 C -3.550161 -2.515143 1.601889
15 C -1.350680 3.728264 0.276039
16 C -1.513887 2.548775 -1.971751
17 C 0.306532 -2.769561 0.336145
18 H -0.583212 2.033345 -2.238566
19 H -1.483644 3.537517 -2.427897
20 H -2.335952 1.971675 -2.411117
21 H -1.426366 3.624630 1.358307
22 C -0.935010 5.059554 -0.134803
23 H -4.318722 2.913099 0.878087
24 H -4.365532 1.544031 1.998822
25 H -5.571024 1.673284 0.705657
26 H -2.933973 -2.997784 2.367318
27 H -4.569985 -2.425904 1.993245
28 H -3.576073 -3.164038 0.723032
29 H -2.697906 -0.854689 -1.445310
30 C -0.620424 6.093864 0.700034
31 N -0.792809 5.513191 -1.451731
32 O -0.284123 7.178660 -0.060589
33 H -0.582955 6.220324 1.770620
34 C -0.412660 6.747402 -1.350766

35 C -0.104479 7.716486 -2.436290
36 H 0.936347 8.054920 -2.376742
37 H -0.746572 8.602184 -2.368636
38 H -0.265457 7.230644 -3.400205
39 O 1.239831 -2.410761 1.187214
40 S 0.769192 -4.115765 -0.739981
41 C 2.459390 -4.474162 -0.260804
42 C 3.506570 -3.606980 -0.597927
43 H 3.306211 -2.672439 -1.109985
44 C 4.812464 -3.941920 -0.253265
45 H 5.616707 -3.254181 -0.503995
46 C 5.108925 -5.144782 0.405671
47 C 6.536410 -5.504589 0.743402
48 C 4.050926 -6.004026 0.722987
49 H 4.255135 -6.939697 1.238456
50 C 2.734170 -5.674291 0.399908
51 H 1.920777 -6.342653 0.665748
52 H 7.074831 -4.649179 1.166961
53 H 7.087857 -5.820437 -0.152052
54 H 6.583479 -6.325848 1.465502
55 H -0.897113 -0.823995 1.744603
56 C 2.115668 0.381766 -0.448448
57 O 1.053244 0.824254 0.145130
58 C 1.911002 0.096245 -1.959716
59 F 2.953571 -0.552827 -2.499108
60 F 0.805384 -0.664181 -2.160612
61 F 1.736118 1.244345 -2.653502
62 O 3.213156 0.186830 0.048642
63 H -1.590674 -2.741705 -0.572601
64 H -0.293032 0.473033 -0.140909
65 O 1.223885 -0.188712 2.563245
66 H 2.151069 -0.211614 2.852384
67 H 1.085452 -1.566748 1.731241
68 H 1.243486 0.404708 1.757563
69 C -0.968619 -2.271514 0.180489
Electronic energy: -2250.91041 au

Trifluoroacetate - hydroxonium ion mediated cyclisation boat-like transition state leading to 2,6-*trans* (376)

Cartesian Coordinates (Angstroms)
Atom X Y Z
--------- ------------ ------------ ------------
1 C C -3.1097417 -1.5584273 1.3276895
2 C C1 -3.7689805 -1.5386234 -0.0679830
3 C C2 -3.6544553 -0.1524389 -0.7345591
4 O O -3.2502370 -2.5715751 -0.9058736
5 H H -4.8310198 -1.7831767 0.0427043
6 C C3 -2.2749369 0.5017167 -0.4807914
7 H H1 -3.7710079 -0.3350604 -1.8085183
8 C C4 -4.7664232 0.8132239 -0.2997808
9 O O1 -1.2889340 -0.5567836 -0.1481067

10 C C5 -1.7419194 1.2740065 -1.6632786
11 H H2 -2.3316919 1.1615861 0.3916765
12 C C6 -1.5936287 -1.5440977 1.2064254
13 H H3 -3.4308701 -0.6626469 1.8777300
14 C C7 -3.5275690 -2.8001477 2.1336105
15 C C8 -1.5901610 2.6086555 -1.5438002
16 C C9 -1.4284574 0.5001791 -2.9209652
17 C C10 0.3801090 -1.6297416 2.7296068
18 H H4 -1.9267906 -0.4734582 -2.9364977
19 H H5 -0.3540529 0.3096335 -3.0132501
20 H H6 -1.7434363 1.0557523 -3.8123383
21 H H7 -1.8552766 3.0875850 -0.6037085
22 C C11 -1.1084474 3.5441404 -2.5459187
23 H H8 -4.6327554 1.7938064 -0.7693756
24 H H9 -4.7739767 0.9623962 0.7872724
25 H H10 -5.7490041 0.4301228 -0.5945672
26 H H11 -3.0064700 -2.8484894 3.0945966
27 H H12 -4.6048675 -2.7736687 2.3307102
28 H H13 -3.3078615 -3.7114740 1.5683856
29 H H14 -2.3532347 -2.3077076 -1.1685992
30 C C12 -0.3744842 3.3684787 -3.6860286
31 N N -1.3482630 4.9168162 -2.3920058
32 O O2 -0.1576263 4.5949613 -4.2480097
33 H H15 0.0907822 2.5294249 -4.1744038
34 C C13 -0.7786950 5.4792252 -3.4096040
35 C C14 -0.7185763 6.9222062 -3.7657853
36 H H16 -1.1855581 7.1079986 -4.7398072
37 H H17 0.3190928 7.2696890 -3.8233386
38 H H18 -1.2455705 7.4968116 -3.0023677
39 O O3 1.2191672 -1.0545626 3.5656642
40 S S 0.8356939 -3.2941826 2.2470618
41 C C15 2.6119537 -3.1323619 2.0234331
42 C C16 3.1144004 -2.5715338 0.8443802
43 H H19 2.4302681 -2.2315476 0.0748474
44 C C17 4.4885075 -2.4387999 0.6685370
45 H H20 4.8607379 -1.9684116 -0.2377599
46 C C18 5.3885337 -2.8872536 1.6460376
47 C C19 6.8782532 -2.7584414 1.4340555
48 C C20 4.8686079 -3.4649495 2.8108622
49 H H21 5.5489525 -3.8142240 3.5840876
50 C C21 3.4923682 -3.5839196 3.0083959
51 H H22 3.1038764 -4.0116561 3.9271864
52 H H23 7.2441134 -3.5095039 0.7214266
53 H H24 7.4306359 -2.8950280 2.3690308
54 H H25 7.1375952 -1.7748436 1.0267232
55 H H26 -1.2159300 -2.4646525 0.7682464
56 C C22 1.9056705 0.9142197 0.0980716
57 O O4 0.6717756 0.8242135 0.4474748
58 C C23 2.2191432 0.3716921 -1.3224805
59 F F 3.5108855 0.0557878 -1.4785616
60 F F1 1.4915528 -0.7463665 -1.6021378
61 F F2 1.8978994 1.2895938 -2.2636542
62 O O5 2.8303148 1.4105547 0.7328343
63 H H27 -1.1364429 -0.1731166 2.8374288
64 H H28 -0.3506485 -0.0483978 0.0257307
65 O O6 1.1728237 1.4972031 3.0687171

66 H H29 2.0777814 1.6582040 2.7327567
67 H H30 1.1654170 -0.0334497 3.4855289
68 H H31 0.7079599 1.4279574 2.2024108
69 C C24 -0.8068706 -1.0731226 2.3225189
Electronic energy: -2250.91453 au

2,6-*trans* cyclised thioester - trifluoroacetic acid - water complex low energy conformation

Cartesian Coordinates (Angstroms)
Atom X Y Z
--- --- --- ---
1 C C -0.5752740 -0.6079779 -4.4312271
2 C C1 -1.9092754 -0.2476379 -3.7469152
3 C C2 -1.7325709 0.8445097 -2.6715936
4 O O -2.8172329 0.1329523 -4.7790859
5 H H -2.2963469 -1.1487272 -3.2398763
6 C C3 -0.6701342 0.3583786 -1.6619905
7 H H1 -1.3605805 1.7482798 -3.1682699
8 C C4 -3.0543211 1.1745443 -1.9630547
9 O O1 0.5598473 0.0160085 -2.3406871
10 C C5 -0.2884154 1.3885464 -0.6123892
11 H H2 -1.0621956 -0.5345385 -1.1591370
12 C C6 0.4763864 -0.9744340 -3.3614655
13 C C7 0.2701426 -2.4159961 -2.7926590
14 H H3 -0.7634180 -1.4953498 -5.0514887
15 C C8 -0.0481801 0.5095295 -5.3461404
16 C C9 -0.5564183 1.0984753 0.6769881
17 C C10 0.3547933 2.6568484 -1.1111019
18 C C11 0.9172498 -2.5584285 -1.4325230
19 H H4 1.1678124 2.4131502 -1.8041488
20 H H5 0.7432026 3.2601629 -0.2913021
21 H H6 -0.3671013 3.2662744 -1.6732815
22 H H7 -1.0172994 0.1350032 0.8765021
23 C C12 -0.3494851 1.8871977 1.8848652
24 H H8 -2.9108029 1.9646962 -1.2197399
25 H H9 -3.4602563 0.3012411 -1.4372193
26 H H10 -3.8068352 1.5365496 -2.6734094
27 H H11 0.7909411 0.1407889 -5.9474815
28 H H12 -0.8329182 0.8550254 -6.0230959
29 H H13 0.3122407 1.3647481 -4.7659156
30 H H14 -3.6942578 0.2219549 -4.3773110
31 C C13 -0.8988372 1.6280008 3.1090704
32 N N 0.4479760 3.0338060 2.0039195
33 O O2 -0.4685788 2.5878741 3.9865593
34 H H15 -1.5881511 0.8876717 3.4844908
35 C C14 0.3395478 3.3977557 3.2438484
36 C C15 0.9724076 4.5576366 3.9282329
37 H H16 1.5778398 4.2320378 4.7817803
38 H H17 0.2139450 5.2521784 4.3074117

39 H H18 1.6108475 5.0834992 3.2163776
40 O O3 0.2623340 -2.5517294 -0.4103640
41 S S 2.7234541 -2.6534788 -1.4503288
42 C C16 3.0775852 -2.1856380 0.2439535
43 C C17 2.7915623 -0.8824806 0.6685523
44 H H19 2.3343047 -0.1777200 -0.0187913
45 C C18 3.0733799 -0.5066838 1.9819696
46 H H20 2.8431112 0.5072957 2.3017852
47 C C19 3.6650000 -1.4051024 2.8844781
48 C C20 4.0108516 -0.9765305 4.2910094
49 C C21 3.9520473 -2.7016464 2.4362305
50 H H21 4.4005584 -3.4179297 3.1203382
51 C C22 3.6586146 -3.0963003 1.1310034
52 H H22 3.8708645 -4.1102000 0.8054540
53 H H23 5.0582945 -0.6536721 4.3566873
54 H H24 3.8789751 -1.7962636 5.0052409
55 H H25 3.3902005 -0.1360565 4.6178930
56 C C23 -3.1803712 -1.3256584 1.6176206
57 O O4 -2.9048357 -1.7132656 0.5041961
58 C C24 -4.5181209 -0.6152033 1.9246269
59 F F -5.2952781 -1.3853566 2.7073944
60 F F1 -4.3001682 0.5498923 2.5662072
61 F F2 -5.1836598 -0.3545005 0.7931811
62 O O5 -2.4455039 -1.4109729 2.7106785
63 H H26 -1.5286880 -1.8196800 2.5123111
64 O O6 -0.0247618 -2.2914784 2.3294039
65 H H27 0.6249700 -1.6033790 2.5467527
66 H H28 0.1535358 -2.4984657 1.3865702
67 H H29 1.4722060 -0.9511681 -3.8157008
68 H H30 0.7000871 -3.1288457 -3.5066049
69 H H31 -0.7868422 -2.6600178 -2.6592846
Electronic energy: -2250.96536 au

2,6-*trans* cyclised thioester - trifluoroacetic acid - water complex low energy conformation

Cartesian Coordinates (Angstroms)
Atom X Y Z
--------- ------------ ------------ ------------
1 C C -0.4800229 -3.7393121 1.3932075
2 C C1 -1.7279574 -3.4439330 2.2465008
3 C C2 -2.8013737 -2.6573996 1.4627903
4 O O -2.2148723 -4.6903036 2.7413697
5 H H -1.4073357 -2.8121772 3.0949766
6 C C3 -2.1473675 -1.3869375 0.8601385
7 H H1 -3.1408748 -3.2922962 0.6365365
8 C C4 -4.0017242 -2.3038433 2.3496710
9 O O1 -0.9937878 -1.7408521 0.0858579
10 C C5 -3.0598870 -0.5805460 -0.0461012
11 H H2 -1.8219740 -0.7475876 1.6992346

12 C C6 0.0211531 -2.3863835 0.8548824
13 H H3 0.2833443 -4.1369669 2.0764960
14 C C7 -0.7406871 -4.7805257 0.2942429
15 C C8 -3.4170924 0.6576088 0.3503361
16 C C9 -3.4776480 -1.2473952 -1.3309393
17 C C10 1.7997049 -1.0962168 -0.3704391
18 H H4 -2.5916355 -1.6249732 -1.8536636
19 H H5 -4.0247748 -0.5658400 -1.9806353
20 H H6 -4.1214845 -2.1153266 -1.1304529
21 H H7 -3.0118814 1.0141651 1.2974353
22 C C11 -4.2785393 1.6391486 -0.2935414
23 H H8 -4.7553838 -1.7384786 1.7937278
24 H H9 -3.6913234 -1.6887105 3.2055761
25 H H10 -4.4902305 -3.2058519 2.7366640
26 H H11 0.1988120 -5.1346290 -0.1432535
27 H H12 -1.2630113 -5.6445409 0.7125600
28 H H13 -1.3515031 -4.3650740 -0.5138022
29 H H14 -2.8906511 -4.5016454 3.4091143
30 C C12 -4.5583973 2.8889266 0.1804285
31 N N -4.9657112 1.4784250 -1.5042614
32 O O2 -5.3998790 3.5122706 -0.7017332
33 H H15 -4.2676036 3.4516102 1.0534142
34 C C13 -5.5969444 2.5943158 -1.6922077
35 C C14 -6.4810224 2.9818622 -2.8246149
36 H H16 -6.0845351 3.8574694 -3.3512065
37 H H17 -7.4870584 3.2348915 -2.4711396
38 H H18 -6.5485870 2.1466618 -3.5238335
39 O O3 1.8738880 -0.2179692 0.4735152
40 S S 2.3527593 -0.9370832 -2.0632526
41 C C15 3.2367944 0.6207038 -2.0383216
42 C C16 2.6334036 1.7826047 -2.5281124
43 H H19 1.6090687 1.7510343 -2.8869166
44 C C17 3.3506864 2.9786704 -2.5491930
45 H H20 2.8727908 3.8801488 -2.9247332
46 C C18 4.6713725 3.0390976 -2.0879336
47 C C19 5.4337877 4.3420439 -2.0676333
48 C C20 5.2640638 1.8594337 -1.6120923
49 H H21 6.2904071 1.8848623 -1.2522941
50 C C21 4.5609473 0.6572690 -1.5819041
51 H H22 5.0122282 -0.2413794 -1.1727964
52 H H23 6.4676743 4.2074868 -2.4046417
53 H H24 5.4716895 4.7464137 -1.0486957
54 H H25 4.9619397 5.0947916 -2.7066811
55 H H26 0.2774042 -1.7419117 1.7108734
56 C C22 3.9682686 2.0496945 1.7355249
57 O O4 4.5980279 1.0331234 1.9454263
58 C C23 4.4547971 3.4183159 2.2639531
59 F F 5.6977822 3.3277103 2.7448796
60 F F1 4.4444207 4.3447122 1.2852782
61 F F2 3.6426728 3.8449083 3.2483835
62 O O5 2.8309591 2.1868535 1.0922665
63 H H27 2.5136573 1.3005562 0.7483755
64 O O6 4.4639534 -1.7102015 0.8959487
65 H H28 4.3697291 -0.8251225 1.2955876
66 H H29 5.3201432 -2.0227999 1.2226857
67 C C24 1.2503446 -2.4715837 -0.0462447

68 H H30 1.0262605 -3.0204982 -0.9658194
69 H H31 2.0678254 -2.9914948 0.4712319
Electronic energy: -2250.96261 au

Thioester - trifluoroacetic acid complex low energy conformation

Cartesian Coordinates (Angstroms)
Atom X Y Z
--- --- --- ---
1 C C -1.3564502 -0.1879429 2.3866860
2 C C1 -2.2956241 0.0273133 1.1777751
3 C C2 -3.7826946 -0.3301596 1.3937611
4 O O -2.1750070 1.4190566 0.7978559
5 H H -1.9160528 -0.5944086 0.3574572
6 C C3 -4.5659695 -0.3458229 0.0461833
7 H H1 -3.8210632 -1.3649080 1.7565711
8 C C4 -4.4752804 0.5742724 2.4254160
9 O O1 -4.4447626 0.9722522 -0.5310349
10 C C5 -4.1424229 -1.4526826 -0.9107800
11 H H2 -5.6256214 -0.5089172 0.2981357
12 C C6 0.0478034 0.1059985 1.9348249
13 C C7 0.8938134 0.9869687 2.4841683
14 H H3 0.3993044 -0.4531446 1.0665568
15 H H4 -1.6371321 0.5156341 3.1801545
16 C C8 -1.4294778 -1.6278957 2.9356020
17 C C9 -3.1542082 -1.2280348 -1.8027474
18 C C10 -4.8875806 -2.7507193 -0.7342429
19 C C11 2.2392016 1.1821676 1.8954471
20 H H5 0.6240242 1.5798188 3.3555025
21 H H6 -4.5029231 -3.5307491 -1.3904729
22 H H7 -5.9571839 -2.6138984 -0.9490333
23 H H8 -4.8250921 -3.0970353 0.3076448
24 H H9 -2.6712642 -0.2532259 -1.7879364
25 C C12 -2.5611968 -2.1219149 -2.7858492
26 H H10 -5.5230807 0.2796722 2.5523936
27 H H11 -4.4514413 1.6213988 2.1135558
28 H H12 -3.9899148 0.5038901 3.4046300
29 H H13 -2.4114989 -1.8457528 3.3673129
30 H H14 -0.6805906 -1.7687080 3.7208766
31 H H15 -1.2301344 -2.3655244 2.1487939
32 H H16 -2.9065099 1.5771733 0.1602556
33 C C13 -1.4129727 -1.8784902 -3.4845603
34 N N -3.0526103 -3.3742046 -3.1770716
35 O O2 -1.1749469 -2.9491893 -4.3008570
36 H H17 -0.6890260 -1.0784760 -3.4803027
37 C C14 -2.2087769 -3.8079239 -4.0602239
38 C C15 -2.2373495 -5.0835944 -4.8251313
39 H H18 -2.3158605 -4.8954641 -5.9021989
40 H H19 -3.0991606 -5.6711140 -4.5039767
41 H H20 -1.3238983 -5.6652736 -4.6568782
42 O O3 2.6189608 0.6845217 0.8559159

```
43 S S 3.2636301 2.2854739 2.9199576
44 C C16 4.8386091 2.2506206 2.0723444
45 C C17 4.9591866 2.6223830 0.7281913
46 H H21 4.0806784 2.8959583 0.1567567
47 C C18 6.2130619 2.6122586 0.1223900
48 H H22 6.2960509 2.8893499 -0.9262126
49 C C19 7.3676356 2.2555307 0.8335751
50 C C20 8.7235822 2.2816451 0.1679434
51 C C21 7.2283146 1.8928881 2.1782818
52 H H23 8.1069845 1.6026303 2.7498939
53 C C22 5.9775915 1.8817235 2.7950569
54 H H24 5.8837607 1.5805028 3.8343028
55 H H25 8.6662610 1.9339121 -0.8693988
56 H H26 9.4431672 1.6491752 0.6980751
57 H H27 9.1362863 3.2992762 0.1453073
58 H H28 -4.6585124 0.8972859 -1.4749579
59 C C23 1.5466189 2.2081529 -2.1769922
60 F F 2.2442123 3.1080531 -1.4645994
61 F F1 1.0809964 2.8287732 -3.2832333
62 C C24 0.3488000 1.6247586 -1.3968499
63 F F2 2.3734185 1.2313607 -2.5615973
64 O O4 -0.1671247 0.5829647 -1.7499266
65 O O5 -0.0278150 2.4084325 -0.4111951
66 H H29 -0.8137225 1.9919267 0.0727076
Electronic energy: -2174.52533 au
```

Trifluoroacetatic acid mediated cyclisation transition state leading to 2,6-*trans* (378)

```
Cartesian Coordinates (Angstroms)
Atom X Y Z
--------- ------------- ------------- -------------
1 C C -0.5588661 -3.4608716 -1.1821157
2 C C1 -1.8463902 -3.4788577 -0.3152251
3 C C2 -2.7784282 -2.2682106 -0.5353133
4 O O -2.5473398 -4.7078300 -0.4938301
5 H H -1.5510124 -3.4986834 0.7401580
6 C C3 -2.0650892 -0.9179891 -0.3634840
7 H H1 -3.1413077 -2.3206987 -1.5707820
8 C C4 -3.9874471 -2.3349065 0.4111785
9 O O1 -0.8426282 -0.9358311 -1.1923952
10 C C5 -2.8838442 0.2855000 -0.7887890
11 H H2 -1.7426632 -0.8033692 0.6783716
12 C C6 0.3198659 -2.2741513 -0.8410455
13 C C7 0.8764260 -2.1524207 0.4683739
14 H H3 0.0123053 -4.3489276 -0.8765725
15 C C8 -0.8208319 -3.5747477 -2.6918435
16 C C9 -2.8430082 1.3757660 0.0040757
17 C C10 -3.5987253 0.2006550 -2.1140777
18 C C11 1.9640776 -1.3313291 0.6841704
19 H H4 -2.9189526 -0.1785994 -2.8877789
20 H H5 -3.9780521 1.1754008 -2.4181495
```

```
21 H H6 -4.4572483 -0.4844175 -2.0731968
22 H H7 -2.2160051 1.3267224 0.8915865
23 C C12 -3.4622860 2.6781896 -0.1784047
24 H H8 -4.7000259 -1.5320197 0.2010006
25 H H9 -3.6696961 -2.2335743 1.4568136
26 H H10 -4.4962583 -3.2965295 0.3109401
27 H H11 0.1275104 -3.6474092 -3.2351764
28 H H12 -1.3891992 -4.4814832 -2.9258758
29 H H13 -1.3610778 -2.7086759 -3.0846946
30 H H14 -2.9408318 -4.6982134 -1.3809062
31 C C13 -3.1554218 3.8098883 0.5217246
32 N N -4.4637211 3.0009672 -1.1036221
33 O O2 -3.9350264 4.8299469 0.0556233
34 H H15 -2.4322085 4.0515715 1.2830625
35 C C14 -4.6986133 4.2625258 -0.9247434
36 C C15 -5.6718722 5.1373982 -1.6320006
37 H H16 -6.4151402 5.5446825 -0.9368282
38 H H17 -6.1847409 4.5521092 -2.3971822
39 H H18 -5.1648946 5.9839743 -2.1086728
40 O O3 2.5932479 -0.7375731 -0.2950397
41 S S 2.4702669 -1.0755347 2.3846220
42 C C16 4.2009929 -0.6109049 2.2479554
43 C C17 5.1821894 -1.5893643 2.4469322
44 H H19 4.8888299 -2.6190074 2.6286856
45 C C18 6.5300976 -1.2376140 2.4159999
46 H H20 7.2854342 -2.0044094 2.5732784
47 C C19 6.9267711 0.0867419 2.1851357
48 C C20 8.3895058 0.4572846 2.1147003
49 C C21 5.9304139 1.0536056 1.9977220
50 H H21 6.2146240 2.0885530 1.8218231
51 C C22 4.5773891 0.7191262 2.0326883
52 H H22 3.8232219 1.4803941 1.8689265
53 H H23 9.0028069 -0.2063447 2.7333968
54 H H24 8.5583041 1.4865773 2.4478519
55 H H25 8.7646447 0.3825269 1.0853022
56 H H26 0.9867454 -1.9504670 -1.6359094
57 C C23 1.1726760 2.0207979 -0.1078264
58 O O4 2.3934191 1.7163903 -0.0198429
59 C C24 0.8019557 3.4477099 0.3751392
60 F F 0.1625199 4.1347083 -0.5895066
61 F F1 -0.0434152 3.3579884 1.4379662
62 F F2 1.8644323 4.1641728 0.7655844
63 O O5 0.2011388 1.3469342 -0.5000250
64 H H27 0.4581409 -2.7025966 1.3040803
65 H H28 -0.3252852 -0.0845983 -0.9826001
66 H H29 2.6076004 0.3293519 -0.1914136
Electronic energy: -2174.48490 au
```

Trifluoroacetatic acid mediated cyclisation transition state leading to 2,6-*cis* (377)

Cartesian Coordinates (Angstroms)

Atom	X	Y	Z
1 C	C	1.6705497	-3.4023464	0.2153709
2 C	C1	0.4283043	-3.9643217	0.9375569
3 C	C2	-0.9202591	-3.5785771	0.2942954
4 O	O	0.6131920	-5.3782614	0.9741559
5 H	H	0.4365814	-3.5653669	1.9685015
6 C	C3	-1.0888633	-2.0508425	0.2505129
7 H	H1	-0.9241440	-3.9543242	-0.7348209
8 C	C4	-2.0967031	-4.2152915	1.0502690
9 O	O1	0.0885076	-1.5011970	-0.4359115
10 C	C5	-2.3277010	-1.5635700	-0.4750139
11 H	H2	-1.0855665	-1.6572734	1.2761254
12 C	C6	1.7280189	-1.8960057	0.3391148
13 C	C7	2.6996305	-1.1415151	-0.3596479
14 H	H3	2.5257622	-3.7611713	0.8091764
15 C	C8	1.8393275	-3.9305209	-1.2167836
16 C	C9	-3.1048854	-0.6698359	0.1693295
17 C	C10	-2.5439725	-2.0650238	-1.8799080
18 C	C11	3.1856060	0.0780115	0.0834598
19 H	H4	-1.6301288	-1.9315637	-2.4718312
20 H	H5	-3.3673348	-1.5411349	-2.3642077
21 H	H6	-2.7790897	-3.1385100	-1.8935867
22 H	H7	-2.7887980	-0.3597480	1.1628671
23 C	C12	-4.3053812	0.0191893	-0.2732527
24 H	H8	-3.0546646	-3.8974840	0.6293742
25 H	H9	-2.0932042	-3.9278716	2.1102223
26 H	H10	-2.0586889	-5.3081028	0.9874342
27 H	H11	2.8485626	-3.7314117	-1.5896932
28 H	H12	1.6849389	-5.0121277	-1.2285361
29 H	H13	1.1267359	-3.4632567	-1.9018617
30 H	H14	-0.0448421	-5.7519924	1.5783693
31 C	C13	-4.8714903	1.0954680	0.3477128
32 N	N	-5.0736153	-0.2821159	-1.4047871
33 O	O2	-5.9711788	1.4766644	-0.3680217
34 H	H15	-4.6103155	1.6862357	1.2107331
35 C	C14	-6.0270816	0.5954092	-1.4109545
36 C	C15	-7.1412567	0.7512297	-2.3843124
37 H	H16	-8.1143389	0.6463756	-1.8909533
38 H	H17	-7.0488061	-0.0155488	-3.1554375
39 H	H18	-7.1143001	1.7393081	-2.8577307
40 O	O3	2.8129572	0.7672094	1.1243954
41 S	S	4.5557060	0.7635637	-0.8307582
42 C	C16	4.5260378	2.4890659	-0.3467810
43 C	C17	3.4391373	3.3080861	-0.6810468
44 H	H19	2.5755431	2.8869099	-1.1871579
45 C	C18	3.4639965	4.6573746	-0.3456488
46 H	H20	2.6113770	5.2827970	-0.6010794
47 C	C19	4.5698750	5.2264461	0.3060259
48 C	C20	4.5810768	6.6949557	0.6588802
49 C	C21	5.6500607	4.3955839	0.6207750
50 H	H21	6.5168159	4.8126996	1.1280069

```
51 C C22 5.6314640 3.0349614 0.3075145
52 H H22 6.4712875 2.4006194 0.5748223
53 H H23 3.7932719 6.9350291 1.3839578
54 H H24 4.4046543 7.3190789 -0.2257009
55 H H25 5.5388435 6.9943422 1.0957630
56 H H26 1.4698538 -1.5237024 1.3297287
57 C C23 -0.2650344 1.3081677 1.0819036
58 O O4 -0.2636359 1.0629136 -0.1436023
59 C C24 -1.2964351 2.3512899 1.5887363
60 F F -0.7131877 3.2926717 2.3494245
61 F F1 -1.9464385 2.9636125 0.5891095
62 F F2 -2.2361514 1.7304195 2.3591960
63 O O5 0.4463443 0.7933467 1.9886774
64 H H27 3.1018652 -1.5222138 -1.2914365
65 H H28 0.0299436 -0.4782301 -0.3974729
66 H H29 1.8416645 0.6214231 1.4664388
Electronic energy: -2174.48791 au
```

2,6-*trans* cyclised thioester - trifluoroacetic acid complex low energy conformation

```
Cartesian Coordinates (Angstroms)
Atom X Y Z
--------- ------------ ------------ ------------
1 C C1 0.7306710 2.4290441 2.0004298
2 C C2 -0.1981218 2.0520280 3.1812304
3 C C3 -1.6154766 2.6673190 3.0210568
4 O O4 -0.2423832 0.6555656 3.4477768
5 H H5 0.2398313 2.4805013 4.0930169
6 C C6 -2.1887009 2.4443868 1.6023586
7 H H7 -2.2547619 2.1752551 3.7620549
8 C C8 -1.6162932 4.1738948 3.3359938
9 O O9 -1.2374377 2.9013163 0.6294166
10 C C10 -2.7243322 1.0596200 1.2191820
11 H H11 -3.0304982 3.1383500 1.4614610
12 C C12 0.0093180 2.1870733 0.6641505
13 C C13 0.7924221 2.6625562 -0.5728450
14 H H14 0.9085645 3.5121156 2.0693831
15 C C15 2.0800457 1.7009510 2.0867876
16 C C16 -3.0404375 0.1303361 2.1398180
17 C C17 -2.9614504 0.8880802 -0.2636400
18 C C18 1.3878953 1.5160494 -1.3754463
19 H H19 -2.0269175 0.6890608 -0.8020692
20 H H20 -3.3726372 1.8113999 -0.6880257
21 H H21 -3.6494263 0.0667241 -0.4738367
22 H H22 -2.8708149 0.3459458 3.1891862
23 C C23 -3.5870484 -1.2050190 1.8891375
24 H H24 -2.6410444 4.5617634 3.3810535
25 H H25 -1.0817282 4.7419884 2.5684505
26 H H26 -1.1436118 4.3731759 4.3044432
27 H H27 2.5164655 1.8285178 3.0836232
28 H H28 1.9694056 0.6276737 1.9093453
```

```
29 H H29 2.7963539 2.0955916 1.3571844
30 H H30 -0.2876058 0.1416612 2.6234072
31 C C31 -4.5201379 -1.8822315 2.6124756
32 N N32 -3.1685967 -2.0612662 0.8583481
33 O O33 -4.6956399 -3.1249903 2.0539559
34 H H34 -5.1160535 -1.6545398 3.4813138
35 C C35 -3.8449263 -3.1651687 1.0046878
36 C C36 -3.7785136 -4.4052394 0.1860168
37 H H37 -4.6950108 -4.5384550 -0.4008113
38 H H38 -3.6607971 -5.2854532 0.8262361
39 H H39 -2.9296293 -4.3430951 -0.4977643
40 O O40 0.8191988 0.4643196 -1.5621695
41 S S41 3.0066012 1.9190845 -2.0878052
42 C C42 3.3741716 0.4327795 -3.0149348
43 C C43 2.7016650 0.1527040 -4.2091598
44 H H44 1.9413466 0.8360912 -4.5743359
45 C C45 3.0070870 -1.0032955 -4.9226880
46 H H46 2.4748037 -1.2145017 -5.8475509
47 C C47 3.9896437 -1.8960085 -4.4717282
48 C C48 4.2932708 -3.1631004 -5.2354196
49 C C49 4.6632977 -1.5928328 -3.2827057
50 H H50 5.4319637 -2.2686333 -2.9153210
51 C C51 4.3580817 -0.4453452 -2.5518460
52 H H52 4.8779422 -0.2348672 -1.6224098
53 H H53 3.5835229 -3.9591665 -4.9738134
54 H H54 5.2982950 -3.5355270 -5.0117942
55 H H55 4.2204709 -3.0068213 -6.3172366
56 C C56 0.2105474 -1.8941622 0.1852233
57 O O57 0.2090848 -1.2534846 1.2165030
58 C C58 1.5376467 -2.3749069 -0.4410774
59 F F59 1.8360658 -3.5946525 0.0653349
60 F F60 1.4711436 -2.4840880 -1.7709909
61 F F61 2.5334010 -1.5394757 -0.1172626
62 O O62 -0.8327575 -2.3269980 -0.4882913
63 H H63 -1.6921729 -2.0846100 -0.0011239
64 H H67 -0.1934008 1.1156138 0.5485980
65 H H68 1.5558891 3.4066402 -0.3239971
66 H H69 0.0722505 3.1527569 -1.2405409
Electronic energy: -2174.53729 au
```

2,6-*cis* cyclised thioester - trifluoroacetic acid complex low energy conformation

```
Cartesian Coordinates (Angstroms)
Atom X Y Z
--------- ------------ ------------ ------------
1 C C1 2.8976757 -3.0318821 1.3283224
2 C C2 1.7223803 -3.4286276 2.2616516
3 C C3 0.3415981 -3.2960856 1.5806868
4 O O4 1.9155797 -4.7163091 2.8440743
5 H H5 1.7392428 -2.7431924 3.1191027
6 C C6 0.2168358 -1.8913089 0.9445432
```

7 H H7 0.2933539 -4.0392989 0.7706493
8 C C8 -0.7944815 -3.5693270 2.5739012
9 O O9 1.3397437 -1.6452065 0.0748074
10 C C10 -1.0372922 -1.6613677 0.1218125
11 H H11 0.2482000 -1.1479218 1.7528521
12 C C12 2.5748412 -1.6292370 0.7840543
13 H H13 3.7923849 -2.9594206 1.9626218
14 C C14 3.1710943 -4.0616707 0.2235403
15 C C15 -1.8211630 -0.6175499 0.4637027
16 C C16 -1.2641576 -2.5906487 -1.0424222
17 C C17 3.1613608 0.3807312 -0.5176687
18 H H18 -0.3572613 -2.6397641 -1.6575166
19 H H19 -2.1046597 -2.2714036 -1.6577641
20 H H20 -1.4703495 -3.6139121 -0.6979439
21 H H21 -1.4995590 -0.0089460 1.3065795
22 C C22 -3.0535482 -0.1302163 -0.1399091
23 H H23 -1.7691406 -3.5689201 2.0758175
24 H H24 -0.8215703 -2.7996399 3.3559294
25 H H25 -0.6509181 -4.5353470 3.0658226
26 H H26 4.0995594 -3.8343106 -0.3113859
27 H H27 3.2954239 -5.0632295 0.6494819
28 H H28 2.3622654 -4.0913195 -0.5141001
29 H H29 1.7467794 -5.3774763 2.1542319
30 C C30 -3.7104515 1.0131966 0.2175179
31 N N31 -3.7772398 -0.7344705 -1.1773817
32 O O32 -4.8249950 1.1378392 -0.5688318
33 H H33 -3.5322682 1.7891495 0.9444708
34 C C34 -4.7933703 0.0431097 -1.3833896
35 C C35 -5.8990160 -0.1150943 -2.3664395
36 H H36 -5.7326231 -1.0263611 -2.9433291
37 H H37 -5.9446642 0.7390042 -3.0518359
38 H H38 -6.8685605 -0.1849095 -1.8599882
39 O O39 3.1187459 1.2590677 0.3278243
40 S S40 2.6430370 0.5762636 -2.2210525
41 C C41 1.7139593 2.1053159 -2.1489993
42 C C42 0.3375032 2.0387971 -1.8921642
43 H H43 -0.1336836 1.0765912 -1.7158309
44 C C44 -0.4139895 3.2090420 -1.8480283
45 H H45 -1.4790877 3.1467138 -1.6370079
46 C C46 0.1818254 4.4622613 -2.0550135
47 C C47 -0.6384498 5.7251225 -1.9545459
48 C C48 1.5548417 4.5072816 -2.3247845
49 H H49 2.0358169 5.4678927 -2.4926442
50 C C50 2.3217820 3.3424915 -2.3739647
51 H H51 3.3857841 3.3962964 -2.5833937
52 H H52 -0.9298246 5.9101615 -0.9132710
53 H H53 -1.5611282 5.6525856 -2.5418774
54 H H54 -0.0797331 6.5978373 -2.3062344
55 H H55 2.4845826 -0.9362910 1.6360351
56 C C56 0.4493606 2.4916991 1.8401248
57 O O57 0.4562747 1.3273810 2.1671637
58 C C58 -0.7306944 3.4187590 2.2129542
59 F F59 -1.8158801 2.6798495 2.5091955
60 F F60 -0.4238272 4.1626097 3.2887490
61 F F61 -1.0584611 4.2481760 1.2057296
62 O O62 1.3768137 3.1542297 1.1749194

63 H H63 2.0705553 2.5151736 0.8522467
64 C C67 3.6213405 -1.0231718 -0.1699121
65 H H68 3.7358731 -1.6344865 -1.0690740
66 H H69 4.5856338 -0.9563057 0.3465883
Electronic energy: -2174.53966 au

Low energy oxo-ester - trifluoroacetic acid complex conformation

Cartesian Coordinates (Angstroms)
Atom X Y Z
--------- ------------ ------------ ------------
1 C C 0.0930813 1.7790225 -1.8401192
2 C C1 1.1782386 1.7344731 -0.7385888
3 C C2 2.3654240 2.7061486 -0.9386514
4 O O 0.5196149 2.0073194 0.5183976
5 H H 1.5797084 0.7128054 -0.7106149
6 C C3 3.5239425 2.4136344 0.0597367
7 H H1 2.7827900 2.5049673 -1.9321603
8 C C4 1.9500748 4.1845283 -0.8754805
9 O O1 2.9851501 2.5920472 1.3834616
10 C C5 4.1952670 1.0603721 -0.1417411
11 H H2 4.2880015 3.1899278 -0.1076969
12 C C6 -0.9681925 0.7668230 -1.5056786
13 C C7 -2.2575264 1.0339587 -1.2731219
14 H H3 -0.3620707 2.7766693 -1.8401646
15 C C8 0.6727131 1.4842197 -3.2385876
16 C C9 3.8459810 0.0147630 0.6360899
17 C C10 5.2232010 1.0285462 -1.2437965
18 C C11 -3.1729660 -0.0515922 -0.8522626
19 H H4 6.0240572 1.7544339 -1.0438730
20 H H5 4.7781151 1.3177503 -2.2064354
21 H H6 5.6681874 0.0398288 -1.3490776
22 H H7 3.0686517 0.1844826 1.3752757
23 C C12 4.3208969 -1.3606009 0.6288531
24 H H8 2.8198429 4.8344182 -1.0235618
25 H H9 1.5031058 4.4276861 0.0914064
26 H H10 1.2200145 4.4257047 -1.6547075
27 H H11 1.2272785 0.5378851 -3.2469441
28 H H12 -0.1361598 1.4007067 -3.9710133
29 H H13 1.3458506 2.2780030 -3.5776176
30 H H14 1.2359968 2.1623889 1.1706991
31 C C13 3.7959870 -2.3871195 1.3616406
32 N N 5.3806755 -1.8715495 -0.1307743
33 O O2 4.5005918 -3.5236755 1.0780229
34 H H15 2.9740919 -2.4828358 2.0534877
35 C C14 5.4404673 -3.1310812 0.1695614
36 C C15 6.3818628 -4.1640479 -0.3401054
37 H H16 5.8407939 -4.9828690 -0.8273972
38 H H17 6.9721041 -4.5963348 0.4759823
39 H H18 7.0570765 -3.7020660 -1.0621213
40 O O3 -2.8761415 -1.2192793 -0.7268290

41 O O4 -4.4154382 0.4611477 -0.6002820
42 C C16 -5.4007377 -0.3766147 -0.0651412
43 C C17 -5.2471352 -0.9613453 1.1910944
44 H H19 -4.3288193 -0.8299955 1.7544107
45 C C18 -6.2947330 -1.7203292 1.7080597
46 H H20 -6.1733894 -2.1813352 2.6857743
47 C C19 -7.4929745 -1.9015197 1.0015368
48 C C20 -8.6254378 -2.7092253 1.5925624
49 C C21 -7.6132000 -1.2963746 -0.2544613
50 H H21 -8.5307781 -1.4201810 -0.8252629
51 C C22 -6.5742199 -0.5354578 -0.7926487
52 H H22 -6.6663677 -0.0662878 -1.7674055
53 H H23 -9.1540896 -2.1478230 2.3746891
54 H H24 -8.2598976 -3.6341879 2.0533606
55 H H25 -9.3624543 -2.9818437 0.8301433
56 H H26 -0.6464308 -0.2716961 -1.4172590
57 C C23 -1.2361548 -0.4118947 2.3726713
58 O O5 -2.0434965 -1.0624941 2.9865229
59 C C24 0.2280372 -0.9042061 2.2336551
60 F F 0.4323546 -2.0577161 2.8700631
61 F F1 0.5705837 -1.0718030 0.9379010
62 F F2 1.0807181 0.0169993 2.7584893
63 O O6 -1.4828148 0.7521996 1.7976068
64 H H27 -2.6625232 2.0407264 -1.3200829
65 H H28 3.6341909 2.2519066 2.0198902
66 H H29 -0.7205717 1.1388884 1.2706204
Electronic energy: -1851.55815 au

10. Abbreviations

Å	Ångstrom
a.u.	atomic units
Ac	acetyl
acac	acetylacetonate
BHT	butylated hydroxy toluene (2,6-di-*t*-butyl-4-methylphenol)
BINOL	1,1'-bi-2-naphthol
Bn	benzyl
Boc	*t*-butyloxycarbonyl
brsm	based on recovered starting material
Bu	butyl
Bz	benzoyl
cdk4	cycline-dependent kinase 4
CSA	camphorsulfonic acid
Cy	cyclohexyl
Cp	cyclopentadienyl
d	day
DBU	1,8-diazabicyclo[5.4.0]undec-7-ene
DCC	*N*,*N*'-dicyclohexylcarbodiimide
DCE	1,2-dichloroethane
DCM	dichloromethane
DDQ	2,3-dichloro-5,6-dicyano-1,4-benzoquinone
DET	diethyl tartrate
DFT	density functional theory
DHA	docosahexaenoic acid

DIBAL	diisobutylaluminum hydride
DIPEA	diisopropylethylamine
DMAP	4-dimethylaminopyridine
DME	dimethyl ether
DMF	dimethylformamide
DMP	Dess-Martin periodinane
DMSO	dimethysulfoxide
DNA	deoxyribonucleic acid
ESI	electrospray ionization
Et	ethyl
eV	electronvolt
FDA	US Food and Drug Administration
g	gram
h	hour
HG II	Hoveyda-Grubbs 2nd generation catalyst
HMDS	hexamethyldisilazide
HMPA	hexamethylphosphoramide
HOMO	highest occupied molecular orbital
HRMS	high resolution mass spectrometry
Hz	hertz
Ipc	isopinocampheyl
***i*-Pr**	isopropyl
IR	infrared spectroscopy
IUPAC	International Union of Pure and Applied Chemistry
J	coupling constant (Hz)

kg	kilogram
kJ	kilojoule
LDA	lithium diisopropylamide
LUMO	lowest unoccupied molecular orbital
M	molar
***m*-CPBA**	*meta*-chloroperoxybenzoic acid
Me	methyl
Mes	mesityl (2,4,6-trimethylphenyl)
Ms	mesyl (methanesulfonyl)
mg	milligram
MHz	megahertz
MMFF94	Merck Molecular Force Field '94
MOM	methoxymethyl
MS	mass spectrometry
NBS	*N*-bromosuccinimide
***n*-Bu**	*n*-butyl
NCI	National Cancer Institute
nM	nanomolar
NMO	*N*-methylmorpholine-*N*-oxide
NMR	nuclear magnetic resonance spectroscopy
NOE	nuclear Overhauser effect
PCC	pyridinium chlorochromate
Ph	phenyl
Piv	pivaloyl
PMB	*p*-methoxybenzyl

Pr	propyl
py	pyridine
RNA	ribonucleic acid
rt	room temperature
TBAF	tetra-*n*-butylammonium fluoride
TBDPS	*t*-butyldiphenylsilyl
TBHP	*t*-butylhydroperoxide
TBS	*t*-butyldimethylsilyl
***t*-Bu**	*tert*-butyl
TES	triethylsilyl
Tf	triflate
TFA	trifluoroacetic acid
THF	tetrahydrofuran
THP	tetrahydropyran
TIPS	triisopropylsilyl
TPS	triphenylsilyl
TLC	thin layer chromatography
TMEDA	*N*,*N*,*N*',*N*'-tetramethylethylenediamine
TMS	tetramethylsilyl
Tol	*p*-tolyl
TPS	triphenylsilyl
Ts	tosyl
TS	transition state
ν	vibration frequency (cm^{-1})

11. References

1. Nicolaou, K. C.; Vourloumis, D.; Winssinger, N.; Baran, P. S. *Angew. Chem Int. Ed.* **2000**, *46*, 769.
2. Nicolaou, K. C.; Snyder, S. A. *Angew. Chem Int. Ed.* **2005**, *44*, 1012.
3. Lindquist, N.; Fenical, W. *J. Am. Chem. Soc.* **1991**, *113*, 2303.
4. Li, J.; Jeong, S.; Esser, L.; Harran, G. H. *Angew. Chem Int. Ed.* **2001**, *40*, 4765.
5. Barton, D. H. R. *Experientia*, **1950**, *6*, 316
6. Evans, D. A.; Kaldor, S. W.; Jones, K. T.; Clardy, J.; Sout, T. J. *J. Am. Chem. Soc.* **1990**, *112*, 7001.
7. Newman, D. J.; Cragg, M. G. *J. Nat. Prod.*, **2012**, *75*, 311.
8. Vangapandu, S.; Jain, M.; Kaur, K.; Patil, P.; Patel, S. R.; Jain, R. *Med. Res. Rev.*, **2007**, *27*, 65
9. Wolff, A. C.; Donehower, R. C.; Carducci, M. K. *Clin. Cancer Res.*, **2003**, *9*, 3589
10. Smith, A. B.; Tomioka, T.; Risatti, C. A.; Sperry, J. B.; Sfouggatakis, C. *Org. Lett.* **2008**, *10*, 4359.
11. Paterson, I.; Florence, G. J. *Top. Curr. Chem.*, **2009**, *286*, 73.
12. Yu, M. J.; Zheng, W.; Seletsky, B. M. *Nat. Prod. Rep.*, **2013**, *30*, 1158.
13. Searle, P. A.; Molinski, T. F. *J. Am. Chem. Soc.* **1995**, *117*, 8126.
14. Searle, P. A.; Molinski, T. F. *J. Am. Chem. Soc.* **1996**, *118*, 9422.
15. Molinski, T. F. *Tetrahedron Lett.* **1996**, *37*, 7879.
16. Forsyth, C. J.; Ahmed, F.; Cink, R. D.; Lee C. S. *J. Am. Chem. Soc.* **1998**, *120*, 5597.
17. Uckun F. M.; Forsyth C. J. *Bioorg. Med. Chem. Lett.* **2001**, *11*, 1181.
18. Smith, A. B.; Hogan, A. L.; Liu, Z.; Razler, T. M.; Meis, R. M.; Morinaka, B. I., Molinski T. F., *Tetrahedron*, **2011**, *67*, 5069.
19. Forsyth, C. J.; Ying, L.; La Clair, J. *J. Am. Chem. Soc.* **2006**, *128*, 3858.

20. Malumbres, M.; Barbacid, M. *Nat. Rev. Cancer*, **2009**, *9*, 153

21. Smith, A. B., III; Verhoest, P. R.; Minbiole, K. P.; Schelhaas, M. *J. Am. Chem. Soc.* **2001,** *123*, 4834.

22. Smith, A. B.; Razler, T. M.; Pettit, G. R.; Chapuis J. C. *Org. Lett.* **2005**, *7*, 4403.

23. Williams, D. R.; Kiryanov, A. A.; Emde, U.; Clark, M. P.; Berliner, M. A.; Reeves, J. T. *Angew. Chem., Int. Ed.* **2003,** *42*, 1258.

24. Pattenden, G.; González, M. A.; Little, P. B.; Millan, D. S.; Plowright, A. T.; Tornos, J. A.; Ye, T. *Org. Biomol. Chem.* **2003,** *1*, 4173.

25. White, J. D.; Kuntiyong, P.; Lee, T. H. *Org. Lett.* **2006**, *8*, 6043.

26. Wang, B.; Hansen, T. M.; Weyer, L.; Wu, D.; Wang, T., Christmann, M.; Lu, Y.; Ying, L.; Engler, M. M.; Cink, R. D.; Lee, C. S.; Ahmed, F.; Forsyth, C. J. *J. Am. Chem. Soc.* **2011,** *133*, 1506

27. Kuntiyong, P.; Lee, T. H.; Kranemann, C. L.; White, J. D.; *Org. Biomol. Chem.*, **2012**, *10*, 7884

28. Evans, D. A.; Fitch, D. M.; Smith, T. E.; Cee, V. J. *J. Am. Chem. Soc.* **2000,** *122*, 10033.

29. Li, De-Run; Zhang, Dong-Hui; Sun, Cai-Yun; Zhang, Ji-Wen; Yang, Li; Chen, Jian; Liu, Bo; Su, Ce; Zhou, Wei-Shan; Lin, Guo-Qiang *Chem. Eur. J.* **2006,** *12*, 1185.

30. Lucas, B. S.; Gopalsamuthiram, V.; Burke, S. D. *Angew. Chem Int. Ed.* **2007**, *46*, 769.

31. Lee, Chi Sing; Forsyth, C. J.; *Tetrahedron Lett.* **1996,** *37*, 6449.

32. Pattenden, G.; Yet, T. *Tetrahedron Lett.* **1998**, *39*, 319.

33. Paterson, I.; Arnott, E. A. *Tetrahedron Lett.* **1998**, *39*, 7185.

34. Williams, D. R.; Clark, M. P., Berliner, M. A. *Tetrahedron Lett.* **1999**, *40*, 2287.

35. White, J. D.; Kuntiyong, P.; Lee, T. H. *Org. Lett.* **2001**, *3*, 4003.

36. Smith, III, A. B.; Minbiole, K. P.; Verhoest, P. R.; Beauchamp, T. J. *J. Am. Chem. Soc.* **1999**, *1*, 913.

37. Rychnovsky, S. D.; Thomas, C. R.; *Org. Lett.* **2000**, *2*, 1217.

38. Lucas, B. S.; Luther, L. M.; Burke, S. D. *J. Org. Chem.* **2005**, *70*, 3757.

39. Hoffmann, H. M. R.; Misske, A. M. *Tetrahedron* **1999**, *55*, 4315.

40. Yadav, J. S.; Satyanarayana, M.; Srinivasulu, G., Kunwar, A. C. *Synlett*, **2007**, *10*, 1577.

41. Chakraborty, T. K.; Reddy, V. R.; Reddy, T. J. *Tetrahedron*, **2003**, *59*, 8613.

42. Huang, H.; Panek, J. S. *Org. Lett.* **2001**, *3*, 1693.

43. Clarke, P. A.; Martin, W. H. C. *Tetrahedron Lett.*, **2004**, *45*, 9061

44. Clarke, P. A.; Sellars, P. B.; Mistry, N. *Tetrahedron Lett.* **2011**, *52*, 3654

45. Clarke, P. A.; Santos, S.; Mistry, N.; Burroughs, L.; Humphries, A. C. *Org. Lett.* **2011**, *13*, 624

46. Clarke, P. A.; Hargreaves, J. M.; Woollaston, D. J.; Rodriguez Sarmiento, R. M. *Tetrahedron Lett.* **2010**, *51*, 4731.

47. Evans, D. A.; Bartroli, J.; Shih, T. L. *J. Am. Chem. Soc.* **1981**, *103*, 2127

48. Walker, M. A.; Heathcock, C. H. *J. Org. Chem.* **1991**, *56*, 5747

49. Evans, D. A.; Tedrow, J. S.; Shaw, J. T.; Downey, C. W. *J. Am. Chem. Soc.* **2002**, *124*, 392

50. Abiko, A.; Liu, J.; Masamune, S. *J. Am. Chem. Soc.* **1997**, *119*, 2586

51. Maleczka, R. E.; Terrell, L. R.; Geng, F.; Ward, J. S. *Org. Lett.* **2002**, *4*, 2841.

52. Dieckmann, M.; Kretschmer, M.; Li, P.; Rudolph, S.; Herkommer, D.; Menche, D. *Angew. Chem. Int. Ed.* **2012**, *51*, 5667.

53. Willwacher, J.; Kausch-Busies, N.; Fürstner, A. *Angew. Chem.* **2012**, *124*, 12207.

54. Yamashita, Y.; Ishitani, H.; Shimizu, H.; Kobayashi, S. *J. Am. Chem. Soc.* **2002**, *124*, 3292

55. Denmark, S. E.; Beutner, G. L.; Wynn, T.; Eastgate, M. D. *J. Am. Chem. Soc.* **2005**, *127*, 3774

56. Abiko, A. *Org. Synth.* **2002**, *79*, 103

57. Benoit, G.; Carey, J. S.; Chapman, A. M.; Chima, R.; Hussain, N.; Popkin, M. E.; Roux, G.; Tavassoli, B.; Vaxelaire, C.; Webb, M. R.; Whatrup, D. *Org. Process Res. Dev.* **2008**, *12*, 88

58. Hargreaves, J. M. PhD Thesis, *Towards The C19-C32 Fragment of The Phorboxazoles*, **2009**, The University of York.

59. Bahmanyar, S.; Houk, K. N. *J. Am. Chem. Soc.* **2001**, *123*, 11273

60. Kleinbeck, F.; Carreira, E. M. *Angew. Chem. Int. Ed.* **2009**, *48*, 578.

61. Frigerio, M.; Santagostino, M.; Sputore, S.; *J. Org. Chem.* **1999,** *64*, 4537

62. Lachance, H.; Hall, D. G. *Organic Reactions*, **2008**, *73*, 1

63. Hoffmann, R. W., Zeiss, H. J. *J. Org. Chem.* **1981**, *46*, 1309

64. Brown, H. C.; Jadhav, P. K.; Bhat, K. S. *J. Am. Chem. Soc.* **1985**, *107*, 2564

65. Yamamoto, Y.; Takahashi, M.; Miyaura, N. *Synlett*, **2002**, 128

66. Ishiyama, T.; Ahiko, T.; Miyaura, N. *Tetrahedron Lett.* **1996**, *37*, 6889

67. Roush, W. R. *J. Org. Chem.* **1991**, *56*, 4151

68. Yus, M.; González-Gómez, J. C.; Foubelo, F. *Chem. Rev.* **2011**, *111*, 7774

69. Ogawa, A. K.; Armstrong, R. W. *J. Am. Chem. Soc.* **1998**, *120*, 12435

70. Grubbs, H, R.; *Handbook of Metathesis*, **2003**, *1*, 1

71. Chatterjee, A. L.; *Handbook of Metathesis*, **2003**, *1*, 246

72. Truett, W. L.; Johnson, D. R., Robinson, I. M.; Montague, B. A. *J. Am. Chem. Soc.* **1960**, *82*, 2337

73. Nguyen, S. T.; Johnson, L. K.; Grubbs, R. H. *J. Am. Chem. Soc.* **1992**, *114*, 3974

74. Vougioukalakis, G. C.; Grubbs, R. H. *Chem. Rev.* **2010**, *110*, 1746

75. Nelson, D. J.; Manzini, S.; Urbina-Blanco, C. A.; Nolan, S. P. *Chem. Commun*., **2014**, *50*, 10355

76. Herisson, J.-L.; Chauvin, J. *Makromol. Chem.* **1971**, *141*, 161

77. Fuwa, H.; Saito, A.; Naito, S.; Konoki, K.; Yotsu-Yamashita, M.; Sasaki, M. *Chem. Eur. J.* **2009**, *15*, 12807

78. Yu, M.; Wang, C.; Kyle, A. F.; Dixon, D. J.; Shrock, R. S.; Hoveyda, A. H. *Nature*, **2011**, *479*, 88

79. Weatherhead, G. S.; Cortez, G. A.; Shrock, R. S.; Hoveyda, A. H *Proc. Natl. Acad. Sci. U.S.A.*, **2004**, *101*, 5805

80. Fuwa, H.; Noto, K.; Sasaki, M. *Org. Lett.* **2011**, *13*, 1820.

81. Fuwa, H.; Ichinokawa, N.; Noto, K.; Sasaki, M. *J. Org. Chem.* **2012**, *77*, 2588

82. Fürstner, A.; Langemann, K. *J. Am. Chem. Soc.* **1997**, *119*, 9130

83. Samojlowicz, C.; Bieniek, M.; Zarecki, A.; Kadyrov, R.; Grela, K. *Chem. Commun*., **2008**, 6282

84. Voigtritter, K.; Ghorai, S.; Lipshutz, B. H. *J. Org. Chem.* **2011**, *76*, 4697

85. Hoffman, T. J.; Rigby, J. H.; Arseniyadis, S.; Cossy, J. *J. Org. Chem.* **2008**, *73*, 2400

86. Nising, C. F.; Bräse, S. *Chem. Soc. Rev.* **2012**, *41*, 988

87. Zhang, X.; Zhang, S.; Wang, W. *Angew. Chem. Int. Ed.* **2010**, *49*, 1481.

88. Gu, Q.; Rong, Z.-Q.; Zheng, C.; You, S.-L. *J. Am. Chem. Soc.* **2010**, *132*, 4056

89. Lee, K.; Kim, H.; Hong, J. *Org. Lett.* **2011**, *13*, 2722

90. Houk, K. N.; Strozier, R. W. *J. Am. Chem. Soc.* **1973**, *95*, 4094

91. Pellicena, M.; Krämer, K.; Romea, P.; Urpí, F.; *Org. Lett.* **2011**, *13*, 5350

92. Clarke, P. A., Ermanis , K. *Org. Lett.* **2012**, *14*, 5550

93. Paterson, I.; Haslett, G. W. *Org. Lett.* **2013**, *15*, 1338

94. Computational Chemistry: Introduction to the Theory and Applications of Molecular and Quantum Mechanics, Lewars, G. E., *Springer*, **2011**

95. Whitford, P. C.; Geggier, P.; Altman, R. B.; Blanchard, S. C.; Onuchic, J. N.; Sanbonmatsu, K. Y. *RNA*, **2010**, *16*, 1196

96. Zhao, G.; Perilla, J. R.; Yufenyuy, E. L., Meng, X.; Chen, B.; Ning, J.; Ahn, J.; Gronenborn, A. M.; Schulten, K.; Aiken, C.; Zhang, P. *Nature*, **2013**, *497*, 643

97. Bikadi, Z.; Hazai, E. *J. Chem. Inf.* **2009**, *1*, 15

98. Becke, A. D; *J. Chem. Phys.* **1993**, *98*, 1372

99. Zhao, Y.; Truhlar, D. G. *Theor. Chem. Acc.* **2008**, *119*, 525

100. Chai, J. D., Head-Gordon, M. *Phys. Chem. Chem. Phys.* **2008**, *10*, 6615

101. El-Aasar, A. M. M.; Nash, C. P.; Ingraham, L. L. *Biochemistry*, **1982**, *21*, 1972

102. Narasaka, K.; Pai, F.-C. *Tetrahedron* **1983**, *40*, 2233

103. Saksena, A. K.; Mangiaracina, P. *Tetrahedron Lett.* **1983**, *24*, 273

104. Evans, D. A.; Chapman, K. T.; Carreira, E. M. *J. Am. Chem. Soc.* **1988**, *110*, 3560

105. Lafontaine, J. A.; Provencal, D. P.; Gardelli, C.; Leahy, J. W. *J. Org. Chem.* **2003**, *68*, 4215.

106. Williams, D. R.; Lowder, P. D.; Gu, Y. G.; Brooks, D. A. *Tetrahedron Lett.* **1997**, *38*, 331.

107. Gilbert, A. B; Peters, F. B; Johnson, H. W. *J. Org. Chem.*, **1983**, *48*, 2724.

108. Crimmins, M.T.; Kirincich, S. J.; Wells, A. J.; Choy, A. L. *Synthetic Communications* **1998**, *28*, 3675.

109. Vita, M.; Waser, J. *Org. Lett.*, **2013**, *15*, 3246.

110. Hiebel, M.A.; Pelotier, B.; Piva, O. *Tetrahedron*, **2007**, *63*, 7874.

111. Kumaraswamy, G.; Rambabu, D. *Tetrahedron Asym.*, **2013**, *24*, 196.

112. Karlubíková, O.; Babjak, M.; Gracza, T. *Tetrahedron*, **2011**, *67*, 4980.